e-ISSN: 2147-2092

GAZI MEDICAL JOURNAL

2026
July
Volume 37 • Issue 3

galenos yayınevi

medicaljournal.gazi.edu.tr

GAZI MEDICAL JOURNAL

medicaljournal.gazi.edu.tr

Editorial Team

GAZI MEDICAL JOURNAL

medicaljournal.gazi.edu.tr

Section Editors and Scientific Editorial Board

Ethical Board

Statistical Board

Scientific Advisory Board

GAZI MEDICAL JOURNAL

medicaljournal.gazi.edu.tr

Please refer to the journal's webpage (https://medicaljournal.gazi.edu.tr/) for "About the Journal" and "Submissions".

The editorial and publication process of Gazi Medical Journal are shaped in accordance with the guidelines of the International Committee of Medical Journal Editors (ICMJE), World Association of Medical Editors (WAME), Council of Science Editors (CSE), Committee on Publication Ethics (COPE), European Association of Science Editors (EASE), and National Information Standards Organization (NISO). The journal is in conformity with the Principles of Transparency and Best Practice in Scholarly Publishing.

Gazi Medical Journal is indexed in Emerging Sources Citation Index, Scopus, Directory of Open Access Journals, EuroPub, Islamic World Science Citation Center, ABCD Index.

The online published articles are freely available on the public internet.

Owner: Musa Yıldız on Behalf of Gazi University

Responsible Manager: Mehmet Ali Ergün

Publisher Contact

Address: Molla Gürani Mah. Kaçamak Sk. No: 21/1 34093 İstanbul, Türkiye

Phone: +90 (539) 307 32 03

E-mail: info@galenos.com.tr/yayin@galenos.com.tr

Web: www.galenos.com.tr

Publisher Certificate Number: 14521

Publication Date: July 2026

e-ISSN: 2147-2092

International scientific journal published quarterly.

GAZI MEDICAL JOURNAL

medicaljournal.gazi.edu.tr

CONTENTS

Original Investigations - Özgün Araştırmalar

GAZI MEDICAL JOURNAL

medicaljournal.gazi.edu.tr

CONTENTS

GAZI MEDICAL JOURNAL

medicaljournal.gazi.edu.tr

CONTENTS

Case Reports - Olgu Sunumları

Literature Review with Case | Olgularla Literatür İncelemesi

Original Investigation | Özgün Araştırma

Gazi Med J 2026;37(3):330-340

DOI: http://dx.doi.org/10.12996/gmj.2026.4012

The Effect of Symptoms Seen in Inpatients Receiving Treatment Due to a Diagnosis of COVID-19 on Functional Independence Status and Anxiety Levels: A Descriptive Study

COVID-19 Tanısı ile Hastanede Yatarak Tedavi Uygulanan Hastalarda Görülen Semptomların Fonksiyonel Bağımsızlık Durumuna ve Anksiyete Düzeyine Etkisi: Tanımlayıcı Bir Çalışma

Arife Altın Çetin[1], Sultan Akçimen[2], Hicran Bektaş[3], Dilara İnan[4], Fatma Gökalp[5]

[1]Department of Nursing, Antalya Bilim University, Faculty of Health Sciences, Antalya, Türkiye
[2]Infection Control Committee, Akdeniz University Hospital, Antalya, Türkiye
[3]Department of Internal Medicine Nursing, Akdeniz University, Faculty of Nursing, Antalya, Türkiye
[4]Department of Infectious Diseases and Clinical Microbiology, Akdeniz University, Faculty of Medicine, Antalya, Türkiye
[5]COVID-19 Clinic, Akdeniz University Hospital, Türkiye

ABSTRACT

Objective: The aim of this research is to determine the effects of symptoms seen in inpatients receiving treatment due to a diagnosis of coronavirus disease 2019 (COVID-19) on functional independence status and anxiety levels.

Methods: This research was conducted as a descriptive study between July 2021 and April 2022. It included 150 patients diagnosed with COVID-19. Data were collected using a Personal Information Form, the Modified Barthel Index, the Beck Anxiety Inventory, and the Coronavirus Anxiety Scale. Percentage calculations, Kruskal-Wallis Analysis of Variance, and the Mann-Whitney U test were used in data analysis.

Results: The mean age of the participants was 52.3 ± 13.18, 55.3% were male, 80% were married, 32% were university graduates, and 72.7% had at least one accompanying disease. The most common symptoms on admission to the hospital and during the hospital stay were dyspnea (63.3%, 64%), cough (58.7%, 46%), fever (56%, 32%), and fatigue (40.7%, 22.7%), respectively. It was determined that participants were slightly functionally dependent (95.7±8.98), most of them had high levels of anxiety (82%), and about half of them had COVID-19-related dysfunctional anxiety (46%).

ÖZ

Amaç: Bu araştırmanın amacı, koronavirüs hastalığı 2019 (COVID-19) tanısı ile hastanede yatarak tedavi uygulanan hastalarda görülen belirtilerin fonksiyonel bağımsızlık durumuna ve anksiyete düzeyine etkisinin belirlenmesidir.

Yöntemler: Bu araştırma tanımlayıcı bir çalışma olarak Temmuz 2021-Nisan 2022 tarihleri arasında yürütüldü. Çalışma COVID-19 tanısı olan 150 hasta ile gerçekleştirildi. Veriler, Kişisel Bilgi Formu, Modifiye Barthel İndeksi, Beck Anksiyete Envanteri ve Koronavirüs Anksiyete Ölçeği kullanılarak toplandı. Verilerin analizinde yüzdelik hesaplamaları, Kruskal-Wallis Varyans Analizi ve Mann-Whitney U testi kullanıldı.

Bulgular: Katılımcıların %55,3'ünün erkek, %80'inin evli, %32'sinin üniversite mezunu olduğu ve %72,7'sinin en az bir ek hastalığı bulunduğu saptandı. Hastaneye başvuru anında ve hastanede yatarken en sık yaşanan semptomlar sırasıyla nefes darlığı (%63,3; %64), öksürük (%58,7; %46), ateş (%56; %32) ve yorgunluktu (%40,7; %22,7). Katılımcıların fonksiyonel yönden hafif derecede (95,7 ± 8,98) bağımlı olduğu, çoğunun (82%) yüksek düzeyde anksiyete ve yaklaşık yarısının (46%) COVID-19 ilişkili işlevsiz anksiyete yaşadığı saptandı.

Cite this article as: Altın Çetin A, Akçimen S, Bektaş H, İnan D, Gökalp F. The effect of symptoms seen in inpatients receiving treatment due to a diagnosis of COVID-19 on functional independence status and anxiety levels: a descriptive study. Gazi Med J. 2026;37(3):330-340

Address for Correspondence/Yazışma Adresi: Arife Altın Çetin, Department of Nursing, Antalya Bilim University, Faculty of Health Sciences, Antalya, Türkiye
E-mail / E-posta: arife.altin@antalya.edu.tr
ORCID ID: orcid.org/0000-0002-9743-6454

Received/Geliş Tarihi: 25.09.2023
Accepted/Kabul Tarihi: 01.06.2026
Publication Date/Yayınlanma Tarihi: 10.07.2026

ABSTRACT

CONCLUSION: These findings highlight the importance of early symptom management and anxiety screening in hospitalized COVID-19 patients. Nursing interventions should be individualized and aimed at improving functional independence while reducing anxiety levels. Future nursing practices and healthcare policies should integrate mental health support as a core component of inpatient COVID-19 care.

Keywords: Anxiety, COVID-19, functional independence, nursing, symptom

ÖZ

Sonuç: Elde edilen bulgular, hastanede yatan COVID-19 hastalarında erken semptom yönetimi ve anksiyete taramasının önemini ortaya koymaktadır. Hemşirelik girişimleri bireyselleştirilmiş olmalı; işlevsel bağımsızlığı artırmayı ve anksiyete düzeylerini azaltmayı hedeflemelidir. Gelecekteki hemşirelik uygulamaları ve sağlık politikaları, yatarak tedavi gören COVID-19 hastalarının bakımında ruhsal destek hizmetlerini temel bir bileşen olarak içermelidir.

Anahtar Sözcükler: Anksiyete, COVID-19, fonksiyonel bağımsızlık, hemşirelik, semptom

INTRODUCTION

Coronavirus disease 2019 (COVID-19) was first detected in Wuhan, Hubei province, China, in December 2019 and subsequently spread rapidly throughout China and then worldwide. The World Health Organization (WHO) declared the case a pandemic (1,2). Around 760 million people worldwide have been affected by COVID-19 infection (3).

The physiological impacts of COVID-19, which has high transmissibility and infectivity, are broad and variable. It has been shown that many of the physiological systems and tissues are affected by the virus in individuals who develop symptoms after contacting with the virus (4). Accordingly, these patients develop many symptoms, such as impaired gas exchange, hyperthermia, pain, nausea-vomiting, fluid-electrolyte loss, aspiration risk, activity intolerance, deterioration in sleep patterns, deterioration in skin integrity, anxiety, and hopelessness, and these symptoms lead to increased morbidity and mortality rates (5). Some studies have indicated that individuals experience limitations in daily living activities, such as walking, moving, bathing, dressing, lifting, performing daily routines, and entertainment (6-8). Activities of daily living (ADL) include aspects of individuals' functional independence, such as nutrition, self-care, dressing, bathing, toileting, mobility, hand function, and social perception. Therefore, it has been emphasized that the functional independence status of an individual should be evaluated to determine whether they can perform the ADL (7).

It has been reported that psychological issues like anxiety, depression, and stress have increased as a result of the detrimental impact of COVID-19 pandemic on mental health (1). In addition to medical treatment provided to individuals showing signs of the illness, social isolation is applied. Isolation refers to the separation and restriction of movement of an individual with an infectious disease for protective purposes and is usually carried out in hospital settings (9). Additionally, situations such as excessive information in the media, stigma, and separation from relatives are thought to cause mental problems, such as anxiety and depression.

Recent cohort and rehabilitation studies highlight that maintaining functional independence during and after COVID-19 hospitalization remains a clinically significant concern. Reduced or minimal improvement in Barthel Index (BI) or Modified Barthel Index (MBI) scores during admission has been strongly associated with higher mortality among older adults with COVID-19 pneumonia (10). Observational rehabilitation studies further demonstrate that early, structured inpatient rehabilitation programs substantially improve ADL and mobility performance, although residual deficits frequently persist, particularly among patients recovering from intensive care or with frailty (11,12). These findings underscore the importance of continuous monitoring and tailored rehabilitation strategies to optimize recovery trajectories.

Concurrently, growing evidence indicates that anxiety and other psychological symptoms remain prevalent and persistent among hospitalized and post-acute COVID-19 patients. For instance, Tan et al. (13) reported that 86% of hospitalized patients experienced clinically relevant anxiety levels, while global meta-analyses estimate an anxiety prevalence of approximately 23% among individuals with post-COVID-19 syndrome (14). Longitudinal follow-up studies reveal that psychiatric and cognitive symptoms—including anxiety, depression, and fatigue—can worsen or newly emerge up to 2–3 years after hospital discharge (15). Collectively, these data highlight the dual need to address functional independence and mental health outcomes across the continuum of COVID-19 recovery.

This study was conducted to determine the effects of symptoms observed in inpatients receiving treatment for COVID-19 on their functional independence and anxiety levels.

MATERIALS AND METHODS

Design

A descriptive research design was used. The study was conducted and reported in accordance with the STROBE recommendations.

Participants

The study sample consisted of patients who were hospitalized with a diagnosis of COVID-19 in the pandemic clinics of Akdeniz University Hospital between July 2021 and April 2022. The sample size was calculated to be 150 individuals, based on a statistical power of 80% and a 95% confidence level. Inclusion criteria identified patients who were aged ≥18 years, were literate, had a positive polymerase chain reaction (PCR) test or were COVID-19 positive as shown by computerized tomography, knew their diagnosis and could express it verbally, had no communication barriers (hearing and speaking), had no psychosomatic disorder according to their self-reports, had no physical, cognitive, or mental disability in answering questions, could use a smartphone with an Internet connection, could use the WhatsApp application, and gave consent to participate in the study. An informative message about the purpose of the study and the research team was sent to the phones of the patients who met the inclusion criteria. The infection physician, infection nurse, and COVID-19 clinical nurse on the research team determined which

patients were eligible to participate in the study. Consent of the patients who agreed to participate in the study was obtained online. Questionnaires were sent to the patients' phones via Google Forms. Patients filled out the forms online. Twenty-five patients refused to participate in the study because of fatigue and reluctance.

Data Collection

A Personal Information Form, the MBI, the Beck Anxiety Inventory (BAI), and the Coronavirus Anxiety Scale (CAS) were used to collect data. In the study, functional independence status, anxiety level, and fear of coronavirus outcomes were evaluated.

Personal Information Form

Data on the descriptive and demographic characteristics of patients were collected using a personal information form. The researchers developed this form following a comprehensive literature review. It includes questions about age, gender, marital status, educational status, job, number of cohabitants, presence of chronic diseases, history of organ transplantation, smoking history, and symptoms observed at the time of admission to the hospital and during hospitalization (16-19).

Modified Barthel Index

The MBI was created by the modification of the BI, which was developed by Mahoney and Barthel (1965), by Shah et al. (20). Physical independence in ADL (transfer, ambulation/wheelchair use, climbing stairs, feeding, dressing, grooming, bathing, toilet use, bladder incontinence, and bowel incontinence) is assessed using a 10-item scale. A score of "0" indicates total dependency, while a score of "100" indicates total independence (20). The total score ranges from 0 to 100. Cronbach's alpha value for the overall scale was determined to be 0.93 in the study by Yavuzer et al. (21,22). In our study, the alpha value of the scale was 0.82.

Beck Anxiety Inventory

Beck et al. (23) created the Beck Anxiety Inventory. It is a 4-point Likert-type scale with 21 questions, each assigned 0 to 3 points and used to gauge the level of anxiety. The total scale scores are interpreted as follows to indicate anxiety levels: low for scores from 8 to 15; moderate for scores from 16 to 25; and high for scores from 26 to 63 (23). Ulusoy et al. (24) conducted a validity and reliability assessment of the scale in Türkiye, and they reported that Cronbach's alpha was 0.93. In our analysis, the alpha value was 0.90.

Coronavirus Anxiety Scale

Lee (25) created the CAS to detect potential instances of dysfunctional anxiety linked to COVID-19. It has one dimension and five questions. A five-point Likert scale with the following options is used to grade the questions: 0, never; 1, rarely, less than one or two days; 2, a few days; 3, more than 7 days; 4, almost daily in the last two weeks (25). In a validity and reliability research done in Türkiye by Biçer et al. (26), Cronbach's alpha was found to be 0.83. In our analysis, the alpha value was 0.85.

Ethical Considerations

Written approval for the study was obtained from the Clinical Research Ethics Committee of Akdeniz University Faculty of Medicine (KAEK-231/28.04.2021) and from the Antalya Provincial Health Directorate (date: 28.06.2021). Permission from the authors who developed the scales used in the study was obtained by e-mail. Informed consent forms prepared following the Declaration of Helsinki were obtained online from the patients who agreed to participate in the study.

Statistical Analysis

IBM SPSS Statistics for Windows, Version 23.0, was used for statistical analysis (IBM Corp., Armonk, NY). The Shapiro-Wilk test was used to assess the normality of the data. Descriptive statistics were summarized using frequency (n), percentage (%), mean, standard deviation (SD), median, range (minimum–maximum), interquartile range (25^{th}–75^{th} percentile). For non-parametric comparisons of scale scores between independent groups, the Mann-Whitney U test and the Kruskal-Wallis test were used. The Bonferroni correction was used for post hoc analysis. For the reliability analysis, Cronbach's alpha coefficients were calculated. A two-sided p-value < 0.05 was considered statistically significant.

RESULTS

Sociodemographic and COVID-19 Characteristics of the Participants

A total of 150 patients who were hospitalized with a diagnosis of COVID-19 participated in the research. The mean age of the participants was 52.3 ± 13.18 years, 55.3% were male, 80% were married, 32% were university graduates, and 30.7% were housewives. 72.7% of the participants at least one comorbidity, 24% were smokers, and 21.3% used immunosuppressive drugs. The participants lived with an average of 3.02 ± 1.05 household members (median = 3, range = 1–4) (Table 1). The most common symptoms experienced by the participants on admission and during hospitalization were dyspnea (63.3%, 64%), cough (58.7%, 46%), fever (56%, 32%), and fatigue (40.7%, 22.7%) (Table 2). The mean anxiety level of the participants was 5.3±2.89 (minimum-maximum: 1–10). They experienced anxiety due to shortness of breath (62.7%), hospitalization (57.3%), and oxygen therapy (50%).

Findings Related to Functional Dependence and Anxiety Levels of the Participants According to their Sociodemographic Characteristics

The mean score for the functional independence status of the participants was 95.7 ± 8.98 according to MBI. The MBI scores of participants aged 60 and over ($p < 0.001$) and of those with chronic diseases ($p = 0.010$) were significantly lower. In addition, MBI scores were significantly higher among university graduates ($p = 0.006$) and among participants with a history of organ transplantation ($p = 0.004$). No significant relationship was found between the participants' MBI scores and their gender, marital status, job, cohabitants, smoking status, or immunosuppressive drug use ($p > 0.05$). It was found that the mean anxiety score of the participants was 33.8 ± 11.40 according to the BAI, and 82% of them had high levels of anxiety. The BAI scores were significantly higher in women and in secondary school graduates than in primary school graduates, and were higher in housewives or unemployed participants than in self-employed participants, workers, or civil servants ($p < 0.05$). In addition, it was found that the mean anxiety score of the participants

was 8.9 ± 4.96 according to the CAS and that 46% of them had dysfunctional anxiety associated with the coronavirus. CAS scores were higher in secondary school and university graduates than in primary school graduates, and higher in participants living with four or more cohabitants than in those with two or fewer cohabitants ($p < 0.05$) (Table 3).

Table 1. Socio-demographic and COVID-19 characteristics of the participants (n = 150).

Socio-demographic characteristics	n	%
Age	52.3 ± 13.18	54 (21–89)
$\bar{X}$ ± SD/median (minimum-maximum)		
Gender		
Female	67	44.7
Male	83	55.3
Marital status		
Married	120	80.0
Single	30	20.0
Educational status		
Literate	4	2.7
Primary school	27	18.0
Secondary school	27	18.0
High school	44	29.3
University	48	32.0
Occupation		
Housewife	46	30.7
Retired	22	14.7
Self-employed	45	30.0
Workers-civil servants	16	10.7
Student	2	1.3
Unemployed	19	12.7
Number of people living together at home	3.02 ± 1.05/3 (1–4)	
$\bar{X}$ ± SD/median (minimum-maximum)		
One person	1	0.7
Two person	63	42.0
Three person	45	30.0
Four people and more	41	27.3
Comorbidities[a]	109	72.7
Kidney disease	25	16.7
Cardiovascular disease	26	17.3
Hypertension	38	25.3
Cancer	21	14.0
Diabetes mellitus	39	26.0
Smoking	36	24.0
Organ transplant history	26	17.3
Immunosuppressive drug use	32	21.3

[a]Participants could report more than one comorbidity; therefore, percentages do not total 100%. SD: Standard deviation.

Findings Related to the Functional Independence Status and Anxiety Level of the Participants According to the Symptoms at the Time of Admission and Hospitalization

BAI scores were significantly higher in participants with nausea or vomiting at hospital admission ($p = 0.034$), and CAS scores were significantly higher in participants with cough during hospitalization ($p = 0.002$). No significant relationship was observed between the participants' symptoms, either at admission or during hospitalization, and their MBI scores ($p > 0.05$) (Table 4).

Findings Related To The Functional Independence And Anxiety Level Of Participants According To Their Anxiety Levels

BAI scores were higher in participants who feared they would not recover and who had dyspnea ($p < 0.05$). Although the BAI scores of the participants who were afraid of not seeing their family members were higher, this difference was not significant ($p > 0.05$). CAS scores were significantly higher among participants who feared they would not recover and significantly lower among those who

Table 2. Symptoms of the patients at the time of admission to the hospital and during hospitalization (n =150).

Symptoms[a]	n	%
At the time of admission		
Dyspnea	95	63.3
Cough	88	58.7
Fever	84	56.0
Fatigue	61	40.7
Musculoskeletal pain	34	22.7
Nausea-vomiting	22	14.7
Diarrhea	12	8.0
Sore throat	9	6.0
Chest pain	6	4.0
Expectoration	6	4.0
Loss of taste and smell	2	1.3
Hospitalization		
Dyspnea	96	64.0
Cough	69	46.0
Fever	48	32.0
Fatigue	34	22.7
Nausea-vomiting	7	4.7
Sore throat	6	4.0
Diarrhea	3	2.0
Loss of taste and smell	1	0.7

[a]Participants could report more than one comorbidity; therefore, percentages do not total 100%.

Table 3. Scale scores according to the sociodemographic characteristics of the patients (n = 150).

Variables	MBI, median (IQR)	BAI, median (IQR)	CAS, median (IQR)
Age			
Under 60	100 (100–100)	35 (28–42)	8 (6–12)
60 and over	100 (90–100)	34 (27–39)	8 (5–12)
z/p	**z = -4.206; p < 0.001**	z = -0.912; p = 0.362	z = -0.727; p = 0.467
Gender			
Female	100 (95–100)	39 (32–45)	8 (5–13)
Male	100 (100–100)	31 (26–38)	8 (5–12)
z/p	z = 0.503; p = 0.615	**z = -3.520; p<0.001**	z = -0.032; p = 0.974
Marital status			
Married	100 (100–100)	36 (29–42)	8 (5.5–12)
Single	100 (95–100)	33 (25–42)	8 (5–14)
z/p	z = -1.499; p = 0.134	z = -1.020; p = 0.308	z = -0.094; p = 0.925
Educational status			
Primary school and before	100 (90–100)[a]	31 (26–36)[a]	6 (2–9)[a]
Secondary school	100 (95–100)[a.b]	39 (31–45)[b]	9 (5–13)[b]
High school	100 (95–100)[a.b]	35.5 (29.5–45.5)[a.b]	8 (5.5–13)[a.b]
University	100 (100–100)[b]	34 (27–42.5)[a.b]	9 (7–13)[b]
KWH/p	**KWH = 12.371; p = 0.006**	**KWH = 7.851; p = 0.049**	**KWH = 9.754; p = 0.021**
Occupation			
Housewife	100 (95–100)	37 (31–44)[a]	8 (6–12)
Retired	100 (95–100)	35.5 (31–41)[a.b]	7.5 (5–10)
Self–employed	100 (100–100)	33 (23–38)[b]	8 (5–12)
Workers–civil servants	100 (100–100)	28 (26–39)[b]	7.5 (6.5–14.5)
Unemployed	100 (100–100)	39 (29–46)[a]	10 (6–16)
KWH/p	KWH = 4.186; p = 0.381	**KWH = 12.682; p = 0.013**	KWH = 4.211; p = 0.378
Number of people living together at home			
Two people and fewer	100 (95–100)	36 (28–41.5)	7 (5–10)[a]
Three people	100 (100–100)	31 (27–39)	8 (6–13)[a.b]
Four people or more	100 (100–100)	38 (31–43)	9 (7–14)[b]
KWH/p	KWH = 3.733; p = 0.155	KWH = 2.517; p = 0.284	**KWH = 8.214; p = 0.016**
Chronic disease			
No	100 (100–100)	31 (27–38)	9 (7–13)
Yes	100 (95–100)	36 (29–42)	8 (5–12)
z/p	**z = -2.582; p = 0.010**	z = 1.525; p = 0.127	z = -1.370; p = 0.171
Smoking			
No	100 (95–100)	36 (29–42)	8 (6–12)
Yes	100 (100–100)	30.5 (26.5–40)	8 (5–12.5)
z/p	z = 1.396; p = 0.163	z = -1.466; p = 0.143	z = 0.163; p = 0.870
Organ transplant history			
No	100 (95–100)	35 (28–42)	8 (5–12.5)
Yes	100 (100–100)	33.5 (28–41)	7.5 (6–10)
z/p	**z = 2.873; p = 0.004**	z = -0.124; p = 0.901	z = 0.035; p = 0.972
Immunosuppressive drug use			
No	100 (95–100)	33.5 (28–41)	8 (5–12)
Yes	100 (100–100)	39 (32–46)	8.5 (7–12.5)
z/p	z = 1.872; p = 0.061	z = 1.781; p = 0.075	z = 0.920; p = 0.358

The same lowercase letters in a column indicate no significant difference between groups. *p < 0.05. BAI: Beck Anxiety Inventory, CAS: Coronavirus Anxiety Scale, IQR: Interquartile range, KWH: Kruskal-Wallis H test, MBI: Modified Barthel Index, z: Mann-Whitney U test.

Table 4. Scale scores according to the symptoms of the patients at the time of admission to the hospital and hospitalization (n = 150).

Symptoms	MBI, median (IQR)	BAI, median (IQR)	CAS, median (IQR)
At the time of admission			
Dyspnea			
No	100 (100–100)	36 (29–45)	8 (5–13)
Yes	100 (95–100)	34 (28–40)	8 (5–12)
z/p	z = -0.476; p = 0.634	z = -1.264; p = 0.206	z = -0.080; p = 0.936
Cough			
No	100 (95–100)	36 (29–42)	8 (5–12)
Yes	100 (100–100)	33 (27.5–42)	8 (5.5–13)
z/p	z = 0.854; p = 0.393	z = -0.945; p = 0.345	z = 0.764; p = 0.445
Fever			
No	100(95–100)	36 (25–42)	8.5(5–13)
Yes	100(100–100)	34.5 (29–42)	8(6–12)
z/p	z = 0.670; p = 0.503	z = 0.968; p = 0.333	z = -0.051; p = 0.959
Fatigue			
No	100 (95–100)	34 (27–42)	8 (6–13)
Yes	100 (100–100)	36 (29–41)	8 (5–12)
z/p	z = 0.861; p = 0.389	z = 0.373; p = 0.709	z = -0.848; p = 0.396
Musculoskeletal pain			
No	100 (95–100)	35 (28–42)	8 (5–12.5)
Yes	100 (100–100)	33 (29–42)	8 (6–11)
z/p	z = 1.604; p = 0.109	z = -0.011; p = 0.991	z = 0.266; p = 0.791
Nausea-vomiting			
No	100 (95–100)	33 (27–41.5)	8 (5–12)
Yes	100 (95–100)	39 (34–44)	8 (7–13)
z/p	z = -0.231; p = 0.817	**z = 2.121; p = 0.034**	z = 0.919; p = 0.358
Diarrhea			
No	100 (95–100)	34 (28–42)	8 (5–12)
Yes	100 (92.5–100)	39 (34–47)	7 (5.5–11.5)
z/p	z = -0.103; p = 0.918	z = 1.851; p = 0.064	z = -0.340; p = 0.734
Hospitalization			
Dyspnea			
No	100 (95–100)	33.5 (28–41)	7.5 (5–12)
Yes	100 (95–100)	35 (28–42.5)	9 (6–13)
z/p	z = 0.069; p = 0.945	z = 0.541; p = 0.589	z = 1.133; p = 0.257
Cough			
No	100 (95–100)	33 (25–42)	7 (5–11)
Yes	100 (100–100)	36 (31–43)	9 (7–13)
z/p	z = 0.448; p = 0.654	z = 1.709; p = 0.087	**z = 3.123; p = 0.002**
Fever			
No	100 (95–100)	35.5 (27–42)	8 (5–13)
Yes	100 (100–100)	33.5 (29–43)	8 (6–12)
z/p	z = 1.348; p = 0.178	z = 0.877; p = 0.381	z = 0.420; p = 0.674
Fatigue			
No	100 (95–100)	33 (28–42)	8 (5–12)
Yes	100 (100–100)	36 (29–42)	8 (5–13)
z/p	z = 0.049; p = 0.961	z = 0.485; p = 0.628	z = -0.257; p = 0.798
Nausea-vomiting			
No	100 (95–100)	35 (28–42)	8 (5–12)
Yes	100 (95–100)	34 (25–41)	10 (7–14)
z/p	z = -0.127; p = 0.899	z = -0.120; p = 0.904	z = 0.389; p = 0.698

*p < 0.05. BAI: Beck Anxiety Inventory, CAS: Coronavirus Anxiety Scale, IQR: Interquartile range, MBI: Modified Barthel Index, z: Mann-Whitney U test.

feared hospitalization ($p < 0.05$). There was no significant correlation between participants' anxiety states and their MBI scores ($p > 0.05$) (Table 5).

DISCUSSION

Although the symptoms associated with COVID-19 infection vary from person to person, it is reported that fever, dyspnea, cough, fatigue, and musculoskeletal system symptoms (muscle pain and joint pain) are most common in individuals who present to the hospital (27-31). Additionally, dyspnea, fatigue, and myalgia have been reported as the most common symptoms in post-COVID-19 patients (32). In our study, consistent with the literature, the most common symptoms experienced by individuals diagnosed with COVID-19 on admission and during hospitalization were dyspnea, fever, cough, and fatigue. These findings highlight the importance of early nursing assessments focused on respiratory and systemic symptoms. Nurses should be vigilant in monitoring dyspnea and fatigue, as these symptoms significantly affect daily functioning and increase psychological distress. Proactive symptom management protocols may improve both physical outcomes and emotional well-being.

Disorders in body functions and structures such as dyspnea, weakness, myalgia, and pain limit the functional independence of individuals (7,32). Functional independence is the capacity to carry out ADL that are required to meet fundamental needs, carry out daily tasks, and preserve one's health and well-being (8). Our results showed that the functional independence of most individuals diagnosed with COVID-19 was adversely affected. Similar findings have been reported in the literature (33-36). Chung et al. (16) found that 36% of individuals diagnosed with COVID-19 were fully independent, 28% were moderately dependent, and 15% were severely dependent. Triantafyllaki et al. (36) reported that the BI scores of patients who were followed up in the clinic after intensive care treatment due to COVID-19 was found to be low. Similarly, it has been reported that most patients hospitalized with COVID-19 have low functional status 6 months after hospitalization (32,37). Belli et al. (33) reported that individuals who survived after hospital treatment due to COVID-19 depended on or needed someone else's help to perform their daily living activities. Heras et al. (38), in their study with elderly patients, found that the functional independence status of elderly patients was slightly low. In our study, the participants were slightly functionally dependent, and the MBI scores of participants aged 60 and over and of those with an additional disease were significantly lower.

Table 5. Scale scores according to patients' anxiety levels in daily life (n = 150).

Anxiety levels	MBI, median (IQR)	BAI, median (IQR)	CAS, median (IQR)
Dyspnea			
No	100 (95–100)	32 (19.5–41.5)	7.5 (5–12)
Yes	100 (100–100)	36 (29–42)	8 (6–12)
z/p	z = 1.860; p = 0.063	**z = 2.142; p = 0.032**	z = 1.642; p = 0.101
Hospitalization			
No	100 (92.5–100)	36.5 (28.5–42.5)	9.5 (7–14)
Yes	100 (100–100)	33 (28–41)	7.5 (5–10)
z/p	z = 1.587; p = 0.112	z = -1.011; p = 0.312	**z = -2.345; p = 0.019**
Oxygen therapy			
No	100 (95–100)	34 (27–41)	8 (5–10)
Yes	100 (100–100)	36 (29–43)	9 (6–13)
z/p	z = 1.424; p = 0.154	z = 1.053; p = 0.292	z = 1.841; p = 0.066
Fear of not recovering			
No	100 (95–100)	32 (25–40)	8 (5–10)
Yes	100 (100–100)	38 (32–45)	10 (7–14)
z/p	z = 0.402; p = 0.688	**z = 3.144; p = 0.002**	**z = 3.376; p = 0.001**
Inability to do daily activities			
No	100 (95–100)	35 (29–42)	8 (5–12)
Yes	100 (97.5–100)	35 (27–41)	8.5 (6–12.5)
z/p	z = 0.285; p = 0.776	z = -0.410; p = 0.682	z = 0.740; p = 0.459
Not seeing their relatives			
No	100 (95–100)	33 (27–42)	8 (5–12)
Yes	100 (100–100)	39 (35–42)	7 (5–12)
z/p	z = 0.451; p = 0.652	z = 1.937; p = 0.053	z = -1.184; p = 0.236

*p < 0.05. BAI: Beck Anxiety Inventory, CAS: Coronavirus Anxiety Scale, IQR: Interquartile range, MBI: Modified Barthel Index, z: Mann-Whitney U test.

Similarly, Frontera et al. (39) demonstrated that older adults diagnosed with COVID-19 exhibited significantly lower BI scores.

Our findings are consistent with recent evidence demonstrating that post-acute functional trajectories following COVID-19 hospitalization remain heterogeneous. Although inpatient rehabilitation programs have been shown to enhance ADL performance, many patients—particularly older adults and those with multiple comorbidities—continue to experience residual functional limitations after discharge. Declines or limited improvement in BI or MBI scores during hospitalization have been associated with higher mortality and poorer long-term outcomes (10,40). Similarly, rehabilitation studies report that early, structured, and multidisciplinary programs can promote significant but incomplete recovery of functional independence, closing the gap between intensive-care and medical-unit survivors (11,12). These results underscore the necessity of sustained monitoring and targeted interventions to maintain functional gains throughout the post-acute phase.

These results underscore the necessity for geriatric-sensitive and comorbidity-aware nursing care plans. Functional assessments should be performed routinely for elderly or chronically ill individuals, and rehabilitation interventions should focus on preserving autonomy and preventing complications related to immobility. Similar to our research, it was reported that the functional independence levels of elderly individuals who were treated for COVID-19 diagnosis and those who had an additional disease were low (16,19,33). Bayat et al. (41) stated that while advanced age affected functional independence, there was no relationship between the presence of additional disease and functional independence, unlike our study.

In our study, the MBI scores of the participants who were university graduates and who had a history of organ transplantation were significantly higher. These individuals' knowledge of COVID-19, its treatment, and how to respond in an acute situation may increase their level of functional independence. Similar findings have been reported in the literature (42). It is emphasized that individuals possess a high level of knowledge about COVID-19, that the body of information has expanded as the pandemic has progressed, and that such information has been accessed through radio, television, and the internet. It has been reported that higher levels of health literacy among individuals are associated with greater knowledge about COVID-19 (43). Health literacy may play a mediating role in this relationship by enabling individuals to interpret medical information accurately, engage effectively with healthcare professionals, and perform self-care activities with confidence. Similarly, prior experience with the healthcare system—such as regular medical follow-up in organ transplant patients—can enhance one's ability to navigate hospital environments and adhere to rehabilitation plans, thereby supporting functional independence. From a clinical nursing perspective, these findings suggest that health literacy and prior medical experience may serve as protective factors in maintaining functional independence. Individuals with greater knowledge of the disease process and acute care responses may navigate hospitalization more effectively. Therefore, nurses should assess patients' baseline knowledge and provide tailored educational interventions, especially for those with limited healthcare experience, to support functional recovery and promote self-care autonomy. In our study, no significant relationship was found between functional independence status and gender, marital status, occupation, cohabitants, smoking, use of immunosuppressive drugs, symptoms at the time of admission or hospitalization, or anxiety ($p > 0.05$). Since the research was conducted with patients whose general condition was sufficiently good to complete the questionnaire, it is thought that their functional independence status may not have been substantially affected.

In addition to its physical effects, COVID-19 has significantly contributed to increased mental health problems in society, particularly among patients (44). Recent systematic reviews and longitudinal cohort studies indicate that anxiety and other psychological symptoms remain highly prevalent among hospitalized COVID-19 patients and those in the post-acute phase. Meta-analytic data show that approximately one-quarter of individuals experience clinically significant anxiety during the recovery period (14), while hospital-based studies report even higher rates (13). Furthermore, long-term follow-up findings demonstrate that psychiatric and cognitive symptoms—including anxiety, depression, and fatigue may worsen or newly emerge up to two to three years after hospitalization (15). These data reinforce the importance of incorporating validated anxiety screening tools, such as the BAI, alongside functional measures in the comprehensive care of COVID-19 survivors. According to the literature, it has been reported that the most common mental health problem in individuals treated with a diagnosis of COVID-19 is anxiety, ranging from 6.5% to 63% (45,46). In a study examining mental health problems in individuals hospitalized because of COVID-19, 34.7% of patients experienced anxiety. Additionally, it was emphasized that there was a relationship between the development of anxiety and advanced age, the severity of the disease, low education level, presence of another family member diagnosed with the disease, female gender, and lack of social support (18). Nie et al. (47) reported that nearly half of the participants (38%) experienced anxiety, and older individuals who were female, had a high level of education, had a family history of COVID-19, or had a family member who had died due to COVID-19 had a higher level of anxiety. In a study conducted with patients recovering from COVID-19 treatment, it was reported that participants who were female, had advanced age, and were university graduates had higher anxiety levels (48). In a systematic review, it was stated that female gender, younger age (≤40 years), presence of chronic/psychiatric diseases, unemployment, being a student, and exposure to more information about COVID-19 in social media/news increased anxiety (49). Bocek and colleagues also stated that age and gender are important factors affecting anxiety levels (50). The high level of anxiety in women has been attributed to greater sensitivity to stressors or to a higher rate of reporting psychological symptoms (46). In line with these findings, our study found that 82% of participants had high levels of anxiety. Women, secondary school graduates, housewives, and unemployed individuals exhibited significantly higher anxiety scores. These findings emphasize the need for gender-sensitive and psychosocially- informed care models. Nurses should proactively identify patients at higher risk of anxiety and provide counseling, emotional support, and access to mental health services tailored to gender- and social-role vulnerabilities.

In our study, 46% of participants experienced dysfunctional anxiety associated with COVID-19. COVID-19-related dysfunctional anxiety levels were higher among participants with secondary school

or university education than among those with primary school education. This finding can be explained by patients with higher educational levels having greater access to information, which increases their awareness of potential complications of their condition and may, in turn, increase their anxiety levels. Participants living with four or more cohabitants had higher COVID-19-related dysfunctional anxiety levels than those living with two or fewer individuals. This finding suggests that higher household density may heighten anxiety due to increased perceived infection risk, increased caregiving burden, and increased fear of transmitting the virus to family members. Recent evidence supports this interpretation, indicating that confinement and the sudden disruption of intergenerational support systems intensified stress and emotional distress among families, especially when household responsibilities were unequally distributed (51,52). Studies conducted in Israel and Italy have likewise shown that families with more members in close quarters experienced greater strain on coping resources and higher anxiety levels, as maintaining caregiving, remote work, and emotional regulation simultaneously proved challenging (53,54). From a nursing perspective, these findings underscore the importance of assessing household structure and caregiving roles when planning psychosocial interventions. Nurses should identify patients and caregivers living in crowded or multigenerational households and provide them with tailored stress-management strategies, family-centered counseling, and social support linkages to mitigate the psychological burden of caregiving in constrained living conditions. Consistent with this interpretation, previous studies have shown that separation from family and friends, reduced caregiving support, and worries about relatives significantly increase anxiety and emotional exhaustion during health crises (55,56).

In the literature, it has been reported that physical symptoms (fever, cough, dyspnea, gastrointestinal symptoms, etc.) due to COVID-19 increase individuals' anxiety levels (28,57). In our study, participants who had nausea/vomiting at hospital admission and those who had cough during hospitalization had significantly higher anxiety levels. These results highlight the need for integrated somatic and psychological care. Nurses should recognize that certain physical symptoms may serve as anxiety triggers and adopt holistic nursing approaches that simultaneously target symptom relief and emotional regulation. Additionally, participants who were afraid that they would not recover or who had dyspnea had higher anxiety levels. The level of COVID-19-related dysfunctional anxiety was high among participants who feared they would not recover, but low among those who feared hospitalization. The high level of anxiety among individuals who fear they may not recover may be due to excessive information in the press and social media about the disease or to fear of death. This underscores the need for clear, empathetic, and evidence-based communication from nurses. Addressing patients' fears about prognosis and survival through therapeutic dialogue may significantly alleviate dysfunctional anxiety.

Study Limitations

This study has some limitations. Conducting the study at a single centre limits the generalisability of the results. The data were collected through self-reporting, which may have introduced social desirability bias. Moreover, because data were collected online and patients with poor general condition were excluded, only clinically stable inpatients able to complete the questionnaire independently were included. As a result, the sample likely represents a healthier, functionally less impaired subset of the inpatient population and may therefore underestimate the true levels of functional dependence and anxiety among more severely affected COVID-19 patients. Additionally, the duration of hospitalization was not collected as part of the demographic data. Because the study focused on functional independence and anxiety rather than hospital-stay characteristics, it was not possible to explore associations between length of hospitalization, functional outcomes, and anxiety. These factors may have influenced the representativeness and generalizability of the findings. Future studies should consider hybrid or in-person data collection methods and include patients with varying disease severity and functional dependence to better reflect the broader clinical population.

CONCLUSION

This study demonstrated that hospitalized patients with COVID-19 commonly experienced high levels of anxiety and mild functional dependence, with nearly half showing dysfunctional anxiety specifically related to COVID-19. Among the symptoms examined, nausea/vomiting and coughing were significantly associated with increased anxiety levels. These findings emphasize the necessity of incorporating routine anxiety screening and functional independence assessments into the standard nursing care of hospitalized patients. Individualized and holistic nursing interventions are essential not only to manage physical symptoms but also to reduce psychological distress and to promote recovery. Furthermore, the results highlight the essential role of nursing in addressing the dual burden of physical and emotional symptoms during infectious disease outbreaks. Special attention should be paid to at-risk populations—such as women, unemployed individuals, and those with lower educational levels—through targeted psychosocial support and education. Future research should aim to include patients with varying levels of disease severity, functional capacity, and sociodemographic backgrounds and investigate the long-term effects of COVID-19 on mental health and daily functioning. In light of ongoing viral mutations and the evolving symptomatology of COVID-19, nursing strategies must remain flexible, evidence-based, and tailored to the complex needs of patients.

Ethics

Ethics Committee Approval: Written approval for the study was obtained from the Clinical Research Ethics Committee of Akdeniz University Faculty of Medicine (decision number: KAEK- 231, date. 28.04.2021) and from the Antalya Provincial Health Directorate (date: 28.06.2021). Permission from the authors who developed the scales used in the study was obtained by e-mail.

Informed Consent: Informed consent forms prepared following the Declaration of Helsinki were obtained online from the patients who agreed to participate in the study.

Footnotes

Authorship Contributions

Concept: A.A.Ç., S.A., H.B., Design: A.A.Ç., S.A., H.B., D.İ., Data Collection or Processing: A.A.Ç., S.A., F.G., Analysis or Interpretation:

A.A.Ç., S.A., H.B., D.İ., Literature Search: A.A.Ç., S.A., H.B., D.İ., Writing: A.A.Ç., S.A., H.B., D.İ.

Conflict of Interest: No conflict of interest was declared by the authors.

Financial Disclosure: The authors declared that this study received no financial support.

REFERENCES

1. Erdoğdu Y, Koçoğlu F, Sevim C. An investigation of the psychosocial and demographic determinants of anxiety and hopelessness during COVID-19 pandemic. J Clin Psy. 2020; 23: 24-37.
2. Argüder E, Kılıç H, Civak M, Kacar D, Kaya G, Yılmaz A, et al. Anxiety and depression levels in hospitalized patients due to COVID-19 infection. Ankara Med J. 2020; 4: 971-81.
3. World Health Organization. Coronavirus (COVID-19) Dashboard. Available from: https://covid19.who.int.
4. Bostan S, Erdem R, Öztürk YE, Kılıç T, Yılmaz A. The effect of COVID-19 pandemic on the Turkish society. Electron J Gen Med. 2020; 17: 1-6.
5. Çelebi C. Nursing care in patients with COVID-19. Medical Journal of Aegean Clinics. 2020; 58: 35-40.
6. Iwashyna TJ, Ely EW, Smith DM, Langa KM. Long-term cognitive impairment and functional disability among survivors of severe sepsis. JAMA. 2010; 304: 1787-94.
7. Pizarro-Pennarolli C, Sánchez-Rojas C, Torres-Castro R, Vera-Uribe R, Sanchez-Ramirez DC, Vasconcello-Castillo L, et al. Assessment of activities of daily living in patients post COVID-19: a systematic review. PeerJ. 2021; 9: e11026.
8. Marques A. Functional status in the COVID-19 era: ALERT, ALERT, ALERT! Pulmonology. 2021; 27: 481-3.
9. Parkinson D. Investigating the increase in domestic violence post disaster: an Australian case study. J Interpers Violence. 2019; 34: 2333-62.
10. Hao Y, Zhang L, Zhang F. Association between Barthel's Index change and all-cause mortality among COVID-19 pneumonia patients aged over 80 years old: a retrospective cohort study. Clin Interv Aging. 2024; 19: 1351-9.
11. Notarstefano C, Bertolucci F, Miccoli M, Posteraro F. Recovery of activities of daily living in COVID-19 patients requiring intensive care unit or medical care unit: an observational study on the role of rehabilitation in the subacute phase. Front Rehabil Sci. 2023; 4: 1256999.
12. Tay SS, Visperas CA, Zaw EM, Tan MMJ, Samsudin F, Koh XH. Functional outcomes of COVID-19 patients who underwent acute inpatient rehabilitation and the exploration of the benefits of adjunct robotic therapy and the effects of frailty. Proc Singapore Healthc. 2023; 32: 20101058221150078.
13. Tan HJ, Shahren AAH, Khoo CS, Ng CF, Zaidi WAW, Kori N, et al. Anxiety among hospitalized COVID-19 patients: a case-control study from a tertiary teaching hospital in Malaysia. Front Psychiatry. 2023; 14: 1148019.
14. Seighali N, Abdollahi A, Shafiee A, Amini MJ, Teymouri Athar MM, Safari O, et al. The global prevalence of depression, anxiety, and sleep disorder among patients coping with post COVID-19 syndrome (long COVID): a systematic review and meta-analysis. BMC Psychiatry. 2024; 24: 105.
15. Taquet M, Vannorsdall TD. Cognitive and psychiatric symptom trajectories 2-3 years after hospital admission for COVID-19. Lancet Psychiatry. 2024; 11: 523-34.
16. Chung CCY, Wong WHS, Fung JLF, Hong Kong RD, Chung BHY. Impact of COVID-19 pandemic on patients with rare disease in Hong Kong. Eur J Med Genet. 2020; 63: 104062.
17. Wang C, Horby PW, Hayden FG, Gao GF. A novel coronavirus outbreak of global health concern. Lancet. 2020; 395: 470-3.
18. Kong X, Zheng K, Tang M, Kong F, Zhou J, Diao L. Prevalence and factors associated with depression and anxiety of hospitalized patients with COVID-19. MedRxiv. 2020; 1-12.
19. Kaçmaz AB, Soysal P, Tan SG, Durdu B, Akkoyunlu Y, Ogün H, et al. The effects of polypharmacy, nutritional, functional status on the progression of COVID-19 in older adults. Infect Dis Clin Microbiol. 2021; 3: 70-7.
20. Shah S, Vanclay F, Cooper B. Improving the sensitivity of the Barthel Index for stroke rehabilitation. J Clin Epidemiol. 1989; 42: 703-9.
21. Yavuzer G, Süldür N, Küçükdeveci A, Elhan A. The role of functional independence measure and Modified Barthel Index in the assessment of neurorehabilitation patients in Turkey. Journal of Rheumatology Medical Rehabilitation. 2000; 11: 26-31.
22. Küçükdeveci AA, Yavuzer G, Tennant A, Süldür N, Sonel B, Arasil T. Adaptation of the Modified Barthel Index for use in physical medicine and rehabilitation in Turkey. Scand J Rehabil Med. 2000; 32: 87-92.
23. Beck AT, Epstein N, Brown G, Steer RA. An inventory for measuring clinical anxiety: psychometric properties. J Consult Clin Psychol. 1988; 56: 893-7.
24. Ulusoy M, Sahin NH, Erkmen H. Turkish version of the Beck Anxiety Inventory: psychometric properties. J Cogn Psychother. 1998; 12: 163-72.
25. Lee SA. Coronavirus Anxiety Scale: a brief mental health screener for COVID-19 related anxiety. Death Stud. 2020; 44: 393-401.
26. Biçer İ, Çakmak C, Demir H, Kurt ME. Coronavirus Anxiety Scale Short Form: Turkish validity and reliability study. Anatol Clin. 2020; 25: 216-25.
27. Adhikari SP, Meng S, Wu YJ, Mao YP, Ye RX, Wang QZ, et al. Epidemiology, causes, clinical manifestation and diagnosis, prevention and control of coronavirus disease (COVID-19) during the early outbreak period: a scoping review. Infect Dis Poverty. 2020; 9: 29.
28. Wang C, Pan R, Wan X, Tan Y, Xu L, Ho CS, et al. Immediate psychological responses and associated factors during the initial stage of the 2019 coronavirus disease (COVID-19) epidemic among the general population in China. Int J Environ Res Public Health. 2020; 17: 1729.
29. Trevissón-Redondo B, López-López D, Pérez-Boal E, Marqués-Sánchez P, Liébana-Presa C, Navarro-Flores E, et al. Use of the Barthel Index to assess activities of daily living before and after SARS-COVID 19 infection of institutionalized nursing home patients. Int J Environ Res Public Health. 2021; 18: 7258.
30. Akova I, Kuzu F, Kilic E. Symptom changes in COVID-19 patients in the disease process and differences in symptoms according to some demographic and clinical characteristics. Journal of Health Sciences Institute. 2021; 7: 39-45.
31. Koç Z, Akın S. The most common persistent symptoms in patients with COVID-19 who were evaluated in the Internal Medicine polyclinic. Eur Res J. 2023; 9: 97-107.
32. Kesikburun B, Ata AM, Borman P, Ozdemir EE, Becenen E, Metin N, et al. The effect of comprehensive rehabilitation on post-COVID-19 syndrome. Egypt Rheumatol Rehabil. 2023; 50: 60.
33. Belli S, Balbi B, Prince I, Cattaneo D, Masocco F, Zaccaria S, et al. Low physical functioning and impaired performance of activities of daily life in COVID-19 patients who survived hospitalisation. Eur Respir J. 2020; 56: 2002096.
34. Paneroni M, Simonelli C, Saleri M, Bertacchini L, Venturelli M, Troosters T, et al. Muscle strength and physical performance in

patients without previous disabilities recovering from COVID-19 pneumonia. Am J Phys Med Rehabil. 2021; 100: 105-9.

35. Simonelli C, Paneroni M, Vitacca M, Ambrosino N. Measures of physical performance in COVID-19 patients: a mapping review. Pulmonology. 2021; 27: 518-28.
36. Triantafyllaki P, Marios C, Kapadohos T, Toulia G, Pavlatou N, Liveri A, et al. Assessment of the functional recovery and stress in ICU survivor patients with acute respiratory distress syndrome due to COVID-19. Int J Caring Sci. 2024; 17: 677-84.
37. Taboada M, Carinena A, Moreno E, Rodriguez N, Dominguez MJ, Casal A, et al. Post-COVID-19 functional status six-months after hospitalization. J Infect. 2021; 82: e31-e33.
38. Heras E, Garibaldi P, Boix M, Valero O, Castillo J, Curbelo Y, et al. COVID-19 mortality risk factors in older people in a long-term care center. Eur Geriatr Med. 2021; 12: 601-7.
39. Frontera JA, Sabadia S, Yang D, de Havenon A, Yaghi S, Lewis A, et al. Life stressors significantly impact long-term outcomes and post-acute symptoms 12-months after COVID-19 hospitalization. J Neurol Sci. 2022; 443: 120487.
40. Elmer N, Reißhauer A, Brehm K, Drebinger D, Schaller SJ, Schwedtke C, et al. Functional outcome after interdisciplinary, acute rehabilitation in COVID-19 patients: a retrospective study. Eur Arch Psychiatry Clin Neurosci. 2024; 274: 1993-2001.
41. Bayat M, Raeissadat SA, Lashgari S, Bolandnazar NS, Taheri SN, Soleimani M. Post-COVID-19 functional limitations in hospitalized patients and associated risk factors: a 3-month follow-up study. Physiother Res Int. 2022; 27: e1965.
42. De Oliveira Silva AS, da Silveira Moreira R, Pereira AM, De Lima Silva V. Association between functionality and knowledge, attitudes, and practices of COVID-19 prevention in the older people. Rev Bras Geriatr Gerontol. 2023; 26: e230063.
43. Dirik Kınıcı E, Paslı Gürdoğan E, Aksoy Kahraman B. The relationship between the levels of health literacy and knowledge of about COVID-19 of individuals with chronic diseases. J Acad Res Nurs. 2025; 11: 33-40.
44. Largani MH, Gorgani F, Abbaszadeh M, Arbabi M, Reyhan SK, Allameh SF, et al. Depression, anxiety, perceived stress and family support in COVID-19 patients. Iran J Psychiatry. 2022; 17: 257-64.
45. Arab-Zozani M, Hashemi F, Safari H, Yousefi M, Ameri H. Health-related quality of life and its associated factors in COVID-19 patients. Osong Public Health Res Perspect. 2020; 11: 296-302.
46. Shanbehzadeh S, Tavahomi M, Zanjari N, Ebrahimi-Takamjani I, Amiri-Arimi S. Physical and mental health complications post-COVID-19: scoping review. J Psychosom Res. 2021; 147: 110525.
47. Nie XD, Wang Q, Wang MN, Zhao S, Liu L, Zhu YL, et al. Anxiety and depression and its correlates in patients with coronavirus disease 2019 in Wuhan. J Psychiatry Clin Pract. 2021; 25: 109-14.
48. Yılbaş B. Psychiatric evaluation of individuals treated with the diagnosis of COVID-19 following recovery period. Clin Psychiatry. 2021; 24: 239-45.
49. Xiong J, Lipsitz O, Nasri F, Lui LMW, Gill H, Phan L, et al. Impact of COVID-19 pandemic on mental health in the general population: a systematic review. J Affect Disord. 2020; 277: 55-64.
50. Bocek J, Koncelikova DK, Vanek J, Latalova K, Genzor S, Mizera J. Anxiety in patients with post-COVID syndrome: associated factors. Psychol Res Behav Manag. 2024; 17: 3255-65.
51. Rico-Blázquez M, Sánchez-Ruano R, Oter-Quintana C, Polentinos-Castro E, Martín-García Á, Otones-Reyes P, et al. Family caregivers' experiences during the COVID-19 pandemic: qualitative study. Healthcare. 2024; 12: 970.
52. Zartler U, Suwada K, Kreyenfeld M. Family lives during the COVID-19 pandemic in European societies: introduction to the special issue. J Fam Res. 2022; 34: 1-15.
53. Fogel Y, Sela Y, Hen-Herbst L. Coping strategies of families and their relationships with family quality of life during COVID-19 pandemic. PLoS One. 2022; 17: e0273721.
54. Zeduri M, Vigezzi GP, Carioli G, Lugo A, Stival C, Amerio A, et al. COVID-19 lockdown impact on familial relationships and mental health in a large representative sample of Italian adults. Soc Psychiatry Psychiatr Epidemiol. 2022; 58: 1-11.
55. Carvalho PMM, Moreira MM, de Oliveira MNA, Landim JMM, Neto MLR. The psychiatric impact of the novel coronavirus outbreak. Psychiatry Res. 2020; 286: 112902.
56. Zhou X, Snoswell CL, Harding LE, Bambling M, Edirippulige S, Bai X, et al. The role of telehealth in reducing the mental health burden from COVID-19. Telemed J E Health. 2020; 26: 377-9.
57. Júnior FJS, de-Carvalho Neto AE, Freitas FRN, Alves AS, Pontes CEB, Barros ILCB, et al. Anxiety and dyspnea in patients infected with the new coronavirus. Revista Neurocienc. 2022; 30: 1-18.

Gazi Med J 2026;37(3):341-349

DOI: http://dx.doi.org/10.12996/gmj.2026.4507

Gender-Stratified Hematological Predictors of Pulmonary Involvement in COVID-19: A Retrospective CT-Correlated Analysis

COVID-19'da Pulmoner Tutulumun Cinsiyete Göre Hematolojik Öngörücüleri: BT-Korelasyonlu Retrospektif Bir Analiz

Tuğçe Yenigün Altaş[1], Cenk Aypak[1,2]

[1]Clinic of Family Medicine, University of Health Sciences Türkiye, Dışkapı Yıldırım Beyazıt Training and Research Hospital, Ankara, Türkiye
[2]Clinic of Family Medicine, University of Health Sciences Türkiye, Ankara Etlik City Hospital, Ankara, Türkiye

Objective: This study investigated the association between hematological parameters and thoracic computed tomography (CT) findings in coronavirus disease-2019 (COVID-19) patients with a focus on gender-specific platelet dynamics.

Methods: Four hundred thirty-seven patients who underwent both reverse transcriptase polymerase chain reaction and thoracic CT scans were analyzed retrospectively. Hemogram data, inflammatory markers, and CT findings were compared by sex.

Results: CT positivity was significantly associated with elevated neutrophil/lymphocyte ratio, C-reactive protein, D-dimer, and neutrophil counts, and with reduced lymphocyte, monocyte (MONO), eosinophil, and basophil (BASO) counts ($p < 0.01$). Mean platelet volume (MPV) showed a significant correlation with CT findings only in female patients ($p = 0.024$). Monocytopenia emerged as a strong predictor of CT positivity, explaining 9.4% of the variance in females and 17.6% in males.

CONCLUSION: These findings underscore the need for gender-specific approaches to COVID-19 triage and suggest that MPV and MONO counts may serve as cost-effective, readily accessible biomarkers of pulmonary involvement when imaging is unavailable.

Keywords: COVID-19, platelet, mean platelet volume, platelet activation, gender analysis, thorax CT, hematological markers.

Amaç: Bu çalışmada, koronavirüs hastalığı-2019 (COVID-19) tanılı hastalarda hematolojik parametreler ile toraks bilgisayarlı tomografi (BT) bulguları arasındaki ilişki, cinsiyete özgü trombosit dinamikleri odağında araştırılmıştır.

Yöntemler: Hem revers transkriptaz polimeraz zincir reaksiyonu hem de toraks BT incelemesi yapılan 437 hasta retrospektif olarak değerlendirilmiştir. Hemogram verileri, enflamatuvar belirteçler ve BT bulguları cinsiyete göre karşılaştırılmıştır.

Bulgular: BT pozitifliği; yüksek nötrofil/lenfosit oranı, C-reaktif protein, D-dimer ve nötrofil sayısı ile anlamlı şekilde ilişkili bulunmuş; düşük lenfosit, monosit (MONO), eozinofil ve bazofil sayıları ile ilişkilendirilmiştir ($p < 0,01$). Ortalama trombosit hacmi (MPV), BT bulguları ile yalnızca kadın hastalarda anlamlı korelasyon göstermiştir ($p = 0,024$). Monositopeni, BT pozitifliğinin güçlü bir öngörücüsü olarak ortaya çıkmış; kadınlarda varyansın %9,4'ünü, erkeklerde ise %17,6'sını açıklamıştır.

Sonuç: Bu bulgular, COVID-19 triyajında cinsiyete özgü yaklaşımların gerekliliğini ortaya koymakta ve görüntüleme imkânı bulunmadığında MPV ile MONO sayımlarının pulmoner tutulumun maliyet etkin ve kolay erişilebilir biyobelirteçleri olarak kullanılabileceğini düşündürmektedir.

Anahtar Sözcükler: COVID-19, trombosit, ortalama trombosit hacmi, trombosit aktivasyonu, cinsiyet analizi, toraks BT, hematolojik belirteçler

Cite this article as: Yenigün Altaş T, Aypak C. Gender-stratified hematological predictors of pulmonary involvement in COVID-19: a retrospective CT-correlated analysis. Gazi Med J. 2026;37(3):341-349

Address for Correspondence/Yazışma Adresi: Tuğçe Yenigün Altaş, Clinic of Family Medicine, University of Health Sciences Türkiye, Dışkapı Yıldırım Beyazıt Training and Research Hospital, Ankara, Türkiye
E-mail / E-posta: tugceyenigunaltas@gmail.com
ORCID ID: orcid.org/0009-0001-2489-8068

Received/Geliş Tarihi: 27.07.2025
Accepted/Kabul Tarihi: 05.06.2026
Publication Date/Yayınlanma Tarihi: 10.07.2026

INTRODUCTION

Coronavirus Disease 2019 (COVID-19), caused by the severe acute respiratory syndrome coronavirus 2 (SARS-CoV-2) virus, was initially found in Wuhan, China, in December 2019 and quickly spread worldwide (1). The World Health Organization declared COVID-19 a global public health danger on January 30, 2020 and gave pandemic status on March 11, 2020 putting enormous strain on healthcare systems around the world. This global health crisis has demonstrated the critical need for timely and precise diagnostic tools.

COVID-19, caused by the SARS-CoV-2 virus, exhibits a wide clinical spectrum, ranging from asymptomatic infection to critical lung infection. Lung involvement is the primary factor determining the prognostic course of COVID-19 and affecting mortality rates. Therefore, early recognition and management of respiratory complications has become a primary goal in the clinical approach (2-4).

Reverse transcriptase polymerase chain reaction (RT-PCR) examination of nasopharyngeal samples, which is regarded as the reference method in COVID-19 diagnosis, has become the standard practice in the field of molecular diagnosis. However, the RT-PCR approach has some drawbacks in clinical practice (5). According to published research, the RT-PCR test has lower sensitivity than thoracic computed tomography (CT) imaging. In patient groups with negative PCR findings, the discovery of COVID-19-specific pathological alterations on radiological imaging modalities emphasizes the importance of multi-parameter evaluation in the diagnostic approach. As a result, a multidisciplinary approach to COVID-19 diagnosis is advocated, with clinical symptoms, laboratory testing, and imaging modalities all being assessed simultaneously (6-8).

During the global health crisis, when maximum efficiency is required with limited resources, the demand for promptly accessible, cost-effective, and minimally invasive biomarkers for illness detection and prognosis has skyrocketed (9). In this critical moment, when health-care systems' capacities are stretched thin, developing diagnostic and monitoring methods based on cost-benefit analysis has become a strategic priority. Among the laboratory abnormalities observed in COVID-19 infection, decreases in lymphocyte (LYM) count, increases in acute phase reactant C-reactive protein (CRP) values, increases in iron storage protein ferritin concentrations, elevations in coagulation marker D-dimer levels, and increases in cellular damage marker lactate dehydrogenase activity are frequently reported (10).

In recent years, the importance of hematological parameters in the diagnosis and prognostic evaluation of COVID-19 has received increasing attention. The systemic inflammatory response induced by SARS-CoV-2 is reflected in characteristic hematological changes. In the meta-analysis by Henry et al. (4), leukocytosis, neutrophilia, lymphopenia, thrombocytopenia and high neutrophil/lymphocyte ratio (NLR) values were shown to be associated with poor prognosis in COVID-19 patients. Yang et al. (5) reported that NLR is an independent predictive factor in predicting COVID-19 severity, and its diagnostic value is as high as the area under the curve (AUC) of 0.841.

Mean platelet volume (MPV), a measure of platelet activation and reactivity, has been linked to increased inflammatory and prothrombotic states, such as those observed in COVID-19. Platelets in COVID-19 individuals are not only numerically but functionally changed, with hyperreactivity and procoagulant characteristics (11). High MPV levels have been linked to illness severity, intensive care unit admission, and mortality, according to research. However, there is limited information on the relationship between MPV and radiological abnormalities, particularly thoracic CT, which provides direct proof of pulmonary pathology (12).

Furthermore, the COVID-19 pandemic has highlighted gender-based immunological and hematological disparities. Sex hormones, notably estrogen and progesterone, alter coagulation pathways and platelet function, which may result in distinct biomarker patterns between males and females. Despite this, few studies have explored the gender-specific diagnostic or prognostic usefulness of platelet indices in COVID-19.

Previous research has primarily focused on general hematological markers or their correlation with disease severity scores (13-15). However, comprehensive studies evaluating the association between specific hemogram parameters—such as MPV, NLR, and monocyte (MONO) count—and thoracic CT findings, stratified by gender, remain scarce.

In this study, we aimed to investigate the relationship between hematological parameters and thoracic CT findings in COVID-19 patients, with a focus on platelet activation markers and gender-specific differences. We hypothesized that MPV, NLR, and MONO levels could serve as potential biomarkers for predicting pulmonary involvement, and that their diagnostic value may differ between male and female patients. Our findings may contribute to a more individualized and cost-effective diagnostic approach, especially in healthcare settings with limited access to advanced imaging.

MATERIALS AND METHODS

Study Design and Population

This retrospective, single-center study was conducted between October and December 2020 after obtaining ethical approval from the University of Health Sciences Türkiye, Dışkapı Yıldırım Beyazıt Training and Research Hospital Ethics Committee (approval number: 104-14, dated: 08.02.2021). The inclusion criteria were: age ≥18 years, simultaneous availability of thoracic CT and hemogram results, and either RT-PCR positivity or thoracic CT findings consistent with COVID-19. After excluding 31 patients because of extreme values that distorted the normal distribution, 437 patients were included in the final analysis.

Data Collection

Demographic information, RT-PCR results, and laboratory parameters—including complete blood count [white blood cells (WBC), neutrophils (NEU), LYM, MONO, eosinophils (EOS), BASO, MPV, and NLR]—were retrieved from electronic hospital records. Inflammatory and coagulation markers, such as CRP, procalcitonin, and D-dimer, were also recorded.

Thoracic CT scans were evaluated by two experienced radiologists who were blinded to the patients' laboratory and clinical data. CT findings were categorized as COVID-19 positive (CT+) or negative (CT–) based on standardized diagnostic criteria. CT positivity was defined by the presence of radiological features typical of COVID-19

pneumonia, such as bilateral ground-glass opacities, crazy paving patterns, and peripheral consolidations, in line with COVID-19 Reporting and Data System scores of ≥4. Reference ranges for all laboratory parameters were defined according to institutional standards.

Statistical Analysis

All statistical analyses were performed using SPSS version 23.0 (IBM Corp., Armonk, NY, USA). The normality of data distribution was assessed using the Kolmogorov–Smirnov test. Skewness and kurtosis coefficients were also examined to confirm the normality of the variables, allowing the use of parametric tests.

Descriptive statistics were presented as means ± standard deviation for continuous variables and as frequencies and percentages for categorical variables. Categorical variables were compared using the chi-square test, while continuous variables were compared using the independent-samples t-test and one-way analysis of variance, as appropriate. Point-biserial correlation analysis was conducted to assess the relationship between continuous hematological parameters and CT positivity (a dichotomous variable). Since the point-biserial correlation is mathematically equivalent to the Pearson product-moment correlation when one variable is dichotomous, it was computed using the Pearson correlation procedure in SPSS, yielding the same r coefficient. The coefficient of determination (r^2) was used to quantify the proportion of variance in CT positivity explained by each hematological parameter. Sex-stratified analyses were performed to explore potential sex-specific patterns. Receiver operating characteristic (ROC) curve analysis was performed to evaluate the diagnostic performance of hematological parameters in predicting CT positivity. The AUC with 95% confidence intervals was calculated for each parameter. Optimal cut-off values were determined using the Youden index. Sensitivity and specificity were calculated for the selected thresholds. To assess potential gender-related differences, ROC analyses were conducted separately for males and females. Parameters of clinical relevance and those identified in preliminary analyses were included in the ROC analysis. The discriminatory power of each parameter was interpreted according to AUC values (0.5–0.6: poor, 0.6–0.7: fair, 0.7–0.8: acceptable, >0.8: excellent). A p-value <0.05 was considered statistically significant.

RESULTS

Patient Characteristics

A total of 437 COVID-19 patients were included in the study (Table 1). Approximately half of the patients (49.9%) were female and the mean age was 55.19 years. The majority of patients (64.1%) were aged 65 years or younger. The RT-PCR test was positive in 79.4% of patients, and thorax CT was positive in 71.6%. In the PCR-CT group distribution, the largest group was PCR (+)/CT (+) (51%), followed by PCR (+)/CT (-) (28.4%) and PCR (-)/CT (+) (20.6%).

Comparison of Hematological Parameters Between CT-Positive and CT-Negative Patients

Significant differences in hematological parameters were observed between patients with CT findings consistent with COVID-19 (CT-positive) and those without (CT-negative), as presented in Table 2. Inflammatory markers, including NEU count, NLR, CRP, and D-dimer levels, were significantly elevated in the CT-positive group (all $p < 0.05$). Conversely, immune cell-related parameters—LYM, MONO, EOS, and BASO counts—were significantly lower in CT-positive than in CT-negative patients *(all* $p < 0.001$). MPV values did not differ significantly between the two groups *(*$p > 0.05$).

Gender-Specific Analyses

Significant differences were observed in the stratified analysis according to sex (Table 3). In female patients, significant increases were detected in CT positivity and in WBC, NEU, MPV, NLR, CRP, and D-dimer values. In particular, MPV values showed a significant correlation with CT positivity only in females. In male patients, CT positivity, NLR, and CRP values increased significantly, whereas LYM, MONO, EOS, and BASO values decreased significantly. No significant relationship was detected between MPV and CT positivity in males. MPV values showed a significant correlation with CT positivity in females but not in males ($p = 0.726$).

Gender-Stratified Predictive Parameters

In the gender-stratified point-biserial correlation analysis, the parameters most strongly associated with CT positivity differed by sex, as reflected by their r^2 values (Table 4). Among female patients, MONO count explained 9.4% of the variance in CT positivity ($r^2 = 0.094$), BASO levels explained 7.0% ($r^2 = 0.070$), and NEU count explained 5.5% ($r^2 = 0.055$). Among male patients, MONO count demonstrated the highest explanatory value at 17.6% ($r^2 = 0.176$), followed by LYM count at 14.4% ($r^2 = 0.144$). These findings support the existence of gender-specific differences in the immune response to COVID-19. Monocytopenia showed the strongest association with CT positivity in both sexes, but its explanatory value was

Table 1. Patient characteristics.

Variable	n (%)
Gender	
Female	218 (49.9)
Male	219 (50.1)
Age groups	
≤65 years	280 (64.1)
>65 years	157 (35.9)
RT-PCR result	
Positive	347 (79.4)
Negative	90 (20.6)
Chest CT result	
Positive	313 (71.6)
Negative	124 (28.4)
PCR-CT group distribution	
PCR(+)/CT(+)	223 (51.0)
PCR(+)/CT(-)	124 (28.4)
PCR(-)/CT(+)	90 (20.6)
Total	437 (100.0)

RT-PCR: Reverse transcriptase polymerase chain reaction, CT: Computed tomography, PCR: Polymerase chain reaction.

Table 2. Comparison of hematological parameters according to CT results.

Parameter	CT-positive (n = 313)	CT-negative (n = 124)	p-value
WBC (×10³/µL)	6.35 ± 2.52	6.12 ± 2.12	0.363
RBC (×10⁶/µL)	4.86 ± 0.58	4.91 ± 0.60	0.430
HGB (g/dL)	13.68 ± 1.72	14.01 ± 1.77	0.074
HCT (%)	41.64 ± 4.73	42.26 ± 4.67	0.221
MCV (fL)	85.76 ± 5.70	86.28 ± 4.59	0.367
RDW (%)	13.59 ± 1.46	13.48 ± 1.15	0.454
PLT (×10³/µL)	224.36 ± 90.00	223.85 ± 57.51	0.953
MPV (fL)	10.40 ± 0.89	10.22 ± 0.91	0.063
PCT (%)	0.28 ± 0.95	0.22 ± 0.05	0.486
PDW (%)	12.03 ± 2.07	11.74 ± 1.98	0.181
NEU (×10³/µL)	4.52 ± 2.38	3.69 ± 1.79	0.001*
LYM (×10³/µL)	1.31 ± 0.57	1.68 ± 0.84	0.001*
MONO (×10³/µL)	0.46 ± 0.20	0.65 ± 0.25	0.001*
EOS (×10³/µL)	0.03 ± 0.06	0.06 ± 0.08	0.001*
BASO (×10³/µL)	0.01 ± 0.01	0.02 ± 0.02	0.001*
NLR	4.21 ± 3.12	2.81 ± 2.31	0.001*
Procalcitonin (ng/mL)	-0.93 ± 0.43	-0.91 ± 0.52	0.597
D-dimer (µg/mL)	-0.23 ± 0.35	-0.32 ± 0.38	0.016*
CRP (mg/L)	1.61 ± 0.46	1.32 ± 0.59	0.001*

*p < 0.05, BASO: Basophil count, CRP: C-reactive protein, CT: Computed tomography, EOS: Eosinophil count, HCT: Hematocrit, HGB: Hemoglobin, LYM: Lymphocyte count, MCV: Mean corpuscular volume, MONO: Monocyte count, MPV: Mean platelet volume, NEU: Neutrophil count, NLR: Neutrophil-to-lymphocyte ratio, PCT: Plateletcrit, PDW: Platelet distribution width, PLT: Platelet count, RBC: Red blood cell, RDW: Red cell distribution width, WBC: White blood cell.

approximately twice as high in males as in females. The predictive value of MPV was found to be significant only in females ($r^2 = 0.023$, p = 0.024), while no significant association was observed in males (p = 0.726).

ROC Curve Analysis

ROC curve analysis was performed to evaluate the diagnostic performance of selected hematological parameters for predicting CT positivity in female and male patients separately. The AUC, optimal cut-off values, sensitivity, specificity, and p-values were calculated for each parameter.

Among female patients, CRP demonstrated the highest diagnostic performance (AUC = 0.698, p < 0.001), followed by NLR (AUC = 0.641, p < 0.001) and D-dimer (AUC = 0.624, p = 0.001), indicating fair discriminatory ability. In contrast, WBC (AUC = 0.573, p = 0.070) and PLT (AUC = 0.484, p = 0.699) did not show statistically significant discrimination between CT-positive and CT-negative cases.

Similarly, among male patients, CRP (AUC = 0.654, p < 0.001), NLR (AUC = 0.680, p < 0.001), and D-dimer (AUC = 0.635, p < 0.001) demonstrated statistically significant discriminatory ability. NLR showed the highest AUC in males, suggesting a stronger predictive value for pulmonary involvement than in females. Conversely, WBC (AUC = 0.466, p = 0.435) and PLT (AUC = 0.477, p = 0.596) failed to achieve statistical significance, and therefore exhibited no meaningful discriminatory capacity.

Overall, CRP, NLR, and D-dimer showed significant but moderate diagnostic performance for predicting CT positivity in both sexes, whereas WBC and platelet count were not useful discriminators. These findings indicate that inflammatory biomarkers, particularly CRP and NLR, may provide clinically relevant information regarding pulmonary involvement in COVID-19 patients, while the diagnostic contribution of WBC and PLT appears limited.

Gender-stratified ROC-derived cut-off values, sensitivity, specificity, AUC values, and corresponding p-values are presented in Table 5 and Figure 1.

DISCUSSION

This study comprehensively investigated the relationship between hemogram parameters and thoracic CT findings in COVID-19 patients. Our findings indicate that some parameters obtained from simple blood tests may be clinically valuable biomarkers for predicting the presence and severity of COVID-19 pneumonia. CT-positive cases had significantly higher NLR, CRP, NEU, D-dimer, and MPV values than CT-negative cases; conversely, LYM, MONO, EOS, and BASO levels were lower. The synergistic relationship between these hematological parameters comprehensively reflects the systemic inflammation and immune response pattern of COVID-19.

Table 3. Gender-specific hematological parameters associated with CT positivity.

Parameter	Female, (n = 218)			Male, (n = 219)		
	CT negative (n = 65)	CT positive (n = 153)	p-value	CT negative (n = 59)	CT positive (n = 160)	p-value
WBC (×10³/µL)	5.37 ± 1.31	6.04 ± 2.27	0.028	6.94 ± 2.53	6.65 ± 2.71	0.478
RBC (×10⁶/µL)	4.71 ± 0.49	4.68 ± 0.51	0.686	5.12 ± 0.64	5.02 ± 0.61	0.310
HGB (g/dL)	13.26 ± 1.33	12.99 ± 1.54	0.235	14.84 ± 1.84	14.33 ± 1.63	0.051
HCT (%)	40.39 ± 3.71	40.05 ± 4.42	0.584	44.31 ± 4.78	43.16 ± 4.53	0.104
MCV (fL)	85.84 ± 4.51	85.4 ± 5.95	0.662	86.75 ± 4.66	86.02 ± 5.46	0.361
RDW (%)	13.58 ± 1.19	13.78 ± 1.56	0.343	13.38 ± 1.10	13.41 ± 1.33	0.871
PLT (×103/µL)	233.78 ± 51.08	235.87 ± 90.61	0.862	212.91 ± 62.47	213.35 ± 88.30	0.972
MPV (fL)	10.17 ± 0.97	10.48 ± 0.88	0.024	10.28 ± 0.84	10.33 ± 0.89	0.726
PCT (%)	0.23 ± 0.04	0.24 ± 0.08	0.391	0.21 ± 0.06	0.32 ± 1.32	0.532
PDW (%)	11.62 ± 2.20	12.10 ± 2.09	0.128	11.87 ± 1.72	11.96 ± 2.05	0.761
NEU (×10³/µL)	3.19 ± 1.07	4.14 ± 2.05	0.001	4.24 ± 2.22	4.89 ± 2.61	0.095
LYM (×10³/µL)	1.53 ± 0.66	1.39 ± 0.63	0.156	1.85 ± 0.97	1.23 ± 0.51	0.001
MONO (×10³/µL)	0.57 ± 0.15	0.44 ± 0.18	0.001	0.70 ± 0.31	0.48 ± 0.21	0.001
EOS (×10³/µL)	0.05 ± 0.07	0.03 ± 0.06	0.009	0.07 ± 0.09	0.03 ± 0.06	0.001
BASO (×10³/µL)	0.02 ± 0.01	0.01 ± 0.01	0.001	0.03 ± 0.02	0.01 ± 0.02	0.001
NLR	2.53 ± 1.58	3.64 ± 2.52	0.001	3.13 ± 2.89	4.76 ± 3.53	0.002
Procalcitonin (ng/mL)	0.20 ± 0.18	0.17 ± 0.28	0.537	0.29 ± 0.52	0.22 ± 0.28	0.165
D-dimer (µg/mL)	0.63 ± 0.55	0.88 ± 0.96	0.048	0.89 ± 1.37	0.80 ± 0.89	0.570
CRP (mg/L)	33.41 ± 29.52	51.90 ± 48.39	0.005	42.71 ± 29.00	73.45 ± 59.19	0.001

BASO: Basophil count, CRP: C-reactive protein, CT: Computed tomography, EOS: Eosinophil count, HCT: Hematocrit, HGB: Hemoglobin, LYM: Lymphocyte count, MCV: Mean corpuscular volume, MONO: Monocyte count, MPV: Mean platelet volume, NEU: Neutrophil count, NLR: Neutrophil-to-lymphocyte ratio, PCT: Plateletcrit, PDW: Platelet distribution width, PLT: Platelet count, RBC: Red blood cell, RDW: Red cell distribution width, WBC: White blood cell.

Table 4. Gender-stratified point-biserial correlation coefficients (r, r^2) between hematological parameters and CT positivity.

Parameter	Female			Male		
	r	r^2	p-value	r	r^2	p-value
WBC (×10³/µL)	0.149	0.022	0.028	0.048	0.002	0.478
RBC (×10⁶/µL)	0.028	0.001	0.686	0.069	0.005	0.310
HGB (g/dL)	0.081	0.007	0.235	0.132	0.017	0.051
HCT (%)	0.037	0.001	0.584	0.110	0.012	0.104
MCV (fL)	0.030	0.001	0.662	0.062	0.004	0.361
RDW (%)	0.065	0.004	0.343	0.011	0.001	0.871
PLT (×10³/µL)	0.012	0.001	0.862	0.002	0.001	0.972
MPV (fL)	0.152	0.023	0.024	0.024	0.001	0.726
PCT (%)	0.058	0.003	0.391	0.042	0.002	0.532
PDW (%)	0.103	0.011	0.128	0.021	0.001	0.761
NEU (×10³/µL)	0.234	0.055	0.001	0.113	0.013	0.095
LYM (×10³/µL)	0.097	0.009	0.156	0.380	0.144	0.001
MONO (×10³/µL)	0.307	0.094	0.001	0.419	0.176	0.001
EOS (×10³/µL)	0.176	0.031	0.009	0.232	0.054	0.001
BASO (×10³/µL)	0.264	0.070	0.001	0.253	0.064	0.001
NLR	0.218	0.047	0.001	0.211	0.044	0.002
Procalcitonin (ng/mL)	0.042	0.002	0.537	0.094	0.009	0.165
D-dimer (µg/mL)	0.134	0.018	0.048	0.039	0.001	0.570
CRP (mg/L)	0.191	0.036	0.005	0.251	0.063	0.001

r: Correlation coefficient; r^2: Variance explained (%). BASO: Basophil count, CRP: C-reactive protein, CT: Computed tomography, EOS: Eosinophil count, HCT: Hematocrit, HGB: Hemoglobin, LYM: Lymphocyte count, MCV: Mean corpuscular volume, MONO: Monocyte count, MPV: Mean platelet volume, NEU: Neutrophil count, NLR: Neutrophil-to-lymphocyte ratio, PCT: Plateletcrit, PDW: Platelet distribution width, PLT: Platelet count, RBC: Red blood cell, RDW: Red cell distribution width, WBC: White blood cell.

Table 5. ROC-derived cut-off values and diagnostic performance of hematological parameters stratified by gender.

Gender	Parameter	AUC (95% CI)	p-value	Cut-off	Sensitivity	Specificity
Female	NLR	0.641	<0.001	3.292	0.440	0.797
Female	CRP	0.698	<0.001	28	0.500	0.899
Female	D-dimer	0.624	0.001	0.62	0.512	0.725
Female	WBC	0.573	0.070	6.29	0.422	0.768
Female	PLT	0.484	0.699	287	0.235	0.942
Male	NLR	0.680	<0.001	2.587	0.727	0.656
Male	CRP	0.654	<0.001	55	0.442	0.902
Male	D-dimer	0.635	<0.001	0.50	0.535	0.738
Male	WBC	0.466	0.435	3.66	0.965	0.082
Male	PLT	0.477	0.596	330	0.110	0.951

AUC: Area under the curve, CI: Confidence interval, CRP: C-reactive protein, NLR: Neutrophil-to-lymphocyte ratio, PLT: Platelet count, ROC: Receiver operating characteristic, WBC: White blood cell.

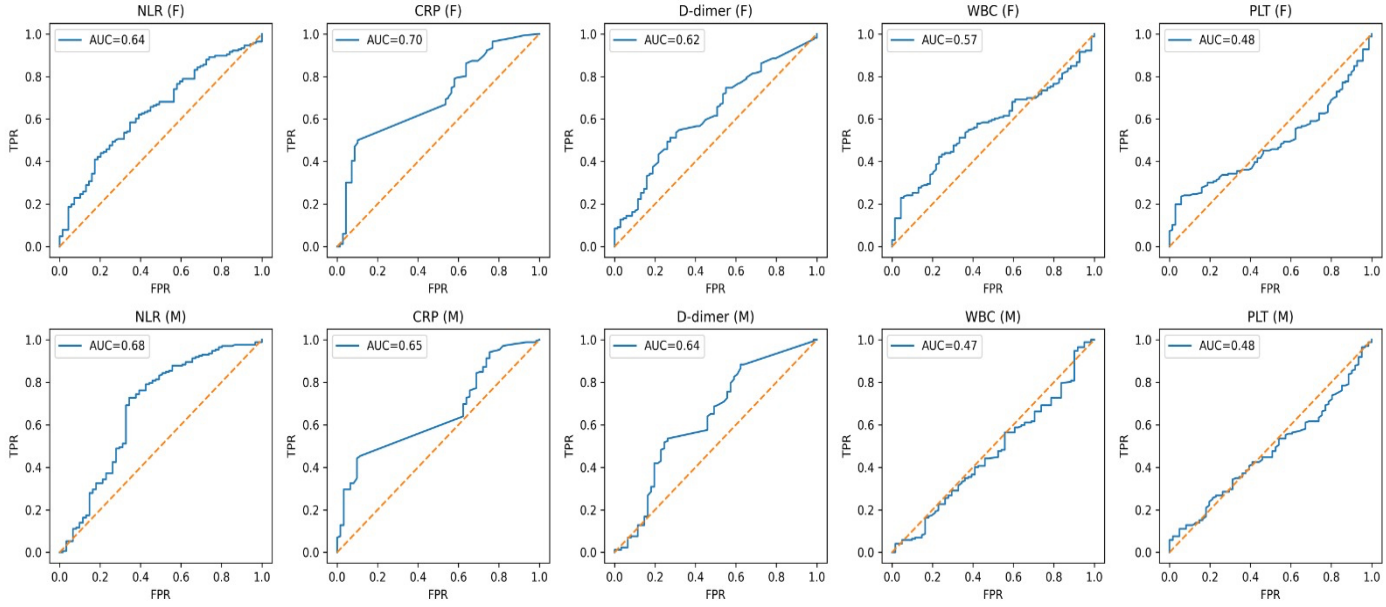

Figure 1. Receiver operating characteristic (ROC) curve analysis of hematological parameters for predicting computed tomography positivity stratified by gender. The upper panel represents females and the lower panel represents males. Each subplot shows the ROC curve and corresponding AUC for the respective parameter. CRP: C-reactive protein, NLR: Neutrophil-to-lymphocyte ratio, PLT: Platelet count, WBC: White blood cell, FPR: False positive rate, AUC: Area under the curve.

Providing a stronger diagnostic value than the parameters evaluated alone. Indeed, it is well known in the literature that NEU count increases, LYM count decreases significantly (lymphopenia) and NLR ratio increases in severe COVID-19 cases (7,8).

Lymphopenia in COVID-19 infection is accepted in the literature as a parameter of critical importance in determining the severity and prognosis of the disease (6). Man et al. (9) reported that lymphopenia and high NLR values showed a strong correlation with the CT severity score in COVID-19 patients. The strong correlation between the LYM level (CT-positive: 1.12 ± 0.58. CT-negative: 1.58 ± 0.71, $p < 0.001$) and NLR values (CT-positive: 4.89 ± 4.12. CT-negative: 2.87 ± 2.43. $p < 0.001$) determined in our study suggests that evaluating these parameters together may increase the diagnostic power. In our study, the significantly lower LYM count in CT-positive patients supports the direct effect of the virus on LYMs or its indirect effect through cytokine storm (10).

The mechanism of lymphocytopenia can be explained by angiotensin-converting enzyme 2 (ACE-2) receptors expressed on LYMs, which facilitate the direct invasion of SARS-CoV-2 into these cells and subsequent cell lysis. In addition, in the study conducted by Huang et al. (16) mediators such as proinflammatory cytokines [especially interleukin (IL)-6, IL-2, IL-7] and tumor necrosis factor-alpha, which are elevated during the fulminant cytokine storm process, can induce LYM apoptosis. These findings explain the molecular basis of

the decrease in LYM count that we detected in CT-positive patients.

NLR stands out as a valuable biomarker in predicting COVID-19 severity as a sensitive indicator of inflammatory response and immune system dysregulation (11). Liu et al. (17) found the AUC value of NLR to be 0.841. while El Hussini et al. (18) reported that NLR >2.5 could predict significant lesions that would require thoracic CT. The mean NLR values detected in our study (4.89 ± 4.12 in the CT positive group) are above the threshold values in the literature, confirming that NLR shows a significant increase in patients with COVID-19 pneumonia.

NLR provides a "bidirectional" inflammatory index by simultaneously reflecting increased NEU and decreased LYM counts, which explains why it is a stronger marker than NEU or LYM counts alone in diseases in which complex immunopathological mechanisms play a role, such as COVID-19. Similarly, Erdogan et al. (12) confirmed this prognostic value in their patient cohort.

One of the most important findings of our study is that the MPV value is significantly correlated with CT positivity, especially in female patients ($p < 0.05$). This gender-specific finding suggests that platelet dynamics in COVID-19 are affected by hormonal factors (13). High MPV is considered a reflection of increased platelet production and megakaryocyte activation. Platelet activation in COVID-19 is a multidimensional process. The direct effect of the virus on endothelial cells, inflammatory mediators released during the cytokine storm, and ACE-2 receptor dysregulation lead to both numerical and functional changes in platelets. The fact that MPV values >10.2 fL in women detected in our study are a significant marker for pulmonary involvement emphasizes the clinical importance of gender-specific platelet reactivity. Current meta-analyses confirm that the prognostic value of MPV in COVID-19 is preserved regardless of gender and age (19). Platelet-endothelium interactions underlie the immunothrombotic complications of COVID-19. Activated platelets promote the formation of neutrophil extracellular traps (NETs), thereby contributing to microthrombus formation. Recent studies suggest that NET activity triggers organ damage and contributes to the development of microthrombosis by increasing endothelial inflammation (20). This mechanism increases the severity of COVID-19 pneumonia, particularly by damaging the pulmonary microvasculature. Although the role of other platelet indices such as PDW and PCT in COVID-19 has not yet been fully elucidated, the evaluation of MPV together with other hematological parameters in our study provides a comprehensive picture of platelet dysfunction.

Our findings regarding MONO and BASO levels are also consistent with the literature. In our gender-stratified correlation analysis, MONO levels explained 17.6% of the variance in CT positivity in males and 9.4% in females (r^2), indicating that monocytopenia is a strong, practical marker for the evaluation of COVID-19 pneumonia. It was concluded that thoracic CT should be considered a priority, especially in patients with MONO counts $<0.4\times10^3/\mu L$, regardless of gender. Zhou et al. (14) reported that monocytopenia may be an indicator of severe immune response in severe COVID-19 patients, and Pehlivan et al. (15) reported that monocytopenia may be a determinant of COVID-19 survival.

Schulte-Schrepping et al. (21) examined in detail the decrease and dysfunction of MONO subpopulations in severe COVID-19 cases and observed a phenotypic change from classical CD14++CD16- MONOs to inflammatory CD14++CD16+ MONOs in COVID-19 patients. This finding supports the association between monocytopenia and severe COVID-19 in our study. Similarly, the decrease in BASO count may be related to the reduction of allergic/immunomodulation capacity in the setting of intense inflammation

In our gender-stratified analyses, significant differences between female and male patients were observed in hemogram parameters that predict CT positivity. These findings indicate that standard approaches are inadequate for COVID-19, and that gender-specific personalized medicine approaches should be developed. MPV and WBC parameters have stronger predictive value in females, whereas LYM and MONO parameters have stronger predictive value in males; this suggests the need to develop gender-specific algorithms in clinical evaluation. Takahashi et al. (22), showed that gender modulates the immune response to COVID-19. T-cell activation was more pronounced in females, whereas inflammatory cytokines were more pronounced in males. The significant difference in MPV among females suggests gender-specific pathophysiological mechanisms in the thrombotic sequelae of COVID-19. Scully et al. (8), showed the modulatory effects of gonadal steroids such as estrogen and progesterone on the coagulation cascade and platelet functions. These hormones are thought to influence endothelial cells and platelets, which may alter platelet dynamics and, therefore, MPV in females. In a meta-analysis conducted by Wang et al. (23), it was emphasized that the endothelial protective and anti-inflammatory effects of estrogen in female patients may positively affect the course of COVID-19. Gender-specific differences in prothrombotic mechanisms may be observed. Klein et al. (7) showed that gender has distinct effects on virus clearance, immune response quality, and inflammatory cytokine production. These findings explain the pathophysiological basis of the gender-specific hematological parameters we detected in our study.

Our findings support the hypothesis that hemogram parameters, particularly MPV, NLR, and MONO values, correlate with thoracic CT findings in COVID-19 patients. These markers may serve as accessible biomarkers for predicting pulmonary involvement when CT imaging is unavailable, offering a cost-effective approach for resource-limited settings. Unlike previous studies, our gender-stratified analysis provides novel insights into how blood parameters can predict CT-confirmed lung involvement, particularly valuable when RT-PCR results are inconclusive. This approach could enhance patient management in centers with limited diagnostic resources during pandemic conditions.

Another important finding in our study was the relationship between PCR results and CT findings, as revealed by the data we obtained in COVID-19 patients. WBC and NEU levels were significantly higher in the PCR (-)/CT (+) group than in the PCR (+)/CT (+) group. These findings indicate the diagnostic value of hematological parameters is further increased in patients who are PCR-negative but radiologically positive. The high NEU levels detected in the PCR (-)/CT (+) group suggest that these patients should be followed more carefully in terms of the risk of bacterial co-infection. Ai et al. (6) reported that the sensitivity of the RT-PCR test was 71% and that 75% of PCR-negative patients had positive CT findings. Wang et al. (24) showed that PCR sensitivity varies significantly depending on the sample

type. In this context, the high NEU and leukocyte levels observed in the PCR (-)/CT (+) group in our study emphasize the diagnostic and prognostic value of inflammatory hemogram parameters, especially in patients with suspected infection but with negative PCR results. These findings emphasize the importance of a holistic evaluation of clinical, laboratory, and imaging modalities, rather than relying on a single diagnostic method in the diagnosis of COVID-19.

An important contribution of our study is determining the role of hematological parameters in differentiating COVID-19 from other pulmonary pathologies. Although similar hemogram changes can be observed in bacterial pneumonia, viral pneumonia, and other lung infections, the co-occurrence of monocytopenia and high MPV in females, especially in COVID-19. is thought to create a pattern specific to this disease.

COVID-19 infection primarily affects the respiratory system, but it can also involve multiple organ systems. The abnormalities in hemogram parameters detected in our study may indicate not only pulmonary involvement but also a systemic inflammatory response. Teuwen et al. (25) showed that COVID-19 can cause multiple organ involvement by causing endothelial cell damage and thrombotic complications. Beceren et al. (26) reported that MPV may be an indicator of cardiac myocyte damage together with troponin elevation in predicting mortality in COVID-19 patients. These findings suggest that the hemogram parameters detected in our study reflect a systemic inflammatory response and may predict extrapulmonary organ involvement.

An important contribution of our study to clinical practice is demonstrating that hematological parameters are cost-effective in the diagnosis and follow-up of COVID-19. A hemogram test is approximately 20-30 times less expensive than thorax CT, and results are available within 15-30 minutes. Especially during pandemics, when healthcare resources are limited, study-specific cut-off values derived from our ROC analysis, such as NLR >3.292 (females) and >2.587 (males), and CRP >28 mg/L (females) and >55 mg/L (males), may support triage decisions and reduce unnecessary CT scans, thus reducing costs and preventing radiation exposure.

Study Limitations

Our study has some methodological limitations. Due to the retrospective design, longitudinal clinical follow-up data for the patients were, and serial changes in hemogram parameters could not be evaluated. In addition, the differential diagnosis of diseases with similar clinical presentations based on hemogram parameters, such as bacterial pneumonia, influenza pneumonia, and other viral pneumonias, could not be evaluated. This situation limits the ability to determine whether the suggested threshold values are specific to COVID-19. The potential effects of confounding variables, such as comorbid diseases, pharmacological treatments, and genetic factors, on hematological parameters could not be fully controlled. However, our number of patients is relatively high and the inclusion of patients without PCR positivity but with radiological findings provides a population suitable for real-world data.

The higher AUC value of NLR observed in males (0.680) than in females (0.641) may indicate stronger discriminatory performance. However, formal comparisons between AUC values were not performed, and this observation should be interpreted cautiously. This is consistent with the existing literature showing that male patients tend to exhibit stronger innate immune and inflammatory responses in COVID-19, which may translate into a higher discriminatory power of NLR for predicting pulmonary involvement in this group. The observed gender differences in optimal cut-off values and AUC levels further suggest that inflammatory biomarkers may behave differently between males and females, highlighting the importance of gender-stratified clinical interpretation. Applying uniform thresholds across both sexes may lead to suboptimal sensitivity or specificity in one group, underscoring the need for sex-specific reference values in clinical triage protocols.

CONCLUSION

This study found between thoracic CT findings and hemogram parameters in COVID-19 patients. In CT-positive patients, NLR, NEU, CRP and D-dimer values were found to be statistically significantly higher; LYM, MONO, EOS and BASO values were found to be significantly lower ($p < 0.01$). In female patients, the MPV value was significantly associated with CT positivity ($p < 0.05$). Point-biserial correlation analysis (r^2) revealed that MONO levels explained 9.4% of the variance in CT positivity in women and 17.6% in men. Leukocyte and NEU levels were significantly higher in the PCR (-)/CT (+) group than in the PCR (+)/CT (+) group ($p < 0.001$). Hemogram parameters, particularly NLR, MPV, and monocytopenia, may aid the evaluation of COVID-19 pneumonia and guide treatment strategies when CT cannot be performed. The fact that MONO levels have twice the predictive value in men compared with women (17.6% in men and 9.4% in women) underscores the need to develop gender-specific triage algorithms. These findings emphasize the inadequacy of standard approaches to COVID-19 and the importance of personalized medicine.

These findings suggest that platelet activation may exhibit sex-specific characteristics in COVID-19 and that MPV may be a useful biomarker, particularly in female patients. Gender-stratified analysis of platelet parameters may offer a new paradigm in thrombotic risk assessment in COVID-19.

Ethics

Ethics Committee Approval: This retrospective, single-center study was conducted between October and December 2020 after obtaining ethical approval from the University of Health Sciences Türkiye, Dışkapı YıldırıM Beyazıt Training and Research Hospital Ethics Committee (approval no: 104-14, date: 08.02.2021).

Informed Consent: Informed consent was not required as this was a retrospective study.

Footnotes

Authorship Contributions

Surgical and Medical Practices: T.Y.A., C.A., Concept: T.Y.A., C.A., Design: T.Y.A., C.A., Data Collection or Processing: T.Y.A., C.A., Analysis or Interpretation: T.Y.A., C.A., Literature Search: T.Y.A., C.A., Writing: T.Y.A., C.A.

Conflict of Interest: No conflict of interest was declared by the authors.

Financial Disclosure: The authors declared that this study received no financial support.

REFERENCES

1. World Health Organization. Naming the coronavirus disease (COVID-19) and the virus that causes it. Geneva: World Health Organization; 2020. Available from: https://www.who.int/emergencies/diseases/novel-coronavirus-2019/technical-guidance/naming-the-coronavirus-disease-covid-2019-and-the-virus-that-causes-it
2. World Health Organization. WHO Director-General's opening remarks at the media briefing on COVID-19 - 13 March 2020. Geneva: World Health Organization; 2020. Available from: https://www.who.int/director-general/speeches/detail/who-director-general-s-opening-remarks-at-the-media-briefing-on-covid-19---13-march-2020
3. Zhu N, Zhang D, Wang W, Li X, Yang B, Song J, et al. A novel coronavirus from patients with pneumonia in China, 2019. N Engl J Med. 2020; 382: 727-33.
4. Henry BM, de Oliveira MHS, Benoit S, Plebani M, Lippi G. Hematologic, biochemical and immune biomarker abnormalities associated with severe illness and mortality in coronavirus disease 2019 (COVID-19): a meta-analysis. Clin Chem Lab Med. 2020; 58: 1021-8.
5. Yang AP, Liu JP, Tao WQ, Li HM. The diagnostic and predictive role of NLR, d-NLR and PLR in COVID-19 patients. Int Immunopharmacol. 2020; 84: 106504.
6. Ai T, Yang Z, Hou H, Zhan C, Chen C, Lv W, et al. Correlation of chest CT and RT-PCR testing for coronavirus disease 2019 (COVID-19) in China: a report of 1014 cases. Radiology. 2020; 296: E32-E40.
7. Klein SL, Dhakal S, Ursin RL, Deshpande S, Sandberg K, Mauvais-Jarvis F. Biological sex impacts COVID-19 outcomes. PLoS Pathog. 2020; 16: e1008570.
8. Scully EP, Haverfield J, Ursin RL, Tannenbaum C, Klein SL. Considering how biological sex impacts immune responses and COVID-19 outcomes. Nat Rev Immunol. 2020; 20: 442-7.
9. Man MA, Rajnoveanu RM, Motoc NS, Bondor CI, Chis AF, Lesan A, et al. Neutrophil-to-lymphocyte ratio, platelets-to-lymphocyte ratio, and eosinophils correlation with high-resolution computer tomography severity score in COVID-19 patients. PLoS One. 2021; 16: e0252599.
10. Wynants L, Van Calster B, Collins GS, Riley RD, Heinze G, Schuit E, et al. Prediction models for diagnosis and prognosis of COVID-19: systematic review and critical appraisal. BMJ. 2020; 369: m1328.
11. Islam MM, Satici MO, Eroglu SE. Unraveling the clinical significance and prognostic value of the neutrophil-to-lymphocyte ratio, platelet-to-lymphocyte ratio, systemic immune-inflammation index, systemic inflammation response index, and delta neutrophil index: an extensive literature review. Turk J Emerg Med. 2024; 24: 8-19.
12. Erdogan A, Can FE, Gönüllü H. Evaluation of the prognostic role of NLR, LMR, PLR, and LCR ratio in COVID-19 patients. J Med Virol. 2021; 93: 5555-9.
13. Stojkovic Lalosevic M, Pavlovic Markovic A, Stankovic S, Stojkovic M, Dimitrijevic I, Radoman Vujacic I, et al. Combined diagnostic efficacy of neutrophil-to-lymphocyte ratio, platelet-to-lymphocyte ratio, and mean platelet volume as biomarkers of systemic inflammation in the diagnosis of colorectal cancer. Dis Markers. 2019; 2019: 6036979.
14. Zhou F, Yu T, Du R, Fan G, Liu Y, Liu Z, et al. Clinical course and risk factors for mortality of adult inpatients with COVID-19 in Wuhan, China: a retrospective cohort study. Lancet. 2020; 395: 1054-62.
15. Pehlivan O, Serin SO, Yesil EE, Demirdag F. Can monocytopenia be a new indicator in determining survival in COVID-19 disease? Clin Lab. 2021; 67.
16. Huang C, Wang Y, Li X, Ren L, Zhao J, Hu Y, et al. Clinical features of patients infected with 2019 novel coronavirus in Wuhan, China. Lancet. 2020; 395: 497-506.
17. Liu J, Liu Y, Xiang P, Pu L, Xiong H, Li C, et al. Neutrophil-to-lymphocyte ratio predicts critical illness patients with 2019 coronavirus disease in the early stage. J Transl Med. 2020; 18: 206.
18. El Hussini M, El Hussieny MS, Heiba A, Elsayed ESM, Hassan NE, El-Masry SA. Correlation between neutrophil-lymphocyte ratio, platelets-lymphocyte ratio, and high-resolution CT in patients with COVID-19. EMJ Radiol. 2023; 10.
19. Zein AFMZ, Sulistiyana CS, Raffaelo WM, Pranata R. The association between mean platelet volume and poor outcome in patients with COVID-19: systematic review, meta-analysis, and meta-regression. J Intensive Care Soc. 2023; 24: 299-308.
20. González-Jiménez P, Méndez R, Latorre A, Lorente B, Fernández-Barat L, et al. Neutrophil extracellular traps and platelet activation for identifying severe episodes and clinical trajectories in COVID-19. Int J Mol Sci. 2023; 24: 6690.
21. Schulte-Schrepping J, Reusch N, Paclik D, Baßler K, Schlickeiser S, Zhang B, et al. Severe COVID-19 is marked by a dysregulated myeloid cell compartment. Cell. 2020; 182: 1419-40.e23.
22. Takahashi T, Ellingson MK, Wong P, Israelow B, Lucas C, Klein J, et al. Sex differences in immune responses that underlie COVID-19 disease outcomes. Nature. 2020; 588: 315-20.
23. Wang X, Dhindsa R, Povysil G, Zoghbi A, Motelow JE, Hostyk JA, et al. Transcriptional inhibition of host viral entry proteins as a therapeutic strategy for SARS-CoV-2. Preprints. 2020; 2020030360.
24. Wang W, Xu Y, Gao R, Lu R, Han K, Wu G, et al. Detection of SARS-CoV-2 in different types of clinical specimens. JAMA. 2020; 323: 1843-4.
25. Teuwen LA, Geldhof V, Pasut A, Carmeliet P. COVID-19: the vasculature unleashed. Nat Rev Immunol. 2020; 20: 389-91.
26. Beceren NG, Armağan HH, Oğuzlar FÇ, Cesur E, Gürdal O, Tomruk Ö. Can mean platelet volume be a prognosis predictor in viral infections: an example of COVID-19. Heliyon. 2023; 9.

Original Investigation | Özgün Araştırma

Gazi Med J 2026;37(3):350-357

DOI: http://dx.doi.org/10.12996/gmj.2026.4610

A Study on Quantification of Maximum Voluntary Contraction of Quadriceps at Various Functional Knee Range of Motion, Using Surface EMG (sEMG)

Yüzey Elektromiyografisi (sEMG) Kullanılarak Kuadriseps Kasının Farklı Fonksiyonel Diz Hareket Açıklıklarında Maksimum İstemli Kasılmasının Nicel Olarak Değerlendirilmesi

Shabiethaa Dharanipathy[1], Jeyakumar Sankarasubbu[1], Saravanan Vinayagamudaliar Selvaraj[1,2], Vincent Prabhakaran Sekar[1]

[1]Department of Physiotherapy, Garden City University, Faculty of Medicine, Bangalore, India
[2]Mohamed Sathak A.J. College of Physiotherapy, Chennai, India

ABSTRACT

Objective: Surface electromyography (sEMG) is an essential tool in physiotherapy education, enabling students to objectively analyze muscle activation and understand joint-angle–dependent changes in force production. Teaching maximum voluntary contraction (MVC) assessment enhances clinical reasoning skills, accuracy of muscle testing, and evidence-based exercise prescription. This study evaluates quadriceps MVC at 70°, 90°, and 110° of knee flexion and highlights its educational relevance for physiotherapy training. Previous studies suggest that mid-range knee flexion allows optimal muscle activation, but comparative evidence across 70°, 90°, and 110° remains limited. Research using sEMG supports the idea that quadriceps activation changes with joint angle, yet findings are inconsistent. Therefore, examining individual differences in MVC at these specific angles is essential. Healthy participants aged 18-25 years who were free from knee injuries, musculoskeletal disorders, and neurological issues were included. All subjects were able to perform isometric quadriceps contractions and provided informed consent.

Methods: Forty-five healthy adults aged 18-25 years were assessed in a controlled laboratory setting. sEMG electrodes were placed over the vastus medialis oblique (VMO) and vastus lateralis (VL) muscles. MVC was recorded during isometric quadriceps contraction at knee flexion angles of 70°, 90°, and 110, which were measured using a universal goniometer. Statistical analysis included one-way analysis of variance, Bonferroni post-hoc tests, and paired t-tests.

ÖZ

Amaç: Yüzey elektromiyografisi (sEMG), kas aktivasyonunun nesnel olarak analiz edilmesini ve eklem açısına bağlı kuvvet üretimindeki değişikliklerin anlaşılmasını sağlayan, fizyoterapi eğitiminde önemli bir değerlendirme yöntemidir. Maksimum istemli kasılmanın (MVC) değerlendirilmesi, öğrencilerin klinik karar verme becerilerini geliştirmekte, kas testlerinin doğruluğunu artırmakta ve kanıta dayalı egzersiz reçetelendirilmesini desteklemektedir. Bu çalışmanın amacı, kuadriseps kasının 70°, 90° ve 110° diz fleksiyon açılarındaki maksimum istemli kasılmasını değerlendirmek ve bulguların fizyoterapi eğitimi açısından önemini ortaya koymaktır.

Yöntemler: Kontrollü laboratuvar ortamında 18–25 yaş aralığında 45 sağlıklı gönüllü değerlendirildi. Yüzey EMG elektrotları vastus medialis oblikus (VMO) ve vastus lateralis (VL) kasları üzerine yerleştirildi. Maksimum istemli kasılma, evrensel gonyometre ile ölçülen 70°, 90° ve 110° diz fleksiyon açılarında izometrik kuadriseps kasılması sırasında kaydedildi. İstatistiksel analizlerde tek yönlü varyans analizi, Bonferroni post-hoc testi ve eşleştirilmiş t-testi kullanıldı.

Bulgular: VMO ve VL kaslarında üç farklı diz fleksiyon açısı arasında MVC değerleri açısından istatistiksel olarak anlamlı farklılık bulundu ($p < 0,001$). Post-hoc analiz sonuçları, VMO için 70°–90° ve 70°–110°; VL için ise 70°–90° ve 70°–110° açıları arasında anlamlı farklılık olduğunu gösterdi. Kuadriseps toplam aktivasyonunda 70°–90° ve 70°–110° açıları arasında anlamlı fark saptanmazken, 90°–110° açıları

Cite this article as: Dharanipathy S, Sankarasubbu J, Selvaraj SV, Sekar VP. A study on quantification of maximum voluntary contraction of quadriceps at various functional knee range of motion, using surface EMG (sEMG). Gazi Med J. 2026;37(3):350-357

Address for Correspondence/Yazışma Adresi: Shabiethaa Dharanipathy, Department of Physiotherapy, Garden City University, Faculty of Medicine, Bangalore, India
E-mail / E-posta: shabiethaa1978@gmail.com
ORCID ID: orcid.org/0009-0009-5556-3525

Received/Geliş Tarihi: 15.12.2025
Accepted/Kabul Tarihi: 29.05.2026
Publication Date/Yayınlanma Tarihi: 10.07.2026

ABSTRACT

Results: VMO and VL showed significant differences in MVC across all three knee angles ($p < 0.001$). Post-hoc analysis indicated significant differences between VMO 70- 90 and VMO 70-110, and between VL 70-90 and VL 70-110. Quadriceps composite activation showed no significant difference between 70°-90° and 70°-110°, while 90°-110° showed significant variation ($p < 0.001$). Mid-range knee flexion demonstrated the highest activation efficiency.

CONCLUSION: Quadriceps MVC is greatest between 70° and 90° of knee flexion. Integrating sEMG-based MVC assessment into physiotherapy education enhances students' understanding of muscle biomechanics, objective evaluation, and optimal exercise positioning. This study supports the incorporation of technology-assisted EMG training into physiotherapy laboratory teaching to improve competency.

Keywords: Surface EMG, maximum voluntary contraction, quadriceps, physiotherapy education, knee biomechanics

ÖZ

arasında anlamlı farklılık belirlendi ($p < 0,001$). Orta düzey diz fleksiyon açılarında en yüksek kas aktivasyonu elde edildi.

Sonuç: Kuadriseps kasının maksimum istemli kasılması 70° ile 90° diz fleksiyon açıları arasında en yüksek düzeydedir. Fizyoterapi eğitiminde sEMG tabanlı MVC değerlendirmesinin kullanılması, öğrencilerin kas biyomekaniği, objektif değerlendirme yöntemleri ve optimal egzersiz pozisyonlandırması konularındaki bilgi ve becerilerini geliştirmektedir. Bu çalışma, teknoloji destekli EMG uygulamalarının fizyoterapi laboratuvar eğitimine entegrasyonunu desteklemektedir.

Anahtar Sözcükler: Yüzey elektromiyografi, sEMG, kuadriseps, maksimum istemli kasılma, diz fleksiyonu, fizyoterapi eğitimi

INTRODUCTION

Surface electromyography (sEMG) has become an essential component of modern physiotherapy education, offering a reliable and objective method for analyzing muscle activation patterns (1). Unlike traditional subjective approaches such as manual muscle testing, sEMG provides quantifiable data on the timing, amplitude, and recruitment order of motor units. For physiotherapy students, learning to interpret sEMG signals enhances clinical reasoning, improves assessment accuracy, and strengthens the application of biomechanical principles in practice (2). As healthcare increasingly incorporates technology-assisted assessment, familiarity with sEMG prepares students to meet contemporary professional standards and deliver evidence-based interventions. Muscle force production varies significantly with joint angle, a concept rooted in the length-tension relationship and mechanical advantage of muscles around a joint. The quadriceps femoris, the primary extensor of the knee, is responsible for functional movements such as stair climbing, sit-to-stand transitions, gait propulsion, and athletic tasks requiring forceful extension. Physiotherapy curricula emphasize quadriceps strength evaluation because weakness or altered activation patterns can cause patellofemoral pain, gait abnormalities, reduced stability, and compromised performance. Teaching students to analyze quadriceps activation across various joint positions helps bridge theoretical knowledge with practical application (3).

The quadriceps muscle group consists of four muscles: rectus femoris, vastus lateralis (VL), vastus medialis, and vastus intermedius, which converge at the patella and function collectively to extend the knee. Among these, the vastus medialis oblique (VMO) and VL play crucial roles in patellar tracking. An imbalance between these components is commonly associated with patellofemoral dysfunction, making their assessment highly relevant to physiotherapy training. sEMG allows students to visualize the differential activation of VMO and VL, helping them understand patellar biomechanics and recognize how variations in muscle control may contribute to clinical symptoms. Knee flexion angles influence quadriceps mechanical efficiency (4). At mid-range flexion (between 70° and 90°), the quadriceps exhibit optimal force production. This is attributable to favorable muscle fiber length, patellofemoral joint alignment, and the mechanical advantage of the extensor mechanism. In physiotherapy education, understanding these biomechanical principles is crucial for teaching appropriate exercise selection, progression, and functional retraining. Students frequently encounter clinical scenarios where they must decide which knee position is best suited for strengthening exercises, pain reduction strategies, or postoperative rehabilitation. Evidence-based training supported by sEMG enhances their decision-making capacity. Historically, assessment of quadriceps strength relied on subjective tools such as the MRC grading system (5). While widely used, these traditional methods lack sensitivity for detecting mild strength deficits or subtle neuromuscular differences. This limitation poses challenges in both research and clinical practice, particularly for early-stage rehabilitation, for high-performance athletes, and for conditions that require precise muscle monitoring. Use of sEMG overcomes these limitations by enabling fine-grained detection of activation patterns and facilitating accurate comparison between muscle groups. When integrated into physiotherapy laboratory sessions, sEMG enhances students' understanding of muscle performance beyond basic clinical palpation or observation. Functional knee positions of 70°, 90°, and 110° are commonly used in daily movements such as sitting, squatting, lifting, and stair negotiation. Evaluating quadriceps MVC at these angles enables students to relate electrophysiological findings to real-world functional biomechanics. As physiotherapy increasingly emphasizes task-oriented training, understanding how muscle activation changes across functional ranges equips students to plan safer and more effective interventions. By engaging with sEMG-based assessments, students gain practical skills, develop a scientific mindset, and strengthen their competence in musculoskeletal evaluation (6).

For educational institutions, incorporating sEMG into teaching offers several advantages. It enhances student engagement, supports blended learning models, and provides objective feedback that can improve technique and performance. Students can observe how electrode placement, posture, joint angle, and contraction type influence muscle activation. This experiential learning fosters deeper comprehension of neuromuscular physiology and facilitates the transition from novice learners to confident clinicians (7). Given the clinical, biomechanical, and educational significance of quadriceps activation, this study investigates, using sEMG, maximum voluntary contraction (MVC) at knee flexion angles of

70°, 90°, and 110° in healthy young adults. In addition to its clinical applications, sEMG has become an important component of modern physiotherapy education, enabling students to analyze muscle activation objectively and to understand joint-angle-dependent changes in force production. Teaching MVC assessment enhances clinical reasoning skills, improves the accuracy of muscle testing, and supports evidence-based exercise prescription. The study not only examines angle-dependent neuromuscular performance but also demonstrates how sEMG-based assessment can be effectively integrated into physiotherapy education to enhance student competency, improve understanding of functional biomechanics, and promote evidence-based practice (8). Despite the growing body of literature on quadriceps activation using sEMG, several gaps remain. Many existing studies have focused on generalized knee positions or isolated joint angles, with limited direct comparisons across multiple functional knee-flexion angles, such as 70°, 90°, and 110°. Furthermore, inconsistencies in reported findings regarding optimal activation angles highlight the need for more standardized evaluation. In addition, relatively few studies have explored the application of sEMG-based quadriceps assessment within a physiotherapy educational context, particularly in relation to teaching MVC and joint angle-dependent muscle performance. Therefore, it is necessary to systematically examine angle-specific quadriceps activation using sEMG and to emphasize its relevance for physiotherapy training.

Review of Literature

sEMG has been widely recognized as a valid and reliable tool for assessing neuromuscular activation during static and dynamic tasks. sEMG provides an objective representation of muscle recruitment patterns, timing, and amplitude, allowing clinicians and students to interpret muscle performance with greater accuracy than traditional manual methods. sEMG is capable of recording the algebraic sum of motor unit action potentials, making it a valuable technique for understanding neuromuscular physiology and fatigue responses during high-intensity contractions. Their foundational work established sEMG as a cornerstone for evaluating muscle behavior in both research and clinical settings. The quadriceps femoris muscle group plays a fundamental role in knee extension and contributes significantly to lower limb stability, gait efficiency, and functional movement performance (9). Studies have demonstrated that quadriceps activation varies with knee joint angle due to changes in muscle length-tension relationships and mechanical leverage. Morrish et al. (10) investigated quadriceps activity at different knee angles and reported increased maximal voluntary contraction (MVC) as flexion increased from 60° to 90°, suggesting that mid-range knee positions may offer a biomechanical advantage. These findings are consistent with the biomechanical principle that muscle force production is optimal when fiber length and joint mechanics are aligned to maximize tension.

The coordination between the VMO and VL plays an essential role in patellar tracking and stabilization. Research comparing EMG ratios of VMO and VL in healthy individuals and individuals with patellofemoral pain indicates that activation imbalances may contribute to lateral patellar maltracking, knee pain, and dysfunction. Souza and Gross (9) reported that altered activation ratios could serve as clinical indicators for patellofemoral disorders (11). Their study highlights the importance of evaluating both components of the quadriceps, particularly when designing rehabilitation programs targeting knee stability. Further studies have explored how joint angle influences quadriceps activation. MVC varies significantly with knee joint position, reinforcing the need to assess quadriceps performance across a range of functional knee angles (12). Similarly, research has demonstrated that the interaction between agonist and antagonist muscles during maximal isometric contractions influences activation patterns that may contribute to injury prevention. These observations support the assessment of muscle performance across multiple joint angles to better understand neuromuscular function (13).

While traditional manual muscle testing, such as the Medical Research Council (MRC) grading system, provides a basic assessment of muscle strength, it lacks sensitivity in detecting subtle deficits or early-stage neuromuscular dysfunction. Several researchers have noted that subjective grading methods may not correlate directly with true muscle force production, as minor changes in strength are often undetectable without the use of objective instruments. sEMG, by contrast, offers precise quantification, improving accuracy in clinical assessment and research applications (14). Studies examining quadriceps activation in functional knee positions emphasize the importance of evaluating MVC at angles commonly encountered during activities of daily living. Knee flexion angles of 70°, 90°, and 110° represent key positions used during squatting, stair climbing, and sit-to-stand transitions. Research suggests that evaluating MVC at these angles provides insight into optimal activation ranges and helps clinicians understand how joint position influences neuromuscular efficiency. Such knowledge aids in designing effective rehabilitation programs and supports physiotherapy students in developing evidence-based decision-making skills (15). Despite extensive research on quadriceps activation, few studies have specifically compared MVC at 70°, 90°, and 110° using sEMG in healthy young adults. Understanding these variations is valuable for both clinical practice and physiotherapy education, as it enhances comprehension of joint biomechanics, exercise prescription, and performance analysis. Therefore, this study aims to address this gap by evaluating angle-specific MVC using sEMG and highlighting its relevance in physiotherapy training and skill development (16).

MATERIALS AND METHODS

Study Design

This study employed an observational cross-sectional design and was conducted in a physiotherapy laboratory. The aim was to analyze MVC of the quadriceps at three functional knee flexion angles 70°, 90°, and 110°using sEMG.

Participants

A total of 45 healthy adults took part in the study. Participants were recruited from the local community and screened using a questionnaire to ensure they met the required criteria. Basic demographic details were collected, and all sessions were scheduled at similar times of day for consistency. Participants were asked to avoid strenuous activity and caffeine before testing. All procedures were conducted in accordance with ethical guidelines.

Inclusion Criteria

Participants were required to be 18-25 years old and free from musculoskeletal or neurological injuries. Only healthy individuals who fully understood the study and were willing to participate were included. Screening procedures ensured that all selected individuals could safely complete the testing protocol.

Exclusion Criteria

Individuals with a lower limb injury in the past three months were excluded. Those who were regularly involved in resistance training, who were using steroids, or who were taking performance-enhancing substances were also not eligible. Anyone with conditions that could interfere with MVCs or pose health risks was excluded.

Ethical Approval Statement

The study protocol received official approval from the Institutional Research Committee (IRC) of Y.M.T. College of Physiotherapy, Navi Mumbai. The research proposal titled "A study on Quantification of Maximum Voluntary Contraction of Quadriceps at Various Functional Knee Range of Motion Using Surface Electromyography (sEMG)" was reviewed and approved by the Chairperson of the IRC (reference number: ymtibpth/1201125, date: 24/03/2025). The Committee confirmed that the proposed research met the ethical standards required for studies involving human participants and granted permission to proceed with data collection.

Instrumentation

The study used a sEMG unit equipped with silver/silver chloride disposable electrodes to record muscle activation. A universal goniometer was utilized to ensure precise measurement of knee flexion angles at 70°, 90°, and 110°. A quadriceps exercise table with adjustable height provided optimal limb positioning, while a stabilization belt was used to minimize compensatory movements during testing. Alcohol swabs were used to clean the skin prior to electrode placement to reduce impedance. All equipment was calibrated before testing to ensure accuracy and consistency in data collection throughout the study. The raw sEMG signals were processed using standard signal conditioning procedures to ensure accuracy and reliability. Signals were sampled at a frequency of 1000 Hz to adequately capture muscle activity without aliasing. A band-pass filter (20-450 Hz) was applied to remove movement artifacts and high-frequency noise. The signals were then full-wave rectified to convert all values to a positive scale, and then smoothed using a root mean square (RMS) algorithm with a 50-ms window to obtain a representative amplitude of muscle activation. All signal processing procedures were performed using the software associated with the sEMG system to ensure consistency and standardization across all participants.

Electrode Placement

Electrodes were positioned following standardized sEMG placement guidelines to ensure reliable data. For the VMO, electrodes were placed approximately 2 cm above and medial to the patella, aligned with the muscle fiber orientation. For the VL, electrodes were positioned on the lateral thigh at one-third of the distance between the greater trochanter and the lateral femoral epicondyle. A ground electrode was placed over a bony prominence, typically the tibial shaft, to minimize electrical noise. Proper skin preparation included shaving and cleaning the electrode sites with alcohol to reduce impedance (17).

Procedure

Participants were seated upright on a quadriceps table, with the tested leg positioned at predetermined knee flexion angles of 70°, 90°, and 110°, as measured using a universal goniometer. A stabilization strap secured the thigh to prevent compensatory movement. For each angle, participants performed a MVC of the quadriceps while sEMG activity was recorded from the VMO and VL. Each contraction was sustained for five seconds, followed by 30-60 seconds of rest to minimize fatigue. Three trials were performed per angle, and the highest amplitude value was selected as the MVC measure for analysis (18).

Outcome Measures

The primary outcome measure was the amplitude of the MVC, recorded in microvolts, for the VMO and VL at knee flexion angles of 70°, 90°, and 110°. sEMG peak values were analyzed to determine angle-dependent variations in muscle activation. A secondary outcome was the comparison of activation differences between VMO and VL at each angle to assess their relative contributions. Composite quadriceps activation patterns across all angles were also evaluated (19). All outcome measures were statistically analyzed to identify significant differences and to interpret their functional relevance. The raw sEMG signals were processed using standard signal conditioning procedures to ensure accuracy and reliability. Signals were sampled at an appropriate sampling frequency (e.g., 1000 Hz) to capture muscle activity without aliasing. A band-pass filter (typically 20-450 Hz) was applied to remove movement artifacts and high-frequency noise. The signals were first full-wave rectified to convert all values to a positive scale and then smoothed using a RMS algorithm over a defined window (e.g., 50 ms) to obtain a representative amplitude of muscle activation. These processing steps were performed using the software associated with the sEMG system to standardize data acquisition and analysis across all participants.

Statistical Analysis

Data analysis was performed using the paired t-test to compare variables within the study groups. Both descriptive and inferential statistical methods were applied to summarize and interpret the collected data. All statistical computations were carried out using the Statistical Package for the Social Sciences (SPSS). Descriptive statistics, including the mean and standard deviation, were calculated for all measured parameters to provide a comprehensive overview of the dataset.

RESULTS

A total of 45 participants were included in the analysis of quadriceps MVC at knee flexion angles of 70°, 90°, and 110° measured using surface EMG. The descriptive characteristics of VMO and VL activation at all three angles are summarized in Table 1, which presents the mean microvolt amplitudes and measures of variability for each muscle. These values provide a clear baseline for understanding muscle recruitment across joint positions. The pattern of activation

across angles establishes the foundation for subsequent inferential testing and comparative analyses performed in this study (Figure 1).

VMO Analysis

These findings confirm that VMO amplitude decreases progressively as the knee flexion angle increases. The overall ANOVA summary for VMO is shown in Table 2, supporting the conclusion that changes in angle substantially influence medial quadriceps activation. VMO activation across the three knee flexion angles showed a significant difference based on one-way ANOVA results (F: 40.392, p < 0.001), indicating angle-dependent variations in recruitment. Post-hoc Bonferroni comparisons, as presented in Table 3, revealed significant reductions in activation for VMO 70-90 (p < 0.001) and VMO 70-110 (p < 0.001).

Table 1. Descriptive statistics of VMO and VL at 70°, 90°, and 110°.

Muscle	Angle	Mean (µV)	Standard deviation	Standard error mean
VMO	70°	233.11	92.01	13.72
	90°	147.93	46.44	6.92
	110°	117.56	37.03	5.52
VL	70°	123.22	39.30	5.86
	90°	186.22	108.92	16.24
	110°	286.56	144.72	21.57

VMO: Vastus medialis oblique, VL: Vastus lateralis.

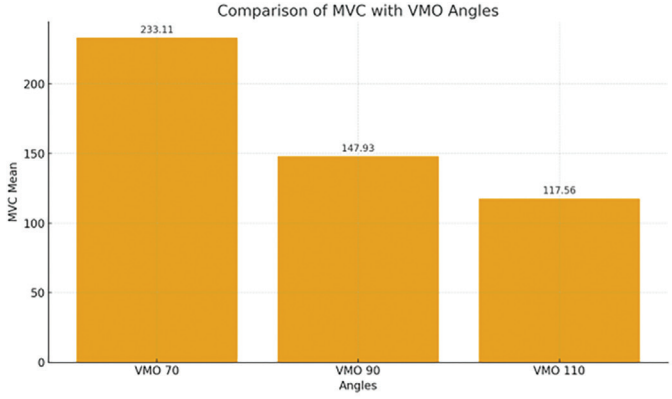

Figure 1. Comparison of mean MVC values of VMO at 70°, 90°, and 110° knee flexion.

MVC: Maximum voluntary contraction, VMO: Vastus medialis oblique.

VMO vs. VL Comparison

A paired t-test comparing overall VMO and VL activation revealed a statistically significant difference, as shown in Table 4. VL demonstrated a higher mean activation than VMO, with the test yielding t: 2.387 and p = 0.018. This suggests that, irrespective of the angle, the VL tends to exhibit a greater EMG amplitude during MVC. The variability in activation between the two muscles highlights functional differences in recruitment patterns, potentially reflecting differences in biomechanical roles and fiber composition. These results emphasize the importance of analyzing both muscles to fully understand quadriceps function during controlled knee flexion tasks.

Quadriceps Composite Activation

Comparisons of quadriceps MVC across angles are also presented in Table 4 and show no significant difference between 70° and 90° (p = 0.330) or between 70° and 110° (p = 0.202). However, activation was significantly higher at 90° than at 110°, with t: 3.849 and p < 0.001. This suggests that deeper knee flexion produces a marked increase in overall quadriceps recruitment. The absence of significant differences in the first two comparisons indicates that moderate changes in flexion angle may not substantially alter quadriceps output, whereas transitions from mid-range to deeper flexion create a more pronounced activation response (Figure 2).

As shown in Tables 1–4, VMO activation was highest at 70° and significantly reduced at 90° and 110°, while VL activation showed the opposite trend, peaking at 110°. A Comparison between VMO and VL confirmed that activation in VL was significantly greater. Quadriceps MVC revealed no significant differences between 70°-90° and 70°-110°, but revealed a highly significant increase between 90°-110°. Overall, these findings demonstrate angle-dependent modulation of quadriceps components, with VMO favoring more extended positions and VL becoming dominant in deeper flexion. This suggests differential neuromuscular strategies for stabilizing and producing force during knee movement.

DISCUSSION

sEMG provides a valuable non-invasive method for capturing muscle activation patterns and quantifying neuromuscular recruitment during voluntary contractions. As a diagnostic and teaching tool, sEMG allows physiotherapists and students to directly visualize the extent, timing, and relative activation of key muscle groups, thereby reducing ambiguity in clinical assessments. Because muscle activity can be recorded objectively during both isolated and functional tasks, sEMG has gained importance not only in research but also

Table 2. One-way ANOVA results for VMO and VL.

Muscle	Source	Sum of squares	df	Mean square	F	p-value
VMO	Between groups	322,967.200	2	161,483.622	40.392	<0.001
	Within groups	527,728.400	132	3,997.942		
	Total	850,695.600	134			
VL	Between groups	610,703.300	2	305,351.667	26.666	<0.001
	Within groups	1,511,507.000	132	11,450.808		
	Total	2,122,210.000	134			

ANOVA: Analysis of variance, VMO: Vastus medialis oblique, VL: Vastus lateralis.

Table 3. Bonferroni post-hoc comparisons for VMO and VL.

Muscle	Comparison	Mean difference (i-j)	Standard error	p-value
VMO	70° vs. 90°	85.18	13.33	<0.001
	70° vs. 110°	115.56	13.33	<0.001
VL	70° vs. 90°	−63.00	22.56	0.018
	70° vs. 110°	−163.33	22.56	<0.001

VMO: Vastus medialis oblique, VL: Vastus lateralis.

Table 4. Paired t-tests: VMO vs. VL and quadriceps at different angles.

Comparison	Mean difference	Standard deviation	Standard error mean	t-value	p-value
VMO vs. VL	32.47	158.02	13.60	2.387	0.018
Quadriceps 70° vs. 90°	11.09	107.33	11.31	0.980	0.330
Quadriceps 70° vs. 110°	23.89	176.40	18.59	1.285	0.202
Quadriceps 90° vs. 110°	34.98	86.21	9.09	3.849	<0.001

VMO: Vastus medialis oblique, VL: Vastus lateralis.

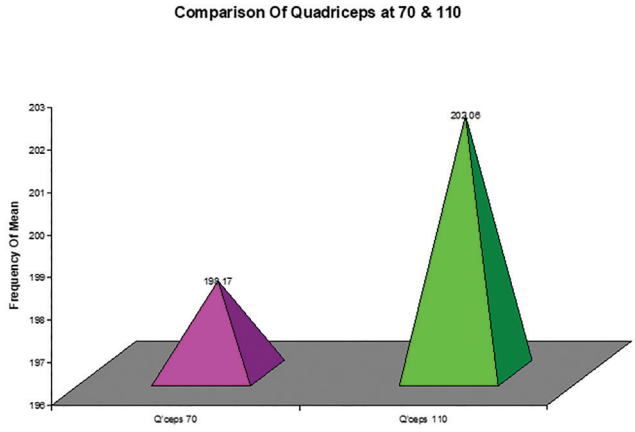

Figure 2. Comparison of mean quadriceps maximum voluntary contraction at 90° and 110° knee flexion demonstrating higher activation at 110°.

in educational environments where students must understand the physiological basis of movement and muscular coordination (20).

The present study demonstrated significant angle-dependent variations in quadriceps activation, with VMO activity highest at 70° and VL activity increasing progressively toward 110°. These findings are consistent with the established length-tension relationship and the mechanical advantage principles governing muscle force production. However, a broader comparison with previous sEMG-based studies provides deeper insight into these observations. Previous research has consistently reported that quadriceps activation varies with knee joint position, with several studies identifying mid-range positions (approximately 60°-90°) as optimal for force generation. The present findings partially align with these observations, as stable activation was observed between 70° and 90°, whereas a significant increase in overall quadriceps recruitment occurred at deeper flexion (110°). More recent sEMG investigations have highlighted that deeper knee flexion angles are associated with increased neuromuscular demand and altered patellofemoral joint mechanics, which support the current finding of higher activation at 110°. This may be attributed to increased mechanical load, changes in moment arm, and greater stabilization requirements at deeper joint angles. In contrast, the higher VMO activation observed at 70° suggests a mechanical advantage for medial stabilization in relatively extended positions. These findings demonstrate that quadriceps components do not function uniformly but instead exhibit angle-specific recruitment patterns.

The paired t-test demonstrated significantly greater overall activation in the VL than in the VMO, indicating lateral dominance in quadriceps recruitment among healthy young adults. While this finding may have potential clinical relevance, it should be interpreted with caution, as the present study was conducted exclusively in healthy individuals (21). This pattern may provide preliminary insight into neuromuscular behavior; however, direct extrapolation to clinical populations, such as individuals with patellofemoral disorders, is not justified without further investigation. Clinical conditions typically involve additional factors such as pain, inflammation, and structural alterations, which were not present in this study. Therefore, the observed activation pattern should be considered representative of normal physiology rather than pathological function.

Comparisons of quadriceps MVC revealed no significant differences between 70°-90° and 70°-110°, whereas a highly significant increase was observed between 90°-110°. While statistical findings indicate whether differences are present, assessing their physiological and practical significance yields a more meaningful interpretation. The absence of significant differences between 70° and 90° suggests that the quadriceps can maintain a relatively stable force output within this functional mid-range, which is commonly used in activities such as sit-to-stand and early-phase squatting. In contrast, the increased activation at 110° indicates that deeper knee flexion requires greater neuromuscular effort, likely due to increased mechanical demand and stabilization requirements. From a practical perspective, this suggests that exercises performed at higher flexion angles may provide a greater strengthening stimulus, although they may also increase joint loading. Therefore, interpretation of results should consider both statistical and functional significance (22).

The findings of this study should also be interpreted in light of certain methodological limitations inherent to sEMG. One important consideration is the potential for cross-talk between adjacent muscles, particularly between the vastus medialis and VL, which may affect signal specificity. Additionally, variations in electrode placement, even when standardized guidelines are followed, can influence signal amplitude due to differences in skin impedance and anatomical variability. Another limitation is the use of non-normalized sEMG amplitude values, which may restrict comparability across individuals and conditions. Furthermore, factors such as participant effort, fatigue, and slight variations in posture during testing may influence EMG recordings. Therefore, the results should be interpreted with caution, and future studies are encouraged to incorporate normalization procedures and advanced signal analysis techniques to enhance reliability (23). The educational relevance of sEMG in physiotherapy training can be more effectively understood when presented in a structured manner. Firstly, sEMG enables students to visualize real-time muscle activation, thereby bridging the gap between theoretical knowledge and practical application. Secondly, it enhances clinical reasoning by facilitating the interpretation of objective data rather than relying solely on subjective assessments. The present study provides a clear example of how joint angle influences muscle activation, helping students understand biomechanical principles and apply them to exercise prescription. Finally, structured integration of sEMG into physiotherapy curricula can support the development of essential skills in assessment, analysis, and decision-making, ultimately improving clinical competency (24). Overall, the present study supports existing literature by demonstrating that quadriceps activation is angle-dependent and underscores the need for cautious interpretation, methodological awareness, and consideration of functional relevance. The findings contribute to both biomechanical understanding and physiotherapy education, while highlighting the need for future research to validate these results in clinical populations (25).

Study Limitations

This study has several limitations that should be acknowledged when evaluating the results. First, the sample only included healthy young adults between 18 and 25 years of age, which limits the generalisability of the data to older adults, athletes, or patients with musculoskeletal and neurological diseases. The relatively small sample size may limit the external validity of the results. Secondly, the muscle activation was investigated only during isometric contractions at three specific knee-flexion angles (70°, 90°, and 110°). Dynamic functional tests such as walking, squatting, stair climbing, and sit-to-stand were not assessed, which may limit the applicability of the results to real-life motions. Third, just two quadriceps components, VMO and VL were studied, while others muscles contributing to knee stability.

CONCLUSION

This study demonstrates that the quadriceps MVC varies with knee flexion angle but not uniformly across all positions. No significant differences were observed between 70° and 90°, or between 70° and 110°, indicating that the quadriceps produce comparable activation levels across these ranges in young adults. However, a highly significant increase in MVC occurred between 90° and 110°, suggesting that deeper knee flexion elicits greater quadriceps recruitment. These findings indicate that while mid-range flexion maintains stable activation, maximal quadriceps output is achieved closer to 110°. This knowledge is valuable for physiotherapy training, exercise prescription, and the understanding of angle-specific muscle performance in functional and rehabilitative contexts.

Ethics

Ethics Committee Approval: This study was approved by the Institutional Research Committee (IRC) of Y.M.T. College of Physiotherapy, Navi Mumbai (reference number: ymtibpth/1201125, date: 24/03/2025).

Informed Consent: Written informed consent was obtained from all participants.

Footnotes

Authorship Contributions

Concept: S.D., J.S., S.V.S., V.P.S., Design: S.D., J.S., S.V.S., V.P.S., Data Collection or Processing: S.D., Analysis or Interpretation: S.D., J.S., S.V.S., V.P.S., Literature Search: S.D., J.S., Writing: S.D., J.S., S.V.S., V.P.S.

Conflict of Interest: No conflict of interest was declared by the authors.

Financial Disclosure: The authors declared that this study received no financial support.

REFERENCES

1. De Luca CJ. The use of surface electromyography in biomechanics. J Appl Biomech. 1997; 13: 135-63.
2. Medved V, Medved S, Kovač I. Critical appraisal of surface electromyography (sEMG) as a taught subject and clinical tool in medicine and kinesiology. Front Neurol. 2020; 11: 560363.
3. Gerdle B, Larsson B, Karlsson S. Criterion validation of surface EMG variables as fatigue indicators using peak torque: a study of repetitive maximum isokinetic knee extensions. J Electromyogr Kinesiol. 2000; 10: 225-32.
4. Enoka RM, Duchateau J. Muscle fatigue: what, why and how it influences muscle function. J Physiol. 2008; 586: 11-23.
5. De Luca CJ, Gilmore LD, Kuznetsov M, Roy SH. Inter-electrode spacing of surface EMG sensors: reduction of crosstalk contamination during voluntary contractions. J Biomech. 2012; 45: 1806-11.
6. Roy SH, De Luca CJ, Cheng MS, Johansson A, Gilmore LD. Electro-mechanical stability of surface EMG sensors. Med Biol Eng Comput. 2007; 45: 447-57.
7. Hermens HJ, Freriks B, Merletti R, Stegeman D, Blok J, Rau G, et al. European recommendations for surface electromyography: results of the SENIAM project. Rofo. 1999; 171: 392-403.
8. Hughes BG, Brown SJ, Lucey A. Reliability of surface electromyographic measurements. Clin Neurophysiol. 1999; 110: 725-34.
9. Souza DR, Gross MT. Comparison of vastus medialis obliquus: vastus lateralis muscle integrated electromyographic ratios between healthy subjects and patients with patellofemoral pain. Phys Ther. 1991; 71: 310-6.
10. Morrish GM, Woledge RC, Haddad FS. Activity in three parts of the quadriceps recorded isometrically at two different knee angles and during a functional exercise. Electromyogr Clin Neurophysiol. 2003; 43: 259-65.

11. Dong C, Li M, Hao K, Zhao C, Piao K, Lin W, et al. Dose atrophy of vastus medialis obliquus and vastus lateralis exist in patients with patellofemoral pain syndrome. J Orthop Surg Res. 2021; 16: 128.
12. Grabiner MD, Owings TM. EMG differences between concentric and eccentric maximum voluntary contractions are evident prior to movement onset. Exp Brain Res. 2002; 145: 505-11.
13. Garner JC, Blackburn T, Weimar W, Campbell B. Comparison of electromyographic activity during eccentrically versus concentrically loaded isometric contractions. J Electromyogr Kinesiol. 2008; 18: 466-71.
14. Lindström L, Petersen I, Gorman RB. An electromyographic index for localized muscle fatigue. Acta Physiol Scand. 1970; 79: 500-8.
15. Dimitrova NA, Dimitrov GV. Interpretation of EMG changes with fatigue: facts, pitfalls, and fallacies. J Electromyogr Kinesiol. 2003; 13: 13-36.
16. Gandevia SC. Neural control and muscle fatigue. Acta Physiol Scand. 1998; 162: 275-83.
17. Linnamo V, Moritani T, Nicol C, Komi PV. Motor unit activation patterns during isometric, concentric and eccentric actions at different force levels. J Electromyogr Kinesiol. 2003; 13: 93-101.
18. Laidlaw DH, Bilodeau M, Enoka RM. Steadiness is reduced and motor unit discharge is more variable in old adults. J Appl Physiol (1985). 2000; 89: 1699-708.
19. Gandevia SC, Petersen NT, Butler JE, Taylor JL. Impaired response of human motoneurones to corticospinal stimulation after voluntary exercise. J Physiol. 1999; 521: 749-59.
20. Gerdle B, Larsson B, Karlsson S. Dependence of the mean power frequency of the electromyogram on muscle force and fibre type. Acta Physiol Scand. 1991; 142: 457-65.
21. Farina D, Merletti R, Enoka RM. The extraction of neural strategies from the surface EMG. J Appl Physiol (1985). 2004; 96: 1486-95.
22. Farina D, Holobar A, Merletti R, Enoka RM. Decoding the neural drive to muscles from the surface electromyogram. Clin Neurophysiol. 2010; 121: 1616-23.
23. Vieira TM, Botter A, Merletti R, et al. Higher specificity of high-density surface electromyography in comparison with traditional surface EMG for detection of muscle fatigue. J Electromyogr Kinesiol. 2019; 44: 102-10.
24. Gerdle B, Karlsson S, Larsson B, et al. Assessment of muscle fatigue: a multidisciplinary approach. Eur J Appl Physiol. 2000; 82: 197-208.
25. Hug F, Tucker K. Muscle coordination and control during dynamic human tasks: insights from surface electromyography. J Electromyogr Kinesiol. 2017; 36: 1-6.

Original Investigation | Özgün Araştırma

Gazi Med J 2026;37(3):358-362

DOI: http://dx.doi.org/10.12996/gmj.2026.4611

To Evaluate Sensitivity of Microcyte% and Macrocyte% Parameters in Comparison with Peripheral Blood Smear in Normocytic Normochromic Anemia Patients

Normositik Normokromik Anemi Hastalarında Mikroset% ve Makroset% Parametrelerinin Periferik Kan Yayması ile Karşılaştırmalı Olarak Duyarlılığını Değerlendirmek

Shramika M. Naik[1], Vikas D. Pathak[1], Harsha Dangare[2]

[1]Department of Pathology, Maharashtra Institute of Medical Education and Research (MAEER MIT PUNE), Dr. Bhausaheb Sardesai Talegaon Rural Hospital, Talegaon, Pune, Maharashtra, India
[2]Department of Pathology, MAEER MIT Pune's MIMER Medical College and Dr. BSTR Hospital, Maharashtra, India

ABSTRACT

Objective: To compare the sensitivity of microcyte and macrocyte percentage given by the automated cell counter with peripheral blood smear (PBS) in normocytic normochromic (NCNC) anaemia, and to set a normal range for microcyte and macrocyte% using the data from normal control samples.

Methods: It is a cross-sectional study; whole blood samples (EDTA vacutainer) were run on a six-part cell counter, and peripheral blood findings were entered into an Excel sheet. Inclusion criteria: Age more than 18 years and having NCNC anemia. Exclusion criteria: Patients with a history of recent blood transfusion or on haematinics.

Results: A total of 240 samples were studied. Research use only (RUO) microcyte% was 44.16%, RUO macrocyte% was 27.5%, and the mixed cell population group was 15.83%. Sensitivities of both research-use-only parameters were 100%, with specificities of 95% for RUO–microcyte% and 97.7% for RUO–macrocyte%, whereas diagnostic accuracy was 97.5% for RUO–microcyte% and 98.3% for RUO–macrocyte%.

CONCLUSION: Microcyte and macrocyte percentages provided by the machine are more sensitive, as they can screen millions of RBCs and are not dependent on the observer's skills, compared to PBS examination. Depending on the percentage of microcytic or macrocytic cells, we can recommend further confirmatory biochemical tests. Thus, we can identify a treatable underlying cause.

Keywords: Whole blood sample, automated cell counter, peripheral blood smear, microcyte% and macrocyte%

ÖZ

Amaç: Normositik normokromik (NCNC) anemide otomatik hücre sayacı tarafından verilen mikroset ve makroset yüzdesinin periferik kan yayması (PBS) ile duyarlılığını karşılaştırmak ve normal kontrol örneklerinden elde edilen verileri kullanarak mikroset ve makroset % için normal bir aralık belirlemek.

Yöntemler: Kesitsel bir çalışmadır; tam kan örnekleri (EDTA vakutainer) altı parçalı bir hücre sayacı üzerinde çalıştırıldı ve periferik kan bulguları bir Excel tablosuna kaydedildi. Dahil etme kriterleri: 18 yaşından büyük olmak ve NCNC anemisi bulunmak. Hariç tutma kriterleri: Yakın zamanda kan transfüzyonu geçirmiş veya hematiniks kullanan hastalar.

Bulgular: Toplamda 240 örnek incelendi. Araştırma amaçlı kullanım (RUO) mikro sit %44,16, RUO makro sit %27,5 ve karışık hücre popülasyonu grubu %15.83 idi. Her iki araştırma amaçlı parametrenin de duyarlılıkları %100 olup, RUO–mikrosit % için özgüllük %95 ve RUO–makrosit % için %97.7 iken, tanısal doğruluk RUO–mikrosit % için %97,5 ve RUO–makrosit % için %98,3'tür.

Sonuç: Makinenin sağladığı mikroasit ve makroasit yüzdeleri, milyonlarca RBC'yi tarayabildiği ve gözlemcinin becerilerine bağlı olmadığı için PBS incelemesine kıyasla daha hassastır. Mikrositik veya makrositik hücrelerin yüzdesine bağlı olarak, daha fazla doğrulayıcı biyokimyasal testler önerebiliriz. Böylece, tedavi edilebilir bir altta yatan nedeni belirleyebiliriz.

Anahtar Sözcükler: Tam kan örneği, otomatik hücre sayacı, periferik kan yayması, % mikrosit ve % makrosit

Cite this article as: Naik SM, Pathak VD, Dangare H. To evaluate sensitivity of microcyte% and macrocyte% parameters in comparison with peripheral blood smear in normocytic normochromic anemia patients. Gazi Med J. 2026;37(3):358-362

Address for Correspondence/Yazışma Adresi: Harsha Dangare, Department of Pathology, Maharashtra Institute of Medical Education and Research (MAEER MIT PUNE), Dr. Bhausaheb Sardesai Talegaon Rural Hospital, Talegaon, Pune, Maharashtra, India
E-mail / E-posta: dr.harshahj@gmail.com
ORCID ID: orcid.org/0000-0002-6347-9130

Received/Geliş Tarihi: 16.12.2025
Accepted/Kabul Tarihi: 05.04.2026
Publication Date/Yayınlanma Tarihi: 10.07.2026

INTRODUCTION

According to the World Health Organization, anaemia is a condition in which either the number of red blood cells (RBCs) or the Hb concentration within them is lower than normal. Anemia is defined as a Hb level <12.0 g/dL in women and <13.0 g/dL in men (1). The two common methods of classification of anaemia are morphologic and pathophysiologic. In the morphological classification, anaemia is subdivided into three major groups based on blood indices, particularly mean corpuscular volume (MCV) (2). According to the RBC morphology system for classifying anemia, there are three basic divisions in the morphologic classification:

a. Microcytic–MCV <80 fL

b. Macrocytic–MCV >100 fL

c. Normocytic–MCV 80–100 fL

MCV is the mean volume of RBCs in a sample. It may serve as a useful parameter to classify anemias based on RBC size (3). The MCV is the average volume of RBCs; it was previously calculated from the hematocrit (volume of packed red cells) and the erythrocyte count. Modern hematology analyzers perform cell sizing; therefore, the MCV is a measured parameter (4).

Since the MCV is the mean volume of RBCs, it does not reflect variation in RBC size within the sample. A sample with a normal MCV may have groups of smaller and/or larger RBCs within the total counted population. The excessive variation in RBC size is known as anisocytosis. It is assessed by a pathologist by reviewing a peripheral blood smear (PBS).

Thus, MCV must always be interpreted in conjunction with a review of the PBS, RDW, RBC graph, and reticulocyte count.

Automated cell counter Mindray BC-6000/BC-6000 Plus has research use only (RUO) parameters named microcyte% and macrocyte% (5). Microcyte% and fraction: in this machine, all cells in the RBC chamber with volumes less than 60 fL are counted. Macrocyte% and fraction—in this machine, all cells in the RBC chamber with volumes greater than 120 fL are counted (6). These indices are rapidly obtained, inexpensive, and can be effective as preliminary screening tools (5). On PBS examination, anisocytosis can be detected, but there are limitations for the observer. In PBS, we can screen up to a thousand cells. The microcyte and macrocyte% (RUO parameters) provided by the machine (Mindray BC6000) are available free of charge and can be used as screening tests to determine microcytic and macrocytic cell percentages. It is more sensitive than PBS examination, as it can screen millions of RBCs and is not dependent on the observer's skills. Depending on the percentage of microcyte or macrocyte cells, we can advise further confirmatory biochemical tests. Thus, we can reach a treatable underlying cause.

These parameters will be useful in cases of falsely normal MCV resulting from two distinct cell populations. Normocytic normochromic (NCNC) anemia causes are anemia of chronic disease (ACD), acute blood loss, chronic renal failure, hemolytic anemia, and mixed nutritional deficiency, etc. The pathogenesis, epidemiology, and clinical characteristics of NCNC anemia of unknown cause are not well established (7).

The study was conducted with the overall aim of evaluating the sensitivity of microcyte and macrocyte percentages given by the cell counter compared with PBS in NCNC anaemia.

Aims and Objectives

1. To compare sensitivity of microcyte and macrocyte percentage given on Mindray BC6000 with morphological findings on PBS in NCNC anaemic patients.

2. To set normal range for microcyte and macrocyte% (RUO parameter) using the data from 120 normal control samples.

MATERIALS AND METHODS

A cross-sectional study was conducted at the central clinical laboratory, Department of Pathology, in a tertiary care hospital. A sample size of 120 was calculated at a precision of 0.1 and a 95% confidence interval using the following formula (8).

Formula used: $n = z^2S (1-S) / d^2$, where z^2 is the area under the curve for the confidence level, S is the sensitivity, and d is the absolute precision. n = (a + b + c + d).

A consecutive and purposive sampling procedure was used. Each of the 120 samples was studied for the anaemic and control groups. Patients above 18 years of age with Hb <12 gm% in females and <13 gm% in males with normal MCV (80–100 fL) were included. The control group includes individuals above 18 years with normal MCV & normal haemoglobin for gender. The control group includes individuals older than 18 years with normal MCV and normal haemoglobin for their gender. Patients who had a recent blood transfusion or were on haematinic supplements were excluded from the study. Venous blood samples were drawn into vacutainers containing K2-EDTA anticoagulant. Samples were stored at ambient temperature and processed within 6 hours of collection. Data obtained from analysis of an EDTA-anticoagulated whole-blood sample on a six-part differential cell counter (Mindray BC 6000), together with peripheral blood findings, were entered into an Excel sheet. The analyzer was calibrated, controlled, and maintained according to the manufacturer's recommendations. The variables studied were MCV, PBS, microcyte% and macrocyte% (RUO parameter).

Maharashtra Institute of Medical Education and Research (MAEER MIT PUNE), Dr. Bhausaheb Sardesai Talegaon Rural Hospital Ethics Committee approval was obtained (EIC reference no MIMER/IEC/1832/09/2021, dated 21.09.2021). Written informed consent was obtained from the study participants. No additional cost was incurred by the study participants.

Statistical Analysis

Statistical analysis: mean, range, and standard deviation were calculated for the control group using IBM SPSS Software version 26.

Using the mean and standard deviation, cut-offs were obtained from the control group, and data from the study group were analyzed and correlated with peripheral smear findings.

RESULTS

A total of 240 samples were included in the study, of which 120 were in the NCNC anemia group (shown in Figure 1) and 120 were in the control group with normal Hb and MCV.

The gender-wise distribution shown in Table 1 indicates an equal distribution of samples between males and females.

Reference ranges were obtained for the parameters MCV, RUO–microcyte%, and RUO–macrocyte% using data from the control group, as depicted in Table 2.

Table 3 shows the study-group analysis from the automated cell counter, reporting RUO–microcyte% as 44.16%, RUO–macrocyte% as 27.5%, and 15.83% in the mixed cell population group.

Table 4 compares all three groups assessed with the automated cell counter and PBS and shows comparable results for RUO–microcyte% and RUO–macrocyte%.

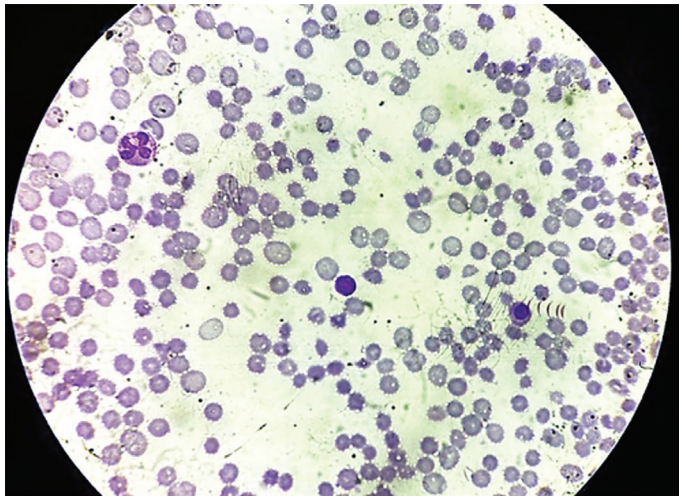

Figure 1. Microphotograph (40x) showing macrocytic and microcytic population of cells on peripheral blood smear.

Table 1. Gender wise distribution of control and study group.

	Control group (normal hemoglobin)	Study group (anemic patients)
Males	64 (53.33%)	65 (54.16%)
Females	56 (46.67%)	55 (45.84%)

Table 2. Reference range of parameters using data from control group.

Parametres	Mean	SD	Reference range, (mean ± SD)
MCV-fL	87.20	8.45	87 ± 16.9
RUO-microcyte%	1.16	1.09	0–3.34
RUO-macrocyte%	2.55	1.51	0–5.57

SD: Standard deviation, RUO: Research use only, MVC: Mean corpuscular volume.

Table 3. RUO percentage values of automated cell counter in study group.

Parameters	Total no of patients	Percentage
RUO-microcyte%	53/120	44.16
RUO-macrocyte%	33/120	27.5
Total	86/120	71.66
Mixed cell population	19/120	15.83

RUO: Research use only.

Table 5 shows 100% sensitivity for both RUO parameters, 95% specificity for RUO–microcyte

%, and 97.7% for RUO–Macrocyte%, whereas the Diagnostic accuracy of RUO–microcyte% is 97.5% and 98.3% for RUO–macrocyte%.

DISCUSSION

With advances in technology over the last 10–15 years, additional RBC parameters have been introduced on automated hematology analyzers. Although many of these advanced indices are currently available on hematology analyzers as RUO parameters, there is increasing evidence of their clinical importance in the diagnosis and in the assessment of the severity of anemia, as well as in monitoring treatment response. These advanced RBC parameters are: mean cellular Hb concentration, calculated cellular Hb, Hb distribution width, percent microcytosis (%MIC), percent macrocytosis (%MAC), percent hypochromia, and percent hyperchromia. The present study focused on %MIC and %MAC.

$$\text{RUO–microcyte\%} = \frac{\text{The number of RBC smaller than 60 fL}}{\text{Total number of RBC}} \times 100\%$$

$$\text{RUO–macrocyte\%} = \frac{\text{The number of RBC larger than 120 fL}}{\text{Total number of RBC}} \times 100\%$$

The percent microcytic RBCs (%MIC) represents the proportion of microcytic RBCs in a sample. The %MIC is derived from the RBC volume distribution histogram and usually includes RBCs with volumes below 60 fL, as shown in Figure 2 (9,10). %MIC can be used in combination with other RBC parameters to help differentiate between iron deficiency anemia (IDA) and thalassemia (11). The percent macrocytic RBC (%MAC) is the proportion of macrocytic RBCs in a sample, reported as a percentage. The %MAC is derived from the RBC volume distribution histogram and usually includes RBCs with volumes above 120 fL. The frequency of microcytic and macrocytic RBCs can be assessed by visual estimation on a stained

Table 4. Comparison of RUO percentage values given by automated cell counter and peripheral blood smear in study group.

Parameters	Automated cell counter	Peripheral smear (gold standard)	Comparison percentage
RUO-microcyte%	53 (44.16%)	50 (41.66%)	94.33%
RUO-macrocyte%	33 (27.5%)	31 (25.83%)	93.93%
Mixed cell population	19 (15.83%)	16 (13.33%)	84.21%

RUO: Research use only.

Table 5. Sensitivity, specificity and diagnostic accuracy of RUO parameters compared to peripheral smear findings.

	RUO-microcyte%	RUO-macrocyte%
Sensitivity	100%	100%
Specificity	95%	97.7%
Diagnostic accuracy	97.5%	98.3%

RUO: Research use only.

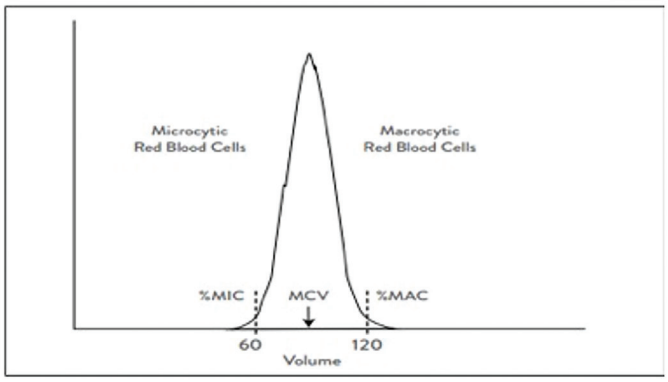

Figure 2. RBC distribution histogram depicting MIC% and MAC%.

MIC%: Percent microcytosis, MAC%: Percent macrocytosis, RBC: Red blood cell.

PBS. The %MIC and %MAC from automated hematology analyzers, however, offer a more precise quantitation. A low degree of anisocytosis cannot be easily diagnosed on a peripheral smear, as a trained and skilled person is required for such interpretation

On PBS, we can screen only a limited number of cells, up to thousands. The microcyte and macrocyte percentages provided by the machine are available at no cost and can be used as screening measures to determine the proportions of microcytic and macrocytic cells. It is more sensitive as it can screen millions of RBC and is not dependent on the observer's skills compared to PBS examination.

NCNC anemia is caused by many conditions. Depending on the percentage of microcytic or macrocytic cells, we recommend further confirmatory biochemical testing. Thus, we can identify a treatable underlying cause, such as nutritional deficiency, and avoid further invasive procedures.

Barton JC conducted a study quantifying microcyte and macrocyte percentages in archived RBC volume histogram images. They used a tool to analyse the RBC graph and calculate the percentage, whereas the present study calculates the percentage using the machine itself (6).

The study conducted by Urrechaga (12) evaluated the discriminant index value of the ratio of % microcytic cells to % hypochromic cells (i.e., M/H ratio) in the differential diagnosis of microcytic anemia. The M/H ratio used by him is a useful parameter to differentiate between IDA and beta thalassemia trait; the latter shows a distinct pattern of microcytic and hypochromic cells that can be detected by this parameter.

There are no studies conducted on the utilisation of micro% and macro% in NCNC anemias.

ACD is the second most common cause of anemia after iron deficiency (13).

A study by Singh et al. (14) showed a 44.88% prevalence of normocytic anemia.

The pathophysiology involves dysregulation of iron metabolism due to chronic inflammation (13). Most patients with ACD present with normocytic, normochromic, or mildly hypochromic RBCs. The MCV is usually in the range of 75–82 fL, and the HGB is rarely less than 9.0 g/dL. MCH, MCHC, and RDW are within normal limits. Additionally, serum iron, transferrin saturation, and total iron-binding capacity may be decreased, but serum ferritin is normal or elevated (15).

Functional iron deficiency occurs when iron stores are transiently unable to meet the demands of increased erythropoiesis, usually during treatment with erythropoietin-stimulating agents (16).

Normocytic, normochromic anemia differs from other forms of anemia because the average size and Hb content of RBCs are typically within normal limits. RBCs typically appear similar to normal cells under microscopic examination; however, in some cases variations in size and shape may offset one another, resulting in mean values within the normal range (17). ACD is usually a mild-to-moderate, normocytic, normochromicanemia; it evolves over time to become hypochromic and, more rarely, microcytic. Less than 25% of NCNC anemia cases progress to microcytic hypochromic anemia; in such cases, the MCV is rarely less than 70 (18).

The dimorphic blood picture reveals a dual- cell population on PBS, whereas indices displayed by automated cell counters may indicate low, normal, or high MCV. Such a diagnosis cannot rely solely on results from an automated cell counter because this may lead to inaccuracies (19). Therefore, it is essential to examine all cell populations using PBS, and it can be better predicted using microcyte% and macrocyte% measured by an automated cell counter.

Iron-deficiency anemia in its early stages can appear as normocytic, normochromic anemia. Iron-deficient erythropoiesis is characterized by the production of RBCs with decreased Hb content, leading to a high percentage of hypochromic cells; these cells also tend to be more microcytic as depletion progresses. Because of their long lifespan, several cohorts of normocytic and microcytic RBCs coexist in the peripheral blood, leading to anisocytosis (20).

Mohammed and Mahmood (21) in their research, concluded that normochromic anemia is the most prevalent anemia associated with renal disease. Anemia frequently occurs as a complication of various chronic illnesses, particularly chronic kidney disease; it is often referred to as anemia of renal disease and is associated with iron deficiency. This condition is typically linked to diminished quality of life and increased mortality and morbidity in patients (21). Thus, these new parameters, microcyte% and macrocyte%, can be helpful in such cases.

Study Limitations

A smaller sample size and confirmatory biochemical tests were not available in this scenario, but they should be used in combination with these parameters.

CONCLUSION

To conclude, this study helped us set cutoffs for microcyte% and macrocyte%: microcyte% greater than 3.34 and macrocyte% greater than 5.57 should be considered abnormal for the given population. Patients with elevated values, depending on the type of measurement, should be evaluated for iron deficiency, vitamin B12 deficiency, or both.

In resource-constrained conditions where a skilled pathologist is not available, RUO–Microcyte% and RUO–macrocyte% provided by the automated cell counter are more sensitive as they can screen

millions of RBC and are not dependent on observer skills compared to PBS examination.

Ethics

Ethics Committee Approval: Maharashtra Institute of Medical Education and Research (MAEER MIT PUNE), Dr. Bhausaheb Sardesai Talegaon Rural Hospital Ethics Committee approval was obtained (EIC reference no MIMER/IEC/1832/09/2021, dated 21.09.2021).

Informed Consent: Written informed consent was obtained from the study participants. No additional cost was incurred by the study participants.

Footnotes

Authorship Contributions

Surgical and Medical Practices: S.M.N., Concept: H.D., Design: H.D., Data Collection or Processing: S.M.N., V.D.P., Analysis or Interpretation: S.M.N., V.D.P., Literature Search: S.M.N., Writing: S.M.N.

Conflict of Interest: No conflict of interest was declared by the authors.

Financial Disclosure: The authors declared that this study received no financial support.

REFERENCES

1. World Health Organization. Handbook for guideline development. Geneva: World Health Organization; 2010. Available from: https://www.who.int/health-topics/anaemia#tab=tab_1
2. Jeong SW, Cho CH. A attempt of morphological classification of anemias using MCV. Korean J Clin Lab Sci. 1998; 30: 34-42.
3. Kuter DJ. Thrombopoietin: biology and clinical applications. Oncologist. 1996; 1: 98-106.
4. Steine-Martin E, Lotspeich-Steininger CA, Koepke JA, editors. Clinical hematology: principles, procedures, correlations. 2nd ed. Philadelphia: Lippincott-Raven Publishers; 1998.
5. Mindray Medical International Limited. BC-6000 Series Auto Hematology Analyzer. Available from: https://www.mindray.com/en/minisite/BC-6000series/6000.html
6. Barton JC, Barton JC. Quantifying microcyte and macrocyte percentages in archived red blood cell volume histogram images. Int J Lab Hematol. 2023; 45: 875-80.
7. Yilmaz G, Shaikh H. Normochromic normocytic anemia. In: StatPearls [Internet]. Treasure Island (FL): StatPearls Publishing; 2026.
8. Pourhoseingholi MA, Vahedi M, Rahimzadeh M. Sample size calculation in medical studies. Gastroenterol Hepatol Bed Bench. 2013; 6: 14-7.
9. Hoffmann JJ, van den Broek NM, Curvers J. Reference intervals of extended erythrocyte and reticulocyte parameters. Clin Chem Lab Med. 2012; 50: 941-8.
10. Sysmex Europe. The Microcytic (MicroR) and Macrocytic (MacroR) red blood cell populations. Available from: https://www.sysmex-europe.com/academy/knowledge-centre/sysmex-parameters/micrormacror/
11. d'Onofrio G, Zini G, Ricerca BM, Mancini S, Mango G. Automated measurement of red blood cell microcytosis and hypochromia in iron deficiency and beta-thalassemia trait. Arch Pathol Lab Med. 1992; 116: 84-9.
12. Urrechaga E. Discriminant value of % microcytic/% hypochromic ratio in the differential diagnosis of microcytic anemia. Clin Chem Lab Med. 2008; 46: 1752-8.
13. Kujovich JL. Evaluation of anemia. Obstet Gynecol Clin North Am. 2016; 43: 247-64.
14. Singh B, Verma SP, Chauhan AS, Verma DP. Prevalence of anemia among reproductive-age females in the Tharu tribe of the Indo-Nepal border region. J Family Med Prim Care. 2022; 11: 2961-4.
15. Wahed A, Dasgupta A. Red blood cell disorders. In: Hematology and coagulation: a comprehensive review for board preparation, certification and clinical practice. 2nd ed. Waltham: Elsevier; 2015. p. 31-49.
16. Piva E, Brugnara C, Spolaore F, Plebani M. Clinical utility of reticulocyte parameters. Clin Lab Med. 2015; 35: 133-63.
17. Smock KJ. Examination of blood and bone marrow. In: Greer JP, Arber DA, Glader B, List AF, Means RT Jr, Rodgers GM, et al., editors. Wintrobe's clinical hematology. 14th ed. Philadelphia: Wolters Kluwer; 2018. p. 1-16.
18. Caporal FA, Comar SR. Evaluation of RDW-CV, RDW-SD, and MATH-1SD for the detection of erythrocyte anisocytosis observed by optical microscopy. J Bras Patol Med Lab. 2013; 49: 324-31.
19. Shrivastav A, Shah N, Goyal S, Shah CK. RBC histogram: utility in diagnosis of various anemia. Int J Clin Diagn Pathol. 2019; 2: 14-7.
20. Juncà J, Flores A, Roy C, Alberti R, Millá F. Red cell distribution width, free erythrocyte protoporphyrin, and England-Fraser index in the differential diagnosis of microcytosis due to iron deficiency or beta-thalassemia trait: a study of 200 cases of microcytic anemia. Hematol Pathol. 1991; 5: 33-6.
21. Mohammed MR, Mahmood B. Morphological types of anemia associated with chronic renal diseases. Open Access Maced J Med Sci. 2022; 10: 905-8.

Gazi Med J 2026;37(3):363-368

DOI: http://dx.doi.org/10.12996/gmj.2026.4631

Short-Term Real-World Clinical Outcomes of the Fixed-Ratio Combination of Insulin Glargine and Lixisenatide in Type 2 Diabetes

Tip 2 Diyabette İnsülin Glarjin ve Liksisenatid Sabit Oranlı Kombinasyonunun Kısa Dönem Gerçek Yaşam Klinik Sonuçları

Enes Üçgül, Burak Menekşe, Burçak Çavnar Helvacı, Bekir Uçan, Erman Çakal

Department of Endocrinology and Metabolism, University of Health Sciences Türkiye, Ankara Etlik City Hospital, Ankara,

Objective: To assess the short-term real-world effects of the fixed-ratio combination of insulin glargine and lixisenatide (iGlarLixi) on glycemic control, body weight, insulin requirements, and the Fibrosis-4 (FIB-4) score in adults with type 2 diabetes mellitus (T2DM).

Methods: This retrospective study screened 122 adults initiated on iGlarLixi between January 1 and April 1, 2025. After excluding 40 patients who were receiving additional antidiabetic therapy and 12 who discontinued treatment due to intolerance or loss to follow-up, 70 patients were included in the final analysis. Body weight, body mass index, HbA1c, daily insulin dose, and FIB-4 were recorded at baseline and at 3 months. Paired t-tests or Wilcoxon signed-rank tests were used for continuous variables, and chi-square or Fisher's exact tests were used for categorical outcomes.

Results: Median age was 57 years, and 85.7% were female. Median baseline HbA1c was 9.05%, and the median FIB-4 was 0.91. At 3 months, weight decreased from 106.5 to 104 kg ($p < 0.001$), HbA1c decreased from 9.05% to 8.4% ($p < 0.001$), and insulin dose decreased from 27 to 24 U/day ($p < 0.001$). FIB-4 decreased modestly but significantly, from 0.91 to 0.85 ($p = 0.03$). In patients who added iGlarLixi to oral therapy, weight, HbA1c, and FIB-4 improved significantly (all $p < 0.03$). Among those switching from basal insulin to iGlarLixi, HbA1c and insulin dose decreased (both $p < 0.001$); weight change was minimal; and FIB-4 was unchanged ($p = 0.308$). Gastrointestinal adverse events occurred in 10% of cases; they were mild to moderate, and did not lead to discontinuation.

Amaç: Bu çalışmanın amacı, tip 2 diyabet mellituslu (T2DM) erişkinlerde insülin glarjin ve liksisenatid sabit oranlı kombinasyonunun (iGlarLixi) kısa dönem gerçek yaşam etkilerini; glisemik kontrol, vücut ağırlığı, insülin gereksinimi ve Fibrozis-4 (FIB-4) skoru üzerindeki değişimler açısından değerlendirmektir.

Yöntemler: Bu retrospektif çalışmada, 1 Ocak ile 1 Nisan 2025 tarihleri arasında iGlarLixi tedavisi başlanan 122 yetişkin hasta tarandı. Ek antidiyabetik tedavi alan 40 hasta ile intolerans veya takip kaybı nedeniyle tedaviyi bırakan 12 hastanın dışlanmasının ardından, 70 hasta nihai analize dahil edildi. Vücut ağırlığı, beden kitle indeksi, HbA1c, günlük insülin dozu ve FIB-4 değerleri başlangıçta ve 3. ayda kaydedildi. Sürekli değişkenler için eşleştirilmiş t-testi veya Wilcoxon işaretli sıralar testi, kategorik değişkenler için ki-kare veya Fisher kesin testi kullanıldı.

Bulgular: Medyan yaş 57 yıl olup hastaların %85,7'si kadındı. Medyan başlangıç HbA1c değeri %9,05 ve medyan FIB-4 skoru 0,91 idi. Üçüncü ayda vücut ağırlığı 106,5 kg'dan 104 kg'a ($p < 0,001$), HbA1c %9,05'ten %8,4'e ($p < 0,001$) ve günlük insülin dozu 27 U/gün'den 24 U/gün'e ($p < 0,001$) düştü. FIB-4 skoru da mütevazı ancak istatistiksel olarak anlamlı şekilde azaldı (0,91'den 0,85'e, $p = 0,03$). iGlarLixi'nin oral tedaviye eklendiği hastalarda vücut ağırlığı, HbA1c ve FIB-4 anlamlı olarak iyileşti (tümü $p < 0,03$). Bazal insülinden iGlarLixi'ye geçilen hastalarda HbA1c ve insülin dozu azaldı (her ikisi için $p < 0,001$), vücut ağırlığındaki değişim minimaldi ve FIB-4 değişmedi ($p = 0,308$). Gastrointestinal yan etkiler olguların %10'unda görüldü, hafif-orta şiddetteydi ve tedavinin kesilmesine yol açmadı.

Cite this article as: Üçgül E, Menekşe B, Çavnar Helvacı B, Uçan B, Çakal E. Short-term real-world clinical outcomes of the fixed-ratio combination of insulin glargine and lixisenatide in type 2 diabetes. Gazi Med J. 2026;37(3):363-368

Address for Correspondence/Yazışma Adresi: Enes Üçgül, Department of Endocrinology and Metabolism, University of Health Sciences Türkiye, Ankara Etlik City Hospital, Ankara, Türkiye
E-mail / E-posta: enes-ucgul@hotmail.com
ORCID ID: orcid.org/0000-0002-6858-751X

Received/Geliş Tarihi: 21.01.2026
Accepted/Kabul Tarihi: 25.03.2026
Publication Date/Yayınlanma Tarihi: 10.07.2026

ABSTRACT

CONCLUSION: iGlarLixi improved glycemic control, reduced insulin requirements, and promoted weight loss in adults with poorly controlled T2DM. When added to oral antidiabetic therapy, iGlarLixi was also associated with a modest but significant reduction in FIB-4, suggesting potential benefits for the liver.

Keywords: Type 2 diabetes mellitus, insulin glargine/lixisenatide fixed-ratio combination, glycemic control, FIB-4 score, body weight

ÖZ

Sonuç: iGlarLixi, kötü kontrollü T2DM'li erişkinlerde glisemik kontrolü iyileştirmiş, insülin gereksinimini azaltmış ve kilo kaybını desteklemiştir. Oral antidiyabetik tedaviye eklendiğinde, iGlarLixi'nin FIB-4 skorunda da mütevazı ancak anlamlı bir azalma ile ilişkili olması, karaciğer açısından potansiyel faydalara işaret etmektedir.

Anahtar Sözcükler: Tip 2 diyabet mellitus, insülin glarjin/liksisenatid sabit oranlı kombinasyonu, glisemik kontrol, FIB-4 skoru, vücut ağırlığı

INTRODUCTION

Type 2 diabetes mellitus (T2DM) is a progressive metabolic disorder characterized by chronic hyperglycemia and insulin resistance, frequently accompanied by obesity and other cardiometabolic comorbidities (1,2). Despite advances in pharmacological treatment, maintaining adequate glycemic control remains difficult, especially in patients with long-standing disease who are already on basal insulin or multiple oral antidiabetic drugs (OADs) (3).

Obesity significantly contributes to the development and progression of T2DM, thereby making the achievement of optimal glycemic targets more challenging in affected individuals (4,5). Consequently, glucagon-like peptide-1 receptor agonists (GLP-1 RAs) have emerged as cornerstones in the management of both diabetes and obesity. These agents have consistently demonstrated efficacy in improving glycemic control, reducing body weight, and providing additional benefits for cardiovascular and liver (6). Moreover, fixed-ratio combinations of basal insulin and GLP-1 RAs, such as insulin glargine/lixisenatide, provide complementary mechanisms of action by simultaneously targeting fasting and postprandial glucose levels and mitigating insulin-associated weight gain. Their therapeutic effects are mediated through multiple pathways, including delayed gastric emptying, glucose-dependent modulation of insulin secretion, and central regulation of appetite. Although randomized trials have demonstrated their efficacy, real-world data on their impact on metabolic and liver parameters are limited (7,8).

Metabolic dysfunction–associated steatotic liver disease (MASLD) is the leading cause of chronic liver disease. Therefore, preventing MASLD and detecting the risk of liver fibrosis (FIB) early are of critical clinical importance. To this end, clinicians frequently use various non-invasive assessment tools, including the fatty liver index, hepatic steatosis index, and the FIB-4 score (9). Notably, the FIB4 score is strongly recommended for monitoring patients with diabetes who are at risk of liver FIB. However, its responsiveness to fixed-ratio combinations of insulin and GLP-1 RAs therapies has not been thoroughly studied (10,11).

This study aimed to evaluate the effects of adding or switching to a fixed-ratio combination of insulin glargine/lixisenatide (iGlarLixi) on glycemic control, body weight, insulin requirements, and FIB-4 scores in patients with type 2 diabetes.

MATERIALS AND METHODS

Study Design and Participants

This retrospective observational study included adult patients (≥18 years) with T2DM who were initiated on iGlarLixi at our Endocrinology and Metabolism Clinic. A total of 70 patients meeting the inclusion criteria between January 1, 2025, and April 1, 2025, were enrolled.

Inclusion criteria were: (1) age ≥18 years, (2) diagnosis of T2DM according to the American Diabetes Association criteria (12), and (3) initiation of iGlarLixi. Exclusion criteria were: (1) addition of any new antidiabetic agents (oral or injectable) at the time of initiation or during the 3-month follow-up period; (2) insufficient baseline or follow-up data; and (3) discontinuation of therapy within the first 3 months due to adverse effects or other reasons.

Out of 122 screened patients, 40 were excluded for receiving additional antidiabetic therapy, and 12 discontinued treatment within the first 3 months due to intolerance or other reasons. Consequently, 70 patients were included in the final analysis. The process of patient selection is summarized in Figure 1.

Data Collection

Data on body weight (kg), body mass index [(BMI), kg/m²], glycated hemoglobin (HbA1c, %), daily total insulin dose (units), FIB-4, and other treatment-related adverse effects were collected at the baseline (month 0) and after 3 months (month 3). Adverse effects were recorded based on patient reports and medical records. The FIB-4 score was calculated using the following validated formula:

$$\text{FIB-4} = \frac{\text{Age [years]} \times \text{AST [U/L]}}{\text{Platelet count [}10^9\text{/L]} \times \sqrt{\text{ALT [U/L]}}}$$

where AST is aspartate aminotransferase and ALT is alanine aminotransferase (13).

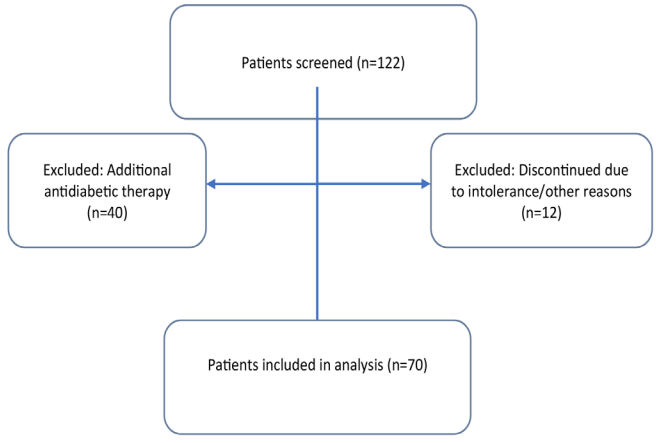

Figure 1. Patient flow chart.

Statistical Analysis

Continuous variables were presented as mean ± standard deviation or median with interquartile range (IQR), depending on their distribution. Comparisons between baseline and 3-month values were performed using paired-sample t-tests or Wilcoxon signed-rank tests, as appropriate. Categorical variables, including hypoglycemic events and other adverse effects, were expressed as counts and percentages and were compared using the chi-square or Fisher's exact tests. The correlation between changes in FIB-4 and body weight over the 3-month period was assessed using Spearman's rank correlation coefficient (for non-normally distributed data). A p-value <0.05 was considered statistically significant. All analyses were conducted using IBM SPSS Statistics (version 27.0).

Ethical Considerations

All study procedures adhered to the Declaration of Helsinki, and ethical approval was obtained from the University of Health Sciences Türkiye, Ankara Etlik City Hospital Ethics Committee (approval number/date: AEŞH-BADEK2-2025-379/05-08-2025, dated 05.08.2025). Due to the retrospective nature of the study, the requirement for informed consent was waived.

RESULTS

Baseline Characteristics

A total of 70 patients were analyzed. The median age was 57 years (IQR: 51.4–62.7), and 85.7% were female. The median BMI and body weight were 41.95 kg/m² (IQR: 38.05–45.85) and 106.5 kg (IQR: 94–114.25), respectively. The median duration of diabetes was 12 years (IQR: 8.0–16.25), with a baseline HbA1c of 9.05% (IQR: 8.35–10.05). The baseline FIB-4 score was 0.91 (IQR: 0.65–1.09). The median total daily insulin dose was 27 units (IQR: 20–56.2). Gastrointestinal adverse events (GI AEs) were reported in 10% of patients. These baseline demographic and clinical characteristics are summarized in Table 1.

Overall Changes from Baseline to the Third Month

Changes in clinical and laboratory parameters from baseline to the third month of treatment are summarized in Table 2. There was a statistically significant reduction in body weight [median 106.5 kg (IQR: 94–114.25) vs. 104 kg (IQR: 93.75–113.25); p < 0.001] and HbA1c levels [median 9.05% (IQR: 8.35–10.05) vs. 8.4% (IQR: 7.3–9.0); p < 0.001]. The FIB-4 score also showed a modest but significant decrease [median 0.91 (IQR: 0.65–1.09) vs. 0.85 (IQR: 0.63–1.03); p = 0.03]. Additionally, the median total daily insulin dose decreased from 27 units (IQR: 20–56.2) to 24 units (IQR: 17.75–50) (p < 0.001). During the 3-month follow-up, 4 patients (5.1%) reported hypoglycemia; all episodes were mild.

Subgroup Analysis: Addition of iGlarLixi to OAD

The changes observed after adding iGlarLixi to ongoing OAD therapy are presented in Table 3. There was a significant reduction in body

Table 1. Baseline demographic and clinical characteristics of the study population.

Demographic and clinical variables	Median [IQR]/n (%)
Age (years)	57 [51.4–62.7]
Sex (female/male)	60 (85.7%) / 10 (14.3%)
BMI (kg/m²)	41.95 [38.05–45.85]
Body weight (kg)	106.5 [94–114.25]
Duration of diabetes (years)	12 [8.0–16.25]
HbA1c (%)	9.05 [8.35–10.05]
Baseline FIB-4 score	0.91 [0.65–1.09]
Total insulin dose (U/day)	27 [20–56.2]
Number of patients with GI AEs	7 (10%)
Hypoglycemia events, n (%)	4 (5.1%)

BMI: Body mass index, FIB-4: Fibrosis-4 score, GI AEs: Gastrointestinal adverse events, HbA1c: Glycated hemoglobin, IQR: Interquartile range.

Table 2. Comparison of clinical and laboratory parameters between baseline and the third month of treatment.

Parameter	Baseline median [IQR]	3rd month median [IQR]	p-value
Body weight (kg)	106.5 [94–114.25]	104 [93.75–113.25]	<0.001
HbA1c (%)	9.05 [8.35–10.05]	8.4 [7.3–9.0]	<0.001
FIB-4 score	0.91 [0.65–1.09]	0.85 [0.63–1.03]	0.030
Total insulin dose (U/day)	27 [20–56.2]	24 [17.75–50]	<0.001
Hypoglycemia events, n (%)	N/A	4 (5.1%)	N/A

FIB-4: Fibrosis-4 index, HbA1c: Glycated hemoglobin, N/A; Not available, IQR: Interquartile range.

Table 3. Changes in clinical and laboratory parameters after adding iGlarLixi to OAD.

Parameter	Baseline median [IQR]	3rd month median [IQR]	p-value
Body weight (kg)	104.5 [90.75–114.25]	102 [90.75–112.25]	0.005
HbA1c (%)	9.15 [8.17–9.9]	8.0 [7.2–9.0]	<0.001
FIB-4	0.92 [0.61–1.21]	0.84 [0.63–1.04]	0.030
Total insulin dose (U/day)	20 [14–21]	26 [18–34]	0.002

FIB-4: Fibrosis-4 score, HbA1c: Glycated hemoglobin, OAD: Oral antidiabetic drug, IQR: Interquartile range.

weight [median 104.5 kg (IQR: 90.75–114.25) vs. 102 kg (IQR: 90.75–112.25); p = 0.005] and HbA1c levels [median 9.15% (IQR: 8.17–9.9) vs. 8.0% (IQR: 7.2–9.0); p < 0.001]. The FIB4 score also decreased significantly [median 0.92 (IQR: 0.61–1.21) vs. 0.84 (IQR: 0.63–1.04); p = 0.03]. The baseline median insulin dose in this subgroup was 20 units/day (IQR: 14–21). Furthermore, the total daily insulin dose increased modestly during the 3-month follow-up [26 (IQR: 18–34); p = 0.002], reflecting treatment intensification and active dose titration to improve glycemic control.

Table 4 examines the correlation between changes in FIB-4 score and changes in body weight among patients on OADs with add-on iGlarLixi therapy. Spearman's rank analysis showed a weak, non-significant positive correlation between ΔFIB-4 and Δbody weight (ρ = 0.191, p = 0.312).

Subgroup Analysis: Switching from Insulin Glargine to iGlarLixi

Among patients who switched from insulin glargine to iGlarLixi, HbA1c [9% (IQR: 8.5–10.4) to 8.5% (IQR: 7.3–9.5); p < 0.001] and total daily insulin dose [50 units (IQR: 26–82) to 34 units (IQR: 20–64); p < 0.001] decreased significantly. Weight reduction was also statistically significant, but minimal [from 107 kg (IQR: 96–116) to 107 kg (IQR: 95–114); p < 0.001]. No significant change was observed in the FIB-4 score (p = 0.308; Table 5).

DISCUSSION

In this study, we evaluated the effects of iGlarLixi combination therapy on glycemic control, FIB-4 score, body weight, and insulin requirements in patients with T2DM. After three months of treatment, we observed significant reductions in HbA1c, body weight, and total daily insulin dose; these changes were accompanied by a modest but statistically significant decrease in FIB-4 in the overall cohort and were particularly evident among patients who received combination therapy in addition to OADs. Notably, patients who switched from insulin glargine to iGlarLixi achieved improved glycemic control with a substantially lower insulin requirement. These findings highlight the potential of combining basal insulin with a GLP-1 RA to enhance glycemic outcomes, reduce insulin need, and favorably impact surrogate markers of liver FIB in patients with long-standing, poorly controlled T2DM.

Table 4. Correlation between FIB-4 score changes and body weight in patients using OAD.

Variables	Spearman's ρ	p-value
ΔFIB-4 vs. Δbody weight	0.191	0.312

Δ: Change; FIB-4: Fibrosis-4 score, OAD: Oral antidiabetic drugs.

In the present study, switching from insulin glargine to iGlarLixi or adding iGlarLixi to OADs improved both glycemic control and weight management. In both groups, significant reductions in HbA1c level and weight were observed. These results are consistent with the existing literature (14,15). In a systematic review and meta-analysis comparing premixed and basal insulin with insulin glargine/lixisenatide, iGlarLixi was superior to premixed insulin and to basal-plus regimens in reducing HbA1c and managing weight. Furthermore, the basal bolus regimen had a similar effect on HbA1c as the insulin glargine/lixisenatide combination (14). In addition, Goldman and Trujillo (16) demonstrated that combination therapy with insulin glargine and lixisenatide resulted in a greater reduction in HbA1c compared with either glargine or lixisenatide alone. Notably, despite this enhanced glycemic effect, the incidence of hypoglycemic events was lower than with monotherapies (16). The combination therapy allows the use of lower doses of both insulin and lixisenatide, thereby reducing the risk of hypoglycemia, improving glycemic control, and exerting a neutral or more favorable effect on weight management. These benefits are attributable to the GLP-1 receptor–mediated mechanisms, including delayed gastric emptying, inhibition of glucagon secretion, and glucose-dependent stimulation of insulin release(17,18).

We demonstrated that switching from insulin glargine to iGlarLixi resulted in a lower total insulin dose. Although 10% of patients experienced dyspeptic symptoms, no patients discontinued treatment because of these adverse effects. These findings are consistent with previous reports (19,20). In the LixiLanL trial, GI AEs were reported in 17% of patients, mostly mild to moderate symptoms such as nausea, vomiting, or diarrhea (19). Importantly, as in our cohort, no patients in that study discontinued treatment due to GI AEs. Severe adverse events, including pancreatitis, were not observed during the three-month follow-up period. Likewise, phase 3 LixiLan trials reported no episodes of pancreatitis, with an overall very low incidence (19,20). Several studies have also shown that improved glycemic control in both premixed and basalbolus regimens can be achieved with lower total insulin doses, consistent with our results (19-22). This effect is attributable to the actions of GLP-1 RAs, which slow gastric emptying, suppress appetite centrally, and enhance glucose-dependent insulin secretion (23,24). Moreover, the use of a lower insulin dose provides additional benefits, including reduced weight gain, fewer injections, and improved quality of life (25,26).

The FIB-4 score is commonly used to assess the risk of hepatic FIB in patients with T2DM. Furthermore, the ADA recommends screening all patients with T2DM for MASLD. If the FIB-4 score is higher than 1.3, this patient should be referred to a gastroenterologist (10). Treatment options for slowing or improving liver FIB are limited,

Table 5. Changes in clinical and laboratory parameters after switching from insulin glargine to iGlarLixi.

Parameter	Baseline median [IQR]	3rd month median [IQR]	p-value
Body weight (kg)	107 [96–116]	106 [95–114]	<0.001
HbA1c (%)	9 [8.5–10.4]	8.5 [7.3–9.5]	<0.001
FIB-4	0.91 [0.65–1.09]	0.85 [0.63–1.03]	0.308
Total insulin dose (U/day)	50 [26–82]	34 [20–64]	<0.001

FIB-4: Fibrosis-4 score, HbA1c: Glycated hemoglobin, IQR: Interquartile range.

and GLP-1 RAs are among the few available options (27,28). In a study evaluating the effect of lixisenatide on non-alcoholic fatty liver disease in T2DM, the aspartate aminotransferase-to platelet count ratio was used to assess liver FIB. Lixisenatide led to improvements in liver inflammation and FIB (29). These findings are consistent with our research. In contrast, a systematic review reported that lixisenatide normalized ALT levels but had no significant effect on AST, alkaline phosphatase, or bilirubin (30). Furthermore, our findings indicate that this effect is independent of weight loss. An improvement in the FIB4 score was observed in the group receiving OAD. In this group, withdrawal of some OADs upon initiation of iGlarLixi therapy may have contributed to the observed improvement in liver enzymes. Importantly, the short-term changes observed in FIB-4 should be interpreted with caution, as they may partly reflect medication adjustments and metabolic improvements rather than true regression of liver FIB. Given the relatively short follow-up period, variations in FIB-4 may primarily reflect dynamic changes in the biochemical parameters comprising the score. Therefore, prospective studies with longer follow-up periods and histological or imaging-based assessments are warranted to better clarify the independent effects of iGlarLixi on liver FIB.

This study has several strengths, including its use of a real-world cohort of patients with long-standing, poorly controlled T2DM and a high BMI, thereby enhancing the clinical relevance of the findings. The comprehensive evaluation of glycemic control, insulin requirements, body weight, and FIB-4 scores provided a multidimensional assessment of treatment effects. However, the three-month follow-up period limits the ability to draw conclusions about long-term efficacy and safety. The modest sample size, particularly in subgroup analyses, may have reduced statistical power. Additionally, relying solely on the FIB-4 score may not fully capture changes in hepatic status. The observed reduction in FIB-4 warrants cautious interpretation because this surrogate index is influenced by biochemical parameters; short-term changes may primarily reflect variations in liver enzyme levels rather than true regression of hepatic FIB. Finally, because this was a single-center study, the results may not be generalizable to all patient populations.

CONCLUSION

iGlarLixi resulted in significant improvements in glycemic control, body weight, and total daily insulin requirements in patients with long-standing T2DM. A modest yet statistically significant reduction in FIB4 scores was observed in the subgroup receiving the combination alongside oral antidiabetic therapy. These results underscore the potential of combining basal insulin with a GLP-1 RA to enhance both metabolic control and a surrogate marker of hepatic status in real-world clinical practice. Further comprehensive, long-term studies are needed to confirm these findings and clarify their clinical implications.

Ethics

Ethics Committee Approval: All study procedures adhered to the Declaration of Helsinki, and ethical approval was obtained from the University of Health Sciences Türkiye, Ankara Etlik City Hospital Ethics Committee (approval number/date: AEŞH-BADEK2-2025-379/05-08-2025, dated 05.08.2025).

Informed Consent: Due to the retrospective nature of the study, the requirement for informed consent was waived.

Footnotes

Authorship Contributions

Surgical and Medical Practices: E.Ü., B.Ç.H., Concept: E.Ü., B.Ç.H., B.U., Design: E.Ü., B.M., B.U., E.Ç., Data Collection or Processing: E.Ü., B.M., Analysis or Interpretation: E.Ü., Literature Search: E.Ü., B.Ç.H., Writing: E.Ü.

Conflict of Interest: No conflict of interest was declared by the authors.

Financial Disclosure: The authors declared that this study received no financial support.

REFERENCES

1. Shah MU, Roebuck A, Srinivasan B, Ward JK, Squires PE, Hills CE, et al. Diagnosis and management of type 2 diabetes mellitus in patients with ischaemic heart disease and acute coronary syndromes - a review of evidence and recommendations. Front Endocrinol (Lausanne). 2025; 15: 1499681.
2. Singh A, Shadangi S, Gupta PK, Rana S. Type 2 diabetes mellitus: a comprehensive review of pathophysiology, comorbidities, and emerging therapies. Compr Physiol. 2025; 15: e70003.
3. Cloete L. Diabetes mellitus: an overview of the types, symptoms, complications and management. Nurs Stand. 2022; 37: 61-6.
4. Piché ME, Tchernof A, Després JP. Obesity phenotypes, diabetes, and cardiovascular diseases. Circ Res. 2020; 126: 1477-500.
5. Malone JI, Hansen BC. Does obesity cause type 2 diabetes mellitus (T2DM)? Or is it the opposite? Pediatr Diabetes. 2019; 20: 5-9.
6. Drucker DJ. GLP-1 physiology informs the pharmacotherapy of obesity. Mol Metab. 2022; 57: 101351.
7. Liu QK. Mechanisms of action and therapeutic applications of GLP-1 and dual GIP/GLP-1 receptor agonists. Front Endocrinol (Lausanne). 2024; 15: 1431292.
8. American Diabetes Association Professional Practice Committee for Diabetes. Obesity and weight management for the prevention and treatment of diabetes: Standards of Care in Diabetes-2026. Diabetes Care. 2026; 49: S166-S82.
9. Abdelhameed F, Kite C, Lagojda L, Dallaway A, Chatha KK, Chaggar SS, et al. Non-invasive scores and serum biomarkers for fatty liver in the era of metabolic dysfunction-associated steatotic liver disease (MASLD): a comprehensive review from NAFLD to MAFLD and MASLD. Curr Obes Rep. 2024; 13: 510-31.
10. Cusi K, Abdelmalek MF, Apovian CM, Balapattabi K, Bannuru RR, Barb D, et al. Metabolic dysfunction-associated steatotic liver disease (MASLD) in people with diabetes: the need for screening and early intervention. A consensus report of the American Diabetes Association. Diabetes Care. 2025; 48: 1057-82.
11. Havranek B, Loh R, Torre B, Redfield R, Halegoua-DeMarzio D. Glucagon-like peptide-1 receptor agonists improve metabolic dysfunction-associated steatotic liver disease outcomes. Sci Rep. 2025; 15: 4947.
12. American Diabetes Association Professional Practice Committee. Diagnosis and classification of diabetes: Standards of Care in Diabetes-2025. Diabetes Care. 2025; 48: S27-49.
13. Rinella ME, Neuschwander-Tetri BA, Siddiqui MS, Abdelmalek MF, Caldwell S, Barb D, et al. AASLD Practice Guidance on the clinical assessment and management of nonalcoholic fatty liver disease. Hepatology. 2023; 77: 1797-835.

14. Home P, Blonde L, Kalra S, Ji L, Guyot P, Brulle-Wohlhueter C, et al. Insulin glargine/lixisenatide fixed-ratio combination (iGlarLixi) compared with premix or addition of meal-time insulin to basal insulin in people with type 2 diabetes: a systematic review and Bayesian network meta-analysis. Diabetes Obes Metab. 2020; 22: 2179-88.
15. Men P, Qu S, Luo W, Li C, Zhai S. Comparison of lixisenatide in combination with basal insulin vs other insulin regimens for the treatment of patients with type 2 diabetes inadequately controlled by basal insulin: systematic review, network meta-analysis and cost-effectiveness analysis. Diabetes Obes Metab. 2020; 22: 107-15.
16. Goldman J, Trujillo JM. iGlarLixi: a fixed-ratio combination of insulin glargine 100 U/mL and lixisenatide for the treatment of type 2 diabetes. Ann Pharmacother. 2017; 51: 990-9.
17. Moiz A, Filion KB, Tsoukas MA, Yu OH, Peters TM, Eisenberg MJ. Mechanisms of GLP-1 receptor agonist-induced weight loss: a review of central and peripheral pathways in appetite and energy regulation. Am J Med. 2025; 138: 934-40.
18. Hinnen D. Glucagon-like peptide 1 receptor agonists for type 2 diabetes. Diabetes Spectr. 2017; 30: 202-10.
19. Rosenstock J, Diamant M, Aroda VR, Silvestre L, Souhami E, Zhou T, et al. Efficacy and safety of LixiLan, a titratable fixed-ratio combination of lixisenatide and insulin glargine, versus insulin glargine in type 2 diabetes inadequately controlled on metformin monotherapy: the LixiLan proof-of-concept randomized trial. Diabetes Care. 2016; 39: 1579-86.
20. Rosenstock J, Aronson R, Grunberger G, Hanefeld M, Piatti P, Serusclat P, et al. Benefits of LixiLan, a titratable fixed-ratio combination of insulin glargine plus lixisenatide, versus insulin glargine and lixisenatide monocomponents in type 2 diabetes inadequately controlled on oral agents: the LixiLan-O randomized trial. Diabetes Care. 2016; 39: 2026-35.
21. Ligthelm RJ, Gylvin T, DeLuzio T, Raskin P. A comparison of twice-daily biphasic insulin aspart 70/30 and once-daily insulin glargine in persons with type 2 diabetes mellitus inadequately controlled on basal insulin and oral therapy: a randomized, open-label study. Endocr Pract. 2011; 17: 41-50.
22. Rosenstock J, Ahmann AJ, Colon G, Scism-Bacon J, Jiang H, Martin S. Advancing insulin therapy in type 2 diabetes previously treated with glargine plus oral agents: prandial premixed insulin lispro protamine suspension/lispro versus basal/bolus glargine/lispro therapy. Diabetes Care. 2008; 31: 20-5.
23. Taylor SI, Yazdi ZS, Beitelshees AL. Pharmacological treatment of hyperglycemia in type 2 diabetes. J Clin Invest. 2021; 131: e142243.
24. Serowik TC, Pantalone KM. The evolution of type 2 diabetes management: glycemic control and beyond with SGLT-2 inhibitors and GLP-1 receptor agonists. J Osteopath Med. 2024; 124: 127-35.
25. Russell-Jones D, Khan R. Insulin-associated weight gain in diabetes: causes, effects and coping strategies. Diabetes Obes Metab. 2007; 9: 799-812.
26. Ishii H, Terauchi Y, Jinnouchi H, Taketsuna M, Takeuchi M, Imaoka T. Effects of insulin changes on quality of life and glycemic control in Japanese patients with type 2 diabetes mellitus: the insulin-changing study intending to gain patients' insights into insulin treatment with patient-reported health outcomes in actual clinical treatments (INSIGHTs) study. J Diabetes Investig. 2013; 4: 560-70.
27. Zhao L, Tang H, Cheng Z. Pharmacotherapy of liver fibrosis and hepatitis: recent advances. Pharmaceuticals. 2024; 17: 1724.
28. Fang L, Li J, Zeng H, Liu J. Effects of GLP-1 receptor agonists on the degree of liver fibrosis and CRP in non-alcoholic fatty liver disease and non-alcoholic steatohepatitis: a systematic review and meta-analysis. Prim Care Diabetes. 2024; 18: 268-76.
29. Koutsovasilis A, Sotiropoulos A, Pappa M, Papadaki D, Kordinas V, Tamvakos C, et al. The effect of lixisenatide and dapagliflozin in nonalcoholic fatty liver disease in patients with type 2 diabetes mellitus compared with sitagliptin and pioglitazone. Diabetes. 2018; 67: 1235-P.
30. Gluud LL, Knop FK, Vilsbøll T. Effects of lixisenatide on elevated liver transaminases: systematic review with individual patient data meta-analysis of randomised controlled trials on patients with type 2 diabetes. BMJ Open. 2014; 4: e005325.

Original Investigation | Özgün Araştırma

Gazi Med J 2026;37(3):369-375

DOI: http://dx.doi.org/10.12996/gmj.2026.4636

Characterization of *FMR1* CGG Repeat Structure and AGG Interruption Patterns in Turkish and Syrian Individuals

Türk ve Suriyeli Bireylerde *FMR1* CGG Tekrar Yapısı ve AGG Kesinti Paternlerinin Karakterizasyonu

Hatice Koçak Eker[1], Sümeyye Kara[1], Fahrettin Duymuş[1,2], Büşra Eser Çavdartepe[1], Ebru Tuncez[1], Özgür Balasar[1], Müşerref Başdemirci[1], Tuğba Akın Duman[1], Levent Şimşek[1]

[1]Clinic of Medical Genetics, Konya City Hospital, Konya, Türkiye
[2]Department of Medical Genetics, Uşak University, Faculty of Medicine, Uşak, Türkiye

ABSTRACT

Objective: This study aimed to characterize *FMR1* CGG repeat length, AGG interruption number and patterns, and uninterrupted CGG tract architecture in Turkish and Syrian individuals referred for *FMR1*-associated phenotypes and evaluate their implications for repeat instability.

Methods: This retrospective study analysed 513 alleles from 351 unrelated individuals (162 females, 189 males), including 476 Turkish and 37 Syrian alleles. CGG repeat length, AGG interruption count and interspersion patterns, and the length and positional distribution of uninterrupted CGG tracts were assessed. Allele classifications and family transmission data were evaluated when available.

Results: Alleles with two AGG interruptions were the most prevalent configuration in both cohorts (70% in Turkish and 58% in Syrian alleles). In the Turkish cohort, 117 patterns were observed, including 56 population-specific variants; in the Syrian cohort, 23 distinct patterns were detected, of which seven were unique. The most common CGG repeat size was 30 in both cohorts. The most frequent AGG interspersion patterns were (CGG)9-AGG-(CGG)9-AGG-(CGG)10 and (CGG)9-AGG-(CGG)9-AGG-(CGG)9. Among 53 normal alleles with uninterrupted CGG tracts of >20 repeats, 94.3% were located at the 5′ end and were significantly associated with a positive family history (p = 0.004). All alleles that expanded to full mutations lacked AGG interruptions.

CONCLUSION: These findings demonstrate marked variability in *FMR1*

ÖZ

Amaç: Bu çalışmanın amacı, *FMR1* ile ilişkili fenotipler nedeniyle yönlendirilen Türk ve Suriyeli bireylerde *FMR1* CGG tekrar uzunluğunu, AGG kesinti sayısı ve paternlerini ve kesintisiz CGG tekrar bölgelerinin mimarisini karakterize etmek ve bu özelliklerin tekrar instabilitesi üzerindeki etkilerini değerlendirmektir.

Yöntemler: Bu retrospektif çalışmada, 351 akraba olmayan bireye (162 kadın, 189 erkek) ait toplam 513 alel analiz edildi; bunların 476'sı Türk, 37'si Suriyeli bireylere aitti. CGG tekrar uzunluğu, AGG kesinti sayısı ve dağılım paternleri ile kesintisiz CGG tekrar bölgelerinin uzunluğu ve pozisyonel dağılımı değerlendirildi. Uygun olan olgularda alel sınıflandırmaları ve aile içi geçiş verileri incelendi.

Bulgular: İki AGG kesintisi içeren aleller her iki kohortta da en sık görülen yapıydı (Türk alellerinde %70, Suriyeli alellerinde %58). Türk kohortunda 56'sı popülasyona özgü olmak üzere toplam 117 patern saptanırken, Suriyeli kohortta yedisi özgün olmak üzere 23 farklı patern belirlendi. En sık gözlenen CGG tekrar sayısı her iki kohortta da 30 idi. En yaygın AGG dağılım paternleri (CGG)9-AGG-(CGG)9-AGG-(CGG)10 ve (CGG)9-AGG-(CGG)9-AGG-(CGG)9 olarak saptandı. Yirmiden fazla kesintisiz CGG tekrarına sahip 53 normal alelin %94,3'ünde bu bölgelerin 5′ uçta yer aldığı ve pozitif aile öyküsü ile anlamlı ilişkili olduğu gösterildi (p = 0,004). Tam mutasyona genişleyen tüm alellerin AGG kesintisi içermediği belirlendi.

Cite this article as: Koçak Eker H, Kara S, Duymuş F, Eser Çavdartepe B, Tuncez E, Balasar Ö, et al. Characterization of *FMR1* CGG Repeat Structure and AGG Interruption Patterns in Turkish and Syrian Individuals. Gazi Med J. 2026;37(3):369-375

Address for Correspondence/Yazışma Adresi: Hatice Koçak Eker, Clinic of Medical Genetics, Konya City Hospital, Konya, Türkiye
E-mail / E-posta: drhaticekocak@hotmail.com
ORCID ID: orcid.org/0000-0003-2735-6739

Received/Geliş Tarihi: 02.02.2026
Accepted/Kabul Tarihi: 09.05.2026
Publication Date/Yayınlanma Tarihi: 10.07.2026

ABSTRACT

CGG repeat length and AGG interruption architecture in Turkish and Syrian populations, although the small sample size of the Syrian cohort warrants cautious interpretation. The data further suggest that repeat instability is associated not only with repeat number but also with repeat structure and positional context. Incorporating AGG interruption analysis into routine *FMR1* testing may improve genetic counseling and risk stratification.

Keywords: AGG interruption, *FMR1* gene, genetic variation, population genetics, trinucleotide repeat expansion, uninterrupted CGG tract

ÖZ

Sonuç: Bu bulgular, Türk ve Suriyeli popülasyonlarda *FMR1* CGG tekrar uzunluğu ve AGG kesinti mimarisinin belirgin değişkenlik gösterdiğini ortaya koymaktadır; ancak Suriye kohortunun küçük örneklem büyüklüğü, bu bulguların dikkatli yorumlanmasını gerektirmektedir. Veriler ayrıca tekrar instabilitesinin yalnızca tekrar sayısından değil, aynı zamanda tekrar yapısı ve pozisyonel bağlamdan da etkilendiğini düşündürmektedir. Rutin *FMR1* testlerine AGG kesinti analizinin eklenmesi, özellikle ailesel ve kuşaklar arası değerlendirmelerde genetik danışmanlık ve risk sınıflandırmasını iyileştirebilir.

Anahtar Sözcükler: AGG kesintisi, *FMR1* geni, genetik değişkenlik, popülasyon genetiği, trinükleotid tekrar genişlemesi, kesintisiz CGG dizisi

INTRODUCTION

Fragile X syndrome is the leading inherited cause of intellectual disability and a primary monogenic contributor to autism spectrum disorder. This condition arises from the expansion of a CGG trinucleotide repeat within the 5′ untranslated region of the *FMR1* gene on the X chromosome (1). Alleles harboring ≥200 CGG repeats typically exhibit hypermethylation and transcriptional silencing of the *FMR1* gene, leading to a deficiency in fragile X mental retardation protein and the characteristic FXS phenotype. Whereas premutation alleles are associated with diverse *FMR1*-associated disorders, including fragile X–associated primary ovarian insufficiency and fragile X–associated tremor/ataxia syndrome (2).

While the total CGG repeat length constitutes the cornerstone of *FMR1* allele classification, the repeat tract architecture—particularly the presence and distribution of AGG interruptions within the CGG array—exerts a pivotal influence on repeat stability (3,4). AGG interruptions are hypothesized to stabilize the CGG repeat tract by interrupting extended runs of pure CGG repeats, thereby preventing DNA slippage during replication and reducing the risk of expansion (3-5). Normal *FMR1* alleles typically contain two or three AGG interruptions, whereas premutation and full mutation alleles frequently exhibit fewer interruptions or are entirely devoid of AGGs (4,6,7).

Beyond the number of AGG interruptions, recent studies suggest that the spatial arrangement of uninterrupted CGG tracts exerts a substantial influence on *FMR1* repeat instability. In intermediate and premutation alleles, AGG interruptions tend to cluster toward the 5′ end of the repeat tract, positioning the longest contiguous CGG stretch at the 3′ end (8,9). Both the length and the position of these uninterrupted CGG tracts have been associated with an increased risk of repeat expansion, underscoring the importance of evaluating repeat tract architecture in addition to total CGG repeat length (5,6,8).

Population studies have identified significant geographic and ethnic differences in CGG repeat length distributions and AGG interruption patterns (5,10-12). Although the most common normal *FMR1* alleles worldwide typically comprise 29–30 CGG repeats, the relative frequencies of specific AGG interruption patterns —e.g., $(CGG)_9$-AGG-$(CGG)_9$-AGG-$(CGG)_9$, $(CGG)_{10}$-AGG-$(CGG)_9$-AGG-$(CGG)_9$— differ considerably between populations, owing to variations in evolutionary history, and population admixture (4,12). Despite the expanding body of literature on this topic, data from Türkiye remain sparse, and in-depth analyses of AGG interruption numbers and configurations are lacking. Furthermore, AGG interruption profiles have not yet been documented in Syrian populations.

Accordingly, this study sought *to* characterize thoroughly FMR1 CGG repeat lengths, AGG interruption counts, and detailed interruption patterns among Turkish and Syrian individuals referred for FMR1-associated phenotypes. By examining 513 FMR1 alleles spanning the normal, intermediate, premutation, and full-mutation categories, this investigation aimed to characterize population-specific AGG interruption patterns, evaluate the distribution and positional characteristics of extended uninterrupted CGG tracts, and investigate the relationships between repeat architecture and family histories of FMR1-related phenotypes. This study contributes to a deeper understanding of FMR1 repeat instability and supports the incorporation of AGG-interruption profiling into genetic counseling and risk assessment.

MATERIALS AND METHODS

Study Population

This multicenter retrospective study evaluated CGG trinucleotide repeat lengths and AGG interruption patterns in 513 *FMR1* alleles obtained from patients who presented to the Medical Genetics Outpatient Clinics of Konya City Hospital and Uşak Training and Research Hospital between January 2021 and December 2024. Individuals were referred because of clinical suspicion of Fragile X syndrome or Fragile X–associated disorders, a positive family history, or both.

A total of 351 unrelated individuals (162 females and 189 males) with normal karyotypes were included. Clinical and family histories were obtained directly from participants or, when necessary, from their parents or legal guardians. Relevant laboratory data and ancillary clinical information were retrieved from existing medical records.

The study protocol, covering both participating centers, was approved by the Uşak University Non-Interventional Clinical Research Ethics Committee (decision number: 710-710-14, dated 12.06.2025). Informed consent was waived due to the retrospective design.

FMR1 Repeat and AGG Interruption Profiling

Genomic DNA was extracted from peripheral blood samples of all participants using the QIAamp DNA Blood Mini Kit (Qiagen, Hilden,

Germany), following the manufacturer's protocol. The extracted DNA underwent polymerase chain reaction (PCR) amplification with specific primers. PCR products were subsequently analyzed by fragment analysis on an ABI 3500 Genetic Analyzer System with the Adellgene Fragile X Screening Kit (BDR, Zaragoza, Spain). The resulting data were interpreted using Gene Mapper software. AGG interruption genotyping was performed to determine both the number of AGG interruptions and the precise CGG repeat configuration. An AGG interruption pattern was defined as the number of uninterrupted CGG repeats between consecutive AGG interruptions, ordered from the 5′ to the 3′ end of the FMR1 CGG repeat tract. In female subjects, when multiple patterns were observed, these were clarified by evaluating family studies when available.

The classification of *FMR1* CGG repeat sizes was performed based on established criteria from previous studies and guidelines from the National Center for Biotechnology Information (13). Alleles containing 5-44 CGG repeats were categorized as normal, 45-54 repeats as intermediate, 55-199 repeats as premutation, and ≥200 repeats as full mutation. The association between categorical variables, including the presence of long uninterrupted CGG tracts and family history status, was evaluated using the chi-square test.

Statistical Analysis

Statistical evaluation of the data was performed using descriptive statistics, including frequencies and percentages. To examine the relationships between categorical variables, Fisher's exact test was used for comparisons involving small sample sizes. All statistical analyses were carried out using SPSS version 27.0 (IBM Corp., Armonk, NY, USA), and a p-value of <0.05 was considered statistically significant.

RESULTS

A total of 513 *FMR1* alleles (n = 476 Turkish and n = 37 Syrian) were analyzed. Their classification and distribution by AGG count in both populations are presented in Supplementary Table 1. In the Turkish cohort, alleles were classified as normal (93.9%), intermediate (1.7%), premutation (1.7%), and full mutation (2.7%) alleles, whereas the Syrian cohort had only normal (97.3%) and intermediate (2.7%) alleles (Table 1). Forty-eight distinct repeat sizes (5 to >200 repeats) were detected in the Turkish cohort, whereas 16 distinct CGG repeat sizes (17–45 repeats) were identified in the Syrian cohort (Supplementary Table 1). In both cohorts, alleles with two AGG interruptions were the most prevalent configuration, accounting for 70% and 58% of alleles in the Turkish and Syrian cohorts, respectively. These were followed, in decreasing order of frequency, by alleles with one, zero, and three AGG interruptions. Notably, a configuration with four AGG interruptions was observed in a single allele exclusively within the Turkish cohort (Figure 1, Supplementary Table 2).

Analysis of FMR1 AGG-interruption patterns in 513 alleles revealed 125 distinct configurations, indicating a high level of allelic diversity (Supplementary Table 2). Of these, five patterns were exclusive to the combined Turkish and Syrian datasets and have not been reported in other populations (Table 2). In the Turkish cohort, 117 AGG interruption patterns were identified across 476 alleles, including 56 population-specific variants. In the Syrian cohort, 23 distinct patterns were observed among 37 alleles, seven of which were unique to this population (Table 2). Supplementary Table 2 presents the distribution of AGG interruption patterns according to allele classification.

Normal alleles were analyzed to assess the distributions of CGG repeat size and AGG configuration in both cohorts. The most common allele was the 30-CGG-repeat allele (34% in the Turkish cohort and 33% in the Syrian cohort), followed by the 29-CGG-repeat allele (28% and 19%, respectively) (Figure 2). In the Turkish cohort, the most common AGG interspersion pattern was $(CGG)_9$-AGG-$(CGG)_9$-AGG-$(CGG)_{10}$ (27.7%), followed by $(CGG)_9$-AGG-$(CGG)_9$-AGG-$(CGG)_9$ (25.1%), whereas in the Syrian cohort, these two patterns were observed with equal frequency (16.7% each) (Supplementary Table 2).

Normal alleles were also examined for uninterrupted CGG segments longer than 20. A total of 53 alleles met this criterion, including 18 pure CGG alleles and 35 alleles containing at least one AGG interruption (Supplementary Table 1). Among alleles with AGG interruptions, uninterrupted CGG tracts were predominantly located at the 5′ end of the *FMR1* gene (94.3%, 33/35), whereas only two alleles showed localization at the 3′ end.

Uninterrupted CGG repeats located at the 5′ end showed a significant association with family history status. While this pattern in normal alleles was observed in both family-history–positive and -negative individuals, all intermediate and premutation alleles with uninterrupted CGG repeats at the 5′ end were detected exclusively in individuals with a positive family history (n = 8 alleles; Fisher's exact test, p = 0.004) (Table 3).

In family screenings of 19 index cases, 57 individuals were analyzed. Among these alleles, those that expanded to full mutations ranged from 56 to 159 CGG repeats, and none contained AGG interruptions. No contractions in the total CGG repeat number were observed

Table 1. Comparative distribution of FMR1 alleles between Turkish and Syrian cohorts according to AGG interruptions and allele classification.

Number of alleles in Turkish patients					AGG number	Number of alleles in Syrian patients				
Normal	**Intermediate**	**Premutant**	**Mutant**	**Total**		**Total**	**Normal**	**Intermediate**	**Premutant**	**Mutant**
21	1	7	13	**42**	0	**4**	3	1	0	0
101	1	0	0	**102**	1	**11**	11	0	0	0
312	5	0	0	**317**	2	**21**	21	0	0	0
12	1	1	0	**14**	3	**1**	1	0	0	0
1	0	0	0	**1**	4	**0**	0	0	0	0
447	**8**	**8**	**13**	**476**		**37**	**36**	**1**	**0**	**0**

Table 2. Distribution of AGG interruption patterns according to allele classification in Turkish and Syrian populations.

Classification	AGG patterns	In Turkish cohorts	In Syrian cohorts	Shared patterns
Normal	**106**	**99**	**22**	**15**
Intermediate	**9**	**8**	**1**	**0**
Premutant	**7**	**7**	**0**	**0**
Mutant	**3**	**3**	**0**	**0**
Total	125	117	23	15

Table 3. Association between family history and uninterrupted CGG repeat patterns (>20 repeats) located at the 5′ end according to allele classification.

Uninterrupted CGG repeat pattern	Family history (+) number (%)	Family history (–) number (%)	Total
Normal alleles (5′ end)	14 (42.4)	19 (57.6)	33
Intermediate and Premutant alleles (5′ end)	8 (100.0)	0 (0.0)	8

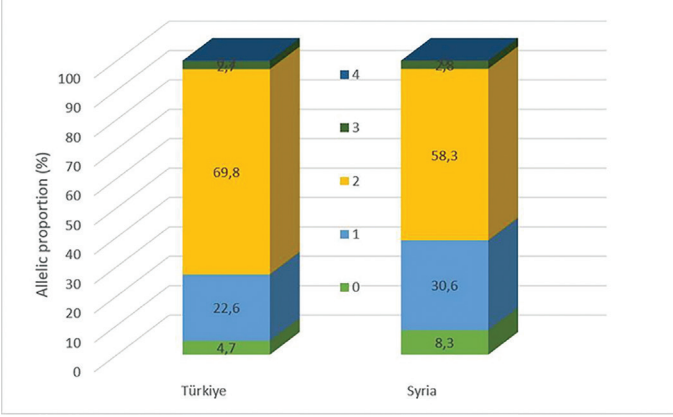

Figure 1. AGG interruption number distribution in *FMR1* normal alleles in Turkish and Syrian populations.

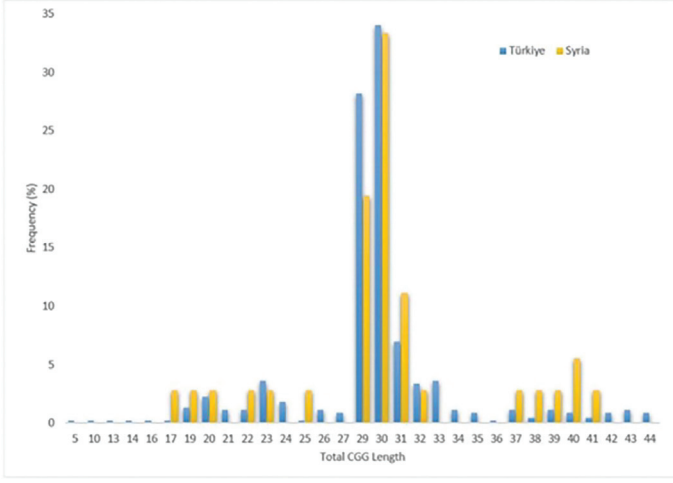

Figure 2. Distribution of *FMR1* CGG repeat lengths in normal alleles from Turkish and Syrian populations.

across generations. Alleles within the normal range containing AGG interruptions demonstrated stable transmission in both repeat size and structure across generations. However, a single exceptional transmission event was identified, in which an allele carrying one AGG interruption (29 + 9) was inherited in the subsequent generation as a pure 33 CGG allele lacking AGG interruptions (Supplementary Table 1).

DISCUSSION

Previous studies have reported on the total number of CGG repeats in the *FMR1* gene, as well as the number and patterns of AGG interruptions and their geographic and ethnic distributions (5,10-12). Although a limited number of studies from Türkiye have reported CGG repeat length distributions and *FMR1* mutation profiles (14-16), comprehensive analyses of AGG interruption number and patterning remain scarce. In addition, AGG interruption data specific to Syrian individuals have not yet been reported in the literature. To address this deficiency, 513 FMR1 alleles from Turkish and Syrian individuals were genotyped, and the total CGG length and the number and patterns of AGG interruptions were evaluated. The findings were compared with those reported in the literature for different populations.

The fact that the most common total CGG repeat length in the Turkish cohort is 30, followed by 29 mirrors the global pattern (5,11). However, it has been shown that the most common allele is 29 repeats in Indonesian, African American, Asian populations, and Malay, Borneo, and Tibetan communities (5,17,18). This consistency supports the evolutionary stability of FMR1 CGG repeat alleles within the common normal range across different populations.

Both the Turkish and Syrian cohorts showed a predominance of alleles carrying two AGG interruptions, followed by alleles with a single AGG interruption, a distribution that is consistent with previously reported population-based studies (5,11). Notably, the identification of an allele harboring four AGG interruptions in the Turkish cohort is of particular interest, as alleles with four AGG interruptions have been reported only in a limited number of populations, including Australia, the United Arab Emirates, Indonesia, and Spain (5). Further studies incorporating comprehensive characterization of such rare AGG patterns in global databases will be required to determine whether these alleles reflect independent mutational events or a shared ancestral origin. In our cohort, 55% (n = 5) of the intermediate alleles carried two AGG interruptions, whereas the vast majority of premutation alleles (87.5%, n = 7) and all full mutation alleles (n = 13) lacked AGG interruptions. These observations align with the established literature indicating that

premutation alleles typically harbor zero to two AGG interruptions, while normal alleles most commonly contain two to three AGG interruptions (4,7). Pure CGG repeats lacking AGG interruptions are generally considered uncommon among normal *FMR1* alleles (10,19). Nevertheless, in our cohort, such alleles were identified in 4.7% of cases (n = 21), indicating that fully uninterrupted CGG tracts may not be as exceptional as previously assumed, at least within certain populations or ascertainment contexts. Although these alleles fall within the normal repeat size range, their structural configuration is noteworthy, given the well-established stabilizing role of AGG interruptions. The presence of a measurable proportion of pure alleles in the normal range may, therefore, represent a latent source of repeat instability, potentially predisposing these alleles to expansion upon intergenerational transmission. This observation underscores the importance of considering not only CGG repeat length but also repeat architecture when evaluating *FMR1* allele stability.

The 125 different AGG interruption patterns identified in this study highlight the high mutational and structural variability of the *FMR1* CGG repeat region in Turkish and Syrian cohorts. Notably, 56 of the 117 AGG interruption patterns observed in the Turkish cohort were exclusive to this population, suggesting a highly heterogeneous genetic structure. Türkiye's historical role as a geographical bridge between Asia and Europe and substantial migration from diverse regions can be considered among the possible reasons for this diversity. The presence of shared AGG configurations between Turkish and Syrian individuals points to a partial overlap in ancestral or regional genetic backgrounds, while distinct population-specific signatures are retained. The limited sample size of the Syrian cohort represents an important constraint in the interpretation of these findings. Nonetheless, the most frequent total CGG repeat lengths observed (29 and 30 repeats) were consistent with existing literature, and the identification of seven population-specific AGG-interruption patterns among a total of 23 distinct patterns suggests the presence of cohort-specific AGG architectures despite the smaller sample size.

With respect to AGG interruption patterns, the Turkish cohort most frequently exhibited the 9 + 9 + 10 pattern, followed closely by the 9 + 9 + 9 pattern. In contrast, most studies report 10 + 9 + 9 as the predominant AGG pattern (17%–53% across studies), with 9 + 9 + 9 ranking second (1–32% across studies) (5,11). However, the opposite of this ordering of patterns has been documented in several populations, including Indonesian (35%–21%), African American (19%–18%), Asian (61%–9%), Malay, Borneo, and Tibetan groups (48%–29%) (17,18). Notably, in African Americans, the 9 + 9 + 9 pattern has been reported at only 1% higher frequency than the 10 + 9 + 9 pattern, highlighting that relatively small frequency shifts can distinguish population-specific AGG architectures (17,18). In the Syrian cohort, the 9 + 9 + 10 and 9 + 9 + 9 AGG interruption patterns were observed at equal frequencies. While this finding should be interpreted cautiously due to the limited sample size, it may suggest a balanced distribution of prevalent AGG configurations in this population. The 9 + 9 + 10 pattern has been reported at its highest relative frequency in African populations (9%), followed by African Americans (4%) and Caucasian and Italian populations (3%) (5,11). However, these proportions remain low in absolute terms, indicating that this AGG configuration is not dominant in any population. The relatively higher frequency of the 9 + 9 + 10 pattern in the Turkish cohort suggests that this AGG configuration is a prominent feature of this population and may reflect regional trends rather than being strictly population-specific. In contrast to most populations in which the 10 + 9 + 9 pattern is reported as the predominant AGG configuration, this pattern was observed in only three alleles (<1%) in the Turkish cohort and was not detected in the Syrian cohort. Following the two most frequent patterns, additional AGG interruption configurations were observed among normal alleles, including 9 + 13 (2.7%), 9 + 10 (2.2%), 19 + 9 (2.2%), and 9 + 10 + 9 (2.2%). Notably, these configurations have been reported in other populations worldwide at comparable frequencies. Specifically, the 9 + 13 pattern has been most frequently reported in Indonesian (3%) and Asian (2%) populations; the 9 + 10 pattern in Basque (2%) and Indian (2%) populations; the 19 + 9 pattern in Guatemalan (3%) and African American (2%) populations; and the 9 + 10 + 9 pattern in Emirati (7%) and Jewish Arabic (4%) populations (5,10,12,20). The presence of these shared patterns across geographically and ethnically distinct populations suggests that certain AGG configurations may be evolutionarily conserved, potentially due to their stabilizing effect on the CGG repeat tract.

Most studies to date investigating AGG interruption patterns in the *FMR1* gene have focused primarily on describing AGG distributions in normal alleles (5,21). In contrast, studies addressing premutation alleles have generally focused on total CGG repeat length and/or AGG interruption number, examining their association with clinical outcomes such as primary ovarian insufficiency, as well as with *FMR1* gene stability (2,6,9,22). However, systematic analyses of AGG interruption patterns specifically within premutation alleles remain scarce (5,10,11). In this context, our study extends the existing literature by characterizing AGG patterns and interruption numbers not only in normal alleles but also in intermediate, premutation, and full mutation alleles (Supplementary Tables 1 and 2), thereby providing a more comprehensive view of AGG architecture across the full spectrum of FMR1 allele classes. In our cohort, the proportion of AGG-less premutation alleles was markedly higher (87.5%) than that reported by Rodrigues et al. (11) (50.3%), whose study population consisted predominantly of Caucasian individuals. Given the established association between the absence of AGG interruptions and increased CGG repeat instability, this difference may provide a biological context for the relatively higher frequencies of premutation (1.7%) and full mutation (2.7%) alleles observed in our clinically selected cohort compared with population-based estimates from Caucasian populations (23,24). However, because both studies used non-population-based samples, these findings should not be interpreted as reflecting true population-level differences. Rather, they highlight potential population-specific variability in AGG interspersion patterns and underscore the need for population-based studies to clarify the contribution of AGG structure to Fragile X–related allele distributions.

Previous studies have reported that, in intermediate and premutation *FMR1* alleles, AGG interruptions preferentially cluster toward the 5′ end of the locus, whereas the longest uninterrupted CGG stretch is typically located at the 3′ end (8,9). By contrast, the present study found that all intermediate and premutation alleles containing AGG interruptions displayed uninterrupted CGG tracts exceeding 20 repeats exclusively at the 5′ end. Notably, the occurrence of this repeat configuration in cases with a positive family history

suggests an association with familial transmission and increased allelic instability of FMR1. However, given the limited number of intermediate and premutation alleles analyzed, this finding should be interpreted with caution.

Supportive evidence for this interpretation is provided by an intergenerational transmission observed in a single family, in which a maternal allele that harbored a long uninterrupted CGG segment at the 5′ end (29 + 9) lost its AGG interruption and expanded to a pure 33 CGG repeat in the offspring. Although anecdotal and not intended to imply causality, this observation is consistent with the hypothesis that uninterrupted CGG segments at the 5′ end may constitute a structurally unstable configuration during transmission, predisposing alleles to AGG loss and early repeat expansion. Taken together with the group-level association observed in the present study, these findings suggest that the contribution of uninterrupted CGG tracts to *FMR1* instability may depend not only on repeat length but also on their positional context within the repeat array.

Although the loss of AGG interruptions during transmission is considered a rare event, it has been previously documented in the literature (25,26). In this context, our observation of an intergenerational AGG loss followed by repeat expansion is consistent with previous reports. Furthermore, none of the alleles that expanded to full mutations during family screening in the present study contained AGG interruptions, which is consistent with a potential stabilizing role of AGG interruptions against large CGG expansions. No contractions in total CGG repeat number were observed across generations, in keeping with the well-established bias of *FMR1* alleles toward repeat expansion rather than contraction (9).

Study Limitations

This study has several limitations. Its retrospective design and the inclusion of a clinically referred, potentially high-risk cohort limit the generalizability of the findings to the general population. In addition, the relatively small sample size reduces statistical power, particularly for the evaluation of rare AGG interruption patterns. This limitation is especially relevant for subgroup analyses, in which the Fisher's exact test is based on very small samples, and for the Syrian cohort; it may limit the robustness and generalizability of the findings. Furthermore, familial data were available only for a subset of cases, and systematic intergenerational assessment of CGG repeat expansion was not feasible across all allele categories. In particular, normal alleles with longer CGG repeat tracts are not routinely subjected to family-based analyses in clinical practice, limiting the ability to directly evaluate transmission dynamics in this group. In addition, AGG interruption patterns cannot be reliably determined in alleles within the full mutation range due to technical limitations in the analysis of large CGG repeat expansions. Moreover, data on the clinical relevance of AGG interruption patterns that deviate from the evolutionarily conserved 9–10 uninterrupted CGG units remain limited. Consequently, the relationship between different repeat architectures and clinical outcomes is not yet fully understood. Prospective, population-based studies with larger cohorts are needed to clarify the clinical and biological significance of distinct AGG interruption patterns, and further investigations addressing this question are currently being planned by our group.

CONCLUSION

This study demonstrates marked variability in *FMR1* CGG repeat length and AGG interruption architecture in Turkish and Syrian cohorts, although the small sample size of the Syrian cohort warrants cautious interpretation. The data further suggest that repeat instability is associated not only with repeat number but also with repeat structure and positional context. The identification of population-specific AGG patterns and long uninterrupted CGG tracts, particularly at the 5′ end, supports the concept that repeat architecture and positional context contribute to *FMR1* instability. Our findings are also consistent with previous studies suggesting that AGG interruptions may contribute to the stabilization of CGG repeat tracts; however, given the limited scope of familial analyses in this study, this interpretation should be viewed with caution. Integrating AGG interruption patterns into routine FMR1 testing may enhance genetic counseling and risk stratification, particularly in families undergoing carrier screening or intergenerational follow-up. However, larger, multicenter studies will be required to confirm these findings and to define their broader clinical significance.

Ethics

Ethics Committee Approval: The study protocol, covering both participating centers, was approved by the Uşak University Non-Interventional Clinical Research Ethics Committee (decision number: 710-710-14, dated 12.06.2025).

Informed Consent: Informed consent was waived due to the retrospective design.

Footnotes

Authorship Contributions

Surgical and Medical Practices: H.K.E., F.D., B.E.C., E.T., Ö.B., M.B., T.A.D., L.Ş., Concept: H.K.E., F.D., Design: H.K.E., S.K., F.D., Data Collection or Processing: H.K.E., S.K., B.E.C., Ö.B., M.B., Analysis or Interpretation: H.K.E., S.K., E.T., T.A.D., Literature Search: H.K.E., B.E.C., L.Ş., Writing: H.K.E., L.Ş.

Conflict of Interest: No conflict of interest was declared by the authors.

Financial Disclosure: The authors declared that this study received no financial support.

Supplementary Tables: https://d2v96fxpocvxx.cloudfront.net/7a593d95-86ec-4d2b-8dd3-26b0d0b79ea4/content-images/e8b95427-9d1a-46ae-b2c0-e41fa768d1f0.pdf

REFERENCES

1. Ciobanu CG, Nucă I, Popescu R, Antoci LM, Caba L, Ivanov AV, et al. Narrative review: update on the molecular diagnosis of fragile X syndrome. Int J Mol Sci. 2023; 24: 9206.
2. Friedman-Gohas M, Kirshenbaum M, Michaeli A, Domniz N, Elizur S, Raanani H, et al. Does the presence of AGG interruptions within the CGG repeat tract have a protective effect on the fertility phenotype of female FMR1 premutation carriers? J Assist Reprod Genet. 2020; 37: 849-54.
3. Domniz N, Ries-Levavi L, Cohen Y, Marom-Haham L, Berkenstadt M, Pras E, et al. Absence of AGG interruptions is a risk factor for full mutation expansion among Israeli FMR1 premutation carriers. Front Genet. 2018; 9: 606.

4. Latham GJ, Coppinger J, Hadd AG, Nolin SL. The role of AGG interruptions in fragile X repeat expansions: a twenty-year perspective. Front Genet. 2014; 5: 244.
5. Yrigollen CM, Sweha S, Durbin-Johnson B, Zhou L, Berry-Kravis E, Fernandez-Carvajal I, et al. Distribution of AGG interruption patterns within nine world populations. Intractable Rare Dis Res. 2014; 3: 153-61.
6. Nolin SL, Glicksman A, Ersalesi N, Dobkin C, Brown WT, Cao R, et al. Fragile X full mutation expansions are inhibited by one or more AGG interruptions in premutation carriers. Genet Med. 2015; 17: 358-64.
7. Yrigollen CM, Durbin-Johnson B, Gane L, Nelson DL, Hagerman R, Hagerman PJ, et al. AGG interruptions within the maternal FMR1 gene reduce the risk of offspring with fragile X syndrome. Genet Med. 2012; 14: 729-36.
8. Eichler EE, Holden JJ, Popovich BW, Reiss AL, Snow K, Thibodeau SN, et al. Length of uninterrupted CGG repeats determines instability in the FMR1 gene. Nat Genet. 1994; 8: 88-94.
9. Nolin SL, Glicksman A, Tortora N, Allen E, Macpherson J, Mila M, et al. Expansions and contractions of the FMR1 CGG repeat in 5,508 transmissions of normal, intermediate, and premutation alleles. Am J Med Genet A. 2019; 179: 1148-56.
10. Arrieta I, Peñagarikano O, Télez M, Ortega B, Flores P, Criado B, et al. The FMR1 CGG repeat and linked microsatellite markers in two Basque valleys. Heredity (Edinb). 2003; 90: 206-11.
11. Rodrigues B, Sousa V, Yrigollen CM, Tassone F, Villate O, Allen EG, et al. FMR1 allelic complexity in premutation carriers provides no evidence for a correlation with age at amenorrhea. Reprod Biol Endocrinol. 2024; 22: 71.
12. Manor E, Gonen R, Sarussi B, Keidar-Friedman D, Kumar J, Tang HT, et al. The role of AGG interruptions in the FMR1 gene stability: a survey in ethnic groups with low and high rate of consanguinity. Mol Genet Genomic Med. 2019; 7: e00946.
13. Hunter JE, Berry-Kravis E, Hipp H, Todd PK. FMR1 disorders. 1998 Jun 16 [updated 2024 May 16]. In: Adam MP, Bick S, Mirzaa GM, et al., editors. GeneReviews® [Internet]. Seattle: University of Washington, Seattle; 1993-2026. Available from: https://www.ncbi.nlm.nih.gov/books/NBK1384/
14. Arikan Y, Bilgen T, Mihci E, Duman O, Karaman T, Keser I. FMR1 gene mutation analysis and CGG repeat number distribution from a single center. Gazi Med J. 2022; 33: 369-74.
15. Sarikaya E, Tokmak A, Cakar ES, Guney G, Duzkale N, Ozaksit MG. Evaluation of FMR1 gene mutations in Turkish women newly diagnosed with primary ovarian failure. Int J Reprod Contracept Obstet Gynecol. 2019; 8: 420-4.
16. Oral E, Toksoy G, Sofiyeva N, Celik HG, Karaman B, Basaran S, et al. Clinical and genetic investigation of premature ovarian insufficiency cases from Turkey. J Gynecol Obstet Hum Reprod. 2019; 48: 817-23.
17. Zhou Y, Tang K, Law HY, Ng IS, Lee CG, Chong SS. FMR1 CGG repeat patterns and flanking haplotypes in three Asian populations and their relationship with repeat instability. Ann Hum Genet. 2006; 70: 784-96.
18. Chiu HH, Tseng YT, Hsiao HP, Hsiao HH. The AGG interruption pattern within the CGG repeat of the FMR1 gene among Taiwanese population. J Genet. 2008; 87: 275-7.
19. Rodrigues B, Vale-Fernandes E, Maia N, Santos F, Marques I, Santos R, et al. Development and validation of a mathematical model to predict the complexity of FMR1 allele combinations. Front Genet. 2020; 11: 557147.
20. Tassone F, Iong KP, Tong TH, Lo J, Gane LW, Berry-Kravis E, et al. FMR1 CGG allele size and prevalence ascertained through newborn screening in the United States. Genome Med. 2012; 4: 100.
21. Eichler EE, Hammond HA, Macpherson JN, Ward PA, Nelson DL. Population survey of the human FMR1 CGG repeat substructure suggests biased polarity for the loss of AGG interruptions. Hum Mol Genet. 1995; 4: 2199-208.
22. Allen EG, Glicksman A, Tortora N, Charen K, He W, Amin A, et al. FXPOI: pattern of AGG interruptions does not show an association with age at amenorrhea among women with a premutation. Front Genet. 2018; 9: 292.
23. Yrigollen CM, Martorell L, Durbin-Johnson B, Naudo M, Genoves J, Murgia A, et al. AGG interruptions and maternal age affect FMR1 CGG repeat allele stability during transmission. J Neurodev Disord. 2014; 6: 24.
24. Crawford DC, Acuña JM, Sherman SL. FMR1 and the fragile X syndrome: human genome epidemiology review. Genet Med. 2001; 3: 359-71.
25. Fernandez-Carvajal I, Lopez Posadas B, Pan R, Raske C, Hagerman PJ, Tassone F. Expansion of an FMR1 grey-zone allele to a full mutation in two generations. J Mol Diagn. 2009; 11: 306-10.
26. Nolin SL, Sah S, Glicksman A, Sherman SL, Allen E, Berry-Kravis E, et al. Fragile X AGG analysis provides new risk predictions for 45-69 repeat alleles. Am J Med Genet A. 2013; 161A: 771-8.

Original Investigation | Özgün Araştırma

Gazi Med J 2026;37(3):376-383

DOI: http://dx.doi.org/10.12996/gmj.2026.4641

Neonatal Outcomes in Infants Born to Mothers Recovered from COVID-19 During Pregnancy: A Single-Center Experience in Türkiye's Level IV NICU

Gebelikte COVID-19 Geçiren Annelerden Doğan Bebeklerde Yenidoğan Sonuçları: Türkiye'de Düzey IV Yenidoğan Yoğun Bakım Ünitesinin Tek Merkez Deneyimi

Elif Keleş[1,2], Gizem Kartal[1,3], Melda Taş[1,4], Münevver Baş[1,5], Nurcan Hanedan[1,6], Ayfer Koyuncu[7], İbrahim Murat Hırfanoğlu[1], Esra Önal[1], Canan Türkyılmaz[1], Ebru Ergenekon[1], Esin Koç[1]

[1]Division of Neonatology, Department of Pediatrics, Gazi University, Faculty of Medicine, Ankara, Türkiye
[2]Department of Radiology, Northwestern University, Hybrid and Machine Intelligence Lab, Chicago, United States of America
[3]Clinic of Pediatrics, University of Health Sciences Türkiye, Gaziantep City Hospital, Gaziantep, Türkiye
[4]Clinic of Pediatrics, University of Health Sciences Türkiye, Ankara Training and Research Hospital, Ankara, Türkiye
[5]Clinic of Pediatrics, University of Health Sciences Türkiye, Balıkesir Atatürk City Hospital, Balıkesir, Türkiye
[6]Clinic of Pediatrics, University of Health Sciences Türkiye, Ankara Etlik City Hospital, Ankara, Türkiye
[7]Department of Biomedical Engineering, Düzce University, Faculty of Medicine, Düzce, Türkiye

ABSTRACT

Objective: The impact of in utero exposure to maternal severe acute respiratory syndrome coronavirus 2 (SARS-CoV-2) infection on neonatal health, particularly in the absence of active infection at delivery, remains incompletely understood. This study evaluated early neonatal outcomes and short-term follow-up among infants exposed to maternal Coronavirus Disease-2019 (COVID-19) during pregnancy, compared with unexposed neonates.

Methods: This retrospective observational cohort study was conducted at Gazi University Faculty of Medicine Hospital, a tertiary university hospital with a Level IV NICU, between March 2020 and August 2021. Neonates who tested polymerase chain reaction (PCR)-negative at delivery and were born to mothers with PCR-confirmed SARS-CoV-2 infection during pregnancy were classified as exposed, while neonates born to mothers without a history of COVID-19 during pregnancy served as controls. Neonatal outcomes during hospitalization and at one-month follow-up were assessed.

Results: A total of 196 neonates were included, of whom 112 were exposed in utero to maternal COVID-19. Neonatal intensive care unit (NICU) admission was more frequent among exposed infants [28.4%

ÖZ

Amaç: Gebelik sırasında maternal şiddetli akut solunum sendromu koronavirüs-2 (SARS-CoV-2) enfeksiyonuna intrauterin maruziyetin yenidoğan sağlığı üzerindeki etkileri, özellikle doğum sırasında aktif enfeksiyon bulunmayan olgularda, tam olarak açıklığa kavuşmamıştır. Bu çalışmada, gebelik sırasında koronavirüs hastalığı-2019 (COVID-19) geçiren annelerden doğan ve doğumda polimeraz zincir reaksiyonu (PCR) testi negatif olan bebeklerin erken yenidoğan dönem sonuçları ve kısa dönem izlemleri, maruziyeti olmayan yenidoğanlarla karşılaştırılarak değerlendirilmiştir.

Yöntemler: Bu retrospektif gözlemsel kohort çalışması, Mart 2020 ile Ağustos 2021 tarihleri arasında üçüncü basamak bir üniversite hastanesinde gerçekleştirildi. Gebelik sırasında PCR ile doğrulanmış SARS-CoV-2 enfeksiyonu geçiren ve doğum sırasında PCR testi negatif olan annelerden doğan bebekler maruz kalan grup olarak tanımlandı. Gebelik sırasında COVID-19 öyküsü bulunmayan annelerden doğan yenidoğanlar ise kontrol grubunu oluşturdu. Hastanede yatış süresince ve yaşamın ilk ayında yenidoğan sonuçları değerlendirildi.

Bulgular: Çalışmaya toplam 196 yenidoğan dahil edildi ve bunların 112'si maternal COVID-19 enfeksiyonuna intrauterin maruz kalmıştı.

Cite this article as: Keles E, Kartal G, Tas M, Baş M, Hanedan N, Koyuncu A, et al. Neonatal outcomes in infants born to mothers recovered from COVID-19 during pregnancy: a single-center experience in Türkiye's level IV NICU. Gazi Med J. 2026;37(3):376-383

Address for Correspondence/Yazışma Adresi: Elif Keleş, Department of Pediatrics, Division of Neonatology, Gazi University Faculty of Medicine, Ankara, Türkiye; Department of Radiology, Northwestern University, Hybrid and Machine Intelligence Lab, Chicago, United States of America
E-mail / E-posta: elif.keles@northwestern.edu
ORCID ID: orcid.org/0000-0001-8103-797X

Received/Geliş Tarihi: 13.02.2026
Accepted/Kabul Tarihi: 20.05.2026
Publication Date/Yayınlanma Tarihi: 10.07.2026

ABSTRACT

vs. 11.9%; relative risk (RR): 2.38, 95% confidence interval (CI): 1.25-4.54; p = 0.007]. In exposed neonates, hyperbilirubinemia requiring phototherapy occurred more frequently (38.8% vs. 22.2%; RR: 1.75, 95% CI: 1.08-2.85; p = 0.017), and the onset of jaundice occurred earlier [median (interquartile range) 3 (2-3) vs. 5.5 (3-8) days; p = 0.006]. Direct Coombs testing (performed in a clinically selected subset) showed similar overall positivity rates, but high-grade positivity (≥2+) occurred exclusively among exposed infants (p = 0.004). In trimester-specific analyses, second-trimester maternal infection was associated with a higher rate of neonatal endotracheal intubation than with first- or third-trimester exposure (10.0% vs. 0%; p = 0.034). No group differences were observed in early postnatal complications or rehospitalizations at one month.

CONCLUSION: Resolved maternal SARS-CoV-2 infection during pregnancy was not associated with major adverse neonatal outcomes, but it was linked to more frequent NICU admissions, earlier onset of clinical jaundice, a higher incidence of hyperbilirubinemia requiring treatment, and distinct patterns of severity on the direct Coombs test, potentially consistent with altered immune or hematologic processes. A trimester-specific association with endotracheal intubation was observed and should be interpreted cautiously.

Keywords: COVID-19, maternal SARS-CoV-2 infection, neonatal outcomes, hyperbilirubinemia, immune reaction, exposed neonate

ÖZ

Yenidoğan yoğun bakım ünitesine (YYBÜ) yatış oranı maruz kalan bebeklerde daha yüksekti [%28,4'e karşı %11,9; göreceli risk (RR): 2,38; %95 güven aralığı (GA): 1,25-4,54; p = 0,007]. Fototerapi gerektiren hiperbilirubinemi maruz kalan grupta daha sık görüldü (%38,8'e karşı %22,2; RR: 1,75; %95 GA: 1,08-2,85; p = 0,017) ve sarılık daha erken dönemde ortaya çıktı [medyan (çeyrekler arası aralık) 3 (2-3) güne karşı 5,5 (3-8) gün; p = 0,006]. Direkt Coombs testi pozitiflik oranları benzer olmakla birlikte, yüksek dereceli pozitiflik (≥2+) yalnızca maruz kalan bebeklerde saptandı (p = 0,004). Trimester bazlı analizlerde, ikinci trimesterde maternal enfeksiyon geçiren annelerin bebeklerinde endotrakeal entübasyon oranı birinci ve üçüncü trimester maruziyetine göre daha yüksekti (%10,0'a karşı %0; p = 0,034). Erken postnatal komplikasyonlar ve bir aylık yeniden hastaneye yatış oranları açısından gruplar arasında anlamlı fark bulunmadı.

Sonuç: Gebelik sırasında geçirilmiş ve doğum öncesinde düzelmiş maternal SARS-CoV-2 enfeksiyonu majör olumsuz yenidoğan sonuçları ile ilişkili bulunmamıştır. Bununla birlikte, daha sık YYBÜ yatışı, sarılığın daha erken başlaması, tedavi gerektiren hiperbilirubinemi sıklığında artış ve direkt Coombs testinde farklı şiddet paternleri ile ilişkili olduğu gösterilmiştir. Ayrıca ikinci trimester maruziyeti ile endotrakeal entübasyon arasında gözlenen ilişki dikkatle yorumlanmalıdır.

Anahtar Sözcükler: COVID-19, maternal SARS-CoV-2 enfeksiyonu, yenidoğan sonuçları, hiperbilirubinemi, immün yanıt, maruz kalan yenidoğan

INTRODUCTION

The Coronavirus Disease-2019 (COVID-19) pandemic challenged global health systems, particularly for pregnant individuals, who are considered an especially vulnerable population (1). Physiological adaptations of pregnancy, including significant changes in the immune, cardiovascular, and respiratory systems, may increase susceptibility and disease severity (2). These considerations raised concerns about potential maternal, fetal, and neonatal consequences of severe acute respiratory syndrome coronavirus 2 (SARS-CoV-2) infection during pregnancy.

During the pandemic, initial clinical focus centered on the possibility of vertical transmission. Evidence demonstrates that transplacental transmission of SARS-CoV-2 is rare, and neonatal infection occurs in only a minority of exposed infants (1,3). As a result, the clinical question has shifted toward the potential indirect effects of maternal infection on the intrauterine environment and neonatal health, even in the absence of direct viral transmission (1,3,4).

Large cohort studies and systematic reviews have demonstrated that maternal SARS-CoV-2 infection during pregnancy is associated with increased risks of adverse perinatal outcomes, including preeclampsia, preterm birth, neonatal respiratory morbidity, stillbirth, and higher rates of neonatal intensive care unit (NICU) admission, particularly among women with severe or symptomatic disease (5-7). However, how resolved maternal infection affects neonatal health remains unclear. Existing studies have yielded diverging results due to variations in disease severity, exposure timing, population characteristics, and study design. Consequently, whether in utero exposure to maternal COVID-19 presents neonatal risk in the absence of active maternal infection at delivery remains an important unanswered clinical question (3,5-7).

Although the global epidemiology of COVID-19 has evolved, SARS-CoV-2 continues to circulate, and a substantial number of pregnancies worldwide have been affected (8,9). Declining vaccination coverage in pregnancy further underscores the ongoing clinical importance of characterizing neonatal outcomes in this context (8). Such understanding has direct relevance for postnatal monitoring strategies and counseling of affected families (10-12).

Our study aimed to evaluate early neonatal outcomes and one-month follow-up among infants born to mothers with documented SARS-CoV-2 infection during pregnancy who tested polymerase chain reaction (PCR)-negative at delivery, and to compare these outcomes with those of unexposed neonates. We assessed birth anthropometrics, early neonatal morbidity, postnatal adaptation, and short-term clinical outcomes to determine whether resolved maternal COVID-19 is associated with risks to neonatal health.

MATERIALS AND METHODS

This retrospective observational cohort study included 196 neonates born at Gazi University Faculty of Medicine Hospital that has a level IV NICU between March 2020 and August 2021. The study population comprised neonates who required NICU admission and those who remained with their mothers and were followed in the postnatal maternal ward.

The study protocol was reviewed and approved by the Gazi University Faculty of Medicine Clinical Research Ethics Committee, approval number 497, date 31.05.2021, and the requirement for informed consent was waived because of the study's retrospective nature.

Neonates were classified as unexposed if they were born to mothers who had no documented history of SARS-CoV-2 infection during pregnancy and who tested PCR-negative at delivery. The exposed

group consisted of infants born to mothers with confirmed SARS-CoV-2 infection during pregnancy [diagnosed by reverse transcription (RT)-PCR of nasopharyngeal swabs] whose infection had resolved by delivery, as confirmed by negative RT-PCR testing. Mothers with active infection at delivery (positive RT-PCR) were excluded. None of the mothers in either group had received COVID-19 vaccination, as vaccines were not available or were restricted by priority policies during the study period.

Clinical and demographic data were systematically extracted from electronic medical records. Maternal variables included gravidity, parity, history of preterm labor, and comorbid conditions such as gestational diabetes mellitus, hypertensive disorders of pregnancy, hypothyroidism, and smoking status. Maternal COVID-19-related data included trimester of infection, symptom severity, pharmacologic treatment history, and prenatal fetal evaluations, including routine ultrasound examinations and fetal echocardiography when available.

Perinatal and neonatal data included gestational age at birth, birth weight, length, head circumference, and their corresponding percentile values based on standard growth charts. Apgar scores at 1 and 5 minutes, the need for delivery-room resuscitation (including positive-pressure ventilation), NICU admission, respiratory support requirements [supplemental oxygen, continuous positive airway pressure (CPAP), or invasive mechanical ventilation], and NICU course and duration were recorded.

Neonatal clinical course variables included primary admission diagnosis, timing of hyperbilirubinemia onset, initiation of phototherapy, presence of intrauterine growth restriction, antibiotic therapy, inotropic support, and laboratory parameters, when available, including complete blood count, C-reactive protein, and interleukin-6. All neonatal complications occurring within the first four weeks of life were documented to assess early postnatal outcomes.

Categorical variables were compared using Pearson's χ^2 test or Fisher's exact test, and the Fisher-Freeman-Halton exact test was applied for trimester-based analyses. The normality of continuous variables was assessed using the Shapiro-Wilk or Kolmogorov-Smirnov test, and the homogeneity of variances was evaluated using Levene's test. Parametric tests (independent-samples t-test or one-way analysis of variance with Tukey post-hoc test) were used when assumptions were met; otherwise, non-parametric tests (Mann-Whitney U test or Kruskal-Wallis test) were applied. Continuous data are presented as mean ± standard deviation or median [interquartile range (IQR)], as appropriate (13,14).

For trimester-specific analyses with sparse data or zero-event cells, exact methods were employed, including the Freeman-Halton extension of Fisher's exact test with Monte Carlo simulation (100,000 resamples). Relative risks (RR) with corresponding 95% confidence intervals (CIs) were calculated for key clinical outcomes, including NICU admission and hyperbilirubinemia (15).

Statistical Analysis

All statistical analyses were performed using IBM SPSS Statistics (version 29.0; IBM Corp., Armonk, NY). A two-sided p-value was considered statistically significant.

RESULTS

A total of 196 neonates were included: 112 (57.1%) were classified as exposed, born to mothers who had documented SARS-CoV-2 infection during pregnancy but who tested PCR-negative at delivery, and 84 (42.9%) were unexposed, born to mothers with no history of SARS-CoV-2 infection during pregnancy.

Baseline maternal and obstetric characteristics were comparable between groups (Tables 1 and 2). Mean maternal age was 30 ± 5 years in both cohorts (p = 0.68). Gravidity, parity, number of living children, and gestational age at delivery did not differ significantly between groups (all p > 0.05; Supplementary Table 1). Gestational ages were predominantly clustered at term, with a median of 38 weeks (IQR: 37-39; range 29+3 to 41+0). Preterm birth (<37 weeks) occurred in 21 of 112 infants (18.8%) with in utero SARS-CoV-2 exposure and in 10 of 84 unexposed infants (11.9%), with no statistically significant difference between groups (p = 0.19). Early preterm birth (<34 weeks) was uncommon in both groups (5.4% vs. 2.4%, p = 0.47). Among exposed mothers, SARS-CoV-2 infection occurred in the first, second, and third trimesters in 22 (19.6%), 45 (40.2%), and 45 (40.2%), respectively. Fourteen mothers (12.5%) were symptomatic during infection, most commonly with fever and cough, and six (5.4%) received pharmacologic treatment. Maternal characteristics and key neonatal outcomes by exposure status are summarized in Table 1.

Maternal comorbidities, pregnancy characteristics, antenatal screening results, and mode of delivery were similar between the exposed and unexposed groups (all p > 0.05) (Table 1).

Neonatal anthropometric measurements at birth and growth percentiles did not differ significantly between groups (Table 2). Apgar scores at 1 and 5 minutes did not differ significantly between infants born to COVID-19-exposed mothers and unexposed controls (p > 0.05). Intrauterine growth restriction was not significantly associated with maternal COVID-19 infection during pregnancy (p = 0.17).

Although delivery room positive-pressure ventilation was more frequently required in exposed infants (7.3% vs. 2.4%), this difference did not reach statistical significance (p > 0.05) (Table 3). NICU admission occurred more frequently among exposed infants compared with unexposed infants [28.4% vs. 11.9%, p = 0.007; RR 2.38, 95% CI: 1.25-4.54] (Table 1). The distribution of indications for NICU admission by exposure status is presented in Table 4. Among admitted infants, rates of respiratory support (CPAP, intubation), resuscitation, antibiotics, and vasoactive support did not differ (all p > 0.05) (Table 3).

Admission indications (tachypnea, hyperbilirubinemia, and prematurity) were similarly distributed between groups (p > 0.05; Table 4). Analysis of a subset of infants revealed no significant differences in length of NICU stay or in postnatal inflammatory markers between the COVID-19-exposed and -unexposed groups (p > 0.05) (Supplementary Table 2).

Hyperbilirubinemia requiring treatment was more frequent among exposed infants (38.8% vs. 22.2%, p = 0.017; RR: 1.75, 95% CI: 1.08-2.85) (Table 3). In addition, the onset of jaundice occurred earlier in exposed infants [median 3 days (IQR 2-3)] than in unexposed controls [median 5.5 days (IQR 3-8), p = 0.006], whereas peak total

Table 1. Maternal and neonatal outcomes according to in utero SARS-CoV-2 exposure.

Variable	Exposed (n = 112)	Unexposed (n = 84)	p-value	RR (95% CI)
Maternal characteristics				
Gestational diabetes mellitus	16 (14.4%)	12 (14.3%)	0.99	
Hypothyroidism	24 (21.4%)	20 (23.8%)	0.68	
Hypertension	5 (4.5%)	5 (6.0%)	0.64	
Preeclampsia	3 (2.7%)	4 (4.8%)	0.46	
Smoking	8 (7.1%)	6 (7.1%)	0.99	
Cesarean delivery	88 (79.3%)	62 (74.7%)	0.44	
Antenatal steroids	14 (12.5%)	17 (20.2%)	0.14	
IVF pregnancy	16 (14.8%)	8 (9.6%)	0.27	
Neonatal outcomes				
Preterm birth (<37 weeks)	21 (18.8%)	10 (11.9%)	0.19	1.57 (0.80–3.08)
Early preterm (<34 weeks)	6 (5.4%)	2 (2.4%)	0.47	2.25 (0.47–10.7)
Positive-pressure ventilation	8 (7.3%)	2 (2.4%)	1.00	3.00 (0.66–13.6)
CPAP support	4 (3.8%)	3 (3.8%)	0.70	1.00 (0.23–4.29)
Endotracheal intubation	4 (3.8%)	2 (2.5%)	0.70	1.50 (0.29–7.65)
Antibiotic requirement	9 (9.2%)	3 (4.3%)	0.21	2.25 (0.64–7.87)
NICU admission	31 (28.4%)	10 (11.9%)	0.007	2.38 (1.25–4.54)
Hyperbilirubinemia	38 (38.8%)	18 (22.2%)	0.017	1.75 (1.08–2.85)

SARS-CoV-2: Severe acute respiratory syndrome coronavirus 2, RR: Relative risk, CI: Confidence interval, IVF: *In vitro* fertilization, CPAP: Continuous positive airway pressure, NICU: Neonatal intensive care unit.

Table 2. Key neonatal clinical outcomes according to in utero COVID-19 exposure.

Variable	Exposed n (IQR range)	Unexposed n (IQR range)	p-value
Birth weight (g)	3090 (2805–3510)	3188 (2925–3455)	0.31
Apgar score (1 min)	9 (8–9)	9 (9–9)	0.91
Apgar score (5 min)	9 (9–10)	9 (9–10)	0.23
NICU stay (days)	3 (1–7)	5 (2–8)	0.30
Day of jaundice onset	3 (2–3)	5.5 (3–8)	0.006
Phototherapy treatment threshold	18.0 [15.6–18.2]	15 18.0 [17.0–18.9]	0.58
Day regained birth weight	8 (6–11)	8 (6–10)	0.50
Day full enteral feeding	1 (1–1)	1 (1–1)	0.06

Data are presented as median (IQR). COVID-19: Coronavirus Disease-2019, IQR: Interquartile range, NICU: Neonatal intensive care unit.

Table 3. Neonatal respiratory and clinical outcomes.

Outcome	Exposed n (%)	Unexposed n (%)	p-value	RR (95% CI)
CPAP support	4 (3.8)	3 (3.8)	>0.05	
Endotracheal intubation	4 (3.8)	2 (2.5)		
Positive-pressure ventilation	8 (7.3)	2 (2.4)		
Antibiotic requirement	9 (9.2)	3 (4.3)		
NICU admission	31 (28.4)	10 (11.9)	0.007	2.38 (1.25–4.54)
Hyperbilirubinemia	38 (38.8)	18 (22.2)	0.017	1.75 (1.08–2.85)

RR: Relative risk, CI: Confidence interval, CPAP: Continuous positive airway pressure, NICU: Neonatal intensive care unit.

bilirubin levels did not differ significantly between groups (Table 2).

Direct Coombs testing was available for a subset of the cohort (n = 57) and was performed when clinically indicated. While the overall prevalence of Coombs positivity did not differ significantly between groups, the distribution of the severity of positivity varied by exposure status. All cases of high-grade (≥2+) Coombs positivity occurred in the exposed group, whereas moderate positivity (1-2+) was more frequent among unexposed infants (p = 0.004) (Table 5). In trimester-specific analyses of exposed infants, the frequency of endotracheal intubation varied by trimester. Infants exposed during the second trimester had a higher rate of intubation (10.0%) compared with infants exposed in the first or third trimesters, in which no intubations were observed (p = 0.034) (Table 6). This signal was not accompanied by consistent differences in related respiratory endpoints (e.g., CPAP or combined respiratory support) or in non-respiratory outcomes. Second-trimester exposure was associated with an increased risk of endotracheal intubation compared with first- and third-trimester exposure combined (RR: 5.2, 95% CI: 1.1-24.6; p = 0.034). Duration-based analyses showed a significant difference in intubation duration across trimesters (Kruskal-Wallis p = 0.036), driven by longer intubation durations among infants exposed in the second trimester.

Feeding progression, postnatal weight loss, time to regain birth weight, achievement of full enteral feeding, and early postnatal complications within the first four weeks of life did not differ significantly between exposed and unexposed infants (all p > 0.05).

Table 4. Indications for NICU admission according to exposure status.

Indication	Exposed (n = 31)	Unexposed (n = 10)	p-value
Tachypnea/respiratory distress	12 (38.7%)	4 (40.0%)	0.93
Hyperbilirubinemia	10 (32.3%)	3 (30.0%)	0.88
Prematurity	7 (22.6%)	2 (20.0%)	0.85
Other	2 (6.4%)	1 (10.0%)	0.69

NICU: Neonatal intensive care unit.

Table 5. Distribution of direct coombs test results.

Direct Coombs result	Exposed n (%)	Unexposed n (%)
Negative	31 (75.6)	10 (24.4)
Positive (0.5–1+)	4 (80.0)	1 (20.0)
Positive (1–2+)	1 (12.5)	7 (87.5)
Positive (≥2+)	3 (100.0)	0 (0.0)

Direct Coombs testing was performed based on clinical indication (n = 57).

DISCUSSION

In our single-center cohort of 196 neonates, infants exposed in utero to maternal SARS-CoV-2 infection exhibited higher rates of hyperbilirubinemia, earlier onset of jaundice, increased NICU admissions, and distinct patterns of direct Coombs test positivity compared with unexposed controls. Notably, these associations were observed despite maternal PCR negativity at delivery and in the absence of increased severe respiratory morbidity or mortality. Together, these findings suggest that resolved maternal COVID-19 may not confer substantial risk for major neonatal complications but may be associated with subtler metabolic and immunologic alterations that are not captured by conventional neonatal outcome measures (12,16). Our results extend prior population-based studies, including large nationwide cohorts, which have reported modest increases in NICU admission and neonatal jaundice following maternal SARS-CoV-2 infection, while consistently demonstrating low rates of severe neonatal disease (12).

Birth anthropometry, Apgar scores, early feeding milestones, postnatal weight trajectories, and respiratory support requirements did not differ between groups. These findings align with large systematic reviews and population-based studies showing that major neonatal outcomes are generally preserved following resolved maternal SARS-CoV-2 infection, even as more subtle metabolic or immunologic alterations may be detectable (7,17-20).

Although NICU admission was more frequent among exposed infants, indications for admission were similarly distributed between groups, and no differences were observed in indicators of disease severity, including length of stay, intensity of respiratory support, and inflammatory markers. This suggests that increased admissions were not accompanied by greater severity of illness. Throughout the study, NICU admission was based on standard clinical indications; no formal category of observation-only admission solely attributable to maternal COVID-19 exposure was established at our institution. Of note, no formal changes in institutional NICU admission criteria occurred during the study period (12,21-23).

A key finding of this study was the higher incidence and earlier onset of hyperbilirubinemia among exposed neonates. Although peak bilirubin levels did not differ significantly between groups, exposed infants developed jaundice earlier and were more likely to require treatment (Table 2). These findings are consistent with reports from multicenter cohorts and case series describing increased rates of neonatal jaundice following maternal SARS-CoV-2 infection during pregnancy and point toward subtle alterations in bilirubin handling rather than overt hepatic dysfunction (24,25).

Table 6. Trimester-specific neonatal respiratory outcomes among exposed infants.

Outcome	1st trimester (n = 22)	2nd trimester (n = 45)	3rd trimester (n = 45)	p-value
Endotracheal intubation (%)	0 (0.0%)	4 (10.0%)	0 (0.0%)	0.034
Intubation duration (days, mean ± SD)	0	1.97 ± 9.51	0	0.036
CPAP requirement (%)	1 (4.8%)	3 (7.5%)	0 (0.0%)	0.41
Combined respiratory support (%)	3 (14.3%)	6 (14.0%)	1 (2.2%)	0.18

SD: Standard deviation, CPAP: Continuous positive airway pressure.

Several mechanisms may account for these observations. Maternal SARS-CoV-2 infection may induce systemic inflammation and cytokine release that alter placental function and disrupt fetal immune programming (16). Altered transplacental transfer of maternal antibodies may subsequently contribute to immune-mediated hemolytic processes in the neonate, while even subtle respiratory adaptation challenges can augment bilirubin production through increased erythrocyte turnover (24,26). Together, these interacting pathways provide a biologically plausible explanation for the earlier onset and higher frequency of hyperbilirubinemia observed in exposed infants, as well as for the distinct patterns of Coombs test severity described below (16,24,26).

Within this context, the pattern of severity on the direct Coombs test provides additional insight. While overall Coombs positivity rates were comparable between groups, high-grade positivity occurred exclusively among exposed infants, whereas weaker positivity predominated among unexposed controls. Direct Coombs testing was performed in a clinically selected subset of infants rather than systematically across the cohort, thereby introducing selection bias. In addition, the relatively small sample size of this subgroup limits statistical power and reduces the generalizability of these findings. Therefore, the observed differences in Coombs test severity should be interpreted with caution (24).

When the timing of maternal infection is considered, our findings provide nuanced insights. In trimester-specific analyses, infants exposed during the second trimester demonstrated a higher frequency of endotracheal intubation than those exposed during the the first or third trimesters, and second-trimester exposure was associated with an increased RR of intubation when first- and third-trimester exposures were combined as the reference. Notably, this association was confined to intubation and was not accompanied by consistent trimester-related differences in other admission-related respiratory outcomes, including CPAP use or combined respiratory support during hospitalization. Given the low absolute number of events and the absence of concordant differences across related endpoints, this finding should be interpreted cautiously and regarded as hypothesis-generating rather than confirmatory. In addition, several RR estimates exceeded 1.0 with wide CIs, reflecting limited event counts and statistical precision.

Placed within the context of existing population-based and longitudinal evidence, these observations are broadly consistent with data suggesting that neonatal morbidity following maternal SARS-CoV-2 infection is generally modest and that adverse neonatal outcomes often occur in the absence of direct neonatal infection (12,27-29). In a Swedish nationwide cohort, maternal SARS-CoV-2 infection during pregnancy was associated with modest increases in neonatal care admission, respiratory morbidity, and hyperbilirubinemia, while neonatal test positivity remained rare; notably, the median interval from maternal test positivity to delivery was 36 days (12). In that study, preterm birth emerged as an important mediator of neonatal respiratory morbidity (12). Similarly, in our cohort, the absence of trimester-related differences across most respiratory endpoints and the low overall frequency of severe respiratory outcomes support the conclusion that serious neonatal respiratory disease is uncommon among exposed but uninfected infants. At the same time, the isolated, trimester-specific intubation signal observed in our data suggests that vulnerability may not be uniform across gestation and raises the possibility that a narrow window of exposure could be associated with more severe respiratory adaptation in a small subset of infants.

Evidence from longitudinal cohorts further clarifies why trimester-dependent effects are not consistently detected when broader respiratory distress endpoints are examined (29). In the COVID Outcomes in Mother Infant Pairs study, respiratory distress among exposed but uninfected neonates was defined by typical clinical signs and radiographic findings (29). However, comparisons across earlier and later gestational exposure did not demonstrate clear trimester-dependent differences in respiratory distress at birth (29). This apparent discrepancy likely reflects differences in outcome definitions and cohort characteristics across studies. Endotracheal intubation represents a more specific marker of severe respiratory compromise than composite respiratory distress measures, and may therefore be more sensitive in identifying clinically meaningful impairments in early respiratory adaptation that are not captured by milder forms of respiratory support, such as CPAP.

Trimester-dependent susceptibility is biologically plausible. Placental development, fetal lung maturation, and immune-inflammatory signaling pathways vary across gestation, and mid-gestation has been proposed as a potentially sensitive window for indirect fetal effects of maternal systemic inflammation (30,31). Variations in placental expression of viral entry-related proteins, such as ACE2 and TMPRSS2, across gestation further support this concept (31,32). However, given the sparse event counts and lack of corroborating trimester differences across other outcomes in our cohort, definitive conclusions cannot be drawn. Larger prospective studies that incorporate standardized neonatal respiratory phenotyping, placental pathology, and inflammatory profiling will be required to determine whether this signal represents a reproducible gestational window of susceptibility.

Within the broader framework of gestational timing, first-trimester exposure warrants brief consideration (9,33). While several reports suggest that asymptomatic or mild infection in early pregnancy is not associated with major adverse neonatal outcomes, systematic reviews have reported increased risks of adverse pregnancy outcomes in the setting of more severe maternal disease (9,34,35). In our cohort, maternal infection that had resolved before delivery was not associated with an increased risk of preterm birth or growth restriction. Several cohorts have found no increase in preterm birth, NICU admission, or growth restriction when maternal infection resolved before delivery (35-37). Taken together, these findings suggest that early pregnancy exposure, when mild or resolved, may spare major neonatal outcomes, while subtle effects related to timing cannot be excluded (36).

Reassuringly, early postnatal follow-up during the first month of life did not reveal differences between exposed and unexposed infants in feeding tolerance, growth, rehospitalization, or screening outcomes, which further indicates that short-term post-discharge health is generally preserved after resolution of maternal infection.

These findings support a risk-stratified approach to postnatal surveillance in which infants exposed to maternal SARS-CoV-2 infection during pregnancy do not require routine escalation of care

based solely on exposure history. However, awareness of potential early bilirubin elevation or challenges in respiratory adaptation may inform individualized monitoring strategies.

Study Limitations

Several limitations should be acknowledged. The retrospective single-center design limits causal inference and generalizability; residual confounding cannot be excluded. Most maternal infections were mild or clinically resolved before delivery, which may limit the generalizability of these findings to severe maternal SARS-CoV-2 infection. Some laboratory and clinical parameters were available only for small subsets of infants and were therefore analyzed descriptively. In addition, all pregnancies in this cohort occurred prior to the availability of COVID-19 vaccination, and our findings may not apply to vaccinated populations or to infections caused by later viral variants.

CONCLUSION

Overall, major neonatal outcomes were largely unaffected by resolved maternal COVID-19; however, our findings suggest subtle, possibly trimester-related differences in neonatal adaptation following in utero exposure. The increased risk of endotracheal intubation among infants exposed during the second trimester suggests a possible window of heightened susceptibility related to respiratory adaptation, while concurrent abnormalities in bilirubin metabolism and patterns consistent with immune-mediated hemolysis may reflect additional physiological processes not captured by conventional neonatal morbidity measures. Despite higher NICU admission rates, no parallel increase in major clinical morbidities or supportive care requirements was observed. Together, these observations support the value of trimester-aware clinical surveillance and underscore the need for prospective studies to clarify underlying mechanisms and optimize neonatal care strategies for exposed infants.

Ethics

Ethics Committee Approval: The study protocol was reviewed and approved by the Gazi University Faculty of Medicine Clinical Research Ethics Committee (approval number 497, dated 31.05.2021).

Informed Consent: The requirement for informed consent was waived because of the study's retrospective nature.

Footnotes

Authorship Contributions

Surgical and Medical Practices: E.K., G.K., M.T., M.B., N.H., İ.M.H., E.Ö., C.T., E.E., E.Ko., Concept: E.K., İ.M.H., E.Ö., C.T., E.E., E.Ko. Design: E.K., G.K., M.T., N.H., İ.M.H., E.Ö., C.T., E.E., E.Ko., Data Collection or Processing: E.K., G.K., M.T., M.B., N.H., A.K., İ.M.H., E.Ö., C.T., E.E., E.Ko., Analysis or Interpretation: E.K., M.T., N.H., A.K., İ.M.H., E.Ö., C.T., E.E., E.Ko., Literature Search: E.K., G.K., M.B., N.H., A.K., İ.M.H., E.Ö., C.T., E.E., E.Ko., Writing: E.K., G.K., M.T., M.B., N.H., A.K., İ.M.H., E.Ö., C.T., E.E., E.Ko.

Conflict of Interest: No conflict of interest was declared by the authors.

Financial Disclosure: The authors declared that this study received no financial support.

Supplementary Table 1 Link: https://d2v96fxpocvxx.cloudfront.net/13b035c5-551c-4fd4-a824-19a1febb0519/content-images/3601da28-83e0-45b2-9171-2c364629244a.pdf

REFERENCES

1. Boettcher LB, Metz TD. Maternal and neonatal outcomes following SARS-CoV-2 infection. Semin Fetal Neonatal Med. 2023; 28: 101428.
2. Baud D, Pomar L, editors. Emerging virus infections in adverse pregnancy outcomes. Basel: MDPI; 2022.
3. Shabil M, Gaidhane S, Ballal S, Kumar S, Bhat M, Sharma S, et al. Maternal COVID-19 infection and risk of respiratory distress syndrome among newborns: a systematic review and meta-analysis. BMC Infect Dis. 2024; 24: 1318.
4. Flannery DD, Zevallos Barboza A, Pfeifer MR, Hudak ML, Barnette K, Getzlaff TR, et al. Perinatal COVID-19 maternal and neonatal outcomes at two academic birth hospitals. J Perinatol. 2022; 42: 1338-45.
5. Charuta A, Smuniewska M, Woźniak Z, Paziewska A. Effect of COVID-19 on pregnancy and neonate's vital parameters: a systematic review. J Pregnancy. 2023; 2023: 3015072.
6. Vizheh M, Allahdadian M, Ghasemi-Tehrani H, Muhidin S, Hashemi M, Dehghan M. Maternal and neonatal outcomes of COVID-19 infection in pregnancy. Arch Iran Med. 2023; 26: 43-9.
7. Wei SQ, Bilodeau-Bertrand M, Liu S, Auger N. The impact of COVID-19 on pregnancy outcomes: a systematic review and meta-analysis. CMAJ. 2021; 193: E540-8.
8. World Health Organization. WHO COVID-19 dashboard. Available from: https://data.who.int/dashboards/covid19/cases. Accessed January 19, 2026.
9. Khalil A, Kalafat E, Benlioglu C, O'Brien P, Morris E, Draycott T, et al. SARS-CoV-2 infection in pregnancy: a systematic review and meta-analysis of clinical features and pregnancy outcomes. EClinicalMedicine. 2020; 25: 100446.
10. Yu N, Li W, Kang Q, Xiong Z, Wang S, Lin X, et al. Clinical features and obstetric and neonatal outcomes of pregnant patients with COVID-19 in Wuhan, China: a retrospective, single-centre, descriptive study. Lancet Infect Dis. 2020; 20: 559-64.
11. Smith V, Seo D, Warty R, Payne O, Salih M, Chin KL, et al. Maternal and neonatal outcomes associated with COVID-19 infection: a systematic review. PLoS One. 2020; 15: e0234187.
12. Norman M, Navér L, Söderling J, Ahlberg M, Hervius Askling H, Aronsson B, et al. Association of maternal SARS-CoV-2 infection in pregnancy with neonatal outcomes. JAMA. 2021; 325: 2076-86.
13. Altman DG. Practical statistics for medical research. London: Chapman and Hall/CRC; 1990.
14. Conover WJ. Practical nonparametric statistics. New York: John Wiley & Sons; 1999.
15. Lydersen S, Pradhan V, Senchaudhuri P, Laake P. Choice of test for association in small sample unordered r x c tables. Stat Med. 2007; 26: 4328-43.
16. Gee S, Chandiramani M, Seow J, Pollock E, Modestini C, Das A, et al. The legacy of maternal SARS-CoV-2 infection on the immunology of the neonate. Nat Immunol. 2021; 22: 1490-502.
17. Zhang D, Huang T, Chen Z, Zhang L, Gao Q, Liu G, et al. Systematic review and meta-analysis of neonatal outcomes of COVID-19 vaccination in pregnancy. Pediatr Res. 2023; 94: 34-42.
18. Murphy CA, O'Reilly DP, Edebiri O, Donnelly JC, McCallion N, Drew RJ, et al. The effect of COVID-19 infection during pregnancy; evaluating neonatal outcomes and the impact of the B.1.1.7 variant. Pediatr Infect Dis J. 2021; 40: e475-81.

19. Pashaei Z, SeyedAlinaghi S, Qaderi K, Barzegary A, Karimi A, Mirghaderi SP, et al. Prenatal and neonatal complications of COVID-19: a systematic review. Health Sci Rep. 2022; 5: e510.
20. Mullins E, Perry A, Banerjee J, Townson J, Grozeva D, Milton R, et al. Pregnancy and neonatal outcomes of COVID-19: the PAN-COVID study. Eur J Obstet Gynecol Reprod Biol. 2022; 276: 161-7.
21. Sankaran D, Nakra N, Cheema R, Blumberg D, Lakshminrusimha S. Perinatal SARS-CoV-2 infection and neonatal COVID-19: a 2021 update. NeoReviews. 2021; 22: e284-95.
22. Woodworth KR, Olsen EO, Neelam V, Lewis EL, Galang RR, Oduyebo T, et al. Birth and infant outcomes following laboratory-confirmed SARS-CoV-2 infection in pregnancy - SET-NET, 16 jurisdictions, March 29-October 14, 2020. MMWR Morb Mortal Wkly Rep. 2020; 69: 1635-40.
23. Anderson NB, Calkins KL. Neonatal indirect hyperbilirubinemia. NeoReviews. 2020; 21: e749-60.
24. Al-Matary A, Almatari F, Al-Matary M, AlDhaefi A, Alqahtani MHS, Alhulaimi EA, et al. Clinical outcomes of maternal and neonate with COVID-19 infection - multicenter study in Saudi Arabia. J Infect Public Health. 2021; 14: 702-8.
25. Itriago E, Lingappan K, Teruya J, Dinu D. Hemolysis in neonates born to mothers with history of SARS-CoV-2 infection during pregnancy: a case series. Int J Clin Pediatr. 2022; 11: 27-32.
26. Itriago E, Lingappan K, Teruya J, Dinu D. Hemolysis in neonates born to mothers with history of SARS-CoV-2 infection during pregnancy: a case series. Int J Clin Pediatr. 2022; 11: 27-32.
27. Schell RC, Macias DA, Garner WH, White AM, McIntire DD, Pruszynski J, et al. Examining the impact of trimester of diagnosis on COVID-19 disease progression in pregnancy. Am J Obstet Gynecol MFM. 2022; 4: 100728.
28. Song D, Prahl M, Gaw SL, Narasimhan SR, Rai DS, Huang A, et al. Passive and active immunity in infants born to mothers with SARS-CoV-2 infection during pregnancy: prospective cohort study. BMJ Open. 2021; 11: e053036.
29. Man OM, Azamor T, Cambou MC, Fuller TL, Kerin T, Paiola SG, et al. Respiratory distress in SARS-CoV-2 exposed uninfected neonates followed in the COVID Outcomes in Mother-Infant Pairs (COMP) Study. Nat Commun. 2024; 15: 399.
30. Argueta LB, Lacko LA, Bram Y, Tada T, Carrau L, Rendeiro AF, et al. Inflammatory responses in the placenta upon SARS-CoV-2 infection late in pregnancy. iScience. 2022; 25: 104223.
31. Chen J, Neil JA, Tan JP, Rudraraju R, Mohenska M, Sun YBY, et al. A placental model of SARS-CoV-2 infection reveals ACE2-dependent susceptibility and differentiation impairment in syncytiotrophoblasts. Nat Cell Biol. 2023; 25: 1223-34.
32. Indra S, Chalak K, Das P, Mukhopadhyay A. Placenta a potential gateway of prenatal SARS-CoV-2 infection: a review. Eur J Obstet Gynecol Reprod Biol. 2024; 303: 123-31.
33. Piekos SN, Roper RT, Hwang YM, Sorensen T, Price ND, Hood L, et al. The effect of maternal SARS-CoV-2 infection timing on birth outcomes: a retrospective multicentre cohort study. Lancet Digit Health. 2022; 4: e95-104.
34. Marchand G, Patil AS, Masoud AT, Ware K, King A, Ruther S, et al. Systematic review and meta-analysis of COVID-19 maternal and neonatal clinical features and pregnancy outcomes up to June 3, 2021. AJOG Glob Rep. 2022; 2: 100049.
35. Rodriguez-Wallberg KA, Nilsson HP, Røthe EB, Zhao A, Shah PS, Acharya G. Outcomes of SARS-CoV-2 infection in early pregnancy: a systematic review and meta-analysis. Acta Obstet Gynecol Scand. 2024; 103: 786-98.
36. Tang Y, Chen L, Han T, Hu C, Li P, Tang J, et al. The impact of acute and prior SARS-CoV-2 infection on maternal and neonatal outcomes in pregnant women: a single-center retrospective cohort study. BMC Pregnancy Childbirth. 2025; 25: 181.
37. Cosma S, Carosso AR, Cusato J, Borella F, Bertero L, Bovetti M, et al. Obstetric and neonatal outcomes after SARS-CoV-2 infection in the first trimester of pregnancy: a prospective comparative study. J Obstet Gynaecol Res. 2022; 48: 393-401.

Original Investigation | Özgün Araştırma

Gazi Med J 2026;37(3):384-391

DOI: http://dx.doi.org/10.12996/gmj.2026.4647

Ten-Year Clinical Outcomes in MINOCA: A Clinical Framework for Long-Term Risk Stratification

MINOCA'da On Yıllık Klinik Sonuçlar: Uzun Dönem Risk Sınıflaması için Klinik Bir Çerçeve

Yusuf Bozkurt Şahin[1], Özden Seçkin[2], Serkan Ünlü[2]

[1]Clinic of Cardiology, University of Health Sciences Türkiye, Ankara Etlik City Hospital, Ankara, Türkiye
[2]Department of Cardiology, Gazi University, Faculty of Medicine, Ankara, Türkiye

ABSTRACT

Objective: This study aimed to design and validate myocardial infarction with non-obstructive coronary arteries (MINOCA), a practical bedside prognostic tool for evaluating the long-term risk profiles of patients experiencing myocardial infarction (MI) with MINOCAs.

Methods: A retrospective cohort analysis was carried out at Gazi University between January 2013 and December 2018. MINOCA was diagnosed based on standard biochemical and clinical MI criteria, alongside angiographic evidence of stenosis of <50% in the epicardial arteries. We extracted baseline clinical, laboratory, and echocardiographic data from electronic registries. The primary endpoint was major adverse cardiovascular events (MACEs), defined as a composite of cardiovascular death, non-fatal MI, stroke, and hospitalization for heart failure; outcomes were tracked up to June 2025. Predictor variables were assessed via logistic regression, and the multivariable coefficients were used to assign point values for the PRO-MINOCA score. Statistical evaluations included receiver operating characteristic curves for discrimination, Kaplan-Meier survival curves, and Cox proportional hazards models for survival analysis.

Results: The cohort comprised 658 subjects (mean age 59.2 ± 11.6 years; 52.4% women). During the extended follow-up, 158 individuals (24%) experienced MACE. Multivariable analysis identified several independent risk factors: age ≥65 years, hypertension, diabetes, left ventricular ejection fraction (EF) <50%, estimated glomerular filtration rate <60 mL/min/1.73 m², elevated levels of C-reactive protein, troponin, and N-terminal pro-brain natriuretic peptide (NT-proBNP), incident atrial fibrillation, and a history of peripheral

ÖZ

Amaç: Bu çalışmada, obstrüktif olmayan koroner arterlerle seyreden miyokard infarktüsü (MINOCA) hastalarında uzun dönem kardiyovasküler riskin öngörülmesi için klinik pratikte kolaylıkla kullanılabilecek PRO-MINOCA skorunun geliştirilmesi ve doğrulanması amaçlandı.

Yöntemler: Ocak 2013-Aralık 2018 tarihleri arasında Gazi Üniversitesi'nde MINOCA tanısı alan hastalar retrospektif olarak değerlendirildi. MINOCA tanısı, miyokard infarktüsüne ait klinik ve biyokimyasal kriterlerin varlığına ek olarak koroner anjiyografide epikardiyal koroner arterlerde <%50 darlık saptanması ile konuldu. Hastaların başvuru sırasındaki klinik özellikleri, laboratuvar bulguları ve ekokardiyografik verileri hastane kayıtlarından elde edildi. Birincil sonlanım noktası kardiyovasküler ölüm, ölümcül olmayan miyokard infarktüsü, inme ve kalp yetersizliği nedeniyle hastaneye yatıştan oluşan majör advers kardiyovasküler olay (MACE) olarak belirlendi. Klinik sonlanımlar Haziran 2025'e kadar takip edildi. PRO-MINOCA skorunu oluşturmak için öngördürücü değişkenler lojistik regresyon analizi ile değerlendirildi ve çok değişkenli analizde bağımsız belirleyici olarak saptanan parametreler puanlama sistemine dahil edildi. Skorun ayırt edici gücü alıcı işletim karakteristiği eğrisi analiziyle, uzun dönem prognostik değeri ise Kaplan-Meier sağkalım analizi ve Cox regresyon modeliyle değerlendirildi.

Bulgular: Çalışmaya toplam 658 hasta dahil edildi. Hastaların ortalama yaşı 59,2 ± 11,6 yıl olup %52,4'ü kadındı. Uzun dönem takipte 158 hastada (%24) MACE gelişti. Çok değişkenli analizde ≥65 yaş, hipertansiyon, diabetes mellitus, sol ventrikül ejeksiyon fraksiyonunun <%50 olması, tahmini glomerüler filtrasyon hızının <60 mL/dk/1,73

Cite this article as: Şahin YB, Seçkin Ö, Ünlü S. Ten-year clinical outcomes in MINOCA: a clinical framework for long-term risk stratification. Gazi Med J. 2026;37(3):384-391

Address for Correspondence/Yazışma Adresi: Yusuf Bozkurt Şahin, Clinic of Cardiology, University of Health Sciences Türkiye, Ankara Etlik City Hospital, Ankara, Türkiye
E-mail / E-posta: ybozkurtsahin@gmail.com
ORCID ID: orcid.org/0000-0003-3523-8783

Received/Geliş Tarihi: 22.02.2026
Accepted/Kabul Tarihi: 11.05.2026
Publication Date/Yayınlanma Tarihi: 10.07.2026

ABSTRACT

arterial disease, MI, or prior stroke. The formulated PRO-MINOCA scale (ranging from 0 to 12 points; higher scores indicate greater risk) allocated 2 points each to reduced EF and elevated NT-proBNP and 1 point to the other parameters. The score demonstrated strong discriminative capacity [area under the curve: 0.781; 95% confidence interval (CI): 0.745–0.816; $p < 0.001$]. A threshold of ≥7 provided 74% sensitivity and 70% specificity. Individuals scoring ≥7 exhibited a profoundly reduced event-free survival rate (log-rank χ^2: 61.2; $p < 0.001$) and a more than twofold increase in MACE risk (hazard ratio: 2.67; 95% CI: 2.06-3.44).

CONCLUSION: The PRO-MINOCA score serves as a highly practical, purely clinical instrument that effectively identifies MINOCA patients who are at elevated long-term risk based on baseline diagnostic data. This tool can facilitate early, risk-adjusted management, particularly in environments lacking advanced cardiovascular imaging. Prospective and external validation studies are recommended.

Keywords: Myocardial infarction, non-obstructive coronary arteries, risk assessment, cardiac biomarkers, prognosis, chronic kidney disease

ÖZ

m^2 olması, yüksek C-reaktif protein, troponin ve N-terminal pro-beyin natriüretik peptid (NT-proBNP) düzeyleri, yeni gelişen atriyal fibrilasyon ve geçirilmiş periferik arter hastalığı, miyokard infarktüsü veya inme öyküsü uzun dönem MACE için bağımsız belirleyiciler olarak saptandı. Bu değişkenler temel alınarak oluşturulan PRO-MINOCA skoru 0 ile 12 puan arasında değişmekteydi. Azalmış ejeksiyon fraksiyonu ve yüksek NT-proBNP düzeyi ikişer puan, diğer değişkenler ise birer puan olarak skorlandı. PRO-MINOCA skoru MACE öngörüsünde iyi düzeyde ayırt edici performans gösterdi [eğri altında kalan alan: 0,781; %95 güven aralığı (GA): 0,745–0,816; $p < 0,001$]. ≥7 puan değeri %74 duyarlılık ve %70 özgüllük sağladı. PRO-MINOCA skoru ≥7 olan hastalarda olaysız sağkalım anlamlı olarak daha düşüktü (log-rank χ^2: 61,2; $p < 0,001$) ve MACE riski belirgin olarak artmıştı [hazard oranı: 2,67; %95 GA: 2,06–3,44].

Sonuç: PRO-MINOCA skoru, MINOCA hastalarında başvuru anında elde edilebilen klinik, laboratuvar ve ekokardiyografik verilerle uzun dönem kardiyovasküler riski öngörebilen pratik bir prognostik araçtır. İleri kardiyak görüntüleme yöntemlerine erişimin sınırlı olduğu klinik ortamlarda erken risk sınıflaması ve hasta yönetiminin planlanmasına katkı sağlayabilir. Skorun klinik kullanımını desteklemek için prospektif ve dış doğrulama çalışmalarına ihtiyaç vardır.

Anahtar Sözcükler: Miyokard infarktüsü, obstrüktif olmayan koroner arterler, risk değerlendirmesi, kardiyak biyobelirteçler, prognoz, kronik böbrek hastalığı

INTRODUCTION

Acute myocardial infarction (MI) remains a primary driver of global cardiovascular morbidity and mortality (1). While the traditional diagnosis of MI relies on identifying significant occlusions within the epicardial coronary vessels (2). MI with non-obstructive coronary arteries is characterized by the presence of MI signs despite the absence of obstructive lesions (defined as <50% stenosis) during coronary angiography. This unique clinical entity is estimated to occur in approximately 5% to 15% of all acute coronary syndrome presentations (3).

Although historically perceived as a relatively benign entity, contemporary research highlights that MINOCA is associated with a considerable long-term cardiovascular burden (3,4). Mortality rates at one year can approach 5%, while the five-year occurrence of major adverse cardiovascular events (MACEs) may hit 25% (5). Furthermore, extensive registry data, such as the SWEDEHEART study, indicate that the long-term prognostic profile of individuals with MINOCA closely mirrors that of patients suffering from obstructive MI (6).

The clinical complexity of MINOCA stems from its diverse pathophysiological mechanisms, which encompass microvascular dysfunction, epicardial vasospasm, myocarditis, takotsubo syndrome, and thromboembolic events (7). To identify the precise underlying etiology, advanced imaging modalities—most notably cardiac magnetic resonance (CMR), optical coherence tomography (OCT), and intravascular ultrasound (IVUS)—are of paramount importance. However, the routine application of these modalities is frequently hindered by logistical barriers, limited availability, and high costs (4,8,9). Consequently, a significant proportion of MINOCA patients are managed clinically without a confirmed etiological diagnosis.

Because of these diagnostic hurdles, there is a clear imperative for an accessible, MINOCA-specific risk stratification instrument. Standard prognostic calculators like the GRACE and TIMI scores fail to adequately capture the distinct clinical profile of the MINOCA population (9-11). Currently, no specialized scoring system that relies entirely on standard laboratory and clinical parameters at the time of presentation has achieved widespread clinical integration.

To address this gap, our study sought to formulate and validate the PRO-MINOCA score, a novel prognostic model tailored to forecast long-term MACE in patients with angiographically verified MINOCAs. Using only baseline laboratory and clinical metrics collected at initial presentation, this tool enables rapid risk assessment without the need for advanced imaging or definitive etiological categorization. Ultimately, PRO-MINOCA delivers a pragmatic, real-world strategy to guide clinical decision-making for this complex patient cohort.

MATERIALS AND METHODS

Study Design and Setting

This research was conducted as a single-centre retrospective study at the Cardiology Department of the Gazi University Faculty of Medicine. Our primary aim was to establish a prognostic scoring tool to predict long-term outcomes for patients with non-obstructive MI, relying exclusively on baseline clinical and laboratory data available at admission.

Ethical Approval

The Institutional Ethics Committee of Gazi University Faculty of Medicine provided formal approval for the research (protocol code: 2025-1013, meeting number: 9, date: 27.05.2025). Due to

the retrospective nature of this clinical registry analysis and the use of de-identified data, the committee waived the requirement for individual patient consent. The study's conduct strictly adhered to the ethical principles of the Declaration of Helsinki.

Study Population

We retrospectively evaluated all patients who underwent coronary angiography with a preliminary diagnosis of acute MI between January 2013 and December 2018. Of approximately 5,500 acute MI patients who were catheterized during the five-year window, 658 met the strict criteria for MINOCA and constituted our final study cohort.

The diagnosis of MINOCA requires clinical, biochemical, and electrocardiographic evidence of an acute infarction [e.g., elevated cardiac troponin, dynamic electrocardiography (ECG) alterations, ischemic chest pain] coupled with angiographic evidence of <50% stenosis in all major epicardial arteries. While some individuals underwent advanced imaging (such as CMR, OCT, or IVUS), these findings were not used to inform etiological subclassification in the present analysis. Inclusion depended strictly on the established angiographic criteria for non-obstructive MI. The entire eligible cohort within the specified timeframe was enrolled without an a priori sample size calculation, aiming to reflect real-world prognostic dynamics.

Data Collection

Patient data were extracted from the institutional electronic medical records and historical interventional logs. We documented presenting symptoms, baseline demographics, cardiovascular risk factors, ECG characteristics, comorbidities, and initial medical therapies. Routine laboratory values recorded at diagnosis—including estimated glomerular filtration rate (eGFR), creatinine, complete blood count, lipid profile, C-reactive protein (CRP), haemoglobin, and cardiac biomarkers (troponin and natriuretic peptides)—were integrated into the evaluation as potential prognostic indicators.

Thresholds for specific biomarkers were defined based on current literature and internal receiver operating characteristic (ROC) analyses. We established binary cut-offs of >1000 ng/L for peak high-sensitivity cardiac troponin T and >1000 pg/mL for and N-terminal pro-brain natriuretic peptide (NT-proBNP), reflecting their prognostic relevance demonstrated in prior research (12-15). Cut-off values of <60 mL/min/1.73 m² for eGFR and >10 mg/L for CRP were similarly adopted based on clinical guidelines and previous evidence (16).

Baseline echocardiographic measurements were obtained from digital archives. Extended clinical follow-up was tracked via national death registries, hospital databases, and digital records, and concluded in June 2025. The primary endpoint was the occurrence of MACEs, defined as a composite of cardiovascular death, non-fatal MI, stroke, and hospitalization for heart failure. All laboratory parameters were measured using standardized institutional assays, and the cohort was analyzed without predefined experimental grouping.

Statistical Analysis

Continuous data are presented as medians with interquartile ranges or means ± standard deviations, depending on data distribution, and were compared using the Mann-Whitney U test or Student's t-test. Categorical variables are presented as frequencies and percentages and analyzed using Fisher's exact test or the chi-square test, as dictated by the data.

To identify predictors of MACE, we initially conducted univariable logistic regression analyses for all potential biochemical, clinical, and echocardiographic variables. Candidate predictors achieving a univariable p-value <0.10 were advanced to a forward stepwise multivariable logistic regression model. Because of their inherent prognostic weight, sex and age were maintained as forced covariates in the multivariable analysis, irrespective of their univariable significance. We confirmed the absence of significant multicollinearity by ensuring that variance inflation factors remained below 2 for all predictors.

Variables that maintained independent associations with MACE in the final multivariable construct were selected to form the PRO-MINOCA score. Point values were allocated based on the relative magnitude of the adjusted odds ratios and on clinical relevance. Variables that had stronger independent associations with MACE, particularly reduced left ventricular ejection fraction (LVEF) and elevated NT-proBNP, were assigned 2 points, whereas the remaining independent predictors were assigned 1 point each, to preserve the simplicity and bedside applicability of the score. The model's discriminative capacity was evaluated using ROC curves, reporting the area under the curve (AUC) alongside 95% confidence intervals. The optimal scoring threshold was identified via the Youden index. Survival dynamics were visualized through Kaplan-Meier curves and assessed with the log-rank test, while hazard ratios were derived from Cox proportional hazards models. A two-tailed p-value below the 0.05 threshold was used to determine statistical significance for all comparative analyses. Data processing and statistical computations were conducted using the SPSS software suite, version 26.0 (IBM Corp., Armonk, NY).

RESULTS

Screening of 5,500 patients who underwent coronary angiography for suspected acute MI was performed. From this initial pool, 658 individuals met the specific inclusion criteria for MINOCA and constituted the final study population. Through systematic linkage with national registries, long-term outcome data were successfully obtained for 100% of the participants. The median follow-up duration was 10.5 years with follow-up extending through June 2025. The study group had a mean age of 59.2 ± 11.6 years, with a female representation of 52.4%. During the clinical observation period, MACE was recorded in 158 patients (24%), while the remaining 500 patients (76%) did not experience any primary endpoints.

Detailed baseline clinical, laboratory, and echocardiographic characteristics, categorized by the occurrence of MACE, are presented in Table 1. Comparative analysis revealed that patients in the MACE (+) group were generally older and demonstrated a higher prevalence of cardiovascular risk factors, including diabetes mellitus, hypertension, hyperlipidemia, and active tobacco use. Furthermore, this group exhibited significantly lower LVEF, larger left atrial diameters, and markedly higher baseline concentrations of CRP, creatinine, troponin, and NT-proBNP. Clinical histories of prior MI, peripheral artery disease (PAD), stroke, and new-onset atrial fibrillation were also more frequent among those who experienced MACE (all $p < 0.05$) (Table 2).

Table 1. Baseline clinical, laboratory and echocardiographic characteristics of the study population according to MACE status.

Variable	Total group (n = 658)	MACE (+) (n = 158)	MACE (–) (n = 500)	p-value
Mean age (years)	59.2 ± 11.6	63.1 ± 10.2	57.8 ± 11.4	<0.001
Female sex, n (%)	345 (52.4%)	92 (58.2%)	253 (50.6%)	0.12
BMI (kg/m²)	27.3 ± 4.1	27.9 ± 4.5	27.0 ± 4.0	0.08
Hypertension, n (%)	308 (46.8%)	96 (60.8%)	212 (42.4%)	<0.001
Diabetes mellitus, n (%)	141 (21.5%)	47 (29.7%)	94 (18.8%)	0.002
Hyperlipidemia, n (%)	258 (39.2%)	73 (46.2%)	185 (37.0%)	0.03
Current smoking, n (%)	209 (31.7%)	65 (41.1%)	144 (28.8%)	0.005
LA diameter (mm)	38.5 ± 5.9	40.1 ± 5.7	38.0 ± 5.8	0.04
Enddiastolic LV diameter (mm)	49.8 ± 6.1	51.1 ± 6.4	49.4 ± 5.9	0.09
LV-EF (%)	53.4 ± 7.2	49.8 ± 8.1	54.9 ± 6.6	<0.001
Wall motion abnormality, n (%)	274 (41.6%)	92 (58.2%)	182 (36.4%)	<0.001
Admission troponin (ng/L)	512 (210–1165)	635 (310–1380)	489 (190–1100)	0.002
Peak troponin (ng/L)	1238 (605–2450)	1460 (740–2680)	1165 (580–2100)	<0.001
NT-proBNP (pg/mL)	1050 (410–2280)	1725 (860–3150)	870 (390–1980)	<0.001
Creatinine (mg/dL)	1.01 ± 0.21	1.21 ± 0.24	0.96 ± 0.18	<0.001
Sodium (mmol/L)	137.6 ± 3.5	137.2 ± 3.8	137.8 ± 3.3	0.38
Potassium (mmol/L)	4.2 ± 0.5	4.1 ± 0.6	4.2 ± 0.4	0.44
CRP (mg/L)	9.6 (4.3–22.1)	13.2 (6.1–30.5)	8.4 (3.8–18.5)	0.006
eGFR (mL/min/1.73 m²)	72.3 ± 18.7	64.2 ± 21.4	75.1 ± 17.2	<0.001
Hemoglobin (g/dL)	13.5 ± 1.7	12.8 ± 1.9	13.7 ± 1.6	0.001
Prior PAD, n (%)	60 (9.1%)	27 (17.1%)	33 (6.6%)	<0.001
Prior stroke or TIA, n (%)	44 (6.7%)	21 (13.3%)	23 (4.6%)	0.002
Onset AF, n (%)	51 (7.8%)	23 (14.6%)	28 (5.6%)	0.01
PRO-MINOCA score	5.6 ± 2.4	7.8 ± 1.8	4.9 ± 2.0	<0.001

Baseline demographic profile, comorbidities, laboratory findings, and echocardiographic measurements of the study cohort are displayed according to long-term MACE status. Data distribution determined the method of descriptive reporting: normally distributed variables are expressed as mean ± SD, whereas skewed variables are presented as median with interquartile range. Categorical parameters are reported as frequency and percentage. Group comparisons were performed using distribution-appropriate tests for continuous variables and contingency analysis for categorical data.
AF: Atrial fibrillation, BMI: Body mass index, CRP: C-reactive protein, eGFR: Estimated glomerular filtration rate, EF: Ejection fraction, Hb: Hemoglobin, HT: Hypertension, LA: Left atrium, LV: Left ventricle, MACE: Major adverse cardiovascular events, MINOCA: Myocardial infarction with non-obstructive coronary arteries, NT-proBNP: N-terminal pro-brain natriuretic peptide, PAD: Peripheral artery disease, TIA: transient ischemic attack, SD: Standard deviation.

In the initial univariable logistic regression, several factors were significantly linked to the development of MACE: age ≥65 years, hypertension, diabetes mellitus, diminished EF (EF <50%), renal impairment (eGFR <60 mL/min/1.73 m²), and elevated levels of troponin, NT-proBNP, and CRP. Additionally, new-onset atrial fibrillation and a history of PAD, MI, or stroke/transient ischemic attack (TIA) were identified as significant predictors. When these variables were entered into a multivariable model, each variable remained an independent predictor of adverse outcomes ($p < 0.05$).

Utilizing these regression coefficients, we constructed the PRO-MINOCA score, a novel clinical risk assessment tool. This scoring system ranges from 0 to 12 points. Elevated NT-proBNP and reduced LVEF, which showed the strongest adjusted associations with MACE and represent clinically established markers of myocardial dysfunction and adverse prognosis, were assigned 2 points each. The remaining independent predictors were each assigned 1 point to preserve the practical, bedside-oriented structure of the score. (Table 3). The average PRO-MINOCA score for the entire cohort was 5.6 ± 2.4. Notably, the MACE (+) group exhibited substantially higher mean scores compared to the event-free group (7.8 ± 1.8 vs. 4.9 ± 2.0, $p < 0.001$).

The discriminative efficiency of the PRO-MINOCA score was confirmed via ROC analysis, which yielded an AUC of 0.781(95% CI: 0.745–0.816, $p < 0.001$). Based on the Youden index (0.44), the optimal diagnostic cut-off was determined to be ≥7, providing a sensitivity of 74% and a specificity of 70% (Figure 1).

Survival dynamics, visualized through Kaplan-Meier analysis, indicated a significantly lower event-free survival rate for patients with a PRO-MINOCA score of ≥7 (log-rank test: χ^2: 61.2, $p < 0.001$). The mean survival duration for those with scores <7 was 3738 days, contrasting with 3187 days in the high-risk group (≥7) (Figure 2). Median survival values followed similar trajectories (3842 vs. 3330 days).

Table 2. Univariate and multivariate logistic regression analysis of variables associated with MACE.

Variables	Univariable OR	p-value	95% confidence interval		Multivariable OR	p-value	95% confidence interval	
			Lower	Upper			Lower	Upper
Age ≥65	1.62	0.023	1.07	2.44	1.50	0.041	1.02	2.22
BMI	1.01	0.893	0.68	1.48	—	—	—	—
Diabetes mellitus	1.92	0.008	1.18	3.09	2.06	0.005	1.25	3.39
Hypertension	1.99	0.006	1.23	3.26	2.24	0.004	1.29	3.90
LV-EF <50%	2.72	<0.001	1.74	4.23	3.29	0.001	1.91	5.68
GFR <60	1.84	0.019	1.10	3.08	1.99	0.022	1.10	3.55
Elevated CRP	1.73	0.011	1.13	2.70	1.82	0.015	1.14	2.89
Onset AF	2.05	0.007	1.21	3.49	2.30	0.008	1.24	4.25
Elevated NT-proBNP	3.46	0.001	2.01	6.13	4.11	<0.001	2.15	7.79
Elevated troponin-T	2.48	0.002	1.40	4.42	2.77	0.001	1.58	4.88
Prior PAD/stroke or TIA	1.80	0.033	1.05	3.13	1.93	0.027	1.07	3.47

This table presents the results of univariable and multivariable logistic regression analyses evaluating predictors of major adverse cardiovascular events. Results are expressed as odds ratios with 95% confidence intervals and p-values. Variables with $p < 0.10$ in univariable analysis were considered for inclusion in the multivariable model. OR: Odds ratio, CI: Confidence interval, AF: Atrial fibrillation, BMI: Body mass index, CRP: C-reactive protein, eGFR: Estimated glomerular filtration rate, LVEF: Left ventricular ejection fraction, NT-proBNP: N-terminal pro-B-type natriuretic peptide, PAD: Peripheral artery disease, TIA: Transient ischemic attack.

Table 3. PRO-MINOCA score components, clinical definitions, odds ratios, and assigned points.

PRO-MINOCA component	Definition/clinical criteria	OR	Score
P – Prior stroke/TIA	History of stroke or TIA	1.93	1
R – Reduced EF	LV-EF <50%	3.29	2
O – Older age	Age ≥65 years	1.50	1
M – Myocardial injury	Peak high-sensitivity troponin T >1000 ng/L	2.77	1
I – Impaired renal function	eGFR <60 mL/min/1.73 m²	1.99	1
N – Natriuretic peptide elevated	NT-proBNP >1000 pg/mL	4.11	2
O – Onset atrial fibrillation	New-onset AF on admission	2.30	1
C – CRP elevation	CRP >10 mg/L	1.82	1
A – Additional comorbidity	Presence of diabetes mellitus	2.06	1
	Presence of hypertension	2.24	1

The PRO-MINOCA score is a composite risk tool developed to predict major adverse cardiac events (MACE) in patients diagnosed with myocardial infarction with non-obstructive coronary arteries (MINOCA). Each component of the acronym represents an independent predictor identified through multivariate logistic regression analysis. Variables were assigned points based on both their clinical relevance and statistical strength (odds ratio). Components with stronger associations (OR ≥3 or high clinical weight) were given 2 points, while others were assigned 1 point. The total score reflects the cumulative risk burden for each patient. AF: Atrial fibrillation, CRP: C-reactive protein, LV: Left ventricle, EF: Ejection fraction, eGFR: Estimated glomerular filtration rate, NT-proBNP: N-terminal pro B-type natriuretic peptide, OR: Odds ratio, TIA: Transient ischemic attack.

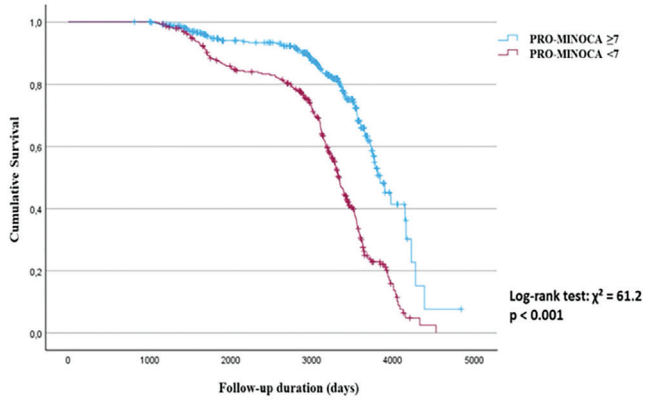

Figure 1. ROC curve of the PRO-MINOCA score for predicting major adverse cardiac events (MACE).

As illustrated by the ROC analysis, the PRO-MINOCA score exhibited significant discriminative ability, with a calculated AUC of 0.781 (95% CI: 0.745-0.816; p < 0.001). ROC: Receiver operating characteristic, MINOCA: Myocardial infarction with non-obstructive coronary artery, AUC: Area under the curve, CI: Confidence interval.

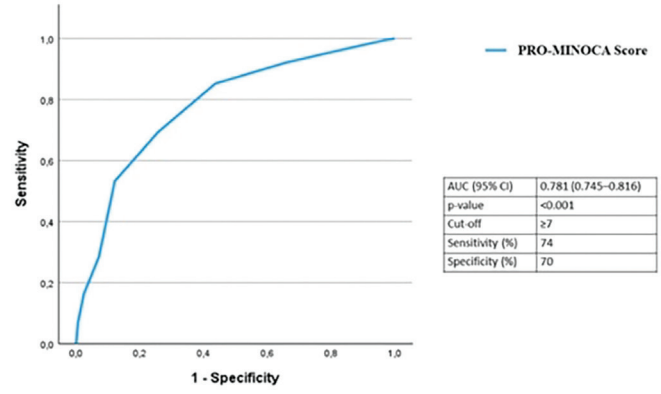

Figure 2. Kaplan-Meier survival curve for major adverse cardiac events (MACEs) stratified by the PRO-MINOCA score cut-off. Survival probabilities were estimated via Kaplan-Meier curves, revealing a substantial divergence in MACE-free survival between the two groups stratified by the PRO-MINOCA threshold (score <7 vs. ≥7). The median survival time was 3842 days in the lower-score group and 3330 days in the higher-score group. The difference was statistically significant according to the log-rank (Mantel-Cox) tes t(χ^2: 61.2, df: 1, p < 0.001). MINOCA: Myocardial infarction with non-obstructive coronary artery.

Finally, the univariable Cox proportional hazards model demonstrated that a PRO-MINOCA score of ≥7 was associated with a more than 2.6-fold increase in the risk of MACE (HR: 2.665; 95% CI: 2.064–3.442; p < 0.001). The model showed an excellent overall fit (likelihood ratio χ^2: 61.2, p < 0.001) in the cohort of 658 patients. These statistical findings confirm that the PRO-MINOCA score is a robust and straightforward clinical instrument for forecasting long-term cardiovascular risk in the MINOCA population.

DISCUSSION

This research aimed to develop and validate the PRO-MINOCA score, a straightforward and clinically reliable tool to predict long-term MACEs in patients with MINOCA. With a median observation period of 10.5 years (extending up to 12 years), our study provides one of the most extensive longitudinal datasets in this area. This prolonged follow-up reinforces the growing consensus that the clinical trajectory of MINOCA is far from benign.

The underlying pathophysiology of MINOCA is notoriously diverse, and the absence of clear obstructive coronary lesions often makes the diagnostic pathway more complex (17). Consequently, there is an urgent clinical requirement for early-stage risk assessment instruments. While CMR imaging is essential for identifying specific etiologies, its routine application in daily practice remains hindered by cost, limited access, and institutional differences in expertise (18-20). This underscores the necessity for non-invasive, accessible, and user-friendly scoring models.

Various established risk scores—including HEART, GRACE, ACEF, and TIMI—have been evaluated in MINOCA cohorts; however, most were originally developed and calibrated for different clinical contexts, such as surgical candidates or patients with general acute coronary syndromes (21,22). Research by Fedele et al. (11) indicated that while the ACEF and GRACE scores can predict one-year mortality in MINOCA, their discriminative performance is only moderate for this specific subset and they lack precision for long-term forecasting. Similarly, Gao et al. (23) explored the ACEF score's utility in MINOCA, but its limited focus on only three variables (age, creatinine, and EF) restricts its overall clinical sensitivity.

To address these gaps, our PRO-MINOCA model integrates variables specific to the MINOCA demographic that are derived entirely from clinical parameters and validated through rigorous multivariable analysis. The components—including age ≥65, prior stroke/TIA, EF <50%, eGFR <60, elevated CRP, new-onset atrial fibrillation, and elevated biomarkers (troponin and NT-proBNP)—have all been previously identified as prognostic markers in MINOCA literature and were strongly linked to MACE in our cohort (17,24-29).

The PRO-MINOCA score demonstrated strong discriminative ability, with an AUC of 0.781 (95% CI: 0.745–0.816). Utilizing the Youden index, we identified ≥7 as the optimal threshold, providing 74% sensitivity and 70% specificity for MACE prediction. This was further validated by Kaplan-Meier analysis, which showed a marked decline in survival for patients whose scores exceeded this threshold. A key advantage of PRO-MINOCA is its reliance on data immediately available at the time of diagnosis, allowing for seamless integration into clinical workflows. Consequently, in clinical settings where advanced modalities like CMR are unavailable, PRO-MINOCA offers a robust and pragmatic alternative for early risk stratification (30).

This study introduces one of the most comprehensive clinical scoring systems for MINOCA, supported by substantial long-term data. The PRO-MINOCA score serves as a vital guide for clinicians, helping to refine risk assessment and inform more personalized management strategies from the moment of diagnosis.

Study Limitations

Several limitations warrant mention. First, the retrospective, single-center framework may limit the generalizability of the findings and preclude causal inferences. While we minimized selection and information bias through standardized electronic records and national registry linkage, these inherent risks remain. Second, the lack of systematic CMR data prevented an etiological subclassification

of MINOCA, meaning we could not assess whether the score's performance varied across different subtypes (e.g., myocarditis vs. plaque rupture). Third, although the statistical validation is robust, the score's direct impact on clinical outcomes and decision-making requires evaluation in prospective, randomized trials. Future multicenter investigations are needed to further validate the PRO-MINOCA score in diverse populations.

CONCLUSION

We propose the PRO-MINOCA score as a novel, pragmatic instrument based purely on clinical parameters to predict long-term adverse outcomes in MINOCA patients. Our model demonstrated strong statistical performance and clinical relevance, supported by a large patient cohort and an extended follow-up. PRO-MINOCA represents an effective alternative for early risk stratification, particularly in resource-limited settings where advanced cardiac imaging is not readily accessible.

Ethics

Ethics Committee Approval: The Institutional Ethics Committee of Gazi University Faculty of Medicine provided formal approval for the research (protocol code: 2025–1013, meeting number: 9, date: 27.05.2025).

Informed Consent: Due to the retrospective nature of this clinical registry analysis and the use of de-identified data, the committee waived the requirement for individual patient consent.

Footnotes

Authorship Contributions

Concept: Y.B.Ş., S.Ü., Design: Y.B.Ş., S.Ü., Data Collection or Processing: Y.B.Ş., Analysis or Interpretation: Y.B.Ş., S.Ü., Literature Search: Y.B.Ş., Ö.S., Writing: Y.B.Ş.

Conflict of Interest: No conflict of interest was declared by the authors.

Financial Disclosure: The authors declared that this study received no financial support.

REFERENCES

1. Salari N, Morddarvanjoghi F, Abdolmaleki A, Rasoulpoor S, Khaleghi AA, Hezarkhani LA, et al. The global prevalence of myocardial infarction: a systematic review and meta-analysis. BMC Cardiovasc Disord. 2023; 23: 206.
2. Canto JG, Shlipak MG, Rogers WJ, Malmgren JA, Frederick PD, Lambrew CT, et al. Prevalence, clinical characteristics, and mortality among patients with myocardial infarction presenting without chest pain. JAMA. 2000; 283: 3223-9.
3. Pasupathy S, Tavella R, Beltrame JF. Myocardial infarction with nonobstructive coronary arteries (MINOCA): the past, present, and future management. Circulation. 2017; 135: 1490-3.
4. Mileva N, Paolisso P, Gallinoro E, Fabbricatore D, Munhoz D, Bergamaschi L, et al. Diagnostic and prognostic role of cardiac magnetic resonance in MINOCA: systematic review and meta-analysis. JACC Cardiovasc Imaging. 2023; 16: 376-89.
5. Nordenskjöld AM, Agewall S, Atar D, Baron T, Beltrame J, Bergström O, et al. Randomized evaluation of beta blocker and ACE-inhibitor/angiotensin receptor blocker treatment in patients with myocardial infarction with non-obstructive coronary arteries (MINOCA-BAT): rationale and design. Am Heart J. 2021; 231: 96-104.
6. Nordenskjöld AM, Lagerqvist B, Baron T, Jernberg T, Hadziosmanovic N, Reynolds HR, et al. Reinfarction in patients with myocardial infarction with nonobstructive coronary arteries (MINOCA): coronary findings and prognosis. Am J Med. 2019; 132: 335-46.
7. Parwani P, Kang N, Safaeipour M, Mamas MA, Wei J, Gulati M, et al. Contemporary diagnosis and management of patients with MINOCA. Curr Cardiol Rep. 2023; 25: 561-70.
8. Gerbaud E, Arabucki F, Nivet H, Barbey C, Cetran L, Chassaing S, et al. OCT and CMR for the diagnosis of patients presenting with MINOCA and suspected epicardial causes. JACC Cardiovasc Imaging. 2020; 13: 2619-31.
9. Sucato V, Testa G, Puglisi S, Evola S, Galassi AR, Novo G. Myocardial infarction with non-obstructive coronary arteries (MINOCA): intracoronary imaging-based diagnosis and management. J Cardiol. 2021; 77: 444-51.
10. Gibson CM, Cannon CP, Murphy SA, Marble SJ, Barron HV, Braunwald E, et al. Relationship of the TIMI myocardial perfusion grades, flow grades, frame count, and percutaneous coronary intervention to long-term outcomes after thrombolytic administration in acute myocardial infarction. Circulation. 2002; 105: 1909-13.
11. Fedele D, Canton L, Bodega F, Suma N, Tattilo FP, Impellizzeri A, et al. Performance of prognostic scoring systems in MINOCA: a comparison among GRACE, TIMI, HEART, and ACEF scores. J Clin Med. 2023; 12: 5687.
12. McCann CJ, Glover BM, Menown IB, Moore MJ, McEneny J, Owens CG, et al. Novel biomarkers in early diagnosis of acute myocardial infarction compared with cardiac troponin T. Eur Heart J. 2008; 29: 2843-50.
13. Fonarow GC, Peacock WF, Phillips CO, Givertz MM, Lopatin M, ADHERE Scientific Advisory Committee and Investigators. Admission B-type natriuretic peptide levels and in-hospital mortality in acute decompensated heart failure. J Am Coll Cardiol. 2007; 49: 1943-50.
14. Elsaka O. Recent evidence on biomarkers for predicting cardiovascular events: a comprehensive review. Journal of Indian College of Cardiology. 2025; 15: 1-12.
15. Katsioupa M, Kourampi I, Oikonomou E, Tsigkou V, Theofilis P, Charalambous G, et al. Novel biomarkers and their role in the diagnosis and prognosis of acute coronary syndrome. Life (Basel). 2023; 13: 1992.
16. Ke J, Liu Q, Liu X, Wu K, Qiu H, Song J, et al. Prognostic value of C-reactive protein predicting all-cause and cause-specific mortality: a prospective cohort study in Shanghai, China. BMJ Open. 2025; 15: e101532.
17. Singh T, Chapman AR, Dweck MR, Mills NL, Newby DE. MINOCA: a heterogenous group of conditions associated with myocardial damage. Heart. 2021; 107: 1458-64.
18. Ardelean AI, Moisi MI, Belenes S, Rus M, Popescu MI. Finding the specific etiology in myocardial infarction with non-obstructive coronary arteries disease (MINOCA) and the best therapeutic approaches. Romanian Journal of Cardiology. 2020; 30.
19. Bil J, Pietraszek N, Pawlowski T, Gil RJ. Advances in mechanisms and treatment options of MINOCA caused by vasospasm or microcirculation dysfunction. Curr Pharm Des. 2018; 24: 517-31.
20. Lima JA, Desai MY. Cardiovascular magnetic resonance imaging: current and emerging applications. J Am Coll Cardiol. 2004; 44: 1164-71.
21. Yin G, Abdu FA, Liu L, Xu S, Xu B, Luo Y, et al. Prognostic value of GRACE risk scores in patients with non-ST-elevation myocardial

infarction with non-obstructive coronary arteries. Front Cardiovasc Med. 2021; 8: 582246.

22. Lopes V, Moreira N, Fernandes R, Cunha G, Ferreira J, Kosta G, et al. Accuracy of the GRACE score for mortality prediction in myocardial infarction with nonobstructive coronary arteries (MINOCA). Eur Heart J. 2023; 44.
23. Gao S, Ma W, Huang S, Lin X, Yu M. Predictive value of the age, creatinine, and ejection fraction score in patients with myocardial infarction with nonobstructive coronary arteries. Clin Cardiol. 2021; 44: 1011-8.
24. Huang S, Yu M, Xu H. Pericoronary fat attenuation index as a novel tool to predict the morbidity of new-onset atrial fibrillation in patients with myocardial infarction with nonobstructive coronary artery disease. Circulation. 2024; 150: A4143007.
25. Zalewska-Adamiec M, Malyszko J, Grodzka E, Kuzma L, Dobrzycki S, Bachorzewska-Gajewska H. The outcome of patients with myocardial infarction with non-obstructive coronary arteries (MINOCA) and impaired kidney function: a 3-year observational study. Int Urol Nephrol. 2021; 53: 2557-66.
26. Hjort M, Lindahl B, Baron T, Jernberg T, Tornvall P, Eggers KM. Prognosis in relation to high-sensitivity cardiac troponin T levels in patients with myocardial infarction and nonobstructive coronary arteries. Am Heart J. 2018; 200: 60-6.
27. Eggers KM, Baron T, Hjort M, Nordenskjöld AM, Tornvall P, Lindahl B. Clinical and prognostic implications of C-reactive protein levels in myocardial infarction with nonobstructive coronary arteries. Clin Cardiol. 2021; 44: 1019-27.
28. Canton L, Fedele D, Bergamaschi L, Foà A, Di Iuorio O, Tattilo FP, et al. Sex- and age-related differences in outcomes of patients with acute myocardial infarction: MINOCA vs. MIOCA. Eur Heart J Acute Cardiovasc Care. 2023; 12: 604-14.
29. Almeida AG. MINOCA and INOCA: role in heart failure. Curr Heart Fail Rep. 2023; 20: 139-50.
30. Bandettini WP, Shanbhag SM, Mancini C, McGuirt DR, Kellman P, Xue H, et al. A comparison of cine CMR imaging at 0.55 T and 1.5 T. J Cardiovasc Magn Reson. 2020; 22: 37.

Gazi Med J 2026;37(3):392-398

DOI: http://dx.doi.org/10.12996/gmj.2026.4663

Knowledge, Attitudes, and Experiences Towards Transcranial Magnetic Stimulation Among Child and Adolescent Psychiatrists

Çocuk ve Ergen Psikiyatristlerinin Transkraniyal Manyetik Stimülasyon Hakkındaki Bilgi, Tutum ve Deneyimleri

Dicle Büyüktaşkın Tunçtürk[1], Senanur Kılıçaslan[1], Berkay Becer[1], Celal Yeşilkaya[2], Ahmet Özaslan[1], Esra Güney[1], Elvan İşeri[1]

[1]Department of Child and Adolescent Psychiatry, Gazi University, Faculty of Medicine, Ankara, Türkiye
[2]Clinic of Child and Adolescent Psychiatry, Konya Ereğli State Hospital, Konya, Türkiye

ABSTRACT

Objective: Transcranial magnetic stimulation (TMS) is a non-invasive modulation technique. While TMS is used in many fields among adult patients, its use in child and adolescent mental health is limited. This study aims to evaluate levels of knowledge, clinical experiences, and attitudes of child and adolescent psychiatrists regarding TMS and to identify potential barriers and facilitators to the application of TMS.

Methods: The study included 115 child and adolescent psychiatrists actively working in various institutions across Türkiye. Data were collected via a structured online questionnaire that inquired about participants' demographic characteristics and their knowledge levels, experiences, perceptions of efficacy and safety, and training regarding TMS protocols.

Results: While 68.7% of participants reported having a "low" general knowledge about TMS, 96.5% had received no formal training in this area. Although the indication for major depressive disorder was known to 93.9% of participants, only 8.7% of physicians had experience with TMS in the pediatric patient group. The biggest barriers to clinical practice were reported to be problems accessing equipment and a lack of information or training. The successful clinical case studies and increased training opportunities emerged as the most important facilitating factors.

CONCLUSION: Although professionals in child and adolescent psychiatry have a positive view of TMS therapy and show strong interest in learning about it, there are deficiencies in training and

ÖZ

Amaç: Transkraniyal manyetik stimülasyon (TMS), invaziv olmayan bir nöromodülasyon tekniğidir. TMS erişkin hastalarda birçok alanda kullanılmakla birlikte, çocuk ve ergen ruh sağlığı alanındaki kullanımı sınırlıdır. Bu çalışmanın amacı, çocuk ve ergen psikiyatristlerinin TMS'ye ilişkin bilgi düzeylerini, klinik deneyimlerini ve tutumlarını değerlendirmek; TMS uygulamasının önündeki olası engelleri ve kolaylaştırıcı faktörleri belirlemektir.

Yöntemler: Çalışmaya, Türkiye'de çeşitli kurumlarda aktif olarak çalışan 115 çocuk ve ergen psikiyatristi dahil edilmiştir. Veriler, katılımcıların demografik özellikleri ile TMS protokollerine ilişkin bilgi düzeylerini, deneyimlerini, etkinlik ve güvenlilik algılarını ve eğitim durumlarını sorgulayan yapılandırılmış bir çevrim içi anket aracılığıyla toplanmıştır.

Bulgular: Katılımcıların %68,7'si TMS hakkında genel bilgi düzeyini "düşük" olarak bildirirken, %96,5'i bu alanda herhangi bir eğitim almadığını belirtmiştir. Majör depresif bozukluk endikasyonu katılımcıların %93,9'u tarafından bilinmesine rağmen, hekimlerin yalnızca %8,7'sinin pediatrik hasta grubunda TMS deneyimi olduğu saptanmıştır. Klinik uygulamanın önündeki en önemli engellerin ekipmana erişim sorunları ile bilgi veya eğitim eksikliği olduğu bildirilmiştir. Başarılı klinik olgu örnekleri ve eğitim olanaklarının artırılması ise en önemli kolaylaştırıcı faktörler olarak öne çıkmıştır.

Sonuç: Çocuk ve ergen psikiyatrisi alanındaki profesyoneller TMS tedavisine olumlu yaklaşmakta ve bu konuda bilgi edinmeye güçlü bir ilgi göstermektedir; ancak eğitim ve deneyim açısından

Cite this article as: Büyüktaşkın Tunçtürk D, Kılıçaslan S, Becer B, Yeşilkaya C, Özaslan A, Güney E, et al. Knowledge, attitudes, and experiences towards transcranial magnetic stimulation among child and adolescent psychiatrists. Gazi Med J. 2026;37(3):392-398

Address for Correspondence/Yazışma Adresi: Dicle Büyüktaşkın Tunçtürk, Department of Child and Adolescent Psychiatry, Gazi University, Faculty of Medicine, Ankara, Türkiye
E-mail / E-posta: dicle.buyuktaskin@gazi.edu.tr
ORCID ID: orcid.org/0000-0003-4679-3846

Received/Geliş Tarihi: 16.3.2026
Accepted/Kabul Tarihi: 22.6.2026
Publication Date/Yayınlanma Tarihi: 10.07.2026

ABSTRACT

experience. To ensure the safe and evidence-based use of TMS, it is implement structured TMS training and to increase its accessibility in hospitals.

Keywords: Transcranial magnetic stimulation, adolescent psychiatry, attitude, clinical competence, major depressive disorder, mental health

ÖZ

eksiklikler bulunmaktadır. TMS'nin güvenli ve kanıta dayalı biçimde kullanılabilmesi için yapılandırılmış TMS eğitimlerinin uygulanması ve hastanelerde erişilebilirliğinin artırılması gerekmektedir.

Anahtar Sözcükler: Transkraniyal manyetik stimülasyon, ergen psikiyatrisi, tutum, klinik yeterlilik, majör depresif bozukluk, ruh sağlığı

INTRODUCTION

Transcranial magnetic stimulation (TMS) is a non-invasive treatment method that induces an electric current in the brain through a magnetic field. TMS aims to induce changes in intracranial actvity through neuronal pathways and neurotransmitter release (1,2). Physiological mechanism of TMS includes neuroplasticity creating long-lasting effects in the brain (3). TMS was first approved by the US Food and Drug Administration (FDA) in 2008 for the treatment of refractory depression in adults. Since then, with the help of developing technological advances, it has become a treatment method applicable to a variety of conditions (4). Currently, various studies are being conducted regarding the use of TMS in many psychiatric and neurological disorders such as major depressive disorder (MDD), obsessive-compulsive disorder (OCD), anxiety disorders, stroke, substance abuse, and schizophrenia (5,6), but its effectiveness in treatment-resistant depression is most consistent (6-8). TMS in anxiety disorders was also suggested to be a viable and safe method (9). Furthermore, the role of TMS treatment in post-stroke rehabilitation and substance use disorders is also being investigated (10,11). Although TMS in adult psychiatry have an extended clinical use, its use in child and adolescent patients is approached cautiously due to the complexity of the developing brain and its safety profile (12,13).

Until recently, TMS had been used experimentally in child and adolescent mental health, including MDD, ASD, and attention deficit hyperactivity disorder (ADHD) (14,15). In 2024, TMS was approved by the FDA for the treatment of depression in adolescents (16). This approval is expected to pave the way for greater use of TMS in clinical practice.

Although experimental studies have been conducted and the recent approval for use in adolescents has been confirmed, child and adolescent psychiatrists may have variable attitudes toward the use of TMS in adolescents. T hat it is not available in every clinic may raise questions regarding TMS. Several studies are currently being conducted to investigate clinicians' perspectives on the use of TMS. A study showed that while 71% of clinicians believed they would refer patients for TMS treatment in the future, 67% were lack of knowledge on TMS referral (17). Another study indicated that 80% of clinicians had sufficient knowledge about TMS, but only 53% said they would accept TMS treatment if they were patients themselves (18). A study about perceptions of psychiatrists in China found that many clinicians had insufficient knowledge of TMS (19). A recent study conducted in Europe found that clinical experience with TMS was limited, and most participants expressed a desire for increased clinical training on TMS (20). A study in 2024 found that knowledge of TMS was higher among those working in academic centers (21); another study conducted in Türkiye emphasized that while most psychiatrists viewed TMS as a positive treatment method, more training and clinical experience were needed (22). Studies show that as training and clinical experience increase, so does the positive attitude towards TMS (17).

Although numerous studies have examined adult psychiatrists' knowledge, attitudes, competencies, and expectations regarding TMS, research in child and adolescent mental health remains limited. The growing body of evidence regarding TMS, coupled with its approval for use in adolescent depression, is leading to increased interest in TMS and its adoption in clinical practice. The gaps in current literature highlight the need to conduct further research on TMS and to clarify clinicians' needs, experiences, perspectives, and expectations toward TMS. Our study aimed to assess the knowledge, attitudes, and clinical experiences of child and adolescent psychiatrists regarding TMS treatment. The primary objectives of the study are to identify clinical training needs and provide data that will facilitate the integration of TMS into clinical practice in child and adolescent psychiatry.

MATERIALS AND METHODS

Methods

Study Design

A descriptive, cross-sectional survey methodology was utilized to examine TMS-related knowledge, perceived barriers, and potential facilitators of clinical implementation among child and adolescent psychiatry professionals in Türkiye. The study was non-interventional in nature and was conducted entirely through an online, self-administered questionnaire format. Ethical approval was granted by the Gazi University Rectorate Ethics Committee (approval number: 2024-1813, meeting date: 26.11.2024, meeting no: 19), and all participants provided electronic informed consent before completing the survey.

Participants

The study targeted professionals in child and adolescent psychiatry who were actively engaged in clinical practice in Türkiye during the data collection period. Inclusion criteria encompassed three groups: board-certified child and adolescent psychiatrists, psychiatry residents undergoing specialty training in child and adolescent psychiatry, and academics in child and adolescent psychiatry. Participants were not excluded based on age, gender, years of clinical experience, or institutional affiliation; institutional affiliations included university hospitals, training and research hospitals, state hospitals, and private practice settings. Participation was entirely voluntary; no identifying information was collected, and no form of compensation was offered.

Survey Administration

Data were collected via an electronic questionnaire developed and distributed through Google Forms. The survey link was disseminated through professional email distribution lists and a closed WhatsApp group consisting of child and adolescent psychiatry specialists, residents, and academic faculty from across Türkiye. All responses were collected without personal identifiers to ensure anonymity, and data were stored in a password-protected institutional database with access restricted to the research team.

Survey Content

The survey consisted of basic demographic items followed by 15 questions assessing child and adolescent psychiatry professionals' knowledge, attitudes, and experiences regarding TMS. The questionnaire was partially adapted from existing literature investigating mental health professionals' attitudes toward diverse treatment modalities (18,23,24).

Demographic variables included age, sex, years of clinical experience in mental health, and geographic location of practice. Knowledge-based items evaluated participants' familiarity with TMS protocols, indications, and underlying mechanisms. Perception-oriented questions assessed professional attitudes regarding the efficacy and safety of TMS in adolescents. Finally, experience-related items focused on the participants' previous clinical use of TMS and formal training history.

Statistical Analysis

All statistical analyses were carried out using IBM SPSS Statistics, Version 26.0. For continuous variables, descriptive statistics were reported as means, standard deviations, medians, and ranges, whereas categorical variables were summarized using frequencies and percentages. The normality assumption was evaluated through skewness and kurtosis indices. Comparisons between groups for categorical variables were conducted using chi-square tests; Fisher's exact test was applied when cell frequencies were insufficient to meet the assumptions of the chi-square test. A p-value of less than 0.05 was considered statistically significant throughout all analyses.

Although year of experience were initially recorded across four categories (≤5, 6–10, 11–20, and ≥21 years), the small cell sizes in the upper categories precluded their use as independent groups in inferential analyses. For chi-square comparisons, experience was dichotomized into two groups: five or fewer years (n = 57) and more than five years (n = 58).

RESULTS

A total of 115 child and adolescent psychiatry professionals participated in the study. The majority of participants were between the ages of 30 and 39 years (59.1%), while 35.7% were under 30 years of age and 5.2% were 40 years or older. Female participants constituted 76.5% of the sample (n = 88). In terms of professional experience, 49.6% of participants had 5 or fewer years, 44.3% had 6 to 10 years, and 6.1% had 11 or more years. Geographically, the largest proportion of respondents worked in the Central Anatolia Region (40.9%), followed by the Marmara Region (21.7%) and the Aegean Region (12.2%). Baseline demographic and professional characteristics of the sample are presented in Table 1.

The knowledge levels and the comparisons between the experience groups are summarized in Table 2. The overall level of knowledge regarding TMS was low across both experience groups. Among participants with 5 or fewer years of experience, 38 (66.7%) reported limited knowledge of TMS, 12 (21.1%) reported moderate knowledge, and only 1 participant reported high knowledge. A similar distribution was observed among participants with more than 5 years of experience, with 41 (70.7%) reporting limited knowledge. No statistically significant difference was found between the two groups with respect to overall TMS knowledge level (p = 0.871). Over half of participants (56.5%) reported no knowledge of TMS protocols, while only 3.5% described their knowledge as high. This distribution also did not differ significantly between the two experience groups (p = 0.954). Regarding knowledge of clinical indications, the majority of participants (93.9%) correctly identified MDD as an indication for TMS. Recognition of MDD was higher among participants with less experience (98.2% vs. 89.7%). A trend toward significance was observed (p = 0.054). In contrast, recognition of alcohol and substance use disorders as an indication for TMS was more prevalent in the more experienced group (24.1% vs. 10.5%), and a trend toward significance was observed for this comparison (p = 0.054). Knowledge of OCD as an indication was significantly more common among participants with more experience than among those with less experience (p = 0.032). No significant between-group differences were observed for anxiety disorders, autism spectrum disorder (ASD), ADHD, or alcohol and substance use disorders. Only a small proportion of participants reported prior experience with TMS in a pediatric population (8.7%), and formal training in TMS was rare in both groups (3.5%).

Table 1. Baseline demographical and professional characteristics.

Variable	Category	n	%
Age	<30	41	35.7
	30–39	68	59.1
	≥40	6	5.2
Sex	Male	27	23.5
	Female	88	76.5
Years of professional experience	≤5	57	49.6
	6–10	51	44.3
	≥11	7	6.1
Geographical regions of Türkiye	Aegean Region	14	12.2
	Black Sea Region	9	7.8
	Central Anatolia Region	47	40.9
	East Anatolia Region	3	2.6
	Mediterranean Region	12	10.4
	Marmara Region	25	21.7
	Southeastern Anatolia Region	5	4.3

Table 2. Comparison of knowledge for TMS in terms of experience.

	≤5 years, (n = 57)	>5 years (n = 58)	Total (n = 115)	X^2	p-value
Overall knowledge level for TMS				0.7	0.871
None	6 (10.5)	5 (8.6)	11 (9.6)		
Few	38 (66.7)	41 (70.7)	79 (68.7)		
Moderate	12 (21.1)	10 (17.2)	22 (19.1)		
High	1 (1.8)	2 (3.4)	3 (2.6)		
Familiarity with TMS protocols				0.1	0.954
None	33 (57.9)	32 (55.2)	65 (56.5)		
Few	22 (38.6)	24 (41.4)	46 (40.0)		
High	2 (3.5)	2 (3.4)	4 (3.5)		
Knowledge of clinical indications					
MDD	56 (98.2)	52 (89.7)	108 (93.9)	3.7	0.054
OCD	36 (63.2)	47 (81.0)	83 (72.2)	4.6	**0.032**
Anxiety disorders	25 (43.9)	27 (46.6)	52 (45.2)	0.1	0.772
ASD	8 (14.0)	11 (19.0)	19 (16.5)	0.5	0.477
ADHD	7 (12.3)	10 (17.2)	17 (14.8)	0.6	0.454
Alcohol/substance use disorders	6 (10.5)	14 (24.1)	20 (17.4)	3.7	0.054
Prior experience with TMS in pediatric populations	4 (7.0)	6 (10.3)	10 (8.7)	FET	0.743
Formal training in TMS	2 (3.5)	2 (3.4)	4 (3.5)	FET	1.000

ADHD: Attention-deficit/hyperactivity disorder, ASD: Autism spectrum disorders, FET: Fisher's exact test, MDD: Major depressive disorder, OCD: Obsessive-compulsive disorder, TMS: Transcranial magnetic stimulation, X^2: Chi-square test.

Perceptions regarding the clinical effectiveness of TMS for MDD in children and adolescents were mixed. The most common response was "moderately effective" (42.6%), while 29.6% of participants indicated they were unsure of TMS's effectiveness. Only 5.2% considered TMS to be highly effective in this population. No statistically significant difference was found between the two experience groups (p = 0.822). With respect to safety, the majority of participants rated TMS as moderately safe (42.6%) or very safe (25.2%) for use in children and adolescents, while 27.0% were unsure. Group differences in safety perceptions were not statistically significant (p = 0.640). Regarding the role of TMS in treatment algorithms, most participants (60.0%) disagreed that TMS should be considered a first-line treatment option for MDD in children and adolescents, while 36.5% neither agreed nor disagreed. Only 3.5% expressed agreement. This distribution did not differ significantly between the two groups (p = 0.408). When asked about the perceived benefits of TMS as an adjunctive treatment for pediatric psychiatric disorders, 49.6% of participants described it as moderately beneficial and 17.4% as highly beneficial. Approximately one-fifth of participants (20.9%) were unsure, whereas only 0.9% considered TMS not beneficial. No significant group differences were identified (p = 0.104; Table 3).

The perceived barriers to, and potential facilitators of, clinical use of TMS, according to participants, are shown in Table 4. Among the identified barriers to gaining experience with TMS, limited accessibility was the most frequently cited concern (75.5%), followed by lack of knowledge and/or education (46.1%), insufficient evidence for efficacy (16.7%), and safety concerns (6.9%). Regarding potential facilitators, the availability of clinical case studies demonstrating successful use was ranked highest (73.9%), followed by greater accessibility of TMS services (61.7%), more education and training opportunities (59.1%), collegial support or consultation (58.3%), and greater accessibility of clinical guidelines (48.7%).

DISCUSSION

This study is one of the pioneering studies evaluating the knowledge, attitudes, and clinical experience of child and adolescent psychiatrists regarding the application of TMS in adolescents. The findings are generally consistent with those reported in other studies. In our study, 68.7% of the professionals had "little knowledge" about TMS, and 96.5% had not received any training on this subject. This data was found to be consistent with studies conducted with adult psychiatrists in the literature (19). Our results were also in line with a study conducted on adult psychiatrists in Türkiye, which highlighted "insufficient clinical experience despite positive attitudes"(22). A similar barrier to practice appears to exist in the field of child and adolescent psychiatry. In our study, 82.6% of professionals expressed a desire to receive training on TMS, which indicates the global training need and gap (20,25).

A large proportion of professionals participating in our study (93.9%) were aware of TMS as a treatment for MDD. This high rate can be explained by the fact that TMS has been approved by the FDA since 2008 (26). Participants with more experience were more aware of the use of TMS to treat OCD than participants with <5 years of experience. This might be due to not having an FDA clearence for TMS use in adolescents with OCD altough it is approved for adults

Table 3. Comparison of perceptions for TMS in terms of experience.

	≤5 years, (n = 57)	>5 years (n = 58)	Total (n = 115)	X^2	p-value
Perceived clinical effectiveness of TMS for MDD in children and adolescents				1.5	0.822
Ineffective	1 (1.8)	2 (3.4)	3 (2.6)		
Slightly Effective	11 (19.3)	12 (20.7)	23 (20.0)		
Moderately effective	24 (42.1)	25 (43.1)	49 (42.6)		
Highly effective	2 (3.5)	4 (6.9)	6 (5.2)		
Not sure	19 (33.3)	15 (25.9)	34 (29.6)		
Perceived safety of TMS in children and adolescents				2.5	0.640
Unsafe	0 (0.0)	1 (1.7)	1 (0.9)		
Slightly safe	2 (3.5)	3 (5.2)	5 (4.3)		
Moderately safe	26 (45.6)	23 (39.7)	49 (42.6)		
Very Safe	12 (21.1)	17 (29.3)	29 (25.2)		
Not sure	17 (29.8)	14 (24.1)	31 (27.0)		
TMS should be considered as a first-line treatment option for MDD in children and adolescents				2.9	0.408
Agree	2 (3.5)	2 (3.4)	4 (3.5)		
Disagree	36 (63.1)	33 (56.9)	69 (60.0)		
Neither agree nor disagree	19 (33.3)	23 (39.7)	42 (36.5)		
Perceived benefits of TMS as an adjunctive treatment for psychiatric disorders in children and adolescents				7.7	0.104
Not beneficial	0 (0.0)	1 (1.7)	1 (0.9)		
Slightly beneficial	3 (5.3)	10 (17.2)	13 (11.3)		
Moderately beneficial	34 (59.6)	23 (39.7)	57 (49.6)		
Highly beneficial	8 (14.0)	12 (20.7)	20 (17.4)		
Not sure	12 (21.1)	12 (20.7)	24 (20.9)		

MDD: Major depressive disorder, TMS: Transcranial magnetic stimulation, X^2: Chi-square test

and has growing evidence on adolescents (27) leading a high percent of knowledge (72.2%) in total for OCD. In addition, some of the participants agreed that TMS is related to neurodevelopmental disorders, including ASD and ADHD. The recent increase in experimental studies on the use of TMS in neurodevelopmental disorders may have improved the awareness of professionals in this area (28). One of the most striking results of our study is that 91.3% of the professionals have never used TMS. Although the FDA's approval of TMS for the treatment of MDD in adolescents in March 2024 (16) is an important development, our findings indicate that this approval has not yet been fully reflected in clinical practice. A study demonstrating a lack of familiarity with the referral process of physicians (17) aligns with the findings in our study, where physicians viewed "lack of knowledge and training" as the primary obstacle to practice. This demonstrates the need for infrastructure and training support for the method to be implemented in clinical practice. Another study found that TMS knowledge was higher among those working in academic centers (21). This also supports increasing TMS units in training and research hospitals in Türkiye and incorporating structured training into the curriculum.

Table 4. Barriers and potential facilitators of TMS ımplementation in clinical practice.

	n (total = 115)	%
Barriers to gaining experience with TMS		
Limited accessibility	77	67.0
Lack of knowledge and/or education	47	46.1
Lack of sufficient evidence for efficacy	17	16.7
Safety concerns	7	6.9
Potential facilitators of TMS ımplementation in clinical practice		
Clinical case studies demonstrating successful use	85	73.9
Greater accessibility of TMS services	71	61.7
More education	68	59.1
Collegial support or consultation	67	58.3
Accessibility of clinical guidelines	56	48.7

TMS: Transcranial magnetic stimulation.

Although the literature highlights that TMS is a non-invasive and safe method that is well-tolerated in the pediatric age group (5,29,30) the fact that 42.6% of the participants were hesitant about safety indicates a need for more clinical practice in child and adolescent mental health clinics. This situation can also be attributed to the fact that the neuroplasticity capacity and developmental complexity of the child and adolescent brain necessitate a cautious approach to the use of TMS (12). To improve clinical comfort, 73.9% of the respondents requested "access to successful case studies", suggesting that these concerns can only be reduced by presenting practical experiences. This result also supports the principle that attitudes become more positive as education and clinical experience increase (17).

Our study is of significant clinical importance, as it is, to our knowledge, the first study to evaluate child and adolescent psychiatrists' perspectives and clinical approaches regarding TMS treatment. Notably, this study was conducted immediately following the FDA's March 2024 approval to treat adolescent depression, providing a timely dataset that reflects the impact of global regulatory developments on clinical practice in Türkiye. Additionally, the inclusion of participants from various regions of the country and of physicians with varying levels of experience enhances the reliability and generalizability of the results.

Study Limitations

Some limitations must be considered when evaluating the findings of our study. First, the study's sample size may not accurately reflect the approaches of the majority of the child and adolescent psychiatrists. Second, the majority of participants had never used TMS, which suggests that responses regarding safety and efficacy may have been based on theoretical knowledge or observations rather than clinical experience. Finally, measuring physicians' interest levels by questionnaire rather than by an objective method may have introduced self-report bias.

CONCLUSION

To address the knowledge and practice gaps identified in this study, several steps are suggested. Given that 96.5% of physicians have not received specific training and 82.6% are willing to receive it, courses and modules related to TMS applications in child and adolescent mental health should be routinely incorporated into specialist training curricula. The biggest obstacle to TMS application is seen as "limited accessibility" (75.5%). Overcoming this problem could increase the use of TMS units in university and training and research hospitals. Most participants reported that awareness of successful case studies would increase their comfort with clinical use. In this context, increasing the number of clinical practice guidelines and fostering research that compiles clinical studies on the use of TMS in children and adolescents will reduce professionals' concerns and encourage evidence-based use. Furthermore, future studies should be designed to include not only the approaches of physicians but also the clinical outcomes of treated child and adolescent patients, as well as the adherence processes and perspectives of families regarding treatment, in order to fill the gap in the literature.

Child and adolescent psychiatrists have a substantial interest in TMS, but they have difficulty translating this interest into clinical practice because of limited education, knowledge, experience, and equipment. To remove obstacles in practice, it is recommended to create structured training programs, to increase access to equipment in hospitals, and to prepare case guides. Structural support and comprehensive training are needed for the safe and widespread use of this non-invasive method in the pediatric population.

Ethics

Ethics Committee Approval: Ethical approval was granted by the Gazi University Rectorate Ethics Committee (approval number: 2024-1813, meeting date: 26.11.2024, meeting no: 19).

Informed Consent: All participants provided electronic informed consent before completing the survey.

Footnotes

Authorship Contributions

Concept: D.C., S.K., B.B., A.Ö., E.G., E.İ., Design: : D.C., C.Y., A.Ö., E.G., E.İ., Data Collection or Processing: D.C., S.K., B.B., A.Ö., Analysis or Interpretation: : D.C., C.Y., Literature Search: : D.C., S.K., B.B., Writing: D.C., S.K.,B.B, C.Y., A.Ö., E.G., E.İ.

Conflict of Interest: No conflict of interest was declared by the authors.

Financial Disclosure: The authors declared that this study received no financial support.

REFERENCES

1. Di Lazzaro V, Ziemann U, Lemon RN. State of the art: physiology of transcranial motor cortex stimulation. Brain Stimul. 2008; 1: 345-62.
2. Diana M, Raij T, Melis M, Nummenmaa A, Leggio L, Bonci A. Rehabilitating the addicted brain with transcranial magnetic stimulation. Nat Rev Neurosci. 2017; 18: 685-93.
3. Klomjai W, Katz R, Lackmy-Vallée A. Basic principles of transcranial magnetic stimulation and repetitive transcranial magnetic stimulation. Ann Phys Rehabil Med. 2015; 58: 208-13.
4. McClintock SM, Reti IM, Carpenter LL, McDonald WM, Dubin M, Taylor SF, et al. Consensus recommendations for the clinical application of repetitive transcranial magnetic stimulation in the treatment of depression. J Clin Psychiatry. 2018; 79: 16cs10905.
5. Lefaucheur JP, Aleman A, Baeken C, Benninger DH, Brunelin J, Di Lazzaro V, et al. Evidence-based guidelines on the therapeutic use of repetitive transcranial magnetic stimulation: an update. Clin Neurophysiol. 2020; 131: 474-528.
6. Guo Q, Li C, Wang J. Updated review on the clinical use of repetitive transcranial magnetic stimulation in psychiatric disorders. Neurosci Bull. 2017; 33: 747-56.
7. Brunoni AR, Sampaio-Junior B, Moffa AH, Aparício LV, Gordon P, Klein I, et al. Noninvasive brain stimulation in psychiatric disorders: a primer. Braz J Psychiatry. 2019; 41: 70-81.
8. Rizvi S, Khan AM. Use of transcranial magnetic stimulation for depression. Cureus. 2019; 11: e4736.
9. Rodrigues PA, Zaninotto AL, Neville IS, Hayashi CY, Brunoni AR, Teixeira MJ, et al. Transcranial magnetic stimulation for the treatment of anxiety disorder. Neuropsychiatr Dis Treat. 2019; 15: 2743-61.

10. Carmi L, Tendler A, Bystritsky A, Hollander E, Blumberger DM, Daskalakis J, et al. Efficacy and safety of deep transcranial magnetic stimulation for obsessive-compulsive disorder: a prospective multicenter randomized double-blind placebo-controlled trial. Am J Psychiatry. 2019; 176: 931-8.
11. Fisicaro F, Lanza G, Grasso AA, Pennisi G, Bella R, Paulus W, et al. Repetitive transcranial magnetic stimulation in stroke rehabilitation: review of the current evidence and pitfalls. Ther Adv Neurol Disord. 2019; 12: 1756286419878317.
12. Krishnan C, Santos L, Peterson MD, Ehinger M. Safety of noninvasive brain stimulation in children and adolescents. Brain Stimul. 2015; 8: 76-87.
13. Chail A, Saini RK, Bhat PS, Srivastava K, Chauhan V. Transcranial magnetic stimulation: a review of its evolution and current applications. Ind Psychiatry J. 2018; 27: 172-80.
14. Hameed MQ, Dhamne SC, Gersner R, Kaye HL, Oberman LM, Pascual-Leone A, et al. Transcranial magnetic and direct current stimulation in children. Curr Neurol Neurosci Rep. 2017; 17: 11.
15. Soltaninejad Z, Nejati V, Ekhtiari H. Effect of anodal and cathodal transcranial direct current stimulation on DLPFC on modulation of inhibitory control in ADHD. J Atten Disord. 2019; 23: 325-32.
16. U.S. Food and Drug Administration. NeuroStar Advanced Therapy System (K231926). Silver Spring: U.S. Food and Drug Administration; 2024. Available from: https://www.accessdata.fda.gov/cdrh_docs/pdf23/K231926.pdf
17. Stern AP, Boes AD, Haller CS, Bloomingdale K, Pascual-Leone A, Press DZ. Psychiatrists' attitudes toward transcranial magnetic stimulation. Biol Psychiatry. 2016; 80: e55-6.
18. AlHadi AN, AlShiban AM, Alomar MA, Aljadoa OF, AlSayegh AM, Jameel MA. Knowledge of and attitude toward repetitive transcranial magnetic stimulation among psychiatrists in Saudi Arabia. J ECT. 2017; 33: 30-5.
19. Deng J, Gong Y, Lin X, Bao Y, Sun H, Lu L. Knowledge and attitudes about transcranial magnetic stimulation among psychiatrists in China. BMC Psychiatry. 2020; 20: 416.
20. Sierra P, Cañada Y, Benavent P, Sabater A, Ribes J, Livianos L, et al. Opinion, use and knowledge about transcranial magnetic stimulation in Spain: a national survey of mental health professionals. Psychiatr Q. 2024; 95: 271-85.
21. Al-Balushi M, Al-Huseini S, Chan MF, Al-Kaabi S, Al-Balushi N, Qashta A, et al. Awareness and attitudes toward transcranial magnetic stimulation among psychiatrists in Oman. New Emirates Med J. 2024; 5: e02506882361774.
22. Ünsalver BÖ, Evrensel A, Sayar GH, Karamustafalıoğlu O, Tarhan N. Attitudes of Turkish psychiatrists regarding transcranial magnetic stimulation. J Neurobehav Sci. 2020; 7: 37-41.
23. Gazdag G, Kocsis N, Tolna J, Lipcsey A, Habil M. Attitudes towards electroconvulsive therapy among Hungarian psychiatrists. J ECT. 2004; 20: 204-7.
24. Mota P, Encantado J, Carvalho LC, Cunha C, Garcia-Romeu A, Johnson MW, et al. Attitudes and perceptions of Portuguese psychiatrists and psychologists on the clinical use of ketamine. Acta Med Port. 2025; 38: 297-306.
25. Bourla A, Chaneac E, Poulet E, Haffen E, Ogorzelec L, Guinchard C, et al. Acceptability, attitudes and knowledge towards transcranial magnetic stimulation among psychiatrists in France. Encephale. 2020; 46: 88-95.
26. Croarkin PE, Aaronson ST, Carpenter LL, Hutton TM, Pages K, Chen B, et al. The effectiveness of transcranial magnetic stimulation in adolescents and young adults with major depressive disorder. JAACAP Open. 2025; 3: 1246-58.
27. Cotovio G, Ventura F, Rodrigues da Silva D, Pereira P, Oliveira-Maia AJ. Regulatory clearance and approval of therapeutic protocols of transcranial magnetic stimulation for psychiatric disorders. Brain Sci. 2023; 13: 1029.
28. Oberman LM, Enticott PG, Casanova MF, Rotenberg A, Pascual-Leone A, McCracken JT. Transcranial magnetic stimulation in autism spectrum disorder: challenges, promise, and roadmap for future research. Autism Res. 2016; 9: 184-203.
29. Zewdie E, Ciechanski P, Kuo HC, Giuffre A, Kahl C, King R, et al. Safety and tolerability of transcranial magnetic and direct current stimulation in children: prospective single center evidence from 3.5 million stimulations. Brain Stimul. 2020; 13: 565-75.
30. Rossi S, Antal A, Bestmann S, Bikson M, Brewer C, Brockmöller J, et al. Safety and recommendations for TMS use in healthy subjects and patient populations, with updates on training, ethical and regulatory issues: expert guidelines. Clin Neurophysiol. 2021; 132: 269-306.

Gazi Med J 2026;37(3):399-406

DOI: http://dx.doi.org/10.12996/gmj.2026.4668

Psychopathology and Psychological Resilience in Adolescents Exposed to Sexual Abuse: A Case-Control Study

Cinsel İstismara Uğramış Ergenlerde Psikopatoloji ve Psikolojik Sağlamlık: Bir Vaka-Kontrol Çalışması

İbrahim Zeyrek[1], Ahmet Özaslan[2,3], Uğur Tekeoğlu[4], Yücel Fidan[5]

[1]Clinic of Child and Adolescent Psychiatry, Memorial Diyarbakır Hospital, Diyarbakır, Türkiye
[2]Psychology Research Centre, Khazar University, Baku, Azerbaijan
[3]Department of Child and Adolescent Psychiatry, Gazi University, Faculty of Medicine, Ankara, Türkiye
[4]Department of Child and Adolescent Psychiatry, Recep Tayyip Erdoğan University, Faculty of Medicine, Rize, Türkiye
[5]Department of Social Work, Sivas Cumhuriyet University, Faculty of Letters, Sivas, Türkiye

ABSTRACT

Objective: This study aimed to investigate the psychological impact of sexual abuse on adolescents by examining differences in depression, anxiety, stress, and post-traumatic stress between those with and without a history of sexual abuse. A further objective was to evaluate the role of psychological resilience, both as a differentiating factor between the groups and as a predictor of mental health outcomes within the abused group.

Methods: The study included 114 adolescents (aged 12–18 years), divided into a case group of 56 with a history of sexual abuse and a control group of 58 with no such history. Participants completed the -21, the Children's Revised Impact of Event Scale, and the Child and Youth Resilience Measure-12. Data were analyzed using multivariate analysis of covariance to compare the groups and hierarchical multiple regression to assess the predictive role of resilience, controlling for age and gender.

Results: The case group reported significantly higher levels of depression [$F(1, 109) = 13.04$, $p < 0.001$], anxiety [$F(1, 109] = 10.31$, $p = 0.002$), stress [$F(1, 109) = 6.40$, $p = 0.013$], and post-traumatic stress [$F(1, 109) = 18.62$, $p < 0.001$], as well as lower levels of psychological resilience [$F(1, 109) = 14.32$, $p < 0.001$], compared to the control group. Within the case group, psychological resilience was a significant negative predictor of depression ($\beta = -0.35$, $p = 0.011$), stress ($\beta = -0.30$, $p = 0.026$), and post-traumatic stress ($\beta = -0.44$, $p = 0.001$), but not anxiety ($\beta = -0.06$, $p = 0.67$).

ÖZ

Amaç: Bu çalışma, cinsel istismar öyküsü olan ve olmayan ergenler arasındaki depresyon, anksiyete, stres ve travma sonrası stres farklılıklarını inceleyerek cinsel istismarın ergenler üzerindeki psikolojik etkisini araştırmayı amaçlamıştır. Bir diğer amaç, psikolojik sağlamlığın rolünü hem gruplar arasında ayırt edici bir faktör olarak hem de istismara uğramış grup içinde ruh sağlığı sonuçlarının bir yordayıcısı olarak değerlendirmektir.

Yöntemler: Çalışmaya 12–18 yaş arası 114 ergen dahil edilmiş, bu grup 56'sı cinsel istismar öyküsü olan bir vaka grubu ve 58'i böyle bir öyküsü olmayan bir kontrol grubu olarak ikiye ayrılmıştır. Katılımcılar Depresyon Anksiyete Stres Ölçeği-21, Çocuklar için Gözden Geçirilmiş Travma Sonrası Stres Ölçeği ve Çocuk ve Genç Psikolojik Sağlamlık Ölçeği-12'yi doldurmuştur. Veriler, grupları karşılaştırmak için çok değişkenli kovaryans analizi ve yaş ve cinsiyet kontrol edilerek psikolojik sağlamlığın yordayıcı rolünü değerlendirmek için hiyerarşik çoklu regresyon kullanılarak analiz edilmiştir.

Bulgular: Vaka grubu, kontrol grubuna kıyasla anlamlı düzeyde daha yüksek depresyon [$F(1, 109) = 13{,}04$, $p < 0{,}001$], anksiyete [$F(1, 109) = 10{,}31$, $p = 0{,}002$], stres [$F(1, 109) = 6{,}40$, $p = 0{,}013$)] ve travma sonrası stres [$F(1, 109) = 18{,}62$, $p < 0{,}001$] düzeyleri ve daha düşük psikolojik sağlamlık [$F(1, 109) = 14{,}32$, $p < 0{,}001$] düzeyleri bildirmiştir. Vaka grubu içinde, psikolojik sağlamlık depresyon ($\beta = -0{,}35$, $p = 0{,}011$), stres ($\beta = -0{,}30$, $p = 0{,}026$) ve travma sonrası stres ($\beta = -0{,}44$, $p = 0{,}001$) için anlamlı bir negatif yordayıcı iken, anksiyete ($\beta = -0{,}06$, $p = 0{,}67$) için anlamlı bir yordayıcı olmamıştır.

Cite this article as: Zeyrek İ, Özaslan A, Tekeoğlu U, Fidan Y. Psychopathology and psychological resilience in adolescents exposed to sexual abuse: a case-control study. Gazi Med J. 2026;37(3):399-406

Address for Correspondence/Yazışma Adresi: İbrahim Zeyrek, Clinic of Child and Adolescent Psychiatry, Memorial Diyarbakır Hospital, Diyarbakır, Türkiye
E-mail / E-posta: dribrahimzeyrek@gmail.com
ORCID ID: orcid.org/0000-0003-2650-0663

Received/Geliş Tarihi: 25.03.2026
Accepted/Kabul Tarihi: 22.06.2026
Publication Date/Yayınlanma Tarihi: 10.07.2026

ABSTRACT

CONCLUSION: Adolescents who have experienced sexual abuse exhibit significant psychopathological symptoms and lower resilience. Psychological resilience appears to be a crucial protective factor, mitigating the severity of depression, stress, and post-traumatic stress. These findings underscore the importance of interventions aimed at fostering resilience in this vulnerable population.

Keywords: Sexual abuse, adolescent, psychopathology, post-traumatic stress, psychological resilience

ÖZ

Sonuç: Cinsel istismar yaşamış ergenler, belirgin psikopatolojik semptomlar ve daha düşük psikolojik sağlamlık sergilemektedir. Psikolojik sağlamlık, depresyon, stres ve travma sonrası stresin şiddetini azaltan önemli bir koruyucu faktör olarak görünmektedir. Bu bulgular, bu hassas popülasyonda psikolojik sağlamlığı artırmayı amaçlayan müdahalelerin önemini vurgulamaktadır.

Anahtar Sözcükler: Cinsel istismar, ergen, psikopatoloji, travma sonrası stres, psikolojik sağlamlık

INTRODUCTION

Sexual abuse is a significant public health problem affecting adolescents worldwide, with substantial documented effects on mental health outcomes. Epidemiological data indicate that approximately 18% of girls and 7.6% of boys experience sexual abuse before the age of 18 (1), with prevalence rates potentially higher in clinical populations. Meta-analytic evidence demonstrates that adolescents with a history of sexual abuse exhibit significantly elevated rates of depression, anxiety, and posttraumatic stress disorder compared to non-abused peers (2). These findings have been consistently replicated across diverse populations and settings (3). While this robust evidence base establishes the detrimental effects of sexual abuse on adolescent mental health, an important clinical and empirical question remains unanswered: among adolescents who have experienced sexual abuse, what factors account for differences in mental health outcomes, and to what extent can psychological resilience explain these differences?

Trauma theory provides a foundational framework for understanding the psychological mechanisms through which sexual abuse exerts its harmful effects. According to trauma theory, exposure to traumatic events such as sexual abuse disrupts normal psychological functioning through multiple pathways (4). Specifically, trauma theory posits that traumatic experiences are encoded in memory in a fragmented and disorganized manner, leading to intrusive memories, avoidance behaviors, and heightened physiological arousal characteristic of posttraumatic stress disorder (5). Beyond post-traumatic stress disorder (PTSD), trauma exposure has been linked to elevated rates of depression, anxiety, and general stress symptoms through several mechanisms: (1) disruption of core beliefs about safety and trust, (2) alterations in emotional regulation capacities, and (3) changes in social functioning and interpersonal relationships (6). These mechanisms collectively contribute to the broad spectrum of psychopathological outcomes observed in trauma-exposed adolescents.

However, not all individuals exposed to trauma develop significant psychopathology, a phenomenon that resilience theory seeks to explain. Resilience is conceptualized as a dynamic process involving the interaction of individual, family, and community factors that enable individuals to maintain or regain psychological well-being in the face of adversity (7). According to the social ecology of resilience framework (8), resilience operates through multiple protective mechanisms: (1) individual capacity factors such as emotional regulation skills, cognitive flexibility, and adaptive coping strategies; (2) family support factors such as parental warmth, secure attachment, and family cohesion; and (3) community resource factors such as access to mental health services, peer support networks, and community connectedness. These protective mechanisms may buffer against the negative psychological consequences of trauma by: (a) enhancing emotional regulation, allowing individuals to process traumatic experiences without becoming overwhelmed; (b) providing social support and validation, which counteracts the isolation and shame often associated with trauma; and (c) facilitating the development of effective coping strategies that enable individuals to manage stress and adversity. The multidimensional nature of resilience suggests that protective factors operate through multiple pathways, potentially explaining why some trauma-exposed adolescents develop significant psychopathology while others maintain relatively good mental health.

Empirical research has consistently documented the detrimental effects of sexual abuse on multiple dimensions of adolescent psychopathology. A meta-analytic review by Hailes et al. (2) examined 124 studies and found that adolescents with a history of sexual abuse exhibit significantly elevated rates of depression, anxiety, and posttraumatic stress disorder compared to non-abused peers, with large effect sizes. Similarly, Dworkin et al. (3) conducted a systematic review of 36 studies on sexual assault victimization and psychopathology and found robust associations between sexual abuse and depression, anxiety, and PTSD across diverse populations. These meta-analytic findings provide strong empirical support for our first hypothesis: adolescents with a history of sexual abuse will report significantly higher levels of depression, anxiety, stress, and posttraumatic stress symptoms compared to their non-abused peers. The consistency and magnitude of these effects across multiple studies and populations underscore the profound psychological impact of sexual abuse on adolescent mental health.

Converging evidence supports the protective role of psychological resilience in mitigating trauma effects. Yang et al. (9) found that resilience partially mediated the relationship between childhood abuse and depression, while Mesman et al. (10) identified resilience as a significant protective factor against depression and anxiety. Domhardt et al. (11) similarly found resilience associated with better psychological outcomes in child sexual abuse survivors. However, a critical distinction exists between demonstrating that resilience is associated with better outcomes and demonstrating that resilience predicts these outcomes. The present study examines the predictive capacity of psychological resilience—the extent to which resilience explains variance in depression, anxiety, stress, and posttraumatic stress symptoms among adolescents with a history of sexual abuse. Thus, we formulate our second hypothesis: psychological resilience will be negatively associated with depression, anxiety, stress,

and posttraumatic stress symptoms, and our third hypothesis: psychological resilience will serve as a significant negative predictor of these outcomes after controlling for demographic variables(age and gender).

Despite substantial literature on the effects of sexual abuse and on the protective role of resilience, important gaps remain. Few studies have examined the predictive capacity of resilience across multiple psychopathology dimensions simultaneously, and research in non-Western populations, particularly in Türkiye, is limited. The present study addresses these gaps by: (1) examining the psychological impact of sexual abuse on Turkish adolescents; (2) investigating resilience's predictive capacity for depression, anxiety, stress, and posttraumatic stress; (3) employing hierarchical multiple regression to quantify resilience's unique contribution beyond demographic variables; and (4) providing evidence to inform resilience-focused interventions in Turkish clinical settings.

This study has two primary objectives. The first objective is to examine whether adolescents with sexual abuse history exhibit significantly higher depression, anxiety, stress, and posttraumatic stress symptoms compared to non-abused peers, grounded in trauma theory (4) and supported by meta-analytic evidence (2,3). The second objective is to determine the predictive role of psychological resilience in the relationship between sexual abuse and psychopathology and to quantify the extent to which resilience explains the variance in these outcomes after controlling for demographic variables. To achieve these objectives, we formulated three hypotheses: Hypothesis 1: Adolescents with sexual abuse history will report significantly higher depression, anxiety, stress, and posttraumatic stress symptoms compared to non-abused peers (2,3). Hypothesis 2: Psychological resilience will be negatively associated with these symptoms in the case group (9-11). Hypothesis 3: Psychological resilience will serve as a significant negative predictor of these outcomes after controlling for age and gender (8).

This study makes several important contributions. It is among the first to examine the predictive capacity of resilience across multiple psychopathology dimensions among Turkish adolescent survivors of sexual abuse, addressing a gap in the non-Western literature. Second, simultaneously examining depression, anxiety, stress, and posttraumatic stress provides a comprehensive understanding of the protective role of resilience. Third, hierarchical multiple regression analysis quantifies the unique contribution of resilience beyond demographic variables. Fourth, recruiting the control group from the same clinical setting (healthy siblings of clinic attendees) enhances ecological validity. Finally, by demonstrating the predictive capacity of resilience, this study provides evidence to inform resilience-focused interventions for adolescent survivors of sexual abuse in Turkish clinical settings.

METHODS

Participants and Procedure

This case-control study was conducted between June and November 2025 at the child and adolescent psychiatry outpatient clinic of a university hospital. The study included 114 adolescents aged 12–18 years. The sample was divided into two groups: a case group of 56 adolescents with a history of sexual abuse and a control group of 58 adolescents with no such history. The case group comprised adolescents referred to the clinic for evaluation and treatment following sexual abuse. The control group consisted of healthy siblings of children and adolescents presenting to the child and adolescent psychiatry outpatient clinic. These siblings were recruited as a comparison group to represent typically developing adolescents without a history of sexual abuse or other significant trauma. The siblings were matched to the case group by age and socioeconomic status to control for potential confounders. Inclusion criteria for the control group required participants to be between 12 and 18 years of age and to be siblings of clinic attendees. Exclusion criteria for the control group included a personal history of any form of abuse (physical, emotional, or sexual), a current or past psychiatric diagnosis, and a current psychological treatment. This recruitment strategy allowed for a more ecologically valid comparison group, as both groups were drawn from the same clinical setting and community context.

Ethical approval for the study was obtained from the university's institutional review board. Ethical approval for the study was obtained from Recep Tayyip Erdoğan University Ethics Committee on 29.05.2025 with the decision number 2025/246. Written informed consent was obtained from all participants and their legal guardians prior to their inclusion in the study. All procedures were conducted in accordance with the Declaration of Helsinki.

Depression Anxiety Stress Scale 21 (DASS 21)

The DASS-21 is a shortened version of the DASS-24, originally developed by Lovibond and Lovibond (12) to assess the adverse effects associated with depression, anxiety, and stress. Each of the three distinct sets of DASS21 scales comprises seven items, and the ultimate scores for each variable are derived by aggregating the scores of the corresponding items (13).

Sarıçam conducted a study on the psychometric properties of the Turkish version of the DASS-21 scale in normal and clinical samples (14). In the control group, test-retest correlation coefficients were reported as follows: r = 0.68 for the depression subscale; r = 0.66 for the anxiety subscale; and r = 0.61 for the stress subscale. The DASS has a Cronbach's alpha of 0.87. It consists of 42 items, with a mean score (M = 50.0) and a [standard deviation (SD) = 21.04]. The alpha reliabilities for its subscales are as follows: stress subscale = 0.58, anxiety subscale = 0.51, and depression subscale = 0.63. This instrument comprises a 4-point Likert-type response format and features seven items dedicated to assessing the dimensions of depression, stress, and anxiety. Scores of 5 or higher on the depression subscale, 4 or higher on the anxiety subscale, and 8 or higher on the stress subscale signify the presence of the corresponding condition.

Child Revised Impact of Event Scale (CRIES)

The CRIES, developed by the Children and War Foundation, has been used for many years in various countries. The 8-item form of the scale consists of intrusive thoughts and avoidance subscales; when a 5-item arousal subscale is added, it becomes the 13-item form. The items are scored on a scale of 0 (not at all), 1 (rarely), 3 (sometimes), and 5 (often). Scores range from 0 to 40 for CRIES-8 and 0 to 65 for CRIES-13, with higher scores indicating more PTSD symptoms. A cut-off score of 30 for CRIES-13 and 17 for CRIES-8 has been reported to provide maximum sensitivity and specificity in detecting PTSD (15,16).

Child and Youth Resilience Measure (CYRM)

The initial 28-item version of this assessment was formulated using data gathered from eleven countries and incorporated three subscales and eight distinct sub-dimensions. This evaluative instrument was developed using both quantitative and qualitative methodologies, with a socio-ecological perspective underlying its design (17). Liebenberg et al. (18) subsequently conducted a short-form study, resulting in a condensed 12-item version following two separate research endeavours. The factor loadings for this scale range from 0.39 to 0.88. and the internal consistency coefficient was 0.84. Responses are captured on a five-point Likert scale ranging from "Describes me completely" (5) to "Does not describe me at all" (1). A higher score indicates a greater degree of resilience. The Turkish validation and reliability analysis were performed by Arslan (19).

All three assessment instruments (DASS-21, CRIES-13, and CYRM-12) have been validated for use with adolescents aged 12–18 years. The DASS-21 has demonstrated adequate internal consistency and test-retest reliability in adolescent populations (20,21), with Turkish validation confirming its psychometric properties in Turkish adolescents (14). The CRIES-13 was specifically designed for children and adolescents aged 8-18 years and has been extensively validated in trauma-exposed youth, including sexual abuse survivors (15,22), with Turkish validation supporting its use in Turkish adolescent samples (16). The CYRM-12 has been validated for youth aged 10–23 years and has demonstrated reliability and validity in Turkish populations and in trauma-exposed youth (23,24). All three instruments are appropriate for the 12–18-year age range in our study sample.

Statistical Analysis

All statistical analyses were performed using IBM SPSS Statistics version 27.0. Before any analyses were initiated, the dataset was scrutinised for missing values and its adherence to the assumptions of normality, linearity, and homogeneity of variance was assessed. Normality was determined by examining skewness and kurtosis coefficients, which confirmed that the distributions of all variables under investigation were suitable. Initial evaluations of disparities in age and gender between groups were conducted using an independent-samples t-test and a chi-square test, respectively. Group differences in scale scores were examined using independent-samples t-tests. Homogeneity of variances was evaluated with Levene's test; when it was violated, Welch's t-test was reported. Prior to conducting the multivariate analysis of covariance (MANCOVA), assumptions of normality, linearity, homogeneity of regression slopes, and equality of covariance matrices were tested. Levene's tests confirmed the homogeneity of error variances across dependent variables. Because Box's M test was significant ($p = 0.002$), Pillai's Trace was used as the multivariate test statistic, given its robustness to covariance heterogeneity. An MANCOVA was conducted to compare the patient and control groups on depression, anxiety, stress, posttraumatic stress, and psychological resilience, controlling for age and gender. Following detection of a significant multivariate effect, individual univariate ANCOVAs were performed for each dependent variable, and partial eta-squared (η^2) was used to report effect sizes. Pearson correlation analyses were employed to investigate the relationships between various factors. Hierarchical multiple regression analyses were then undertaken to ascertain whether psychological resilience could predict depression, anxiety, stress, and PTSD symptoms after accounting for the influence of age and gender. For each analytical model, age and gender were incorporated in the initial step, with psychological resilience introduced in the second step to evaluate the incremental variance explained (ΔR^2). A p-value of less than 0.05 (two-tailed) was established as the threshold for statistical significance.

RESULTS

The sociodemographic and clinical characteristics of the participants are presented in Table 1. The sample consisted of 114 adolescents (71 girls and 43 boys) aged 12–18 years (M = 15.17, SD = 1.68). Preliminary analyses indicated no significant age difference between the patient (M = 15.18, SD = 1.52) and control (M = 15.16, SD = 0.83) groups, $t(112) = -0.07$, $p = 0.94$. However, the gender distribution differed significantly [χ^2 (1, n = 114) = 18.48, $p < 0.001$], with girls overrepresented in the case group (82%) compared with the control group (43%).

As illustrated in Table 2, the case group exhibited significantly higher levels of symptoms of depression, anxiety, and stress compared to the control group (all $p < 0.01$). Furthermore, the analysis revealed

Table 1. Sociodemographic and clinical characteristics of participants.

Characteristic	Control (n = 58), n (%)	Case (n = 56), n (%)
Age (years)		
Mean (standard deviation)	(0.83)	18 (1.52)
Gender, n (%)		
Female	25 (43.1%)	46 (82.1%)
Male	33 (56.9%)	10 (17.9%)
Number of siblings in the family		
1	5 (8.6)	4 (7.1)
2	18 (31.0)	19 (33.9)
3 or more	35 (60.3)	33 (58.9)
Family status		
Parents living together	46 (79.3)	37 (66.1)
Divorced	7 (12.1)	16 (28.6)
Deceased parent	5 (8.6)	3 (5.4)
Socioeconomic status (monthly income)		
Low	6 (10.3)	25 (44.6)
Middle	48 (82.8)	25 (44.6)
High	4 (6.9)	6 (10.7)
Any significant medical illness		
Yes	1 (1.7)	6 (10.7)
No	57 (98.3)	50 (89.3)
Any psychiatric illness		
Yes	0 (0.0)	24 (42.9)
No	58 (100.0)	32 (57.1)

Table 2. Comparison of psychopathology and resilience between groups.

Measure	Control (n = 58) M (SD)	Patient (n = 56) M (SD)	Skewness	Kurtosis	t(df)	p
DASS-depression	81 (5.36)	38 (5.18)	34	−1.00	−4.62 (112)	<0.001
Depression-anxiety	5.12 (4.82)	8.50 (4.30)	0.47	−0.40	−3.95 (112)	<0.001
DASS-stress	6.60 (5.24)	9.66 (4.40)	0.35	−0.26	−3.37 (112)	0.001
CRIES-13	21.53 (17.91)	38.64 (13.26)	−0.06	−0.95	−5.81 (105.01)†	<0.001
Psychological resilience	44.38 (11.57)	35.16 (9.16)	0.04	−0.92	4.71 (112)	<0.001

Skewness and Kurtosis values are reported for the total sample (n = 114). †For CRIES-13, Levene's test indicated heterogeneity of variances (p = 0.009); therefore, Welch's t-test was reported (equal variances not assumed).
DASS: Depression, Anxiety and Stress Scale, CRIES-13: Children's Revised Impact of Event Scale-13, M: Mean, SD: Standard deviation, t(df): t-test statistic (degrees of freedom).

markedly elevated post-traumatic stress symptoms (CRIES-13) and significantly lower psychological resilience in patients compared with healthy controls (both $p < 0.001$).

The overall MANCOVA revealed a significant multivariate main effect of group on the combined dependent variables (Pillai's Trace = 0.20, $F(5,105) = 5.32$, $p < 0.001$, $\eta^2 = 0.20$), indicating that the psychological profiles of the two groups differed significantly after adjusting for age and gender. No significant multivariate effects were found for sex ($p = 0.297$) or for the group × sex interaction ($p = 0.940$). Results of the follow-up univariate ANCOVAs, including adjusted marginal means (SEs) by group, are presented in Table 3. Compared with controls, patients reported significantly higher depression [$F(1,109) = 13.04$, $p < 0.001$, $\eta^2 = 0.11$], anxiety [$F(1,109) = 10.31$, $p = 0.002$, $\eta^2 = 0.09$], stress [$F(1,109) = 6.40$, $p = 0.013$, $\eta^2 = 0.06$], and posttraumatic stress [$F(1,109) = 18.62$, $p < 0.001$, $\eta^2 = 0.15$] scores and significantly lower psychological resilience [$F(1,109) = 14.32$, $p < 0.001$, $\eta^2 = 0.12$] scores. No significant main effects of age or sex were observed across dependent variables.

Within the case group, Pearson correlation analyses demonstrated significant negative associations between psychological resilience and depression ($r = −0.36$, $p = 0.006$), stress ($r = −0.34$, $p = 0.011$), and posttraumatic stress symptoms ($r = −0.48$, $p < 0.001$). The correlation with anxiety was non-significant ($r = −0.08$, $p = 0.58$). The DASS-21 subscales were strongly intercorrelated ($r = 0.50–0.84$, $p < 0.001$) and positively related to CRIES-13 scores ($r = 0.49–0.54$, $p < 0.001$).

To further explore the protective role of psychological resilience, multiple hierarchical regression analyses were conducted within the case group (Table 4). After controlling for age and gender, psychological resilience emerged as a significant negative predictor of depression ($\beta = −0.35$, $p = 0.011$), stress ($\beta = −0.30$, $p = 0.026$), and posttraumatic stress symptoms ($\beta = −0.44$, $p = 0.001$), but not of anxiety ($\beta = −0.06$, $p = 0.67$). The inclusion of resilience in the second step explained an additional 11.4% of the variance in depression, 8.8% in stress, and 18.5% in posttraumatic stress, beyond the effects of age and gender. The final models accounted for 14%, 14%, and 27% of the variance in depression, stress, and posttraumatic stress, respectively (all $p < 0.05$), whereas the model for anxiety was non-significant ($R^2 = 0.009$, $p = 0.92$). Neither age nor gender contributed significantly to any of the models.

DISCUSSION

The present study examined the psychological impact of sexual abuse on Turkish adolescents and the protective role of psychological resilience. Consistent with our first hypothesis and extensive meta-analytic evidence, adolescents with a history of sexual abuse exhibited significantly higher levels of depression, anxiety, stress, and posttraumatic stress symptoms compared to their non-abused peers (2,3). Specifically, the case group reported substantially elevated scores on the DASS-21 depression, anxiety, and stress subscales, as well as on the CRIES-13 posttraumatic stress measure. These findings are consistent with the well-established literature demonstrating that sexual abuse exposure is associated with broad-spectrum psychopathology in adolescents (6). The magnitude of these group differences underscores the profound psychological impact of sexual abuse on adolescent mental health and validates the clinical significance of sexual abuse in Turkish populations.

Table 3. Follow-up univariate ANCOVA results for the effect of group (patient vs. control) on depression, anxiety, stress, posttraumatic stress, and psychological resilience (controlling for age and sex).

Dependent variable	Adjusted mean (control) (SE)	Adjusted mean (patient) (SE)	F(1, 109)	p	Partial η^2
DASS-depression	90 (0.70)	10 (0.93)	04	<0.001*	0.11
DASS-anxiety	5.22 (0.61)	8.46 (0.80)	10.31	0.002*	0.09
DASS-stress	6.75 (0.64)	9.43 (0.84)	6.40	0.013*	0.06
CRIES-13	22.23 (2.05)	36.89 (2.71)	18.62	<0.001*	0.15
Psychological resilience	44.22 (1.38)	35.59 (1.81)	14.32	<0.001*	0.12

Values represent univariate F-tests from the MANCOVA, with age and sex included as covariates. Adjusted means are estimated marginal means. All results remained significant after Bonferroni correction ($\alpha = 0.05$). Group coded as 0 = control, 1 = patient.
DASS: Depression, Anxiety and Stress Scale, CRIES-13: Children's Revised Impact of Event Scale-13, SE: Standard error, ANCOVA: Analysis of covariance, MANCOVA: Multivariate analysis of covariance.

Table 4. Hierarchical multiple regression analyses predicting psychopathology from psychological resilience (controlling for age and gender).

Dependent variable	Model	Predictor	β	t	p	F(Δdf)	R^2	ΔR^2
DASS-depression	1	Age	15	12	27	F(2,53) = 0.73	0.027	—
		Gender	0.07	0.50	0.62			
	2	Psychological resilience	−0.35	−2.62	0.011*	F(1,52) = 6.87	0.140	0.114
DASS-anxiety	1	Age	0.06	0.44	0.66	F(2,53) = 0.16	0.006	—
		Gender	0.01	0.08	0.94			
	2	Psychological resilience	−0.06	−0.43	0.67	F(1,52) = 0.19	0.009	0.004
DASS-stress	1	Age	0.21	1.57	0.12	F(2,53) = 1.34	0.048	—
		Gender	0.07	0.51	0.62			
	2	Psychological resilience	−0.30	−2.30	0.026*	F(1,52) = 5.28	0.136	0.088
CRIES (post-traumatic stress)	1	Age	0.24	1.83	0.07	F(2,53) = 2.44	0.084	—
		Gender	0.17	1.29	0.20			
	2	Psychological resilience	−0.44	−3.63	0.001*	F(1,52) = 13.20	0.270	0.185

β: Standardized regression coefficient, ΔR^2: Change in explained variance after adding psychological resilience in Step 2, DASS: Depression Anxiety Stress Scale, CRIES: Children's Revised Impact of Event Scale.

Our second and third hypotheses were partially supported. As expected, we found a significant negative correlation between psychological resilience and symptoms of depression, stress, and post-traumatic stress within the case group. Furthermore, resilience emerged as a significant negative predictor of these outcomes, even after controlling for age and gender. This finding aligns with previous research highlighting the crucial role of resilience as a buffer against the negative psychological consequences of trauma (9,10,25).

Resilience, conceptualized as the capacity to adapt and recover from adversity (7,26) has been identified as a key protective factor in trauma-exposed populations. Yang et al. (9) demonstrated in their study of adolescent abuse survivors that psychological resilience mediated the relationship between childhood abuse and depression, with higher resilience associated with lower depressive symptoms. Similarly, Milovančević et al. (27) found that resilience was a significant protective factor against psychopathology in youth with histories of childhood abuse. Our findings extend this literature by demonstrating that resilience not only correlates with better mental health outcomes but also serves as a significant predictor of lower levels of depression, stress, and post-traumatic stress symptoms, even when demographic variables are controlled for.

However, contrary to our expectations, we did not find a significant relationship between psychological resilience and anxiety. This finding warrants further consideration. While some studies have reported a negative association between resilience and anxiety in trauma-exposed youth (10), others have suggested that the protective role of resilience against internalizing symptoms, including anxiety, may be relatively minor (25). The complex nature of anxiety, which can manifest as both a state and a trait, may contribute to this discrepancy. T he measure of resilience used in this study may not fully capture the protective factors most relevant to anxiety. Future research should explore this relationship in more detail, perhaps using different measures of anxiety and resilience, and considering the potential mediating role of other factors, such as social support (28).

The non-significant relationship between resilience and anxiety can be explained by several factors. First, anxiety measured by the DASS-21 reflects immediate emotional responses to stress rather than stable personality traits, which may be less influenced by resilience than depression or stress (29,30). Second, the CYRM-12 resilience measure may not capture anxiety-specific protective factors such as emotion regulation or coping skills that directly address threat perception and fear responses in trauma survivors (11). Third, the protective effect of resilience on anxiety may depend on other factors not examined here, such as social support—adolescents with high resilience but weak social networks may still experience significant anxiety (28). Finally, heightened anxiety during adolescence is developmentally normal due to brain changes in threat detection, which may mask resilience's protective effects (31). These findings suggest that anxiety in trauma-exposed adolescents requires targeted interventions beyond resilience-building programs.

While our findings are consistent with existing literature from Western populations, the present study contributes important contextual and cultural insights. This is among the first studies to examine the protective role of resilience in Turkish adolescent survivors of sexual abuse, extending research to a non-Western, culturally distinct population. Cultural factors may influence both the expression of psychological symptoms and the protective mechanisms through which resilience operates. For instance, in Turkish culture, family support and community connectedness are particularly valued protective factors (32), and the CYRM-12's assessment of family and community resilience dimensions may be particularly relevant in this cultural context. Second, the Turkish mental health system and access to trauma-specific interventions may differ from those in Western contexts, making the identification of protective factors, such as resilience, particularly important to inform culturally adapted interventions. Third, the prevalence and presentation of sexual abuse in Turkish adolescents may differ from Western populations due to cultural norms, help-seeking behaviors, and reporting patterns (33). These contextual factors highlight the importance of conducting research in diverse populations

to understand how universal psychological processes (such as resilience) operate within specific cultural and social contexts.

Study Limitations

Several limitations should be considered when interpreting these findings. First, the cross-sectional design of this study precludes causal inferences about the relationship between resilience and mental health outcomes. Longitudinal research would be valuable for understanding the temporal dynamics of these relationships and identifying potential causal pathways. Second, the unequal gender distribution between groups, with a higher proportion of females in the case group, may limit the generalizability of the findings. Future research should aim for more balanced gender representation or explicitly examine gender differences in the relationship between sexual abuse, resilience, and psychopathology. Third, we did not collect detailed information about characteristics of sexual abuse (e.g., timing, duration, and relationship to the perpetrator), which limits our ability to examine how abuse characteristics relate to resilience and mental health outcomes.

Future research should employ longitudinal designs to examine the developmental trajectories of resilience and mental health in adolescent survivors of sexual abuse. Additionally, qualitative research exploring the lived experiences of resilient survivors could provide valuable insights into the mechanisms through which resilience operates in this population. Research examining the effectiveness of resilience-focused interventions combined with anxiety-specific treatments would help develop more comprehensive and effective treatment approaches for adolescent survivors of sexual abuse.

CONCLUSION

This study provides further evidence of the significant and detrimental impact of sexual abuse on adolescent mental health. Our findings indicate that adolescents with a history of sexual abuse exhibit higher levels of depression, anxiety, stress, and post-traumatic stress symptoms and lower levels of psychological resilience than their non-abused peers. While psychological resilience appears to be a crucial protective factor against depression, stress, and post-traumatic stress, its relationship with anxiety is more complex and requires further investigation. These findings have important implications for clinical practice, highlighting the need for interventions that not only address the psychopathological consequences of sexual abuse but also focus on fostering resilience in this vulnerable population. Future research should employ longitudinal designs and more comprehensive assessments to further elucidate the complex interplay between trauma, resilience, and mental health in adolescents.

Ethics

Ethics Committee Approval: Ethical approval for the study was obtained from Recep Tayyip Erdoğan University Ethics Committee on 29.05.2025 with the decision number 2025/246.

Informed Consent: Written informed consent was obtained from all participants and their legal guardians prior to their inclusion in the study.

Footnotes

Authorship Contributions

Surgical and Medical Practices: İ.Z., A.Ö., U.T., Y.F., Concept: İ.Z., A.Ö., U.T., Y.F., Design: İ.Z., A.Ö., U.T., Y.F., Data Collection or Processing: İ.Z., U.T., Y.F., Analysis or Interpretation: İ.Z., A.Ö., Literature Search: İ.Z., A.Ö. Writing: İ.Z., A.Ö., U.T., Y.F.

Conflict of Interest: No conflict of interest was declared by the authors.

Financial Disclosure: The authors declared that this study received no financial support.

REFERENCES

1. Stoltenborgh M, van IJzendoorn MH, Euser EM, Bakermans-Kranenburg MJ. A global perspective on child sexual abuse: meta-analysis of prevalence around the world. Child Maltreat. 2011; 16: 79-101.
2. Hailes HP, Yu R, Danese A, Fazel S. Long-term outcomes of childhood sexual abuse: an umbrella review. Lancet Psychiatry. 2019; 6: 830-9.
3. Dworkin ER, Menon SV, Bystrynski J, Allen NE. Sexual assault victimization and psychopathology: a review and meta-analysis. Clin Psychol Rev. 2017; 56: 65-81.
4. Litz BT, Stein N, Delaney E, Lebowitz L, Nash WP, Silva C, et al. Moral injury and moral repair in war veterans: a preliminary model and intervention strategy. Clin Psychol Rev. 2009; 29: 695-706.
5. van der Kolk B. The body keeps the score: brain, mind, and body in the healing of trauma. New York: Viking; 2014.
6. Teicher MH, Samson JA. Annual research review: enduring neurobiological effects of childhood abuse and neglect. J Child Psychol Psychiatry. 2016; 57: 241-66.
7. Masten AS. Ordinary magic: resilience in development. New York: Guilford Press; 2014.
8. Ungar M, editor. The social ecology of resilience: a handbook of theory and practice. New York: Springer; 2012.
9. Yang Y, Ma X, Kelifa MO, Li X, Chen Z, Wang P. The relationship between childhood abuse and depression among adolescents: the mediating role of school connectedness and psychological resilience. Child Abuse Negl. 2022; 131: 105760.
10. Mesman E, Vreeker A, Hillegers M. Resilience and mental health in children and adolescents: an update of the recent literature and future directions. Curr Opin Psychiatry. 2021; 34: 586-92.
11. Domhardt M, Münzer A, Fegert JM, Goldbeck L. Resilience in survivors of child sexual abuse: a systematic review of the literature. Trauma Violence Abuse. 2015; 16: 476-93.
12. Lovibond PF, Lovibond SH. The structure of negative emotional states: comparison of the Depression Anxiety Stress Scales with the Beck Depression and Anxiety Inventories. Behav Res Ther. 1995; 33: 335-43.
13. Gloster AT, Rhoades HM, Novy D, Klotsche J, Senior A, Kunik M, et al. Psychometric properties of the Depression Anxiety and Stress Scale-21 in older primary care patients. J Affect Disord. 2008; 110: 248-59.
14. Sariçam H. The psychometric properties of Turkish version of Depression Anxiety Stress Scale-21 in health control and clinical samples. J Cogn Behav Psychother Res. 2018; 7: 19.
15. Perrin S, Meiser-Stedman R, Smith P. The Children's Revised Impact of Event Scale: validity as a screening instrument for PTSD. Behav Cogn Psychother. 2005; 33: 487-98.

16. Çeri V, Hamidi F, Çakır B, Bilaç Ö, İz M, Ay İz FB, et al. Child Revised Impact of Event Scale: validity and reliability study of Turkish version. Neuropsychiatr Invest. 2021; 59: 21-6.
17. Liebenberg L, Ungar M, van de Vijver F. Validation of the Child and Youth Resilience Measure-28 among Canadian youth. Res Soc Work Pract. 2012; 22: 219-26.
18. Liebenberg L, Ungar M, LeBlanc JC. The CYRM-12: a brief measure of resilience. Can J Public Health. 2013; 104: e131-5.
19. Arslan G. Çocuk ve Genç Psikolojik Sağlamlık Ölçeği'nin (ÇGPSÖ-12) psikometrik özellikleri: geçerlilik ve güvenirlik çalışması. Ege Eğitim Dergisi. 2015; 16: 1-12.
20. Henry JD, Crawford JR. The short-form version of the Depression Anxiety Stress Scales: construct validity and normative data in a large non-clinical sample. Br J Clin Psychol. 2005; 44: 227-39.
21. Szabó M, Lovibond PF. Anxiety, depression, and tension/stress in children. J Psychopathol Behav Assess. 2006; 28: 192-202.
22. Meiser-Stedman R, Dalgleish T, Glucksman E, Yule W, Smith P. Maladaptive cognitive appraisals mediate the evolution of posttraumatic stress reactions: a 6-month follow-up of child and adolescent assault and motor vehicle accident survivors. J Abnorm Psychol. 2009; 118: 778-87.
23. Ungar M, Liebenberg L. Assessing resilience across cultures using mixed methods: construction of the Child and Youth Resilience Measure. J Mix Methods Res. 2011; 5: 126-49.
24. Arslan G. Çocuk ve Genç Psikolojik Sağlamlık Ölçeği'nin (ÇGPSÖ-12) psikometrik özellikleri: geçerlilik ve güvenirlik çalışması. Ege Eğitim Dergisi. 2015; 16: 1-12. [Mükerrer kaynak: bkz. kaynak 19]
25. Srivastava AV, Brown R, Newport DJ, Rousseau JF, Wagner KD, Guzick A, et al. The role of resilience in the development of depression, anxiety, and post-traumatic stress disorder after trauma in children and adolescents. Psychiatry Res. 2024; 334: 115772.
26. Southwick SM, Bonanno GA, Masten AS, Panter-Brick C, Yehuda R. Resilience definitions, theory, and challenges: interdisciplinary perspectives. Eur J Psychotraumatol. 2014; 5: 25338.
27. Milovančević MP, Tenjović L, Išpanović V, Mitković M, Kirćanski JR, Minčić T, et al. Psychopathology and resilience in relation to abuse in childhood among youth first referred to the psychiatrist. Vojnosanit Pregl. 2014; 71: 565-70.
28. Buchanan M, Walker G, Boden JM, Mansoor Z, Newton-Howes G. Protective factors for psychosocial outcomes following cumulative childhood adversity: systematic review. BJPsych Open. 2023; 9: e197.
29. Spielberger CD, editor. Anxiety: current trends in theory and research. New York: Academic Press; 2013.
30. Suliman S, Mkabile SG, Fincham DS, Ahmed R, Stein DJ, Seedat S. Cumulative effect of multiple trauma on symptoms of posttraumatic stress disorder, anxiety, and depression in adolescents. Compr Psychiatry. 2009; 50: 121-7.
31. Steinberg L. A social neuroscience perspective on adolescent risk-taking. In: Walsh A, Beaver KM, editors. Biosocial theories of crime. New York: Routledge; 2017. p. 435-63.
32. Kağıtçıbaşı Ç. Family, self, and human development across cultures: theory and applications. New York: Routledge; 2017.
33. Baytunca MB, Ata E, Ozbaran B, Kaya A, Kose S, Aktas EO, et al. Childhood sexual abuse and supportive factors. Pediatr Int. 2017; 59: 10-5.

Gazi Med J 2026;37(3):407-410

DOI: http://dx.doi.org/10.12996/gmj.2026.4674

Clinical, Biochemical, and Histopathological Characteristics of Big Adrenal Masses: A Single-Center Retrospective Study

Büyük Adrenal Kitlelerin Klinik, Biyokimyasal ve Histopatolojik Özellikleri: Tek Merkez Deneyimi

Meriç Coşkun[1], Mehmet Muhittin Yalçın[1], Başak Bolayır[1], Begüm Algül[2], Mustafa Akhoroz[2], Mehmet Feyiz Altınsoy[3], Afruz Babayeva[1], Alev Eroğlu Altınova[1], Müjde Aktürk[1], Ayhan Karakoç[1], Sinan Sözen[3], Aylar Poyraz[4], Füsun Baloş Törüner[1]

[1]Division of Endocrinology and Metabolism, Department of Internal Medicine, Gazi University, Faculty of Medicine, Ankara, Türkiye
[2]Gazi University, Faculty of Medicine, Ankara, Türkiye
[3]Department of Urology, Gazi University, Faculty of Medicine, Ankara, Türkiye
[4]Department of Pathology, Gazi University, Faculty of Medicine, Ankara, Türkiye

ABSTRACT

Introduction: Large adrenal tumors (≥8 cm) are associated with a high risk of malignancy, although their pathological distribution varies across institutions. Clarifying their clinical and biochemical features is essential for appropriate surgical decision-making. This study aimed to evaluate the clinical presentation, hormonal activity, surgical management, and histopathological outcomes of adrenal tumors ≥8 cm.

Methods: This retrospective study included patients who underwent adrenalectomy at a tertiary endocrine center and had a tumor size ≥8 cm on histopathology. Demographic data, hormonal evaluation, radiological findings, and follow-up outcomes were analyzed.

Results: Twenty-six patients (mean age 50.85 ± 13.04 years; 57.7% women) were included. Tumors were incidentally detected in 46.2% of cases. Hormonal hypersecretion was present in 46.2% of patients, most commonly catecholamine excess (34.6%). Pheochromocytoma was the most frequent diagnosis (38.5%), followed by adrenocortical carcinoma (15.4%). Overall, 46.2% of masses were malignant. Malignant tumors were significantly larger than benign ones (p = 0.041). Laparoscopic adrenalectomy was performed for smaller lesions than those treated by open surgery (p = 0.003). During follow-up, 58.3% of malignant cases developed metastases; two patients achieved remission.

CONCLUSION: Adrenal tumors ≥8 cm demonstrate marked clinical and pathological heterogeneity. Although tumor size is associated

ÖZ

Amaç: Büyük adrenal tümörler (≥8 cm), yüksek malignite riski ile ilişkilidir; ancak patolojik dağılımları merkezler arasında farklılık gösterebilmektedir. Uygun cerrahi karar verme süreci için bu tümörlerin klinik ve biyokimyasal özelliklerinin net olarak ortaya konulması önemlidir. Bu çalışmada, ≥8 cm adrenal tümörlerin klinik prezentasyonu, hormonal aktivitesi, cerrahi yönetimi ve histopatolojik sonuçlarının değerlendirilmesi amaçlandı.

Yöntemler: Bu retrospektif çalışmaya, üçüncü basamak bir endokrinoloji merkezinde adrenalektomi uygulanan ve histopatolojik incelemede tümör boyutu ≥8 cm olarak saptanan hastalar dahil edildi. Demografik özellikler, hormonal değerlendirme sonuçları, radyolojik bulgular ve takip verileri analiz edildi.

Bulgular: Çalışmaya 26 hasta (ortalama yaş 50,85 ± 13,04 yıl; %57,7 kadın) dahil edildi. Tümörler olguların %46,2'sinde insidental olarak saptandı. Hastaların %46,2'sinde hormonal hipersekresyon mevcuttu ve en sık görülen hormonal aktivite katekolamin fazlalığıydı (%34,6). En sık histopatolojik tanı feokromositoma (%38,5) olup, bunu adrenokortikal karsinom (%15,4) izledi. Tüm kitlelerin %46,2'si malign özellikteydi. Malign tümörler benign tümörlere göre anlamlı olarak daha büyüktü (p = 0,041). Laparoskopik adrenalektomi uygulanan lezyonların boyutu, açık cerrahi uygulananlara göre anlamlı derecede daha küçüktü (p = 0,003). Takip sürecinde malign olguların %58,3'ünde metastaz gelişirken, iki hastada remisyon sağlandı.

Cite this article as: Coşkun M, Yalçın MM, Bolayır B, Algül B, Akhoroz M, Altınsoy MF, et al. Clinical, biochemical, and histopathological characteristics of big adrenal masses: a single-center retrospective study. Gazi Med J. 2026;37(3):407-410

Address for Correspondence/Yazışma Adresi: Meriç Coşkun, Division of Endocrinology and Metabolism, Department of Internal Medicine, Gazi University, Faculty of Medicine, Ankara, Türkiye
E-mail / E-posta: drmericcoskun@gmail.com
ORCID ID: orcid.org/0000-0003-4855-6078

Received/Geliş Tarihi: 28.3.2026
Accepted/Kabul Tarihi: 17.6.2026
Publication Date/Yayınlanma Tarihi: 10.07.2026

ABSTRACT

with malignancy, the high prevalence of pheochromocytoma in referral centers highlights the importance of comprehensive biochemical evaluation. Management should be individualized using a multidisciplinary approach rather than relying solely on tumor size.

Keywords: Adrenal tumor, large adrenal mass, pheochromocytoma, adrenocortical carcinoma, adrenalectomy

ÖZ

Sonuç: ≥8 cm adrenal tümörler belirgin klinik ve patolojik heterojenite göstermektedir. Tümör boyutu malignite ile ilişkili olmakla birlikte, üçüncü basamak merkezlerde feokromositomanın yüksek prevalansı kapsamlı biyokimyasal değerlendirmenin önemini ortaya koymaktadır. Bu hastaların yönetimi yalnızca tümör boyutuna dayanılarak değil, multidisipliner bir yaklaşımla bireyselleştirilmelidir.

Anahtar Sözcükler: Adrenal tümör, büyük adrenal kitle, feokromositoma, adrenokortikal karsinom, adrenalektomi

INTRODUCTION

The widespread use of modern imaging techniques has led to a substantial increase in the incidental detection of adrenal lesions (1). Incidentally identified adrenal lesions are reported in approximately 4–10% of imaging studies, with even higher rates observed in autopsy series (2). Although most adrenal incidentalomas are benign, further radiological and biochemical evaluation of these lesions is essential to reach a specific diagnosis. When an incidental adrenal mass is detected, the patient's clinical features, imaging features for malignant/benign differentiation of the adrenal mass, and biochemical tests for functionality should be reviewed (3). The prevalence of adrenal tumors increases with age (4).

In determining the risk of malignancy of an adrenal tumor, imaging characteristics, especially the tumor size, are essential. Tumor size is considered one of the most important predictors of malignancy in adrenal lesions, with larger tumors carrying a higher probability of being malignant. Intermittent enlargement of adrenal masses is also considered an indicator of malignancy (2). However, the standard threshold for tumor size that indicates malignancy is unclear. While several guidelines suggest that any adrenal mass concerning radiographic characteristics and size ≥4 cm should be resected because of the increased risk of adrenal cancer, recent ones do not recommend a total tumor size for operation (5). Instead, newer guidelines suggest an individualized approach considering adrenalectomy in large tumors (5). Angeli et al. (6) reported a tumor size threshold of 4 cm for 80% sensitivity but 34% specificity for diagnosing a malignant adrenal mass. Sturgeon et al. (7) reported an estimated risk of malignancy with a specificity of 95% and a sensitivity of 77% for tumors larger than 8 cm. Based on this information, we aimed to examine the clinical and histopathological features of patients who underwent surgery for an adrenal mass larger than 8 cm.

MATERIALS AND METHODS

Study Design and Subjects

This retrospective study included patients with tumor size ≥8 cm on the histopathological examination after adrenalectomy, evaluated in the endocrinology outpatient clinic due to the detection of an adrenal mass at our tertiary care centre between 2010 and 2021. Demographic characteristics, clinical presentation, preoperative hormonal work-up, imaging results, surgical approach, pathology findings, and follow-up outcomes were retrieved from hospital records. The study protocol was approved by Ethics Committee of Gazi University (date: 28.06.2021 and no: 594).

Written informed consent was not required due to the retrospective design of the study.

Statistical Analysis

Commercial statistical software, Statistical Package for the Social Sciences (SPSS) version 22.0 (IBM Corp., Armonk, NY, USA), was used for statistical analyses. The Shapiro-Wilk test was used to assess the conformity of continuous variables to the normal distribution, while the homogeneity of variance was evaluated using Levene's test. Continuous variables with a normal distribution were presented as the mean ± standard deviation. Continuous variables that were not normally distributed were presented as the median and interquartile range (25^{th}–75^{th} percentiles). Student's t-test was used for normally distributed continuous data, and the Mann–Whitney U test was used for non-normally distributed data. The relationships between variables that did not meet the assumption of normality were evaluated using Spearman's Rho correlation coefficient. The error rate ($\alpha = 0.05$) was set for all tests, and differences between groups were considered statistically significant when $p < 0.05$.

RESULTS

The study included 26 cases with adrenal masses larger than 8 cm; the mean age was 50.85 ± 13.04 years. Women comprised 57.7% (n = 15) of cases. 50% (13) of masses were located on the left, 46% (11) were on the right, and 3.8% (1) were bilateral. It was detected incidentally in 46.2% (12) of cases. The most prominent symptoms of the patients were abdominal pain, 38.5% (10); high blood pressure, 30.8% (8); and other symptoms, including back pain, fatigue, weakness, and palpitations.

Preoperative biochemical tests were completed for all but one emergency case. Fourteen masses (53.8%) were non-functional; the remaining masses demonstrated hormonal hypersecretion, most commonly of catecholamines [34.6% (9)], followed by hypercortisolism [7.7% (2)], and one case of aldosterone-cortisol co-secretion.

Open surgery was performed in 76.9% of cases, typically for larger tumors, while the remaining cases were performed laparoscopically. Median tumor size was 10.25 cm (8–18 cm). Pheochromocytoma was the most common diagnosis [38.5% (10)], followed by ACC [15.4% (4)], myelolipoma [11.5% (2)], cavernous hemangioma, cysts, cortical hyperplasia, schwannoma, pleomorphic sarcoma, sarcomatoid carcinoma, diffuse large B-cell lymphoma (DLBCL), and renal cell carcinoma (RCC) metastasis (Table 1). Fourteen masses (53.8%) were benign; the remainder were malignant.

Of the cases evaluated as malignant, 33.3% (4) were pheochromocytoma, 33.3% (4) were adrenocortical carcinoma (ACC), and the remaining cases were pleomorphic sarcoma, sarcomatoid carcinoma, DLBCL, and RCC metastasis. During follow-up, metastasis occurred in 58.3% (7) of malignant cases, and the patients died. Of these, 25.0% (3) were metastatic; they received medical treatment, and two patients (one DLBCL, one pheochromocytoma) remained in remission.

Among pheochromocytomas, three were incidental findings. Catecholamine excess was detected in all but one emergency case, which had a tumour diameter of 110 cm in the left adrenal gland, had metastases to the spleen, kidney, and liver, and presented with severe abdominal pain. Forty per cent of cases were classified as malignant pheochromocytoma because of metastasis to non-adrenal organs. Preoperative alpha-blocker treatment was administered to all cases except the case taken for emergency surgery; no intraoperative complications were identified.

The median tumour diameter in benign lesions (9.25 cm; range 8–12 cm) was lower than that in malignant lesions (11.25 cm; range 8–18 cm) (p = 0.041). The median tumour diameter for those who underwent laparoscopic [9 (8–9.5) cm] was lower than that for open surgery [11 (8–18] cm) (p = 0.003). The tumour diameters of non-functional masses [9.55 (8–15) cm] and functional masses [11 (8–18) cm] were similar (p = 0.297) (Table 2). No correlation was found between tumour diameter and age at diagnosis.

Table 1. Histopathological distribution of adrenal tumors ≥8 cm.

Pathological diagnosis	% (n)
Pheochromocytoma	5 (10)
Adrenocortical carcinoma	4 (4)
Myelolipoma	5 (3)
Cavernous hemangioma	7.7 (2)
Benign cyst	3.8 (1)
Cortical hyperplasia	3.8 (1)
Schwannoma	3.8 (1)
Pleomorphic sarcoma	3.8 (1)
Sarcomatoid carcinoma	3.8 (1)
Diffuse large B-Cell lymphoma	3.8 (1)
Renal cell carcinoma metastasis	3.8 (1)

Table 2. Tumor size differences by pathology, functional status, and surgical technique.

Feature	Size	p-value
Benign	9.25 cm (8–12)	0.041
Malign	11.25 cm (8–18)	
Non-functional	9.55 cm (8–15)	0.297
Functional	11 cm (8–18)	
Laparoscopic surgery	9 cm (8–9.5)	0.003
Open surgery	11 cm (8–18)	

DISCUSSION

In this single-center retrospective study, we evaluated the clinical, biochemical, surgical, and pathological characteristics of 26 patients with adrenal tumors ≥8 cm. Although large adrenal masses are frequently reported as malignant in the literature, pheochromocytoma was the most common histopathological diagnosis in our study, which likely reflects referral bias at a tertiary endocrine center. Tumor size was significantly larger in malignant lesions and in those managed with open surgery, whereas functional status was not associated with tumor diameter.

Large adrenal masses pose a significant diagnostic challenge; the likelihood of malignancy increases with tumor size, while the histopathological distribution varies considerably among centers. Previous literature consistently reports ACC as the predominant diagnosis in tumors ≥8–10 cm (8). In contrast, pheochromocytoma was the most common pathology in our cohort, followed by ACC. This difference likely reflects referral bias, as our tertiary endocrine center manages a high proportion of hormonally active adrenal tumors, particularly those suspected of secreting catecholamines.

The malignancy rate in the present study aligns with earlier findings that large adrenal tumors are associated with a substantial risk of malignancy. Abdel-Aziz et al. (9) reported an 84% ACC rate in tumors >8 cm, whereas Cichocki et al. (10) found ACC in 63% of tumors >10 cm. However, more recent multicenter cohorts suggest slightly lower malignancy rates and emphasize the importance of imaging rather than size alone. The 2023 ENSAT update stresses that although size is a strong predictor, it should not be used in isolation for surgical decision-making when imaging and biochemical features are benign (11). Importantly, we found that malignant tumors had significantly larger diameters than benign tumors. Malignant tumors were significantly larger, reinforcing tumor diameter as an important predictor; however, considerable overlap between benign and malignant lesions limits its discriminatory value. Functional status was not linked to malignancy, consistent with recent evidence showing that hormonal hypersecretion—other than androgen excess—does not reliably distinguish malignant from benign disease (11,12).

The high malignancy rate among pheochromocytomas is notable. Malignant pheochromocytoma is difficult to predict preoperatively, as tumor size and catecholamine profile do not reliably differentiate benign from malignant disease (13). Moreover, recent evidence suggests that increasing tumor size itself is associated with a higher likelihood of metastatic behavior in pheochromocytoma and paraganglioma, highlighting the role of tumor diameter as a risk factor for aggressive disease (14).

Regarding surgical management, laparoscopic adrenalectomy was performed for tumors with significantly smaller diameters than those selected for open surgery. This pattern is consistent with current recommendations favoring open adrenalectomy for large or radiographically suspicious masses due to concerns about capsular disruption, incomplete resection, and oncologic upstaging (15,16). Nevertheless, recent evidence indicates that minimally invasive adrenalectomy may still be safely performed in carefully selected patients with pheochromocytomas larger than 5 cm, with comparable perioperative outcomes despite longer operative times (17).

Study Limitations

Strengths of this study include detailed biochemical evaluation, histopathological verification, and long-term outcome data. Limitations include the retrospective design, single-center setting, and relatively small sample size, which may restrict generalizability.

CONCLUSION

Our study shows that adrenal tumors ≥8 cm are pathologically heterogeneous and should not be assumed to represent ACC. The high frequency of pheochromocytoma in our cohort reflects referral patterns and highlights the importance of thorough preoperative endocrine evaluation and perioperative management. These findings support an individualized approach to large adrenal masses that integrates biochemical testing, imaging features, and multidisciplinary decision-making rather than relying on tumor size alone.

Ethics

Ethics Committee Approval: The study protocol was approved by Ethics Committee of Gazi University (date: 28.06.2021 and no: 594).

Informed Consent: Written informed consent was not required due to the retrospective design of the study.

Footnotes

Authorship Contributions

Surgical and Medical Practices: M.C., M.M.Y., B.B., B.A., M.A., M.F.A., A.B., A.E.A., M.A., A.K., S.S., A.P., F.B.T., Concept: M.C., M.M.Y., B.B., B.A., M.A., M.F.A., A.B., A.E.A., M.A., A.K., S.S., A.P., F.B.T., Design: M.C., M.M.Y., B.B., B.A., M.A., M.F.A., A.B., A.E.A., M.A., A.K., S.S., A.P., F.B.T., Data Collection or Processing: M.C., M.M.Y., B.B., B.A., M.A., M.F.A., A.B., A.E.A., M.A., A.K., S.S., A.P., F.B.T., Analysis or Interpretation: M.C., M.M.Y., B.B., B.A., M.A., M.F.A., A.B., A.E.A., M.A., A.K., S.S., A.P., F.B.T., Literature Search: M.C., M.M.Y., B.B., B.A., M.A., M.F.A., A.B., A.E.A., M.A., A.K., S.S., A.P., F.B.T., Writing: M.C., M.M.Y., B.B., B.A., M.A., M.F.A., A.B., A.E.A., M.A., A.K., S.S., A.P., F.B.T.

Conflict of Interest: No conflict of interest was declared by the authors.

Financial Disclosure: The authors declared that this study received no financial support.

REFERENCES

1. Iñiguez-Ariza NM, Kohlenberg JD, Delivanis DA, Hartman RP, Dean DS, Thomas MA, et al. Clinical, biochemical, and radiological characteristics of a single-center retrospective cohort of 705 large adrenal tumors. Mayo Clin Proc Innov Qual Outcomes. 2018; 2: 30-9.
2. Mody RN, Remer EM, Nikolaidis P, Pandharipande PV, Giordano SH, Berland LL, et al. ACR Appropriateness Criteria® adrenal mass evaluation: 2021 update. J Am Coll Radiol. 2021; 18: S251-S267.
3. He X, Peter PR, Auchus RJ. Approach to the patient with an incidental adrenal mass. Med Clin North Am. 2021; 105: 1047-63.
4. Bovio S, Cataldi A, Reimondo G, Sperone P, Novello S, Berruti A, et al. Prevalence of adrenal incidentaloma in a contemporary computerized tomography series. J Endocrinol Invest. 2006; 29: 298-302.
5. Fassnacht M, Arlt W, Bancos I, Dralle H, Newell-Price J, Sahdev A, et al. Management of adrenal incidentalomas: European Society of Endocrinology Clinical Practice Guideline in collaboration with the European Network for the Study of Adrenal Tumors. Eur J Endocrinol. 2016; 175: G1-G34.
6. Angeli A, Osella G, Ali A, Terzolo M. Adrenal incidentaloma: an overview of clinical and epidemiological data from the National Italian Study Group. Horm Res. 1997; 47: 279-83.
7. Sturgeon C, Shen WT, Clark OH, Duh QY, Kebebew E. Risk assessment in 457 adrenal cortical carcinomas: how much does tumor size predict the likelihood of malignancy? J Am Coll Surg. 2006; 202: 423-30.
8. Arshad H, Kawamoto S, Chu LC, Fishman EK. A comprehensive approach to the CT detection and evaluation of large adrenal masses part 2: malignant adrenal lesions and future directions. Abdom Radiol (NY). 2025. Online ahead of print.
9. Abdel-Aziz TE, Rajeev P, Sadler G, Weaver A, Mihai R. Risk of adrenocortical carcinoma in adrenal tumours greater than 8 cm. World J Surg. 2015; 39: 1268-73.
10. Cichocki A, Samsel R, Papierska L, Roszkowska-Purska K, Nowak K, Cichocki O, et al. Adrenal tumour bigger than 5 cm - what could it be? An analysis of 139 cases. Endokrynol Pol. 2017; 68: 411-5.
11. Fassnacht M, Tsagarakis S, Terzolo M, Tabarin A, Sahdev A, Newell-Price J, et al. European Society of Endocrinology clinical practice guidelines on the management of adrenal incidentalomas, in collaboration with the European Network for the Study of Adrenal Tumors. Eur J Endocrinol. 2023; 189: G1-G42.
12. Elhassan YS, Alahdab F, Prete A, Delivanis DA, Khanna A, Prokop L, et al. Natural history of adrenal incidentalomas with and without mild autonomous cortisol excess: a systematic review and meta-analysis. Ann Intern Med. 2019; 171: 107-16.
13. Ayala-Ramirez M, Feng L, Johnson MM, Ejaz S, Habra MA, Rich T, et al. Clinical risk factors for malignancy and overall survival in patients with pheochromocytomas and sympathetic paragangliomas: primary tumor size and primary tumor location as prognostic indicators. J Clin Endocrinol Metab. 2011; 96: 717-25.
14. Wang LL, Wei XJ, Zhang QC, Li F, Chen GY. Analysis of clinicopathological and immunohistochemical features of pheochromocytoma/paraganglioma. Ann Diagn Pathol. 2025; 79: 152525.
15. Libé R. Adrenocortical carcinoma: diagnosis, prognosis, and treatment. Front Cell Dev Biol. 2015; 3: 45.
16. Gaillard M, Razafinimanana M, Challine A, Bricaire L, Bertherat J, Bertagna X, et al. Laparoscopic or open adrenalectomy for stage I-II adrenocortical carcinoma: a retrospective study. J Clin Med. 2023; 12: 3698.
17. Gan Q, Huang Y, Li H, Yao Y, Li Y, Chen Y, et al. Redefining surgical boundaries: outcomes of minimally invasive adrenalectomy in large pheochromocytomas. Ann Med. 2025; 57: 2575300.

Gazi Med J 2026;37(3):411-418

DOI: http://dx.doi.org/10.12996/gmj.026.4683

The Impact of Obesity on the Metabolic Profile of Patients with Polycystic Ovary Syndrome

Polikistik Over Sendromlu Hastalarda Obezitenin Metabolik Profil Üzerine Etkisi

Seher Elif Koçoğlu[1], Mustafa Kavutçu[2], İsmail Güler[3], Nazlı Canpunar[2], Midvar Dashdamirova[3], Leman Nur Nehri[4], Cengiz Karakaya[2]

[1]Department of Medical Biochemistry, Institute of Health Sciences, Gazi University, Faculty of Medicine, Ankara, Türkiye
[2]Department of Medical Biochemistry, Gazi University, Faculty of Medicine, Ankara, Türkiye
[3]Department of Obstetrics and Gynecology, Gazi University Faculty, of Medicine, Ankara, Türkiye
[4]Data Science in Life Sciences Group, Institute for Chemistry and Bioanalytics, School of Life Sciences, FHNW University of Applied Sciences and Arts Northwestern Switzerland, Muttenz, Switzerland

ABSTRACT

Objective: The aim of this study was to evaluate the effects of polycystic ovary syndrome (PCOS) and accompanying obesity on various metabolic and biochemical parameters, particularly body composition, insulin resistance (IR), lipid profile, and inflammatory markers.

Methods: A total of 120 women aged 18–40 years were included in the study: 40 obese patients with PCOS, 40 normal-weight (non-obese) patients with PCOS, and 40 healthy controls. The diagnosis of PCOS was established according to the Rotterdam criteria. Participants were classified based on body mass index (BMI) as obese (BMI ≥30 kg/m^2) or non-obese (BMI <25 kg/m^2). Body composition was assessed using bioelectrical impedance analysis. Serum fasting glucose, insulin, glycated hemoglobin (HbA1c), lipid profile, C-reactive protein (CRP), alanine aminotransferase, aspartate aminotransferase, anti-Müllerian hormone (AMH), luteinizing hormone (LH), follicle-stimulating hormone (FSH), estradiol, and progesterone were analyzed. IR was calculated using the homeostatic model assessment of IR (HOMA-IR) method. Statistical comparisons between groups were performed using the Kruskal–Wallis test followed by Dunn's post-hoc analyses.

Results: Body weight, BMI, total fat mass, and body fat percentage were significantly higher in the obese PCOS group than in the other groups, whereas body water percentage and high-density lipoprotein (HDL) cholesterol levels were significantly lower ($p < 0.001$). Fasting insulin levels and HOMA-IR were significantly higher in the obese PCOS

ÖZ

Amaç: Bu çalışmanın amacı, polikistik over sendromunun (PCOS) ve eşlik eden obezitenin, özellikle vücut kompozisyonu, insülin direnci, lipid profili ve inflamatuvar belirteçler olmak üzere çeşitli metabolik ve biyokimyasal parametreler üzerindeki etkilerini değerlendirmektir.

Yöntemler: Çalışmaya 18–40 yaşları arasında, PCOS tanılı 40 obez hasta, PCOS tanılı 40 normal kilolu hasta ve 40 sağlıklı kontrol olmak üzere toplam 120 kadın dahil edilmiştir. PCOS tanısı Rotterdam kriterlerine göre konulmuştur. Bireyler vücut kütle indeksine (VKİ) göre obez (VKİ ≥30 kg/m²) ve obez olmayan (VKİ <25 kg/m²) olarak sınıflandırılmıştır. Vücut kompozisyonu Biyoelektrik Empedans Analizi ile değerlendirilmiştir. Serum açlık glukozu, insülin, HbA1c, lipid profili, C-reaktif protein (CRP), alanin aminotransferaz (ALT), aspartat aminotransferaz, anti-Müllerian hormon (AMH), luteinizan hormon (LH), folikül uyarıcı hormon (FSH), östradiol ve progesteron düzeyleri analiz edildi. İnsülin direnci HOMA-IR yöntemi kullanılarak hesaplanmıştır. Gruplar arasındaki istatistiksel karşılaştırmalar Kruskal-Wallis testi ve ardından Dunn post hoc analizleri ile gerçekleştirilmiştir.

Bulgular: Obez PCOS grubunda vücut ağırlığı, vücut kütle indeksi (VKİ), toplam yağ kütlesi ve vücut yağ yüzdesi diğer gruplara göre anlamlı derecede daha yüksek iken, vücut suyu yüzdesi ve HDL kolesterol düzeyleri anlamlı derecede daha düşüktür ($p < 0,001$). Açlık insülini ve HOMA-IR düzeyleri obez PCOS grubunda hem kontrol grubuna hem de obez olmayan PCOS grubuna göre anlamlı derecede daha yüksek tespit

Cite this article as: Koçoğlu SE, Kavutçu M, Güler İ, Canpunar N, Dashdamirova M, Nehri LN, et al. The impact of obesity on the metabolic profile of patients with polycystic ovary syndrome. Gazi Med J. 2026;37(3):411-418

Address for Correspondence/Yazışma Adresi: Cengiz Karakaya, Department of Medical Biochemistry, Gazi University, Faculty of Medicine, Ankara, Türkiye
E-mail / E-posta: karakayac@gazi.edu.tr
ORCID ID: orcid.org/0000-0002-0399-9150

Received/Geliş Tarihi: 09.04.2026
Accepted/Kabul Tarihi: 09.05.2026
Publication Date/Yayınlanma Tarihi: 10.07.2026

ABSTRACT

group than in both the control group and the non-obese PCOS group ($p < 0.001$). Additionally, HbA1c levels were higher in the obese PCOS group compared with both the control group ($p < 0.001$) and the non-obese PCOS group ($p < 0.01$). Similarly, triglyceride (TG), CRP, and ALT levels were higher in the obese PCOS group than in the other groups. AMH levels were higher in the non-obese PCOS group than in the control group. In contrast, no statistically significant differences were found among the groups in LH levels, FSH levels, the LH/FSH ratio, or progesterone levels. Correlation analyses showed that BMI and fat mass were positively associated with indicators of IR and with levels of TG, CRP, and ALT, and negatively associated with HDL cholesterol and body water percentage.

Conclusion: The severity of metabolic impairment in PCOS is closely associated with obesity and increased fat mass. Obesity is one of the main determinants of IR, dyslipidemia, and inflammation. Therefore, improving body composition is of great importance in the management of PCOS to reduce metabolic risk.

Keywords: Polycystic ovary syndrome, obesity, insulin resistance, body composition, inflammation, lipid profile

ÖZ

edilmiştir ($p < 0,001$). Ayrıca HbA1c düzeyleri obez PCOS grubunda kontrol grubuna ($p < 0,001$) ve obez olmayan PCOS grubuna ($p < 0,01$) göre daha yüksek bulunmuştur. Benzer şekilde trigliserid, CRP ve ALT düzeyleri de obez PCOS grubunda diğer gruplara göre daha yüksekti. AMH düzeyleri obez olmayan PCOS grubunda kontrol grubuna göre daha yüksektir. Buna karşın, LH, FSH, LH/FSH oranı ve progesteron düzeyleri açısından gruplar arasında istatistiksel olarak anlamlı bir farklılık bulunmamıştır. Korelasyon analizleri, VKİ ve yağ kütlesinin insülin direnci göstergeleri, trigliserid, CRP ve ALT düzeyleri ile pozitif; HDL kolesterol ve vücut suyu yüzdesi ile negatif ilişkili olduğunu göstermiştir.

Sonuç: Sonuç olarak, PCOS'ta metabolik bozulmanın şiddeti obezite ve artmış yağ kütlesi ile yakından ilişkilidir. Obezite, insülin direnci, dislipidemi ve inflamasyonun temel belirleyicilerinden biridir. Bu nedenle metabolik riskin azaltılması amacıyla PCOS yönetiminde vücut kompozisyonunun iyileştirilmesi büyük önem taşımaktadır.

Anahtar Sözcükler: Polikistik over sendromu, obezite, insülin direnci, vücut kompozisyonu, inflamasyon, lipid profili

INTRODUCTION

Polycystic ovary syndrome (PCOS) is a heterogeneous disorder characterized by ovulatory dysfunction and hyperandrogenism, with both metabolic and endocrine features. It is one of the most common hormonal disorders, affecting approximately 6%–20% of women worldwide. Most of the clinical manifestations of PCOS emerge during adolescence (1). The Rotterdam Criteria (2003) are currently the most widely accepted international diagnostic criteria for PCOS (2). According to these criteria, PCOS is diagnosed when at least two of the following are present: clinical or biochemical hyperandrogenism (hirsutism, androgenetic alopecia, acne, or elevated serum testosterone levels), oligo-ovulation or anovulation, and polycystic ovarian morphology on ultrasonography (3,4).

PCOS is a multifactorial syndrome that arises from the interaction of metabolic disturbances, genetic predisposition, environmental factors, and intrauterine developmental processes. Genetic and epigenetic mechanisms are considered major determinants of its etiology. Previous studies have shown that PCOS shares a common genetic background with obesity, insulin resistance (IR), type 2 diabetes, and cardiometabolic diseases (5). In addition, environmental factors such as obesity, IR, and inflammation may influence epigenetic regulation and contribute to the transgenerational transmission of the PCOS phenotype (6,7). In this context, obesity and IR are regarded not only as conditions that accompany PCOS but also as key factors that determine the clinical course and severity of PCOS.

The World Health Organization classifies a body mass index (BMI) of 18.5–24.9 kg/m^2 as normal weight, 25.0–29.9 kg/m^2 as overweight, and ≥30.0 kg/m^2 as obesity (8,9). Epidemiological data indicate that the prevalence of obesity among women with PCOS varies across regions. In Australia, the prevalence of obesity in women with PCOS has been reported as 47%, whereas in India, approximately 20.7% of women diagnosed with PCOS were found to be obese and 7.5% to be overweight (10,11). A systematic review including multiple countries showed that the prevalence of obesity in women with PCOS ranges from 38% to 50% (12).

The aim of this study was to compare body composition, IR, lipid profile, and inflammatory markers between obese and non-obese women with PCOS and to elucidate the impact of metabolic impairment on the relationship between PCOS and obesity.

MATERIALS AND METHODS

Study Design

A total of 120 women aged 18–40 years who presented to the Gynecology and Obstetrics Outpatient Clinic of Gazi University Faculty of Medicine were included in the study. The study included three groups: control (n = 40), obese PCOS (n = 40), and non-obese PCOS (n = 40).

PCOS was diagnosed according to the Rotterdam Criteria, and participants were classified based on BMI as obese (BMI ≥30 kg/m^2) or non-obese (BMI <25 kg/m^2).Overweight individuals with a BMI of 25.0–29.9 kg/m^2 were excluded from the study to preserve group homogeneity.

The control group consisted of healthy women who had regular menstrual cycles, normal ovarian morphology on ultrasonographic evaluation, no signs of hirsutism, acne, or alopecia, had not used oral contraceptives within the previous three months, and had no endocrinological disorders. Individuals who were pregnant or suspected to be pregnant; who had a diagnosis of Cushing syndrome, congenital adrenal hyperplasia, adrenal tumor, hyperprolactinemia, thyroid dysfunction, virilizing tumors, diabetes, hepatic or renal dysfunction, any malignancy, central nervous system disease, or hypertension; or were current smokers were excluded from the study across all groups.

Anthropometric Measurements and Biochemical Analyses

Anthropometric measurements, including BMI, height, body weight, body fat percentage, total fat mass, lean body mass, total body water, and body water percentage, were assessed by bioelectrical impedance analysis (BIA).

In blood samples obtained from the patients, levels of anti-Müllerian hormone (AMH), triglycerides (TG), low-density lipoprotein (LDL), high-density lipoprotein (HDL), total cholesterol, fasting glucose, fasting serum insulin, glycated hemoglobin (HbA1c), alanine aminotransferase (ALT), aspartate aminotransferase (AST), and C-reactive protein (CRP) were analyzed in the Medical Biochemistry Laboratory of Gazi University Faculty of Medicine Hospital. IR was calculated using the homeostatic model assessment of insulin resistance (HOMA-IR) formula: fasting glucose (mg/dL) × fasting insulin (μIU/mL)/405.

Serum AMH levels were analyzed using the electrochemiluminescence immunoassay method. TG levels were measured by the enzymatic colorimetric method, while HDL levels were determined by a photometric method. LDL cholesterol levels were calculated using the Friedewald formula when TG levels were below 400 mg/dL; when TG levels were above 400 mg/dL, LDL cholesterol levels were measured using a homogeneous enzymatic colorimetric method. HbA1c analyses were performed using high-performance liquid chromatography. CRP levels were analyzed using a nephelometric assay, whereas ALT and AST levels were measured using the kinetic photometric method.

Ethics Committee Approval

Ethical approval for this study was obtained from the Non-Interventional Clinical Research Ethics Committee of İzmir Bakırçay University (decision no: 1732, dated: 08.08.2024). Written informed consent was obtained from all participants.

Statistical Analysis

Differences among the groups were analyzed using the Kruskal–Wallis test. For multiple comparisons, Dunn's post-hoc pairwise comparisons were performed with Benjamini–Hochberg correction to control the probability of type I error. Associations among clinical, metabolic, and hormonal variables were evaluated using Spearman's rank correlation analysis, both across the entire sample and within each group, to examine group-specific patterns of relationships. All statistical analyses were conducted in the R software environment using RStudio and relevant R packages. A p-value of <0.05 was considered statistically significant.

RESULTS

Baseline and Anthropometric Characteristics

The analyses revealed statistically significant differences among the groups in anthropometric parameters. The obese PCOS group had significantly higher BMI, body weight, total fat mass, and body fat percentage than both the non-obese PCOS group and the control group ($p < 0.001$). Lean body mass and total body water were also higher in the obese PCOS group than in the other groups ($p < 0.001$), whereas the percentage of body water was significantly lower ($p < 0.001$). In contrast, no statistically significant differences were found between the control group and the non-obese PCOS group with respect to BMI, body weight, fat mass, body fat percentage, lean body mass, total body water, or body water percentage ($p > 0.05$) (Table 1).

Metabolic and Biochemical Parameters

When metabolic parameters were compared, fasting insulin and HOMA-IR levels were significantly higher in the obese PCOS group than in the other groups ($p < 0.001$). Additionally, HbA1c levels were found to be higher in the obese PCOS group compared with both the control group ($p < 0.01$) and the non-obese PCOS group ($p < 0.01$). Fasting glucose levels in the obese PCOS group were higher than those in both the control group ($p < 0.001$) and the non-obese PCOS group ($p = 0.02$). In addition, fasting glucose levels in the non-obese PCOS group were significantly higher than those in the control group ($p = 0.02$).

No statistically significant difference was found between the control and non-obese PCOS groups in terms of HDL cholesterol and TG levels. However, HDL cholesterol levels were significantly lower in the obese PCOS group than those in the other groups ($p < 0.001$), whereas TG levels were significantly higher ($p < 0.01$). No statistically significant differences were observed among the groups with respect to LDL cholesterol or total cholesterol levels.

When liver function parameters were examined, ALT levels were found to be significantly higher in the obese PCOS group than in the other groups. This difference was significant compared with those in both the control group ($p < 0.001$) and the non-obese PCOS group ($p = 0.02$). In contrast, no statistically significant differences in AST levels were observed among the groups. CRP levels were

Table 1. Demographic and anthropometric characteristics of the CONT, NON, and OBESE groups.

Variable	CONT (n = 40)	NON (n = 40)	OBESE (n = 40)
Age	23 (22-27)	23 (21–24.5)	27 (23–30)
Height (cm)	164.9 ± 5.0	162.1 ± 4.9	160.9 ± 6.2
Weight (kg)	59.4 ± 4.7	57.1 ± 7.4	84.8 ± 8.2
BMI (kg/m^2)	21.8 ± 1.4	21.7 ± 2.5	32.6 (30.6-34.5)
Body fat percent (%)	28.4 (25.45-30.78)	26.7 ± 5.4	41.4 ± 3.4
Body fat (kg)	16.7 ± 3.5	15.5 ± 4.7	35.2 ± 5.7
Lean mass (kg)	42.7 ± 2.3	41.7 ± 3.7	49.6 ± 3.7
Body water (kg)	31.3 ± 1.7	30.5 ± 2.5	36.5 (33.9–38.9)
Body water percent (%)	52.5 (50.7–54.51)	53.7 ± 3.9	42.8 (40.9–44.2)

Data are presented as mean ± standard deviation or median (minimum–maximum).
CONT: Control group, NON: Non-obese group, OBESE: Obese group, BMI: Body mass index.

significantly higher in the obese PCOS group than in both the control group ($p < 0.001$) and the non-obese PCOS group ($p < 0.001$). No significant difference in CRP levels was found between the control and non-obese PCOS groups. AMH levels were significantly higher in the non-obese PCOS group than in the control group ($p < 0.05$) (Figure 1, Tables 2 and 3).

No statistically significant differences were found among the groups in FSH, LH, LH/FSH ratio, or progesterone levels ($p > 0.05$).

The global significance profile of variables was evaluated across the control, non-obese, and obese groups. The dots represent the −log10-transformed p-values for each variable after Benjamini–Hochberg false discovery rate (FDR) correction. The vertical dashed line indicates the threshold for statistical significance (FDR-adjusted p = 0.05). Variables related to metabolic regulation, such as body weight, body fat parameters, BMI, indicators of IR, and lipid parameters, showed the most pronounced differences among the groups, whereas no statistically significant differences were observed for some hormonal and biochemical markers (Figure 2).

The distribution of anthropometric and metabolic parameters in the control, non-obese, and obese groups is presented using box plots. The graphs illustrate the distributional characteristics of anthropometric, metabolic, and hormonal variables across the study groups. Overall group differences were analyzed using the Kruskal–Wallis test, and Dunn's post hoc pairwise comparisons were performed with Benjamini–Hochberg correction for multiple testing. Compared with the control and non-obese groups, the obese group had lower HDL cholesterol levels and body water percentage, but higher BMI, body fat mass, body fat percentage, insulin, HOMA-IR, TG, CRP, ALT, and body weight. Statistically significant pairwise comparisons are indicated by asterisks (*$p < 0.05$, **$p < 0.01$, ***$p < 0.001$) (Figure 3).

The Spearman correlation structure among anthropometric, metabolic, and hormonal parameters was evaluated in the entire sample. In the Spearman correlation heatmap, which visualizes anthropometric, metabolic, biochemical, and hormonal variables using hierarchical clustering, color intensity represents the direction and strength of correlations (red: positive; blue: negative).

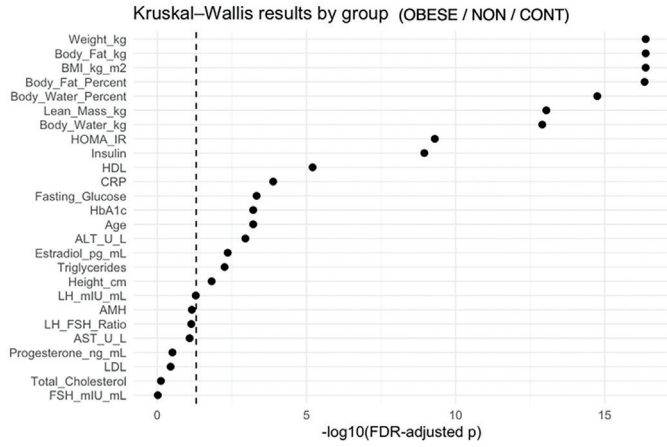

Figure 1. Global significance profile of variables across the CONT, NON, and OBESE groups.

CONT: Control group, NON: Non-obese group, OBESE: Obese group.

Table 2. Comparison of metabolic, biochemical, and hormonal parameters among the CONT, NON, and OBESE groups.

Variable	CONT (n = 40)	NON (n = 40)	OBESE (n = 40)
Fasting glucose (mg/dL)	78.5 ± 7.6	82.3 ± 6.3	86.3 ± 8.4
Insulin (µU/mL)	8.1 ± 3.6	8.6 (5.6–11.1)	15.4 (10.7–22)
HOMA-IR	1.6 ± 0.7	1.8 (1.1–2.3)	3.1 (2.3–4.9)
HbA1c (%)	5.1 ± 0.3	5.2 ± 0.3	5.4 (5.2–5.6)
Triglycerides (mg/dL)	68 (56.1–87.7)	64.5 (58.1–92.2)	87.1 (76.2–104)
Total cholesterol (mg/dL)	167.2 ± 24.2	171.9 ± 20.8	172.1 ± 33.9
LDL (mg/dL)	93.2 ± 18.9	92.7 ± 17.3	99.2 ± 24.6
HDL (mg/dL)	60.1 ± 9.0	63.9 ± 13.4	49.7 ± 11.8
AMH (ng/mL)	2.5 (1.8–4.5)	4.0 (2.9–6.3)	3.9 (1.7–5.4)
CRP (mg/dL)	2.5 (2.5–2.5)	2.5 (2.5–2.5)	2.5 (2.5–5.2)
ALT (U/L)	14 (11.8–20)	16.1 (13–22.7)	21.2 (14.7–29.2)
AST (U/L)	16.5 (15.1–20.6)	18.4 (17–22.2)	19.1 (16.8–21.1)
LH (mIU/mL)	9.1 (5.4–11.6)	14.4 (7.8–20.3)	8.7 (4.8–16.6)
FSH (mIU/mL)	4.8 (4.0–6.7)	5.4 ± 2.1	5.3 ± 2.0
LH/FSH ratio	1.8 (1.2–2.2)	2.7 (1.7–3.6)	2.1 ± 1.1
Progesterone (ng/mL)	0.6 (0.2–3.8)	0.3 (0.1–1.5)	0.3 (0.1–1.7)
Estradiol (pg/mL)	101.9 (59.2–181.5)	73.4 (49.5–123)	51.1 (32.3–79.8)

Data are presented as mean ± standard deviation or median (minimum–maximum).
CONT: Control group, NON: Non-obese group, OBESE: Obese group, BMI: Body mass index, HOMA-IR: Homeostatic model assessment of insulin resistance, HbA1c: Glycated hemoglobin, LDL: Low-density lipoprotein, HDL: High-density lipoprotein, AMH: Anti-Müllerian hormone, CRP: C-reactive protein, ALT: Alanine aminotransferase, AST: Aspartate aminotransferase, LH: Luteinizing hormone, FSH: Follicle-stimulating hormone.

Hierarchical clustering analysis revealed that BMI, body fat mass, insulin, HOMA-IR, TG, and CRP levels were strongly positively correlated with one another, whereas these variables were negatively correlated with HDL cholesterol and body water percentage. In contrast, hormonal parameters exhibited weaker interrelationships and formed a relatively independent cluster separate from the metabolic indicators.

DISCUSSION

PCOS is one of the most common endocrine disorders in women of reproductive age and a complex metabolic and endocrine condition characterized by hyperandrogenism, ovulatory dysfunction, and polycystic ovarian morphology. However, PCOS is not limited to the reproductive system; it is also closely associated with various metabolic disturbances, including IR, obesity, dyslipidemia, and chronic low-grade inflammation. The findings of the present study indicate that the metabolic impairments observed in women with PCOS are largely associated with increased fat mass and obesity. The current literature also reports that the prevalence of obesity, particularly visceral/abdominal adiposity, is higher in women with PCOS than in healthy individuals, and that this higher prevalence markedly worsens the cardiometabolic risk profile. Obesity is considered a major determinant in the pathophysiology of PCOS, and increased visceral adiposity has been suggested to impair insulin signaling, thereby accelerating the development of metabolic complications such as IR and dyslipidemia (13). In addition, adipokines and proinflammatory cytokines secreted by increased adipose tissue are reported to play an important role in the disruption of metabolic and hormonal balance, promoting chronic low-grade inflammation through elevations in inflammatory markers such as CRP (14). These inflammatory processes are thought to adversely affect insulin signaling pathways and to play a critical role in the development of IR and the progression of metabolic dysfunction. Therefore, the combined evaluation of body composition and hormonal and metabolic parameters in individuals with PCOS is important to better understand the metabolic consequences of the disorder and the underlying pathophysiological mechanisms.

Table 3. Significant pairwise comparisons of biochemical and hormonal parameters between groups.

Variables	Groups	p-value
Fasting glucose (mg/dL)	CONT-NON	$p < 0.05$
Fasting glucose (mg/dL)	CONT-OBESE	$p < 0.001$
Fasting glucose (mg/dL)	NON-OBESE	$p < 0.05$
Insulin (µU/mL)	CONT-OBESE	$p < 0.001$
Insulin (µU/mL)	NON-OBESE	$p < 0.001$
HOMA-IR	CONT-OBESE	$p < 0.001$
HOMA-IR	NON-OBESE	$p < 0.001$
HbA1c (%)	CONT-OBESE	$p < 0.001$
HbA1c (%)	NON-OBESE	$p < 0.01$
Triglycerides (mg/dL)	CONT-OBESE	$p < 0.01$
Triglycerides (mg/dL)	NON-OBESE	$p < 0.01$
HDL (mg/dL)	CONT-OBESE	$p < 0.001$
HDL (mg/dL)	NON-OBESE	$p < 0.001$
AMH (ng/mL)	CONT-NON	$p < 0.05$
CRP (mg/dL)	CONT-OBESE	$p < 0.001$
CRP (mg/dL)	NON-OBESE	$p < 0.001$
ALT (U/L)	CONT-OBESE	$p < 0.001$
ALT (U/L)	NON-OBESE	$p < 0.05$
Estradiol (pg/mL)	CONT-OBESE	$p < 0.01$
Estradiol (pg/mL)	NON-OBESE	$p < 0.05$

HOMA-IR: Homeostatic model assessment of insulin resistance, HbA1c: Glycated hemoglobin, LDL: Low-density lipoprotein, HDL: High-density lipoprotein, AMH: Anti-Müllerian hormone, CRP: C-reactive protein, ALT: Alanine aminotransferase, CONT: Control group, NON: Non-obese group, OBESE: Obese group.

In our study, which used BIA, body weight, BMI, total fat mass, and body fat percentage were significantly higher in the obese PCOS group than in the other groups. In addition, lean body mass and total body water were higher in the obese PCOS group, whereas body water percentage was lower in that group. The markedly elevated fat mass and body fat percentage observed in the obese PCOS group are consistent with previous studies in the literature (15-17). In line with our classification criteria, and given that the non-obese PCOS and control groups had similar BMI and body weight, no significant differences were found between the groups in fat mass or body fat percentage. Similarly, other studies comparing healthy women and non-obese women with PCOS have reported no significant differences in fat mass or body fat percentage (18). These findings suggest that obesity, independent of PCOS, has a substantial effect on body composition. The results presented in Figure 1 further demonstrate that the differences among the groups were largely driven by variables related to body composition, IR, and lipid metabolism.

IR is one of the key pathophysiological mechanisms associated with both obesity and PCOS. In our study, levels of fasting insulin, HOMA-IR, fasting glucose, and HbA1c were significantly higher in the obese PCOS group than in both the non-obese PCOS group and the control group. In addition, fasting glucose levels were significantly higher in all PCOS groups than in healthy controls. The literature indicates that, in the presence of PCOS, obesity contributes to increases in fasting insulin, HOMA-IR, fasting glucose, and HbA1c levels (15-21). Consistent with previous reports, fasting insulin and HOMA-IR values were higher in the non-obese PCOS group than in the control group, although this difference did not reach statistical significance ($p > 0.05$) (15,17,18). These findings suggest that, in addition to PCOS itself, obesity plays a determining role in the severity of IR.

In obese individuals, prolonged sedentary behavior and low levels of physical activity adversely affect lipid metabolism. Increased sedentary time has been reported to be particularly associated with decreased HDL cholesterol levels and increased TG levels (22,23). In the systematic review and meta-analysis conducted by Isayeva et al. (22), sedentary lifestyle duration was reported to be associated with abdominal obesity, dyslipidemia, and low HDL cholesterol levels. The authors emphasized that low physical activity negatively affects lipid metabolism and increases metabolic risk (22). Similarly, in the review by Silveira et al. (23), a sedentary lifestyle was reported to be associated with obesity and IR, as well as decreased HDL levels and increased TG levels.

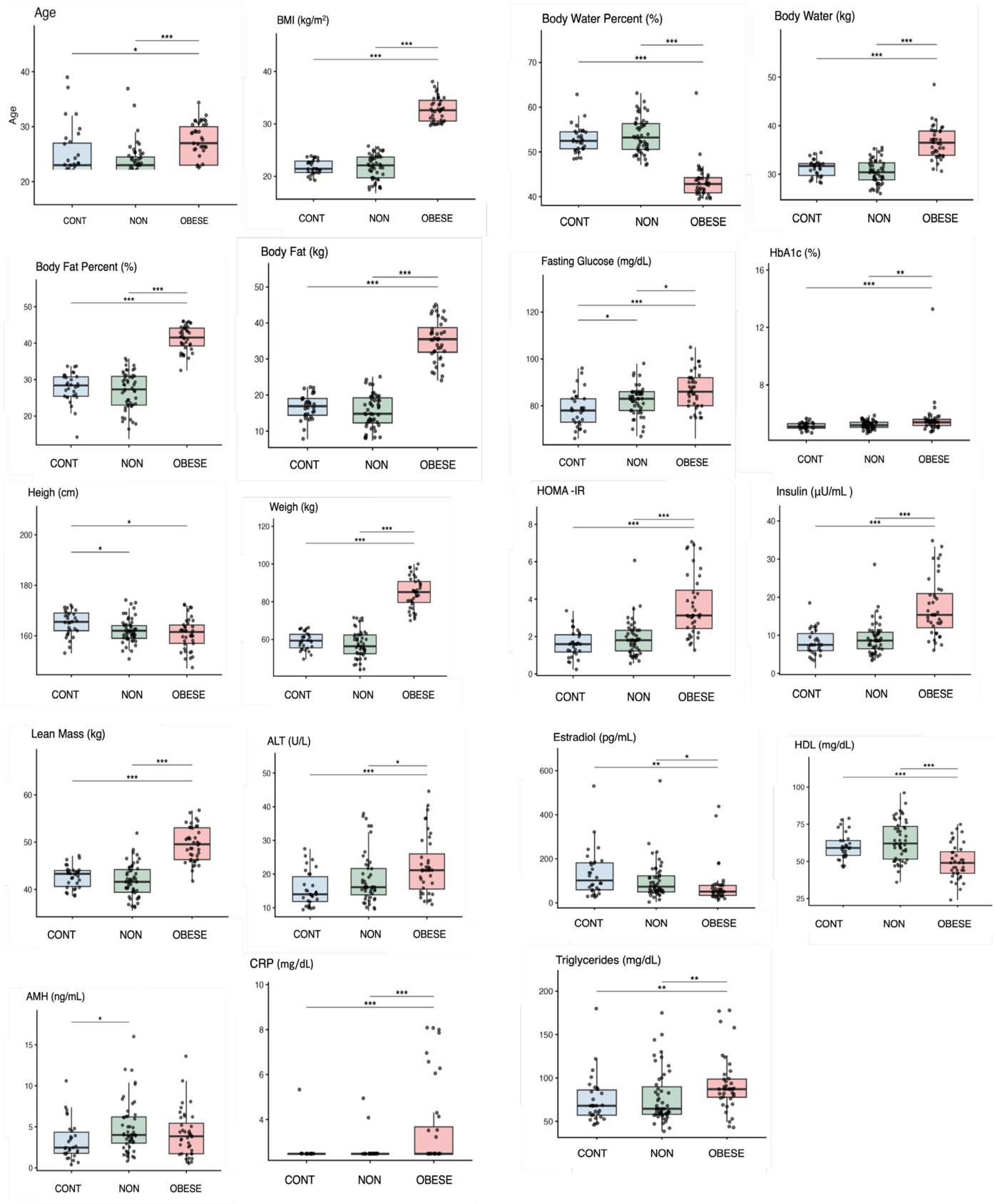

Figure 2. Distribution of anthropometric and metabolic parameters in the CONT, NON, and OBESE groups.

CONT: Control group, NON: Non-obese group, OBESE: Obese group.

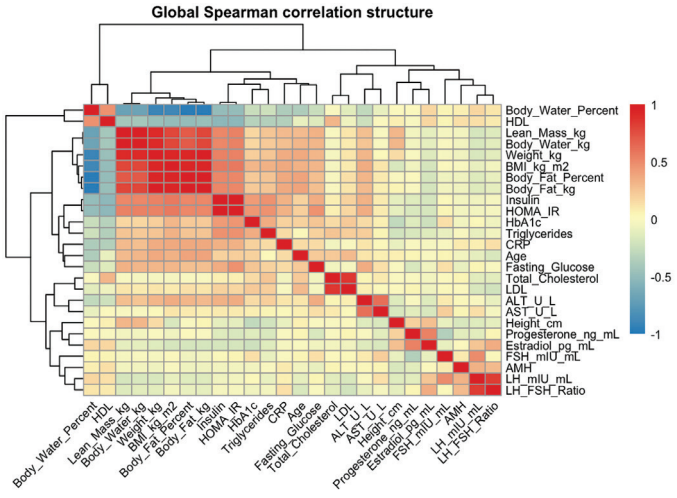

Figure 3. Spearman correlation structure among anthropometric, metabolic, and hormonal parameters in the entire sample.

In our study, HDL cholesterol levels were significantly lower and TG levels were significantly higher in the obese PCOS group than in the other groups. No significant differences were observed among the groups with respect to LDL or total cholesterol levels. Our findings are supported by previous studies reporting lower HDL levels and higher TG levels in individuals with obese PCOS (19,24).

The markedly elevated CRP levels observed in the obese PCOS group may reflect obesity-associated chronic inflammation, given that no significant difference in CRP was found between healthy women and the non-obese PCOS group. Previous studies have likewise reported elevated CRP levels in patients with obese PCOS (21,25). When ALT and AST levels were examined, both parameters were higher in the obese PCOS group; however, the increase was statistically significant only for ALT. The absence of a significant difference in AST levels does not suggest marked hepatocellular injury. No statistically significant differences were found among the groups in terms of FSH, LH, LH/FSH ratio, or progesterone levels.

Correlation analyses showed that BMI and body weight were positively and significantly associated with fat mass, body fat percentage, fasting insulin, HOMA-IR, HbA1c, TG levels, ALT, and CRP levels, and negatively associated with HDL cholesterol and body water percentage.

CONCLUSION

This study demonstrates that metabolic disturbances in PCOS are strongly associated with obesity and increased fat mass. The obese PCOS group exhibited a clearly more unfavorable profile in terms of body composition parameters, markers of IR, and lipid profile, and elevated inflammatory markers. In contrast, no significant differences were observed between the non-obese PCOS group and healthy controls in many metabolic parameters.

The findings of this study indicate that obesity is not merely a condition accompanying PCOS, but also one of the key determinants of the metabolic severity of the disorder. Therefore, we believe that strategies aimed at improving body composition should play a critical role in the management of PCOS, particularly in preventing metabolic complications such as IR, dyslipidemia, and inflammation.

Ethics

Ethics Committee Approval: Ethical approval for this study was obtained from the Non-Interventional Clinical Research Ethics Committee of İzmir Bakırçay University (decision no: 1732, dated: 08.08.2024).

Informed Consent: Written informed consent was obtained from all participants.

Footnotes

Authorship Contributions

Concept: S.E.K., M.K., C.K., Design: S.E.K., C.K., Data Collection or Processing: S.E.K., C.K., N.C., M.D., L.N.N., Analysis or Interpretation: S.E.K., L.N.N., C.K., Literature Search: S.E.K., C.K., Writing: S.E.K., L.N.N., C.K.

Conflict of Interest: No conflict of interest was declared by the authors.

Financial Disclosure: The authors declared that this study received no financial support.

REFERENCES

1. Siddiqui S, Mateen S, Ahmad R, Moin S. A brief insight into the etiology, genetics, and immunology of polycystic ovarian syndrome. J Assist Reprod Genet. 2022; 39: 2439-73.
2. Rotterdam ESHRE/ASRM-Sponsored PCOS Consensus Workshop Group. Revised 2003 consensus on diagnostic criteria and long-term health risks related to polycystic ovary syndrome. Hum Reprod. 2004; 19: 41-7.
3. Teede HJ, Tay CT, Laven JJE, Dokras A, Moran LJ, Piltonen TT, et al. Recommendations from the 2023 international evidence-based guideline for the assessment and management of polycystic ovary syndrome. J Clin Endocrinol Metab. 2023; 108: 2447-69.
4. World Health Organization. Polycystic ovary syndrome. Geneva: World Health Organization; 2026 Jan 22. Available from: https://www.who.int/news-room/fact-sheets/detail/polycystic-ovary-syndrome
5. Day FR, Hinds DA, Tung JY, Stolk L, Styrkarsdottir U, Saxena R, et al. Causal mechanisms and balancing selection inferred from genetic associations with polycystic ovary syndrome. Nat Commun. 2015; 6: 8464.
6. Diamanti-Kandarakis E, Dunaif A. Insulin resistance and the polycystic ovary syndrome revisited: an update on mechanisms and implications. Endocr Rev. 2012; 33: 981-1030.
7. Rattan S, Flaws JA. The epigenetic impacts of endocrine disruptors on female reproduction across generations. Biol Reprod. 2019; 101: 635-44.
8. Tvºrkiye Endokrinoloji ve Metabolizma Dernefüi. Obezite tanf± ve tedavi kf±lavuzu. Ankara: Tvºrkiye Endokrinoloji ve Metabolizma Dernefüi; 2019.
9. World Health Organization. Obesity and overweight. Geneva: World Health Organization; 2025 Dec 8. Available from: https://www.who.int/news-room/fact-sheets/detail/obesity-and-overweight
10. Joshi B, Mukherjee S, Patil A, Purandare A, Chauhan S, Vaidya R. A cross-sectional study of polycystic ovarian syndrome among

adolescent and young girls in Mumbai, India. Indian J Endocrinol Metab. 2014; 18: 317-24.

11. Tay CT, Loxton D, Bahri Khomami M, Teede H, Harrison CL, Joham AE. High prevalence of medical conditions and unhealthy lifestyle behaviours in women with PCOS during preconception. Hum Reprod. 2023; 38: 2267-76.
12. Lim SS, Davies MJ, Norman RJ, Moran LJ. Overweight, obesity and central obesity in women with polycystic ovary syndrome: a systematic review and meta-analysis. Hum Reprod Update. 2012; 18: 618-37.
13. Kim JJ. Obesity and polycystic ovary syndrome. J Obes Metab Syndr. 2024; 33: 239-45.
14. Koleva-Tyutyundzhieva D, Ilieva-Gerova M, Deneva T, Orbetzova M. Metabolic and inflammatory adipokine profiles in PCOS: a focus on adiposity, insulin resistance, and atherogenic risk. Int J Mol Sci. 2025; 26: 9702.
15. Cassar S, Teede HJ, Moran LJ, Joham AE, Harrison CL, Strauss BJ, et al. Polycystic ovary syndrome and anti-Mullerian hormone: role of insulin resistance, androgens, obesity and gonadotrophins. Clin Endocrinol (Oxf). 2014; 81: 899-906.
16. GonzV°lez F, Kirwan JP, Rote NS, Minium J. Glucose ingestion stimulates atherothrombotic inflammation in polycystic ovary syndrome. Am J Physiol Endocrinol Metab. 2013; 304: E375-83.
17. GonzV°lez F, Kirwan JP, Rote NS, Minium J. Evidence of mononuclear cell preactivation in the fasting state in polycystic ovary syndrome. Am J Obstet Gynecol. 2014; 211: 635.e1-7.
18. Aydin K, Cinar N, Aksoy DY, Bozdag G, Yildiz BO. Body composition in lean women with polycystic ovary syndrome: effect of ethinyl estradiol and drospirenone combination. Contraception. 2013; 87: 358-62.
19. Patwari P, Batra N, Sen K, Saha A, Kumari B, Basu M, et al. Nonobese PCOS compared to obese PCOS have similar clinical presentation, hormonal profile, and insulin resistance. Clin Endocrinol (Oxf). 2025; 103: 567-79.
20. Liang Y, Ming Q, Liang J, Zhang Y, Zhang H, Shen T. Gut microbiota dysbiosis in polycystic ovary syndrome: association with obesity. Can J Physiol Pharmacol. 2020; 98: 803-9.
21. Huddleston HG, Quinn MM, Kao C, Lenhart N, Rosen MP, Cedars MI. Women with polycystic ovary syndrome demonstrate worsening markers of cardiovascular risk over the short term despite declining hyperandrogenaemia. Clin Endocrinol (Oxf). 2017; 87: 775-82.
22. Isayeva AS, Vovchenko MM, Petyunina OV. Sedentary lifestyle attenuates positive metabolic effect of regular physical exercise. J Endocrinol Metab. 2022; 12: 59-65.
23. Silveira EA, MendonVßa CR, Delpino FM, Souza GVE, Rosa LPS, Oliveira C, et al. Sedentary behavior, physical inactivity, abdominal obesity and obesity in adults and older adults. Clin Nutr ESPEN. 2022; 50: 63-73.
24. Usta A, Avci E, Bulbul CB, Kadi H, Adali E. The monocyte count to HDL cholesterol ratio in obese and lean patients with polycystic ovary syndrome. Reprod Biol Endocrinol. 2018; 16: 34.
25. Sarray S, Almawi WY. Levels of CD40L and other inflammatory biomarkers in obese and non-obese women with polycystic ovary syndrome. Am J Reprod Immunol. 2016; 76: 285-91.

Original Investigation | Özgün Araştırma

Gazi Med J 2026;37(3):419-427

DOI: http://dx.doi.org/10.12996/gmj.2026.4707

Risky Social Media Use, Fear of Missing Out, Psychological Distress, and Social Media Use Motivations: A Cross-Sectional Study

Riskli Sosyal Medya Kullanımı, Gelişmeleri Kaçırma Korkusu, Psikolojik Sıkıntı ve Sosyal Medya Kullanım Motivasyonları: Kesitsel Bir Çalışma

Hasan Ünver[1], Mehmet Rıdvan Varlı[1], Azat Duman[2], Fatih Yığman[3]

[1]Department of Psychiatry, University of Health Sciences Türkiye, Ankara Etlik City Hospital, Ankara, Türkiye
[2]Clinic of Child and Adolescent Psychiatry, Erciş Şehit Rıdvan Çevik State Hospital, Van, Türkiye
[3]Department of Psychiatry, Yüksek İhtisas University Faculty of Medicine, Ankara, Türkiye

ABSTRACT

Objective: Risky social media use is related to fear of missing out (FoMO) and psychological distress, but the role of specific use motivations remains less clear. This study compares FoMO, psychological distress, and motivations for social media use between individuals with risky social media use and those without.

Methods: This cross-sectional online study included 349 adult social media users. Participants completed the Bergen Social Media Addiction Scale (BSMAS), FoMO, Depression Anxiety Stress Scale-21, and Social Media Use Motivations Scale. Risky social media use was defined as a BSMAS score of ≥19. Group comparisons and correlation analyses were conducted.

Results: Participants with risky social media use had higher FoMO, depression, anxiety, and stress scores, and higher scores on most motivation measures. Information-seeking motivation did not differ between groups and was not correlated with BSMAS scores.

CONCLUSION: Risky social media use was more closely related to FoMO, psychological distress, and social-emotional motives than to information seeking.

Keywords: Risky social media use, FoMO, psychological distress, social media use motivations, depression, anxiety

ÖZ

Amaç: Riskli sosyal medya kullanımı, gelişmeleri kaçırma korkusu (FoMO) ve psikolojik sıkıntı ile ilişkilidir; ancak belirli kullanım motivasyonlarının rolü daha az açıktır. Bu çalışma, riskli sosyal medya kullanımı olan ve olmayan bireyler arasında FoMO, psikolojik sıkıntı ve sosyal medya kullanım motivasyonlarını karşılaştırmayı amaçlamaktadır.

Yöntemler: Kesitsel desenli bu çevrim içi çalışmaya 349 yetişkin sosyal medya kullanıcısı dahil edilmiştir. Katılımcılar Bergen Sosyal Medya Bağımlılığı Ölçeği (BSMAS), FoMO Ölçeği, Depresyon Anksiyete Stres Ölçeği-21 ve Sosyal Medya Kullanım Motivasyonları Ölçeği'ni doldurmuştur. Riskli sosyal medya kullanımı, BSMAS puanının ≥19 olması olarak tanımlanmıştır. Grup karşılaştırmaları ve korelasyon analizleri yapılmıştır.

Bulgular: Riskli sosyal medya kullanımı olan katılımcıların FoMO, depresyon, anksiyete ve stres puanları ile çoğu motivasyon ölçümünden aldıkları puanlar daha yüksektir. Bilgi arama motivasyonu gruplar arasında farklılık göstermemiş ve BSMAS puanlarıyla ilişkili bulunmamıştır.

Sonuç: Riskli sosyal medya kullanımı, bilgi aramadan ziyade FoMO, psikolojik sıkıntı ve sosyal-duygusal motivasyonlarla daha yakından ilişkili bulunmuştur.

Anahtar Sözcükler: Riskli sosyal medya kullanımı, FoMO, psikolojik sıkıntı, sosyal medya kullanım motivasyonları, depresyon, anksiyete

Cite this article as: Ünver H, Varlı MR, Duman A, Yığman F. Risky social media use, fear of missing out, psychological distress, and social media use motivations: a cross-sectional study. Gazi Med J. 2026;37(3):419-427

Address for Correspondence/Yazışma Adresi: Hasan Ünver, Department of Psychiatry, University of Health Sciences Türkiye, Ankara Etlik City Hospital, Ankara, Türkiye
E-mail / E-posta: hasanunver.1989@gmail.com
ORCID ID: orcid.org/0000-0001-5392-5507

Received/Geliş Tarihi: 08.05.2026
Accepted/Kabul Tarihi: 01.06.2026
Publication Date/Yayınlanma Tarihi: 10.07.2026

INTRODUCTION

Social media platforms have become an important part of everyday life, serving multiple functions such as facilitating communication and entertainment, enabling self-expression, supporting information-seeking, and maintaining social relationships. Although social media use may facilitate social connection and access to information, excessive or poorly regulated use may be related to difficulties controlling online behavior and negative consequences for daily functioning. Problematic or risky patterns of social media use are often conceptualized through behavioral addiction models. Within this approach, such use is characterized by core features such as excessive preoccupation with social media, using it to regulate mood, needing increasing engagement over time, discomfort when access is restricted, use-related conflicts, and repeated unsuccessful attempts to reduce use (1,2). In this regard, risky social media use does not necessarily indicate a formal psychiatric diagnosis, but rather refers to a pattern of use that may be related to psychological vulnerability and impaired self-regulation.

Previous studies have widely investigated fear of missing out (FoMO) as a psychological factor associated with problematic patterns of social media use. This term describes individuals' apprehension that others are participating in enjoyable or meaningful experiences without them, accompanied by a persistent need to stay informed about others' activities through ongoing social connection (3). Social media platforms may intensify this experience by providing continuous exposure to others' activities, relationships, achievements, and social events. Existing evidence indicates that higher FoMO is associated with greater social media engagement and a greater tendency toward problematic use (4). In addition, FoMO was linked to psychological distress and maladaptive online behaviors, suggesting that the desire to remain socially updated may contribute to repetitive checking and difficulty disengaging from social media platforms (5,6).

Risky social media use is related to several indicators of emotional strain, including depressive and anxiety symptoms as well as perceived stress. However, this relationship is unlikely to follow a simple one-way pattern. Instead, social media involvement and psychological distress may influence each other through multiple, partly overlapping mechanisms. Individuals experiencing distress may use social media for distraction, reassurance, social contact, or emotion regulation. Conversely, excessive use may increase exposure to social comparison, perceived exclusion, sensitivity to online feedback, and interpersonal stressors, all of which may contribute to negative emotional states. Therefore, examining depression, anxiety, and stress together may provide a broader understanding of the emotional correlates of risky social media use.

In addition to psychological distress, the motivations underlying social media use may help distinguish adaptive or instrumental use from riskier patterns. From a uses and gratifications perspective, individuals may use social media to satisfy various psychological and social needs, including social interaction, entertainment, self-presentation, information seeking, and relationship maintenance (7). These motives may not have the same relationship with risky use. For example, socially driven motives, such as maintaining connection, seeking social recognition, monitoring others, or expressing oneself, may be more closely related to FoMO and emotional distress than instrumental motives, such as obtaining information. The Scale of Motives for Using Social Networking Sites (SMU-SNS) was designed to measure different reasons for engaging with social networking platforms. It covers nine motivational domains: romantic or flirting-related use, forming new friendships, academic use, preserving social ties, observing others' activities, entertainment, gaining social approval, self-presentation, and obtaining information (8).

Previous studies largely focused on the links among problematic social media use, FoMO, and psychological distress. However, relatively little attention has been paid to how these factors operate alongside specific and multidimensional motives for social media use. This distinction is important because similar levels of social media engagement may reflect different underlying motives and may not carry the same psychological meaning. A more detailed motivational approach may therefore contribute to a better understanding of why some individuals show riskier social media use patterns.

This study aims to compare individuals with and without risky social media use with respect to FoMO, psychological distress, and motivations for social media use. This study hypothesized that individuals with risky social media use would report higher FoMO and psychological distress scores and stronger motivations for social media use than individuals without risky social media use. In addition, this study explored whether specific motivational dimensions, including social/interpersonal and information-seeking motivations, differed in their association with risky social media use.

MATERIALS AND METHODS

Study Design and Sample

The study data were collected via a web-based survey between February and March 2025. The sample consists of adult social media users who were reached via Instagram, X, and TikTok. The survey package included online informed consent, a sociodemographic questionnaire, and self-report measures evaluating risky social media use, FoMO, psychological distress, and motives for social media use. After eligibility screening and data cleaning, 349 participants remained in the analytic sample.

Inclusion criteria were: age 18–65 years, use of social media, ability to read and understand the survey content, and provision of voluntary consent to participate in this study. Exclusion criteria were: self-reported past psychiatric disorders, current psychotropic medication use, any medical or neurological condition that could impair capacity to provide informed consent or affect reality testing, and incomplete questionnaires. No structured psychiatric interview was conducted. Instead, psychiatric eligibility was assessed during the collection of sociodemographic data, and participants reporting a previous psychiatric disorder or current psychotropic medication use were excluded.

Ethical Approval and Procedure

Ethical approval was obtained from the University of Health Sciences Türkiye, Ankara Etlik City Hospital's Institutional Ethics Committee (approval number: AEŞH-BADEK-2025-0083; dated 29.01.2025), and the study procedures were conducted in line with the Declaration of Helsinki. Participants were invited to take part in this study through online announcements posted on social media platforms. Before

completing the survey, all participants were informed about the study objectives and provided online informed consent. Participation was voluntary, and participants completed the questionnaires anonymously.

Measures

Sociodemographic Data Form

Participant characteristics were recorded using a form prepared by the research team. The form collected information on demographic variables, including gender, age, educational level, employment status, marital status, and perceived economic status, living arrangements, psychiatric and medical history, family history of psychiatric or medical conditions, medication use, daily screen exposure, duration of social media use, and the most commonly used platform.

Bergen Social Media Addiction Scale (BSMAS)

The BSMAS was used to assess risky social media use patterns. This instrument was originally introduced by Andreassen et al. (9) and later validated in Turkish by Demirci (10). The Turkish version includes six questions addressing key behavioral addiction features related to social media use, namely salience, mood modification, tolerance, withdrawal, conflict, and relapse. Each item is scored using a five-point Likert scale. The overall score ranges from 6 to 30, with higher scores indicating greater severity of problematic social media use.

Participants were grouped based on their BSMAS total scores. A score of ≥19 was used to define the risky social media use group, while participants scoring below 19 were placed in the non-risky use group. The threshold of 19 was adopted from Bányai et al. (11), who identified this value through latent profile analysis as an appropriate cut-off for detecting individuals vulnerable to problematic social media use.

Fear of Missing Out Scale

FoMO was assessed using the Turkish version of the FoMO adapted to the social media context by Çelik and Özkara (12). This scale measures FoMO related to social media use and includes personal and social FoMO dimensions. In the present study, personal, social, and total FoMO scores were used in the analysis. Higher scores indicate a higher level of FoMO.

Depression Anxiety Stress Scale-21 (DASS-21)

Psychological distress was evaluated using the Turkish adaptation of the DASS-21, the validity of which was reported by Yılmaz et al. (13). This 21-item measure provides separate scores for depressive, anxiety, and stress symptoms, with seven items allocated to each domain. Responses are given using a four-point Likert format. No items are reverse-scored, and higher scores indicate greater symptom severity.

Social Media Use Motivations Scale

Motivations for social media use were examined using the Turkish adaptation of the SMU-SNS. The original instrument, developed by Pertegal et al. (8), measures the reasons individuals engage with social networking platforms within the uses and gratifications approach. The original form consists of 27 items grouped into nine subdimensions: flirting, making new friends, academic purposes, maintaining social connectedness, following and monitoring others, entertainment, seeking social recognition, self-expression, and seeking information.

It was adapted to Turkish by Dölay (14). In the present study, the nine motivational dimensions were evaluated separately. Items are rated on a 7-point Likert-type scale, with higher scores indicating stronger motivation in the corresponding dimension.

Statistical Analysis

Statistical analyses were performed using IBM SPSS Statistics for Windows, version 22.0 (IBM Corp., Armonk, NY, USA). For descriptive reporting, continuous variables were presented as means and standard deviations, while categorical variables were summarized using counts and percentages.

Participants were divided into two groups based on the BSMAS cut-off score: those below the risky-use threshold and those meeting the risky-use threshold. The distribution of continuous variables was assessed using histograms, Q-Q plots, and skewness and kurtosis values. An independent-samples t-test was used to compare continuous variables between groups, and chi-square tests were used for categorical comparisons. Fisher's exact test was employed when expected cell counts were low.

Pearson's correlation analysis was employed to examine the relationships among risky social media use severity, FoMO, depression, anxiety, stress, and social media use motivations. All analyses were two-tailed, and statistical significance was set at $p < 0.05$.

RESULTS

The final analysis included 349 participants. Based on the predetermined BSMAS cut-off value, 223 participants were assigned to the non-risky social media use group, whereas 126 participants met the criterion for risky social media use.

Sociodemographic Characteristics

The mean age of participants without risky social media use was 34.78 ± 10.40 years, whereas that of those with risky social media use was 30.47 ± 9.77 years. Participants with risky social media use were significantly younger than those without [$t(347) = 3.802$, $p < 0.001$].

Gender distribution differed significantly between the groups [$\chi^2(1) = 6.245$, $p = 0.012$]. The proportion of women was higher in the risky social media use group than in the non-risky social media use group (66.7% vs. 52.9%, respectively).

Employment status also differed significantly between the groups [$\chi^2(3) = 11.441$, $p = 0.010$]. The risky social media use group had a lower proportion of employed participants and a higher proportion of students than the non-risky social media use group. Specifically, 66.7% of the risky use group were employed compared to 79.8% of the non-risky use group; 19.8% of the risky use group were students compared to 9.9% of the non-risky use group.

No significant group differences were found in marital status [$\chi^2(2) = 2.627$, $p = 0.269$], educational level [$\chi^2(3) = 2.142$, $p = 0.544$], perceived economic status [$\chi^2(2) = 4.985$, $p = 0.083$], living arrangement [$\chi^2(5) = 6.966$, $p = 0.223$], or most frequently used social media platform [$\chi^2(3) = 6.375$, $p = 0.095$].

Comparison of FoMO, Psychological Distress, and Social Media Use Motivations

As anticipated, participants in the risky social media use group had markedly higher BSMAS scores than those in the non-risky group [$t(347) = -25.679$, $p < 0.001$].

FoMO scores were significantly higher among participants with risky social media use. Personal FoMO scores [15.01 ± 7.04 vs. 9.00 ± 4.69, $t(309) = -9.011$, $p < 0.001$], social FoMO scores [7.84 ± 5.08 vs. 5.71 ± 3.12, $t(333) = -4.752$, $p < 0.001$], and total FoMO scores [22.31 ± 10.78 vs. 14.62 ± 6.77, $t(303) = -7.634$, $p < 0.001$] were higher in the risky use group than in the non-risky use group.

Psychological distress scores were significantly higher among participants in the risky social media use group. Specifically, depression scores were higher in this group compared to participants in the non-risky use group [6.95 ± 4.17 vs. 3.95 ± 3.74, $t(347) = -6.906$, $p < 0.001$].

Table 1. Sociodemographic characteristics by risky social media use.

Variable	No risky use, (n = 223)	Risky use, (n = 126)	χ^2/t	df	p-value
Age (years), mean (SD)	34.78 (10.40)	30.47 (9.77)	3.802	347	<0.001
Gender, n (%)			6.245	1	0.012
Female	118 (52.9)	84 (66.7)			
Male	105 (47.1)	42 (33.3)			
Marital status, n (%)			2.627	2	0.269
Single	112 (50.2)	72 (57.1)			
Married	102 (45.7)	52 (41.3)			
Other	9 (4.0)	2 (1.6)			
Education, n (%)			2.142	3	0.544
Primary education	2 (0.9)	1 (0.8)			
High school	15 (6.7)	8 (6.3)			
University	126 (56.5)	81 (64.3)			
Postgraduate	80 (35.9)	36 (28.6)			
Employment status, n (%)			11.441	3	0.010
Not working	15 (6.7)	15 (11.9)			
Working	178 (79.8)	84 (66.7)			
Student	22 (9.9)	25 (19.8)			
Retired	8 (3.6)	2 (1.6)			
Perceived economic status, n (%)			4.985	2	0.083
Income less than expenses	49 (22.0)	29 (23.0)			
Income equal to expenses	100 (44.8)	69 (54.8)			
Income greater than expenses	74 (33.2)	28 (22.2)			
Living arrangement, n (%)			6.966	5	0.223
Alone	46 (20.6)	23 (18.3)			
With family	4 (1.8)	4 (3.2)			
With spouse/children	109 (48.9)	51 (40.5)			
With parents	44 (19.7)	33 (26.2)			
With friends	17 (7.6)	15 (11.9)			
Other	3 (1.3)	0 (0.0)			
Primary social media platform, n (%)			6.375	3	0.095
Instagram	131 (58.7)	76 (60.3)			
Other	33 (14.8)	22 (17.5)			
Twitter	55 (24.7)	21 (16.7)			
TikTok	4 (1.8)	7 (5.6)			

Values are presented as mean (SD) or n (%). Percentages are column percentages. SD: Standard deviation, t: Independent samples t-test, χ^2: Chi-square test.

Anxiety scores [7.60 ± 3.75 vs. 4.63 ± 3.62, t(347) = -7.279, p < 0.001], stress scores [7.05 ± 4.02 vs. 4.13 ± 3.78, t(347) = -6.768, p < 0.001], and DASS-21 total scores [21.60 ± 11.29 vs. 12.71 ± 10.60, t(347) = -7.352, p < 0.001] were also significantly higher in the risky use group.

Regarding motivations for social media use, participants with risky social media use had significantly higher scores on most motivational dimensions. The risky use group reported higher scores for flirting motivation [5.37 ± 3.53 vs. 4.35 ± 3.31, t(347) = -2.695, p = 0.007], making new friendships [5.76 ± 3.73 vs. 4.77 ± 3.43, t(347) = -2.510, p = 0.013], academic purposes [7.51 ± 5.08 vs. 5.82 ± 4.18, t(347) = -3.355, p < 0.001], maintaining social connectedness [12.64 ± 4.74 vs. 9.83 ± 4.76, t(347) = -5.302, p < 0.001], following and monitoring others [10.56 ± 4.79 vs. 7.84 ± 4.30, t(347) = -5.454, p < 0.001], entertainment [15.48 ± 4.04 vs. 13.04 ± 5.05, t(347) = -4.642, p < 0.001], social recognition [6.10 ± 3.41 vs. 4.97 ± 3.17, t(347) = -3.125, p = 0.002], and self-expression [9.17 ± 5.09 vs. 7.50 ± 4.89, t(347) = -3.017, p = 0.003]. However, information-seeking motivation did not differ significantly between the groups [16.48 ± 4.20 vs. 16.15 ± 4.51, t(347) = -0.660, p = 0.510] (Table 2).

Statistical Analyses

Pearson correlation analyses revealed that BSMAS total scores were positively correlated with FoMO scores: moderately with personal FoMO (r = 0.571, p < 0.001) and total FoMO (r = 0.522, p < 0.001), and weakly to moderately with social FoMO (r = 0.295, p < 0.001).

BSMAS total scores were also positively correlated with psychological distress. Significant correlations were found between BSMAS total scores and depression (r = 0.406, p < 0.001), anxiety (r = 0.387, p < 0.001), stress (r = 0.383, p < 0.001), and DASS-21 total scores (r = 0.411, p < 0.001).

Considering social media use motivations, BSMAS total scores were significantly and positively correlated with flirting (r = 0.182, p < 0.001), making new friendships (r = 0.148, p = 0.005), academic purposes (r = 0.230, p < 0.001), maintaining social connectedness (r = 0.407, p < 0.001), following and monitoring others (r = 0.359, p < 0.001), entertainment (r = 0.358, p < 0.001), social recognition (r = 0.182, p < 0.001), and self-expression (r = 0.198, p < 0.001). Information-seeking motivation was not significantly correlated with BSMAS total scores (r = 0.077, p = 0.152) (Table 3).

Table 2. Comparison of psychological scale scores by risky social media use.

Variable	**No risky use, mean (SD)**	**Risky use, mean (SD)**	**t**	**df**	**p-value**
BSMAS					
Total	12.82 (3.49)	21.77 (2.35)	-25.679	347	**<0.001**
FoMO					
Personal FoMO	9.00 (4.69)	15.01 (7.04)	-9.011	309	**<0.001**
Social FoMO	5.71 (3.12)	7.84 (5.08)	-4.752	333	**<0.001**
Total	14.62 (6.77)	22.31 (10.78)	-7.634	303	**<0.001**
DASS					
Depression	3.95 (3.74)	6.95 (4.17)	-6.906	347	**<0.001**
Anxiety	4.63 (3.62)	7.60 (3.75)	-7.279	347	**<0.001**
Stress	4.13 (3.78)	7.05 (4.02)	-6.768	347	**<0.001**
Total	12.71 (10.60)	21.60 (11.29)	-7.352	347	**<0.001**
Motives for social media use					
Flirting	4.35 (3.31)	5.37 (3.53)	-2.695	347	**0.007**
Making new friends	4.77 (3.43)	5.76 (3.73)	-2.510	347	**0.013**
Academic purposes	5.82 (4.18)	7.51 (5.08)	-3.355	347	**<0.001**
Social connectedness	9.83 (4.76)	12.64 (4.74)	-5.302	347	**<0.001**
Following others	7.84 (4.30)	10.56 (4.79)	-5.454	347	**<0.001**
Entertainment	13.04 (5.05)	15.48 (4.04)	-4.642	347	**<0.001**
Social recognition	4.97 (3.17)	6.10 (3.41)	-3.125	347	**0.002**
Self-expression	7.50 (4.89)	9.17 (5.09)	-3.017	347	**0.003**
Information seeking	16.15 (4.51)	16.48 (4.20)	-0.660	347	0.510

Values are presented as mean (SD). Bold values indicate statistically significant group differences (p < 0.05). BSMAS: Bergen Social Media Addiction Scale, DASS: Depression Anxiety Stress Scale, FoMO: Fear of missing out, SD: Standard deviation, t: Independent samples t-test.

Table 3. Correlations among social media addiction, FoMO, psychological distress, and social media use motives.

		BSMAS total	Personal FoMO	Social FoMO	FoMO total	DASS depression	DASS anxiety	DASS stress	DASS total	Dating motive	New friendship motive	Academic motive
BSMAS total	r	—										
	p	—										
Personal FoMO	r	0.571	—									
	p	<0.001	—									
Social FoMO	r	0.295	0.667	—								
	p	<0.001	<0.001	—								
FoMO total	r	0.522	0.949	0.868	—							
	p	<0.001	<0.001	<0.001	—							
DASS depression	r	0.406	0.340	0.300	0.341	—						
	p	<0.001	<0.001	<0.001	<0.001	—						
DASS anxiety	r	0.387	0.356	0.300	0.330	0.868	—					
	p	<0.001	<0.001	<0.001	<0.001	<0.001	—					
DASS stress	r	0.383	0.340	0.304	0.327	0.880	0.860	—				
	p	<0.001	<0.001	<0.001	<0.001	<0.001	<0.001	—				
DASS total	r	0.411	0.362	0.316	0.349	0.960	0.950	0.957	—			
	p	<0.001	<0.001	<0.001	<0.001	<0.001	<0.001	<0.001	—			
Dating motive	r	0.182	0.265	0.323	0.294	0.124	0.118	0.123	0.127	—		
	p	<0.001	<0.001	<0.001	<0.001	0.021	0.028	0.021	0.017	—		
New friendship motive	r	0.148	0.197	0.297	0.244	0.137	0.134	0.115	0.135	0.624	—	
	p	0.005	<0.001	<0.001	<0.001	0.010	0.012	0.031	0.012	<0.001	—	
Academic motive	r	0.230	0.304	0.342	0.361	0.255	0.188	0.236	0.238	0.205	0.251	—
	p	<0.001	<0.001	<0.001	<0.001	<0.001	<0.001	<0.001	<0.001	<0.001	<0.001	—
Social connection motive	r	0.407	0.511	0.411	0.509	0.261	0.243	0.253	0.264	0.309	0.292	0.333
	p	<0.001	<0.001	<0.001	<0.001	<0.001	<0.001	<0.001	<0.001	<0.001	<0.001	<0.001
Following others motive	r	0.359	0.496	0.455	0.513	0.183	0.193	0.170	0.190	0.332	0.281	0.276
	p	<0.001	<0.001	<0.001	<0.001	<0.001	<0.001	0.001	<0.001	<0.001	<0.001	<0.001
Entertainment motive	r	0.358	0.269	0.166	0.235	0.355	0.362	0.365	0.377	0.159	0.127	0.121
	p	<0.001	<0.001	0.002	<0.001	<0.001	<0.001	<0.001	<0.001	0.003	0.018	0.024
Social recognition motive	r	0.182	0.386	0.489	0.445	0.186	0.174	0.174	0.186	0.389	0.455	0.267
	p	<0.001	<0.001	<0.001	<0.001	<0.001	0.001	0.001	<0.001	<0.001	<0.001	<0.001
Self-expression motive	r	0.198	0.292	0.235	0.267	0.261	0.252	0.205	0.250	0.194	0.359	0.255
	p	<0.001	<0.001	<0.001	<0.001	<0.001	<0.001	<0.001	<0.001	<0.001	<0.001	<0.001
Information seeking motive	r	0.077	0.127	0.031	0.096	0.193	0.205	0.199	0.208	0.003	0.062	0.190
	p	0.152	0.026	0.569	0.096	<0.001	<0.001	<0.001	<0.001	0.960	0.252	<0.001

Table 3. Continued.

	Social connection motive	Following others motive	Entertainment motive	Social recognition motive	Self-expression motive	Information seeking motive
BSMAS total						
Personal FoMO						
Social FoMO						
FoMO total						
DASS depression						
DASS anxiety						
DASS stress						
DASS total						
Dating motive						
New friendship motive						
Academic motive						
Social connection motive	—					
	—					
Following others motive	0.642	—				
	<0.001	—				
Entertainment motive	0.447	0.376	—			
	<0.001	<0.001	—			
Social recognition motive	0.429	0.470	0.182	—		
	<0.001	<0.001	<0.001	—		
Self-expression motive	0.446	0.289	0.248	0.484	—	
	<0.001	<0.001	<0.001	<0.001	—	
Information seeking motive	0.409	0.242	0.373	0.154	0.340	—
	<0.001	<0.001	<0.001	0.004	<0.001	—

Bold values indicate statistically significant correlations (p <0.05). BSMAS: Bergen Social Media Addiction Scale, DASS: Depression Anxiety Stress Scales, FoMO: Fear of missing out, r = Pearson correlation coefficient.

DISCUSSION

The present study examined FoMO, psychological distress, and motivations for social media use among individuals with and without risky social media use. The principal findings revealed that participants in the risky social media use group reported greater FoMO, more pronounced symptoms of depression, anxiety, and stress, and higher levels of motivation across most domains of social media use. Correlation analyses also indicated that higher BSMAS scores were related to FoMO, psychological distress, and several motivational dimensions. In contrast, information-seeking motivation neither differed significantly between the risky and non-risky groups nor showed a significant association with BSMAS scores. Taken together, these results suggest that risky social media use may be more closely associated with social, emotional, and interpersonal motives than with instrumental, information-oriented use.

In accordance with the study hypothesis, participants with risky social media use reported higher levels of FoMO than those without risky use. This result is consistent with earlier evidence linking FoMO to excessive and problematic engagement with social media platforms (3,4). Social media platforms provide continuous access to others' activities, social interactions, and rewarding experiences. For individuals with higher FoMO, this constant flow of social information may increase the need to remain connected, frequently check updates, and avoid missing social experiences (3). Therefore, FoMO may serve as an important psychological mechanism that maintains repetitive and poorly controlled social media use. The moderate positive correlation between BSMAS total scores and total FoMO scores in the present study further supports the role of FoMO as a central correlate of risky social media use.

These findings further indicated that risky social media use was related to higher levels of psychological distress. Individuals in the risky use group were found to have higher levels of depression, anxiety, stress, and higher overall DASS-21 scores. This pattern aligns with previous studies showing links between problematic social media use, FoMO, anxiety symptoms, depressive symptomatology, and reduced psychological well-being (5,6). Several mechanisms may explain this relationship. Individuals experiencing emotional distress may use social media for distraction, reassurance, social contact, or temporary emotion regulation. At the same time, excessive social media use may increase exposure to social comparison, perceived exclusion, interpersonal stressors, and sensitivity to online feedback (5,6). The direction of this relationship cannot be determined due to the cross-sectional design of the present study. Nevertheless, the results indicate that risky social media use is significantly related to a broader psychological distress profile, including depressive, anxious, and stress-related symptoms.

A notable contribution of the present study is the evaluation of the multidimensional motivations for social media use. Participants with risky social media use scored higher on most motivational dimensions, including flirting, making new friends, academic purposes, maintaining social connectedness, following and monitoring others, entertainment, social recognition, and self-expression. These findings are consistent with the uses and gratifications perspective, which suggests that individuals use social media to meet different psychological and social needs, including social interaction, entertainment, self-presentation, and information seeking (7). They are also consistent with the multidimensional structure proposed in the SMU-SNS, which addresses different motives for social media use rather than treating social media engagement as a single homogeneous behavior (8). However, these findings also indicate that not all motives are equally related to risky use. Motivations involving social connection, monitoring others, entertainment, recognition, and self-expression seem more relevant to risky use than to information seeking.

The lack of significant group differences in information-seeking motivation is particularly important. Even though individuals may use social media to obtain information, this motive did not distinguish participants with risky use from those without. Similarly, information-seeking motivation was not significantly correlated with BSMAS total scores. This suggests that risky social media use may not simply reflect frequent or active engagement with social media platforms. Rather, it may be more strongly related to social and emotional motives, such as the need to stay socially connected, observe others, gain recognition, express oneself, or regulate mood through entertainment. This distinction may help clarify why some forms of social media use are relatively functional, whereas others may become more difficult to control. From this perspective, the findings of this study support the idea that problematic social media use should be understood not only in terms of frequency or duration of use, but also in terms of the psychological motives underlying use (7,8).

The sociodemographic findings should also be taken into consideration. Participants with risky social media use were significantly younger than those without risky use. This finding is consistent with the idea that younger adults may be more exposed to social media platforms and may integrate them more strongly into daily social interactions. Gender distribution also differed between groups, with a higher proportion of women in the risky use group. Employment status also differed: those with a higher proportion of students and a lower proportion of employed individuals. These variables may reflect differences in social media exposure, daily routines, peer interaction patterns, and availability of unstructured online time. However, these findings should be interpreted cautiously, as this study was not designed to examine demographic predictors of risky social media use.

Study Limitations

This study also has several limitations. Its cross-sectional nature precludes any inference about causality or temporal ordering among FoMO, psychological distress, and risky social media use. Therefore, it remains unclear whether FoMO and distress increase susceptibility to risky use, whether risky use contributes to emotional difficulties, or whether these factors operate in a reciprocal manner. In addition, the data were collected entirely via self-report instruments, which are subject to memory-related inaccuracies, response tendencies, and individual differences in symptom appraisal. Another limitation is the absence of a structured psychiatric interview. Even though participants who reported a previous psychiatric disorder or current use of psychotropic medication were excluded, psychiatric

eligibility was determined solely by self-report. Moreover, because recruitment was conducted online via social media platforms, the findings may not be fully representative of the general population. Finally, the risky use grouping was established based on a previously proposed cut-off score (11); therefore, it should be regarded as a risk classification rather than a formal clinical diagnosis of addiction.

Despite these limitations, this study has several strengths. It evaluated risky social media use alongside FoMO, psychological distress, and a detailed set of motivations for social media use. This multidimensional approach provides a more nuanced understanding of risky social media use. The findings of this study suggest that risky use is not only related to general motivation to use social media, but is also particularly associated with social and emotional motivations. This may have practical implications for prevention and intervention. Interventions targeting risky social media use may benefit from addressing FoMO, emotional distress, and social needs that drive repetitive online engagement, rather than focusing solely on reducing screen time.

CONCLUSION

Risky social media use was associated with higher FoMO, higher levels of psychological distress, and stronger motivations for social media use. Participants with risky use reported higher scores for depression, anxiety, and stress and for several motivational dimensions, particularly those related to social connection, following others, entertainment, recognition, and self-expression. In contrast, information-seeking motivation did not differ significantly between the two groups and was not related to the severity of social media addiction symptoms. Overall, these results indicate that risky social media use is more strongly linked to social and affective motives than to instrumental information-oriented use. Further longitudinal studies are needed to determine the temporal direction of these relationships and to test whether FoMO and particular social media use motives contribute to the emergence or persistence of risky use patterns.

Ethics

Ethics Committee Approval: Ethical approval was obtained from the University of Health Sciences Türkiye, Ankara Etlik City Hospital's Institutional Ethics Committee (approval number: AEŞH-BADEK-2025-0083; dated 29.01.2025), and the study procedures were conducted in line with the Declaration of Helsinki.

Informed Consent: Before completing the survey, all participants were informed about the study objectives and provided online informed consent.

Footnotes

Authorship Contributions

Concept: H.Ü., A.D., F.Y., Design: H.Ü., F.Y., Data Collection or Processing: H.Ü., M.R.V., A.D., Analysis or Interpretation: H.Ü., F.Y., Literature Search: H.Ü., M.R.V., A.D., F.Y., Writing: H.Ü., M.R.V., A.D., F.Y.

Conflict of Interest: No conflict of interest was declared by the authors.

Financial Disclosure: This research received no specific grant and financial support from any funding agency in the public, commercial, or not-for-profit sectors.

REFERENCES

1. Griffiths MD. A components model of addiction within a biopsychosocial framework. J Subst Use. 2005; 10: 191-7.
2. Andreassen CS. Online social network site addiction: a comprehensive review. Curr Addict Rep. 2015; 2: 175-84.
3. Przybylski AK, Murayama K, DeHaan CR, Gladwell V. Motivational, emotional, and behavioral correlates of fear of missing out. Comput Human Behav. 2013; 29: 1841-8.
4. Oberst U, Wegmann E, Stodt B, Brand M, Chamarro A. Negative consequences from heavy social networking in adolescents: the mediating role of fear of missing out. J Adolesc. 2017; 55: 51-60.
5. Dhir A, Yossatorn Y, Kaur P, Chen S. Online social media fatigue and psychological wellbeing: a study of compulsive use, fear of missing out, fatigue, anxiety and depression. Int J Inf Manage. 2018; 40: 141-52.
6. Dempsey AE, O'Brien KD, Tiamiyu MF, Elhai JD. Fear of missing out and rumination mediate relations between social anxiety and problematic Facebook use. Addict Behav Rep. 2019; 9: 100150.
7. Whiting A, Williams D. Why people use social media: a uses and gratifications approach. Qual Mark Res. 2013; 16: 362-9.
8. Pertegal MÁ, Oliva A, Rodríguez-Meirinhos A. Development and validation of the Scale of Motives for Using Social Networking Sites (SMU-SNS) for adolescents and youths. PLoS One. 2019; 14: e0225781.
9. Andreassen CS, Pallesen S, Griffiths MD. The relationship between addictive use of social media, narcissism, and self-esteem: findings from a large national survey. Addict Behav. 2017; 64: 287-93.
10. Demirci İ. Bergen sosyal medya bağımlılığı ölçeğinin Türkçeye uyarlanması, depresyon ve anksiyete belirtileriyle ilişkisinin değerlendirilmesi. Anadolu Psikiyatri Derg. 2019; 20: 15-22.
11. Bányai F, Zsila Á, Király O, Maraz A, Elekes Z, Griffiths MD, et al. Problematic social media use: results from a large-scale nationally representative adolescent sample. PLoS One. 2017; 12: e0169839.
12. Çelik F, Özkara BY. Gelişmeleri kaçırma korkusu (FoMO) ölçeği: sosyal medya bağlamına uyarlanması ve psikometrik özelliklerinin sınanması. Psikoloji Çalışmaları. 2022; 42: 71-103.
13. Yılmaz Ö, Boz H, Arslan A. Depresyon Anksiyete Stres Ölçeğinin (DASS-21) Türkçe kısa formunun geçerlilik-güvenilirlik çalışması. Finans Ekonomi ve Sosyal Araştırmalar Dergisi. 2017; 2: 78-91.
14. Dölay Z. Sosyal medya bağımlılığı, sosyal medya kullanım motivasyonları ve karanlık üçlü kişilik özellikleri arasındaki ilişkilerin incelenmesi [master's thesis]. İstanbul: Maltepe Üniversitesi, Lisansüstü Eğitim Enstitüsü; 2024.

Original Investigation | Özgün Araştırma

Gazi Med J 2026;37(3):428-435

DOI: http://dx.doi.org/10.12996/gmj.2026.4712

Prognostic Value of EASIX (ln-EASIX) in Hospitalized Patients with Cirrhosis

Hastanede Yatan Siroz Hastalarında ln-EASIX'in Prognostik Değeri

Ali Karataş[1], Yunus Emre Börü[1], Güner Kılıç[1], Mehmet Cindoruk[1], Tarkan Karakan[1], Murat Kekilli[1], Çağdaş Kalkan[1], Kenan Moral[2], Ali Levent Güngör[3]

[1]Department of Gastroenterology, Gazi University, Faculty of Medicine, Ankara, Türkiye
[2]Department of Gastroenterology, Başkent University, Faculty of Medicine, Ankara, Türkiye
[3]Department of Internal Medicine, Gazi University, Faculty of Medicine, Ankara, Türkiye

ABSTRACT

Objective: To investigate the prognostic value of the natural logarithm of the Endothelial Activation and Stress Index (ln-EASIX) for mortality and readmission outcomes in hospitalized patients with cirrhosis, and to compare its discriminative performance with the Model for End-Stage Liver Disease–Sodium (MELD-Na) score.

Methods: This retrospective cohort study included 244 hospitalized patients with cirrhosis. Because the EASIX values demonstrated a right-skewed distribution, logarithmic transformation was applied before the analysis. Patients were categorized into low- and high-ln-EASIX groups using the receiver operating characteristic (ROC) curve -derived optimal threshold determined by the Youden index for 30-day mortality in the analytic dataset. Baseline demographic, clinical, and laboratory characteristics were compared between the groups. Mortality and readmission were assessed, and receiver operating characteristic analysis was performed to evaluate the discriminative ability of the selected endpoints. Readmission analyses were considered secondary endpoints.

Results: Thirty-day mortality was higher in the high ln-EASIX group than in the low ln-EASIX group (11.6% vs. 1.6%, p = 0.004). ln-EASIX demonstrated moderate discrimination for 30-day mortality area under the curve (AUC) 0.725, 95% confidence interval (CI) 0.613–0.837, whereas MELD-Na showed numerically higher discrimination (AUC 0.782, 95% CI 0.692–0.872). In a MELD-Na-adjusted logistic regression model, ln-EASIX was not independently associated with 30-day mortality (adjusted OR 1.72, 95% CI 0.82–3.62, p = 0.153).

ÖZ

Amaç: Bu çalışmanın amacı, hastanede yatan siroz hastalarında Endotelyal Aktivasyon ve Stres İndeksi'nin doğal logaritmik dönüşümünün (ln-EASIX) mortalite ve yeniden hastaneye yatış üzerindeki prognostik değerini araştırmak ve ayırt edici performansını Model for End-Stage Liver Disease-Sodium (MELD-Na) skoru ile karşılaştırmaktır.

Yöntemler: Bu retrospektif kohort çalışmasına hastanede yatan toplam 244 siroz hastası dahil edildi. EASIX değerleri sağa çarpık dağılım gösterdiğinden, analiz öncesinde logaritmik dönüşüm uygulanarak ln-EASIX elde edildi. Hastalar, analiz grubunda 30 günlük mortalite için alıcı işletim karakteristiği (ROC) eğrisi ve Youden indeksi kullanılarak belirlenen en uygun eşik değere göre düşük ve yüksek ln-EASIX gruplarına ayrıldı. Gruplar arasında demografik, klinik ve laboratuvar özellikleri karşılaştırıldı. Mortalite ve yeniden hastaneye yatış sonuçları değerlendirildi; seçilen sonlanım noktaları için ayırt edici performans ROC analizi ile incelendi. Yeniden hastaneye yatış analizleri ikincil sonlanım noktası olarak değerlendirildi.

Bulgular: Yüksek ln-EASIX grubunda 30 günlük mortalite, düşük ln-EASIX grubuna göre anlamlı olarak daha yüksekti (%11,6'ya karşı %1,6; p = 0,004). ln-EASIX, 30 günlük mortaliteyi öngörmede orta düzeyde ayırt edici performans gösterdi (EAA/AUC: 0,725; %95 GA: 0,613–0,837). MELD-Na skorunun ayırt edici performansı ise sayısal olarak daha yüksekti (EAA/AUC: 0,782; %95 GA: 0,692–0,872). MELD-Na'ya göre düzeltilmiş lojistik regresyon analizinde ln-EASIX'in 30 günlük mortalite için bağımsız bir belirleyici olmadığı görüldü (düzeltilmiş OR: 1,72; %95 GA: 0,82–3,62; p = 0,153).

Cite this article as: Karataş A, Börü YE, Kılıç G, Cindoruk M, Karakan T, Kekilli M, et al. Prognostic value of EASIX (in-EASIX) in hospitalized patients with cirrhosis. Gazi Med J. 2026;37(3):428-435

Address for Correspondence/Yazışma Adresi: Ali Karataş, Department of Gastroenterology, Gazi University, Faculty of Medicine, Ankara, Türkiye
E-mail / E-posta: alikaratas@gazi.edu.tr
ORCID ID: orcid.org/0000-0002-2464-1975

Received/Geliş Tarihi: 13.05.2026
Accepted/Kabul Tarihi: 19.06.2026
Publication Date/Yayınlanma Tarihi: 10.07.2026

ABSTRACT

CONCLUSION: In hospitalized patients with cirrhosis, a higher ln-EASIX was associated with a more advanced disease profile and worse early outcomes. ln-EASIX may serve as a simple adjunctive marker for early bedside risk stratification; however, the findings should be interpreted cautiously until validated in larger studies with explicit cutoff definitions, multivariable modeling, and formal model-comparison analyses.

Keywords: Cirrhosis, EASIX, ln-EASIX, mortality, readmission, MELD-Na

ÖZ

Sonuç: Hastanede yatan siroz hastalarında yüksek ln-EASIX düzeyi, daha ileri hastalık profili ve daha kötü erken dönem klinik sonuçlarla ilişkili bulundu. ln-EASIX, erken dönemde yatak başında risk sınıflandırması için kolay uygulanabilir tamamlayıcı bir biyobelirteç olarak kullanılabilir. Ancak bu bulguların, daha geniş hasta serilerinde, açıkça tanımlanmış eşik değerleri, çok değişkenli modeller ve formal model karşılaştırmalarını içeren çalışmalarla doğrulanması gerekmektedir.

Anahtar Sözcükler: Siroz, EASIX, ln-EASIX, mortalite, yeniden hastaneye yatış, MELD-Na

INTRODUCTION

Cirrhosis is a dynamic systemic disorder characterized by portal hypertension, impaired hepatic synthetic function, inflammation, endothelial injury, circulatory dysfunction, renal impairment, and progressive multiorgan involvement. In hospitalized patients, especially those with acute decompensation, these interconnected mechanisms may lead to rapid clinical deterioration and death. Consequently, there is increasing interest in pragmatic biomarkers that capture systemic vulnerability beyond conventional liver-centered prognostic scores (1-3).

The Model for End-Stage Liver Disease–Sodium (MELD-Na) is widely used for prognostic assessment in advanced liver disease and remains central to clinical decision-making. Nevertheless, MELD-Na mainly reflects bilirubin, creatinine, the international normalized ratio, and sodium levels, and may not fully capture endothelial dysfunction, inflammatory burden, or microvascular stress. Therefore, biomarkers that complement established scores may be clinically useful, particularly in patients hospitalized with acute instability (4-6).

The natural logarithm of Endothelial Activation and Stress Index (ln-EASIX), derived from lactate dehydrogenase, creatinine, and platelet count, has been investigated as a surrogate marker of endothelial activation and systemic injury in several diseases, including hematopoietic stem cell transplantation, graft-versus-host disease, coronavirus disease 2019 (COVID-19), and cardiovascular disease. Its potential relevance to cirrhosis is biologically plausible, given the central role of endothelial dysfunction, immune dysregulation, thrombocytopenia, renal dysfunction, and tissue injury in the pathogenesis of decompensated liver disease. Recently, EASIX was also evaluated in critically ill patients with advanced liver disease, where it showed clinically meaningful prognostic accuracy for short-term mortality, supporting the relevance of this biomarker in cirrhosis-specific populations (7-12).

In this study, we evaluated the association of ln-EASIX with mortality and readmission outcomes in hospitalized patients with cirrhosis and compared its discriminative performance with that of MELD-Na. This study was designed primarily to explore the potential prognostic utility of ln-EASIX in an inpatient cirrhosis cohort.

MATERIALS AND METHODS

Study Design and Patient Population

This retrospective study included patients hospitalized with cirrhosis between January 2014 and December 2025 at a tertiary care center in Türkiye. A total of 312 hospitalized patients with cirrhosis were initially screened for eligibility using an institutional clinical dataset. Patients were excluded due to missing key laboratory parameters required for EASIX calculation (n = 18), insufficient follow-up data for outcome assessment (n = 27), or incomplete hospitalization records (n = 23). After these exclusions, 244 patients met the inclusion criteria and were included in the final analysis. Only patients with sufficient clinical and laboratory data to calculate the EASIX score during the index hospitalization were included in the analysis. The cohort comprised hospitalized patients with clinically significant disease severity, as reflected by the high prevalence of decompensation-related features and the observed mortality profile. The patient selection process is illustrated in Figure 1. This study was approved by the Gazi University Ethics Committee (approval no: 2025-2240; approval date: December 23, 2025; meeting no: 20). A total of 312 patients were screened; 68 were excluded due to missing data or insufficient follow-up. The final analytic cohort included 244 patients with complete outcome data.

Inclusion Criteria

The inclusion criteria were as follows: (1) age ≥18 years; (2) a confirmed diagnosis of cirrhosis based on clinical, radiological, or histological criteria; and (3) hospitalization due to cirrhosis-related complications between January 2014 and December 2025. To ensure the independence of observations, only the index hospitalization for each patient was included in the analysis.

Exclusion Criteria

The exclusion criteria were as follows: (1) age <18 years; (2) absence of a confirmed diagnosis of cirrhosis; (3) missing key laboratory parameters required for EASIX calculation (including lactate dehydrogenase, creatinine, or platelet count); and (4) insufficient follow-up data to assess the study outcomes.

Patients with hepatocellular carcinoma, prior liver transplantation, hematologic malignancy, or receiving chronic dialysis were not excluded if they met the inclusion criteria and had complete data available, to reflect a real-world hospitalized cirrhosis population.

Definitions and Variables

Cirrhosis was defined according to the criteria used in routine clinical practice at the enrolling center, based on a combination of clinical, laboratory, imaging, and where available, histological data from the patients. Demographic variables, baseline clinical characteristics, laboratory parameters, and hospitalization outcomes were extracted from the analytical dataset. EASIX was calculated using lactate dehydrogenase, creatinine, and platelet count, and a logarithmic transformation was applied because the raw EASIX distribution was right-skewed. MELD-Na was used as the principal comparator. Mortality outcomes included in-hospital, 30-day, short-term, and 365-day mortality. For this analysis, short-term mortality was defined as death occurring within 90 days of the index hospitalization. Readmission outcomes at 30 days, during short-term follow-up, and at 365 days were also evaluated in this study.

Grouping Strategy

Patients were classified into low- and high-ln-EASIX groups according to the ROC-derived optimal threshold (based on the Youden index) for 30-day mortality in the analytic dataset.

Statistical Analysis

Continuous variables were summarized as medians and interquartile ranges, and categorical variables were summarized as numbers and percentages. Comparisons between groups were performed using the Mann–Whitney U test for continuous variables and the chi-square test or Fisher's exact test for categorical variables as appropriate.

Due to the right-skewed distribution of EASIX values, a natural logarithmic transformation was applied, and ln-EASIX was used in all analyses. Receiver operating characteristic (ROC) analysis was performed to assess the discriminative performance of the selected outcomes, and the optimal cutoff value for ln-EASIX was determined using the Youden index.

Multivariable logistic regression analysis was performed to evaluate the association between ln-EASIX and 30-day mortality, adjusting for the MELD-Na score. Given the limited number of events (n=16), the multivariable model was restricted to avoid overfitting.

All analyses were exploratory and hypothesis-generating. Due to the limited number of mortality events, no stepwise variable selection or model optimization procedures were applied.

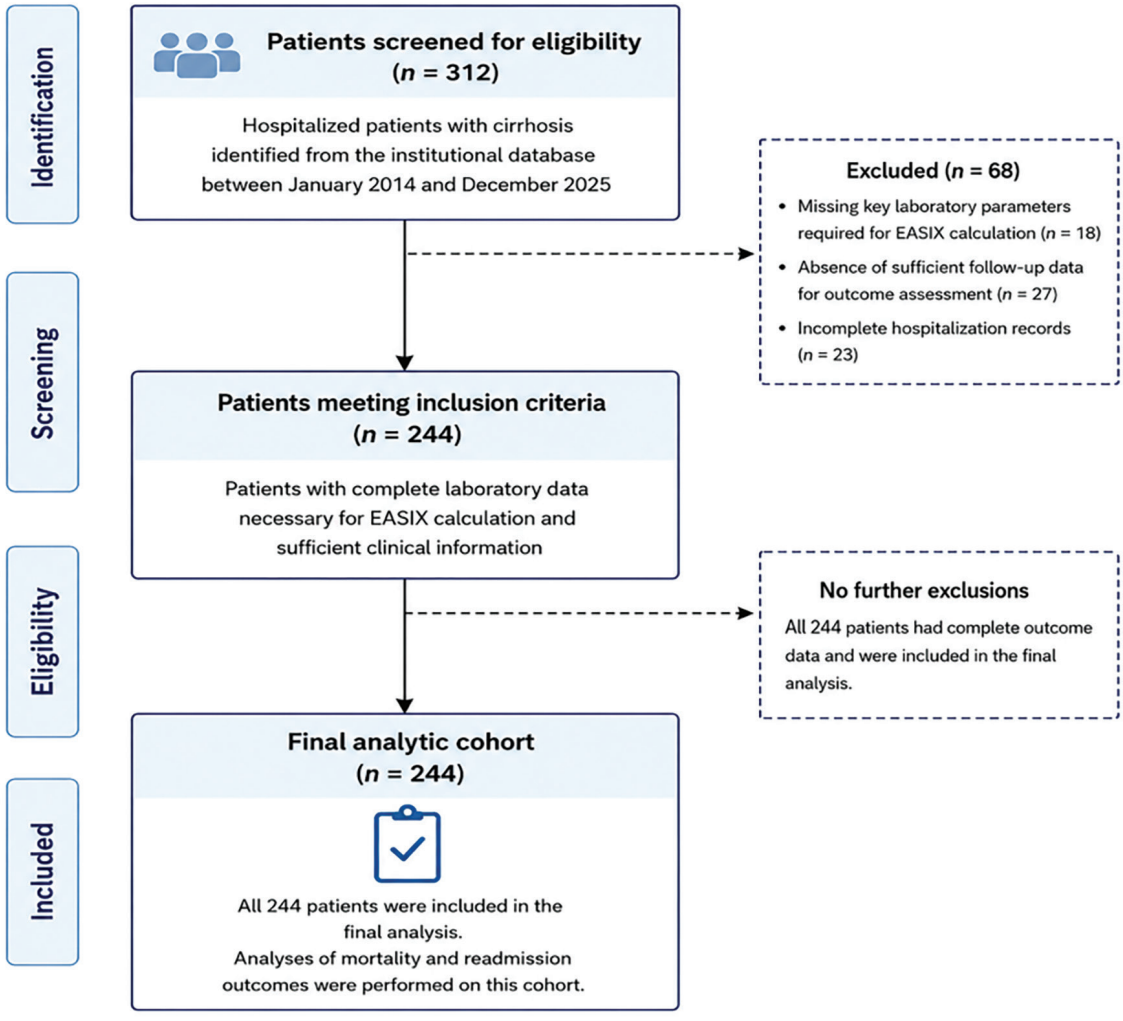

Figure 1. Flow diagram of patient selection.

RESULTS

Baseline Characteristics

The study cohort comprised 244 hospitalized patients with cirrhosis. The baseline characteristics of the overall cohort are presented in Table 1, and comparisons between the low and high ln-EASIX groups are shown in Table 2.

Patients were categorized into low-ln-EASIX (n = 123) and high-ln-EASIX (n = 121) groups based on the ROC-derived cutoff value of 0.76. The median MELD-Na was 18.0 [13.0–24.0]. Patients with high ln-EASIX had a more severe disease profile, characterized by higher MELD-Na scores and laboratory abnormalities consistent with more severe systemic illness. These findings suggest that ln-EASIX reflects broader clinical decompensation rather than isolated laboratory abnormalities.

Mortality Outcomes

Patients were categorized into low (n = 123) and high (n = 121) ln-EASIX groups based on the ROC-derived cutoff value of 0.76. The median MELD-Na was 18.0 [13.0–24.0] (Table 1). Patients in the high ln-EASIX group exhibited a more severe disease profile, characterized by higher MELD-Na scores and more adverse laboratory findings consistent with a greater systemic illness (Table 2). These findings suggest that ln-EASIX reflects broader clinical decompensation rather than isolated laboratory abnormalities.

Table 1. Demographic and laboratory characteristics of the study population.

Characteristic	Overall (n = 244)
Demographic variables	
Age, years	65.5 [58.0–71.0]
Male sex, n (%)	144 (59.0%)
Liver disease severity	
Child–pugh A, n (%)	66 (27.0%)
Child–pugh B, n (%)	123 (50.4%)
Child–pugh C, n (%)	55 (22.5%)
Laboratory variables	
Albumin, g/dL	2.8 [2.5–3.28]
LDH, U/L	251.0 [209.8–300.3]
Platelet, $\times 10^3/\mu L$	119 [87–165]
INR	1.38 [1.20–1.59]
AST, U/L	41.5 [31.0–68.3]
ALT, U/L	25.0 [16.0–36.0]
Clinical characteristics	
Ascites, n (%)	226 (92.6%)
Variceal bleeding, n (%)	38 (15.6%)
Hepatic encephalopathy, n (%)	42 (17.2%)
Hepatorenal syndrome, n (%)	24 (9.8%)
Infection, n (%)	77 (31.6%)

ALT: Alanine aminotransferase, AST: Aspartate aminotransferase, INR: International normalized ratio, LDH: Lactate dehydrogenase, n: Number, U/L: Units per liter, g/dL: Grams per deciliter, µL: Microliter.

A total of 16 30-day mortality events were observed in the cohort, limiting statistical power and constraining the complexity of multivariable modeling. In multivariable logistic regression analysis, adjusted for MELD-Na, ln-EASIX was associated with increased odds of 30-day mortality; however, this association did not reach statistical significance (adjusted OR = 1.72, 95% CI = 0.82–3.62, p = 0.153).

Readmission Outcomes

The findings related to readmission were less robust than those related to mortality (Table 3). Although readmission is a clinically relevant outcome, it is influenced by multiple factors beyond acute physiological status at the index admission, including discharge planning, outpatient follow-up, treatment adherence, competing mortality, and healthcare-system factors.

In the present cohort, MELD-Na demonstrated moderate discriminative ability for 30-day readmission and modest ability for longer-term readmission, whereas ln-EASIX showed limited predictive value for these endpoints.

These findings suggest that readmission may be less directly related to acute disease severity and more strongly influenced by nonbiological and system-level factors. Therefore, readmission was considered a secondary exploratory endpoint in this study.

Discriminative Performance

In the overall cohort, ln-EASIX predicted 30-day mortality with an area under the curve (AUC) of 0.725 (95% CI: 0.613–0.837, p = 0.003). The optimal cut-off value based on the Youden index was 0.76, corresponding to a sensitivity of 87.5% and a specificity of 53.5% (Table 4).

The MELD-Na score demonstrated a higher discriminatory performance for 30-day mortality, with an AUC of 0.782 (95% CI: 0.692–0.872, p < 0.001). The optimal cutoff value was 20.5, with a sensitivity of 81.3% and a specificity of 67.1%.

The MELD-Na also demonstrated consistent predictive performance for longer-term mortality, including 1-year mortality (AUC 0.724) and 2-year mortality (AUC 0.697) (Table 4).

For readmission outcomes, MELD-Na showed moderate discriminative ability for 30-day readmission (AUC 0.729) and modest discriminative ability for long-term readmission.

DISCUSSION

The present study suggests that ln-EASIX is associated with a more severe clinical phenotype and poorer early outcomes in hospitalized patients with cirrhosis. Patients with higher ln-EASIX values had greater biochemical derangement and higher short-term mortality, supporting the concept that this index captures clinically relevant systemic vulnerability at the time of hospitalization. Importantly, these findings should be interpreted as complementary rather than competitive with established prognostic scores. In the current analysis, MELD-Na remained a central marker of liver disease severity, whereas ln-EASIX may reflect an overlapping but not identical biological domain that includes endothelial stress, renal dysfunction, thrombocytopenia, and tissue injury. Therefore, the principal implication of this study is not that ln-EASIX should replace MELD-Na, but that it may serve as a practical adjunct for early inpatient risk stratification (1-6).

The biological plausibility of ln-EASIX in cirrhosis is supported by the current understanding of decompensated cirrhosis and acute-on-chronic liver failure. Cirrhosis is increasingly recognized as a systemic disorder in which portal hypertension, hepatic insufficiency, systemic inflammation, endothelial dysfunction, immune dysregulation, circulatory impairment, and extrahepatic organ failure interact dynamically. In acute decompensation and acute-on-chronic liver failure (ACLF), systemic inflammation can amplify vascular dysfunction and microcirculatory injury, resulting in tissue hypoperfusion and multi-organ failure. Because EASIX combines lactate dehydrogenase, creatinine, and platelet count, it may provide a simple laboratory-based summary of several components of the pathophysiological cascade (1-4,13,14).

Endothelial dysfunction is particularly relevant to the interpretation of EASIX in patients with advanced liver disease. In cirrhosis, liver sinusoidal endothelial cell dysfunction contributes to increased intrahepatic vascular resistance and portal hypertension, whereas systemic and splanchnic endothelial abnormalities contribute to vasodilation, circulatory dysfunction, inflammation, and organ hypoperfusion. These processes are central to the transition from compensated disease to decompensation and may contribute to the development of ACLF. From this perspective, ln-EASIX may be clinically meaningful because it does not merely reflect liver synthetic dysfunction; rather, it may capture the broader vascular and systemic injury phenotype that characterizes high-risk hospitalized patients with cirrhosis (6,13-15).

The creatinine component of the EASIX is clinically important, because renal dysfunction is among the strongest determinants of short-term prognosis in patients with cirrhosis. Acute kidney injury and hepatorenal syndrome are common in patients with decompensated cirrhosis and associated with longer hospital stays, need for intensive care, and increased in-hospital and short-term

Table 2. Baseline characteristics according to ln-EASIX group.

Characteristic	Overall (n = 244)	Low ln-EASIX (≤0.76) (n = 123)	High ln-EASIX (>0.76) (n = 121)	p-value
Female sex, n (%)	100 (41.0%)	55 (44.7%)	45 (37.2%)	0.287
Age, years	66.0 [58.0–71.0]	66.0 [58.0–73.0]	65.0 [58.3–70.0]	0.270
MELD-Na	18.0 [13.0–24.0]	14.0 [11.0–20.0]	20.0 [16.0–25.0]	<0.001
EASIX	2.14 [1.40–3.74]	1.29 [0.90–1.50]	3.39 [2.33–5.01]	<0.001
ln-EASIX	0.76 [0.33–1.32]	0.26 [−0.11–0.40]	1.22 [0.85–1.61]	<0.001
WBC/µL	5,940 [4,295–7,700]	6,320 [4,780–7,730]	5,595 [3,825–7,678]	0.028
Hemoglobin, g/dL	10.2 [8.5–11.7]	10.2 [8.9–12.2]	10.2 [8.4–11.5]	0.153
Platelet, ×10³/µL	118 [87–165]	158 [117–210]	94.5 [68.5–134.3]	<0.001
INR	1.38 [1.20–1.59]	1.27 [1.17–1.51]	1.44 [1.29–1.68]	<0.001
Albumin, g/dL	2.8 [2.5–3.3]	2.8 [2.5–3.4]	2.7 [2.5–3.1]	0.073
Total bilirubin, mg/dL	1.43 [0.94–2.80]	1.21 [0.76–1.88]	1.79 [1.12–3.34]	<0.001
CRP, mg/L	15.0 [7.04–35.3]	13.8 [7.8–33.7]	16.7 [6.7–38.1]	0.431
Sodium, mmol/L	135 [131–138]	135 [132–139]	134 [130–138]	0.128
Baseline creatinine, mg/dL	0.75 [0.60–0.93]	0.70 [0.55–0.80]	0.80 [0.65–1.05]	<0.001
Admission creatinine, mg/dL	0.97 [0.75–1.46]	0.83 [0.67–1.04]	1.12 [0.86–1.76]	<0.001

Grouping was based on the ROC-derived ln-EASIX cutoff value of 0.76 for 30-day mortality. Values are presented as median [interquartile range] or number (%). Continuous variables were compared using the Mann–Whitney U test, and categorical variables were compared using the chi-square test or Fisher's exact test, as appropriate.
CRP: C-reactive protein, EASIX: Endothelial Activation and Stress Index, INR: International normalized ratio, ln-EASIX: Natural logarithm of the Endothelial Activation and Stress Index, MELD-Na: Model for End-Stage Liver Disease Sodium, n: Number, ROC: Receiver operating characteristic, WBC: White blood cell, g/dL: Grams per deciliter, mg/dL: Milligrams per deciliter, mg/L: Milligrams per liter, mmol/L: Millimoles per liter, µL: Microliter.

Table 3. Mortality and readmission outcomes according to ln-EASIX group.

Outcome	Low ln-EASIX (≤0.76) (n = 123)	High ln-EASIX (>0.76) (n = 121)	p-value
30-day mortality	2/123 (1.6%)	14/121 (11.6%)	0.004
Short-term mortality (90-day)	16/123 (13.0%)	29/121 (24.0%)	0.03
365-day mortality	43/123 (35.0%)	49/121 (40.5%)	0.40
30-day readmission	12/123 (9.8%)	24/121 (19.8%)	0.05
Short-term readmission (≤90-day)	38/123 (30.9%)	46/121 (38.0%)	0.25
365-day readmission	76/123 (61.8%)	70/121 (57.9%)	0.56

The differences in the denominators reflect missing follow-up data for specific endpoints. Values are presented as n (%). p-values were calculated using the chi-square test or Fisher's exact test, as appropriate.
ln-EASIX: Natural logarithm of the Endothelial Activation and Stress Index, n: Number.

Table 4. Discriminative performance of ln-EASIX and MELD-Na.

Outcome	Variable	AUC	95% CI	p-value	Cut-off	Sensitivity	Specificity
30-day mortality	ln-EASIX	0.725	0.613–0.837	0.003	0.76	87.5%	53.5%
30-day mortality	MELD-Na	0.782	0.692–0.872	<0.001	20.5	81.3%	67.1%
90-day mortality	MELD-Na	0.724	0.660–0.788	<0.001	17.5	71.9%	62.8%
365-day mortality	MELD-Na	0.697	0.631–0.763	<0.001	14.5	82.8%	50.0%
30-day readmission	MELD-Na	0.729	0.618–0.841	<0.001	20.5	71.4%	68.5%
365-day readmission	MELD-Na	0.641	0.571–0.711	<0.001	16.5	65.3%	59.6%

The optimal ln-EASIX cut-off value for 30-day mortality was 0.76 (Youden index). Although this ROC-derived threshold coincided numerically with the cohort median ln-EASIX value, grouping was based on the Youden index obtained from the ROC analysis for 30-day mortality. The AUC values are presented with 95% confidence intervals. The cut-off values were determined using the Youden index. Low ln-EASIX group: n = 123; High ln-EASIX group: n = 121.
AUC: Area under the curve, CI: Confidence interval, ln-EASIX: Natural logarithm of the Endothelial Activation and Stress Index, MELD-Na: Model for End-Stage Liver Disease Sodium, n: Number, ROC: Receiver operating characteristic.

mortality. In patients with cirrhosis, even modest increases in serum creatinine may indicate clinically meaningful renal impairment, because serum creatinine can underestimate the degree of kidney dysfunction in patients with reduced muscle mass. Thus, the incorporation of creatinine into EASIX plausibly links the index to circulatory failure, renal hypoperfusion, and systemic hemodynamic instability that accompanies advanced decompensation (5,6,16).

The platelet component also has a strong mechanistic basis. Thrombocytopenia is one of the most common hematological abnormalities in chronic liver disease and is closely related to portal hypertension, splenic sequestration, reduced thrombopoietin production, bone marrow suppression, inflammation, and disease severity. Although platelet count should not be interpreted as a pure measure of portal pressure, lower platelet counts often indicate a more advanced portal hypertensive phenotype and may coexist with clinically significant complications, such as ascites, varices, and decompensation. Therefore, its inclusion in the EASIX may help the index capture the portal hypertensive and systemic severity burden of cirrhosis (7-9,17).

Lactate dehydrogenase (LDH), the third component of EASIX, is less specific but may still be informative in acute inpatient settings. Elevated LDH levels can reflect tissue injury, cellular stress, hypoperfusion, hemolysis, infection-related injury, or systemic inflammatory activation. In patients hospitalized with decompensated cirrhosis, these processes may be accompanied by sepsis, gastrointestinal bleeding, acute kidney injury, ACLF, and other acute complications. Therefore, the prognostic relevance of LDH within EASIX is likely related to its role as a nonspecific marker of acute cellular injury rather than a liver-specific mechanism. When combined with creatinine and platelet count, LDH may contribute to multidimensional signals of acute systemic stress (2-4,10-12).

The finding that ln-EASIX is more closely related to early mortality than to longer-term outcomes is clinically relevant. Early mortality in hospitalized patients with cirrhosis is often attributable to acute physiological instability, infection, renal dysfunction, circulatory failure, and other organ failures. These processes are precisely those that EASIX is biologically positioned to reflect. In contrast, 365-day mortality and readmission are influenced by many additional factors, including response to treatment, recurrent decompensation, nutritional status, frailty, outpatient follow-up, alcohol abstinence, access to liver transplantation, and health care system factors. Accordingly, ln-EASIX may be most useful as an early warning marker at the time of hospital admission rather than as a standalone long-term prognostic tool (2-6).

However, a comparison with MELD-Na requires careful interpretation. MELD-Na is a validated and widely used prognostic score for advanced liver disease and transplant allocation. In the present dataset, the numerical performance of MELD-Na and ln-EASIX should be reported without overstating their superiority. If MELD-Na demonstrates a higher AUC than ln-EASIX for a given endpoint, the appropriate interpretation is that ln-EASIX may provide complementary biological information rather than superior discrimination. This distinction is important because ln-EASIX and MELD-Na partially overlap with respect to renal dysfunction, but they emphasize different aspects of illness. MELD-Na reflects liver disease severity and sodium-related circulatory dysfunction, whereas ln-EASIX may better represent endothelial stress, thrombocytopenia, and acute tissue injury (4-6).

These findings are consistent with those of prior studies evaluating EASIX in advanced liver disease and other systemic inflammatory conditions. Schult et al. (12) reported that EASIX had prognostic utility in critically ill patients with advanced liver disease, including patients with ACLF, and showed performance comparable to several established intensive care and liver-related scores. Although that cohort was more severely ill and was ICU-based, it nevertheless supports the concept that EASIX may be relevant to advanced liver disease characterized by endothelial dysfunction and organ failure. Beyond hepatology, EASIX has been associated with adverse outcomes in allogeneic stem cell transplantation, graft-versus-host disease, COVID-19, and cardiovascular disease; conditions in which endothelial activation and systemic injury are central biological features (7-12).

From a clinical standpoint, the ln-EASIX score has several practical advantages. It is calculated from routine laboratory tests, requires no specialized assay, and can be obtained early during hospital admission. This makes it potentially useful in emergency departments, inpatient wards, and high-dependency settings, where early triage decisions are clinically important. A high ln-EASIX value could identify patients requiring closer monitoring, earlier evaluation for renal dysfunction or infection, more aggressive supportive care, or assessment for intensive care. However, this potential clinical role should be regarded as hypothesis-generating

until externally validated and tested in combination with established prognostic models (6,12).

This study also highlights the need for careful methodological interpretation. Group-based analyses depend heavily on the selection of the ln-EASIX threshold. If an ROC-derived cutoff is used, the cutoff value, sensitivity, specificity, confidence intervals, and derivation method should be clearly reported. If a median split was used, it should be described as such and not presented as an optimized prognostic threshold. In addition, comparisons between ln-EASIX and MELD-Na should not rely solely on visual or numerical differences in the AUC; a formal statistical comparison is needed when superiority is claimed. Without such testing, the most defensible conclusion is that ln-EASIX may provide complementary prognostic information (5,6,12).

In summary, ln-EASIX appears to be a promising adjunctive marker of early clinical vulnerability in hospitalized patients with cirrhosis. Its value is likely related to its ability to integrate renal dysfunction, platelet-related severity of portal hypertension, and acute tissue injury into a single laboratory-based severity index. Current evidence supports further investigation of ln-EASIX as a complementary tool for early inpatient risk stratification, but not as a replacement for MELD-Na. Future multicenter studies should validate the optimal threshold, test the adjusted and incremental prognostic value, and determine whether the incorporation of ln-EASIX into clinical decision pathways improves patient outcomes (6,12).

Study Limitations

The main limitations of this study should be emphasized. Its retrospective, single-center design introduces the possibility of selection bias, residual confounding, and incomplete clinical characterization. The relatively high mortality burden suggests that the cohort may represent a particularly high-risk inpatient population rather than the broader cirrhosis population. The limited number of 30-day mortality events restricts the complexity of multivariable modeling and reduces the precision of adjusted estimates. Readmission outcomes are also influenced by nonbiological determinants and should be interpreted as secondary exploratory endpoints. These limitations do not negate the observed association, but they should temper the strength of the clinical conclusions.

Despite these limitations, this study has important strengths. It focuses on a clinically relevant, hospitalized cirrhosis population, examines early outcomes that are directly relevant to bedside decision-making, and evaluates a biomarker that is objective, inexpensive, and immediately available. This study also places ln-EASIX within a biologically plausible framework linking endothelial dysfunction, renal vulnerability, thrombocytopenia, and systemic injury. This framework may help guide future studies evaluating whether ln-EASIX improves risk prediction when added to MELD-Na, chronic liver failure consortium acute-on-chronic liver failure, or other established prognostic models.

CONCLUSION

In hospitalized patients with cirrhosis, a higher ln-EASIX was associated with a more severe disease profile and worse early outcomes, particularly 30-day mortality. ln-EASIX demonstrated moderate-to-good discriminative ability for 30-day mortality in this cohort and may be a practical adjunctive tool for early inpatient risk stratification. However, its role should currently be considered exploratory rather than definitive, pending explicit reporting of the analytic cutoff value, multivariable validation, and formal comparison with established prognostic models.

Ethics

Ethics Committee Approval: This study was approved by the Gazi University Ethics Committee (approval no: 2025-2240, approval date: 23.12.2025, meeting no: 20).

Informed Consent: Informed consent was waived because of the retrospective study design.

Footnotes

Authorship Contributions

Surgical and Medical Practices: A.K., Y.E.B., G.K., M.C., T.K., M.K., Ç.K., K.M., A.L.G., Concept: A.K., Y.E.B., G.K., M.C., T.K., M.K., Ç.K., K.M., A.L.G., Design: A.K., Y.E.B., G.K., M.C., T.K., M.K., Ç.K., K.M., A.L.G., Data Collection or Processing: A.K., Y.E.B., G.K., M.C., T.K., M.K., Ç.K., K.M., A.L.G., Analysis or Interpretation: A.K., Y.E.B., G.K., M.C., T.K., M.K., Ç.K., K.M., A.L.G., Literature Search: A.K., Y.E.B., G.K., M.C., T.K., M.K., Ç.K., K.M., A.L.G., Writing: A.K., Y.E.B., G.K., M.C., T.K., M.K., Ç.K., K.M., A.L.G.

Conflict of Interest: No conflict of interest was declared by the authors.

Financial Disclosure: The authors declared that this study received no financial support.

REFERENCES

1. Bernardi M, Angeli P, Claria J, Moreau R, Gines P, Jalan R, et al. Albumin in decompensated cirrhosis: new concepts and perspectives. Gut. 2020; 69: 1127-38.
2. Arroyo V, Moreau R, Kamath PS, Jalan R, Gines P, Nevens F, et al. Acute-on-chronic liver failure in cirrhosis. Nat Rev Dis Primers. 2016; 2: 16041.
3. Moreau R, Jalan R, Gines P, Pavesi M, Angeli P, Cordoba J, et al. Acute-on-chronic liver failure is a distinct syndrome that develops in patients with acute decompensation of cirrhosis. Gastroenterology. 2013; 144: 1426-37.
4. Kim WR, Biggins SW, Kremers WK, Wiesner RH, Kamath PS, Benson JT, et al. Hyponatremia and mortality among patients on the liver-transplant waiting list. N Engl J Med. 2008; 359: 1018-26.
5. Bittermann T, McCauley M, Merli M, Fraker S, Sorensen S, Brown RS Jr, et al. Mortality risk factors among patients with cirrhosis and a low Model for End-Stage Liver Disease Sodium score. Gastroenterology. 2019; 156: 2314-25.
6. European Association for the Study of the Liver. EASL Clinical Practice Guidelines for the management of patients with decompensated cirrhosis. J Hepatol. 2018; 69: 406-60.
7. Luft T, Benner A, Jodele S, Dandoy CE, Storb R, Carreras E, et al. EASIX in patients with acute graft-versus-host disease: a retrospective cohort analysis. Lancet Haematol. 2017; 4: e414-e423.
8. Penack O, Eder M, Dandoy CE, Lawitschka A, Bertz H, Wolff D, et al. The endothelial activation and stress index predicts complications after allogeneic stem cell transplantation. Transplant Cell Ther. 2021; 27: 518.e1-518.e9.
9. Nawas MT, Devlin SM, Sanchez-Escamilla M, Maloy M, Scordo M, Barker JN, et al. Dynamic EASIX scores predict nonrelapse mortality after allogeneic hematopoietic cell transplantation. Blood Adv. 2022; 6: 5379-89.

10. Schulz A, Gummert J, Mohr M, Bauer T, Fink K, Reichenberger F, et al. Endothelial activation and stress index as a predictor of mortality in hospitalized patients with COVID-19. Front Immunol. 2021; 12: 703289.
11. Finke D, Hund H, Frey N, Luft T, Lehmann LH. EASIX (endothelial activation and stress index) predicts mortality in patients with coronary artery disease. Clin Res Cardiol. 2025; 114: 1008-18.
12. Schult D, Rasch S, Schmid RM, Lahmer T, Mayr U. EASIX is an accurate and easily available prognostic score in critically ill patients with advanced liver disease. J Clin Med. 2023; 12: 2553.
13. Claria J, Stauber RE, Coenraad MJ, Moreau R, Jalan R, Pavesi M, et al. Systemic inflammation in decompensated cirrhosis: characterization and role in acute-on-chronic liver failure. Hepatology. 2016; 64: 1249-64.
14. Sarin SK, Choudhury A, Sharma MK, Maiwall R, Al Mahtab M, Rahman S, et al. Acute-on-chronic liver failure: pathophysiological mechanisms and management. J Clin Exp Hepatol. 2022; 12: 1616-35.
15. Iwakiri Y, Grisham M, Shah V. Vascular biology and pathobiology of the liver: report of a single-topic symposium. Hepatology. 2008; 47: 1754-63.
16. Angeli P, Gines P, Wong F, Bernardi M, Boyer TD, Gerbes A, et al. Diagnosis and management of acute kidney injury in patients with cirrhosis: revised consensus recommendations of the International Club of Ascites. Gut. 2015; 64: 531-537.
17. Mitchell O, Feldman DM, Diakow M, Sigal SH. The pathophysiology of thrombocytopenia in chronic liver disease. Hepat Med. 2016; 8: 39-50.

Original Investigation | Özgün Araştırma

Gazi Med J 2026;37(3):436-445

DOI: http://dx.doi.org/10.12996/gmj.2026.4718

Imaging Characteristics and Diagnostic Spectrum of Pancreatic Masses in Pediatric and Young Adult Patients: A Single-Center Retrospective Series

Pediatrik ve Genç Erişkin Hastalarda Pankreatik Kitlelerin Görüntüleme Özellikleri ve Tanısal Spektrumu: Tek Merkezli Retrospektif Bir Seri

Merve Yazol, İsmail Akdulum

Division of Pediatric Radiology, Department of Radiology, Gazi University, Faculty of Medicine, Ankara, Türkiye

ABSTRACT

Objective: We aimed to describe the imaging characteristics and clinicopathologic features of pancreatic masses in pediatric and young adult patients managed at a single tertiary referral center.

Methods: This retrospective study included 19 patients (aged 4–24 years) with a pancreatic mass evaluated between 2012 and 2025. Cross-sectional imaging included computed tomography (n = 12), magnetic resonance imaging (MRI, n = 16), or both (n = 10). Imaging findings, pathologic results, and surgical outcomes were analyzed descriptively.

Results: Solid pseudopapillary neoplasm (SPN) was the most common diagnosis (n = 12, 63.2%), predominantly affecting female patients (10/12, 83.3%), with a median age of 14 years (range 12–17). A well-defined capsule was present in all 12 SPN cases (100%), and internal hemorrhage was present in 58.3%. Two of eleven MRI-evaluated SPN patients demonstrated an atypical, predominantly cystic pattern with absent T1 hyperintensity, no diffusion restriction, and no internal enhancement; both were preoperatively misinterpreted as pseudocysts. Main pancreatic duct dilatation was absent in all SPN cases, regardless of lesion size or location. Surgical resection was performed in 10 of 12 SPN patients (83.3%); lymphovascular invasion was absent in all confirmed cases. Rare entities included pancreatoblastoma (n = 1), diffuse large B-cell lymphoma with pancreatic involvement (n = 1), undifferentiated/anaplastic carcinoma (n = 1; the only case with nodal metastasis in the cohort), neuroendocrine tumor grade 1 (n = 1), focal nesidioblastosis (n = 1), serous cystadenoma (n = 1), and von Hippel-Lindau-associated pancreatic cysts (n = 1).

ÖZ

Amaç: Üçüncü basamak bir referans merkezinde takip edilen pediyatrik ve genç erişkin hastalardaki pankreas kitlelerinin görüntüleme özelliklerini ve klinikopatolojik bulgularını tanımlamayı amaçladık.

Yöntemler: Bu retrospektif çalışmaya, 2012 ile 2025 yılları arasında değerlendirilen ve pankreas kitlesi olan 19 hasta (4–24 yaş arası) dahil edildi. Kesitsel görüntüleme yöntemleri arasında bilgisayarlı tomografi (n = 12), manyetik rezonans görüntüleme (MRG; n = 16) veya her ikisi (n = 10) yer aldı. Görüntüleme bulguları, patoloji sonuçları ve cerrahi sonuçlar tanımlayıcı olarak analiz edildi.

Bulgular: Solid psödopapiller neoplazm (SPN), medyan yaşı 14 (dağılım 12–17) olan ve ağırlıklı olarak kadın hastaları (10/12, %83,3) etkileyen en yaygın tanıydı (n = 12, %63,2). On iki SPN vakasının tamamında (%100) iyi tanımlanmış bir kapsül mevcuttu ve %58,3'ünde iç kanama izlendi. MRG ile değerlendirilen on bir SPN hastasından ikisi, T1 hiperintensitesinin bulunmadığı, difüzyon kısıtlamasının olmadığı ve iç kontrastlanmanın görülmediği, her ikisi de ameliyat öncesi yanlışlıkla psödokist olarak yorumlanan atipik ağırlıklı olarak kistik bir patern sergiledi. Lezyon boyutu veya lokalizasyonundan bağımsız olarak hiçbir SPN vakasında ana pankreatik kanal (MPD) dilatasyonu saptanmadı. SPN hastalarının 12'sinden 10'una (%83,3) cerrahi rezeksiyon uygulandı; doğrulanmış vakaların hiçbirinde lenfovasküler invazyon görülmedi. Nadir görülen antitelere pankreatoblastom (n = 1), pankreas tutulumlu diffüz büyük B hücreli lenfoma (n = 1), andiferansiye/anaplastik karsinom (n = 1; kohortta nodal metastazı olan tek vaka), derece 1 nöroendokrin tümör (n = 1), fokal nezidioblastozis (n = 1), seröz kistadenom (n = 1) ve von Hippel-Lindau ilişkili pankreas kistleri (n = 1) dahildi.

Cite this article as: Yazol M, Akdulum İ. Imaging characteristics and diagnostic spectrum of pancreatic masses in pediatric and young adult patients: a single-center retrospective series. Gazi Med J. 2026;37(3):436-445

Address for Correspondence/Yazışma Adresi: Merve Yazol, Division of Pediatric Radiology, Department of Radiology, Gazi University, Faculty of Medicine, Ankara, Türkiye
E-mail / E-posta: myazol@gmail.com
ORCID ID: orcid.org/0000-0003-1437-8998

Received/Geliş Tarihi: 20.05.2026
Accepted/Kabul Tarihi: 15.06.2026
Publication Date/Yayınlanma Tarihi: 10.07.2026

ABSTRACT

CONCLUSION: SPN accounts for approximately two-thirds of pancreatic masses in pediatric and young adult patients and displays characteristic imaging features that support a confident preoperative diagnosis. An atypical cystic SPN pattern mimicking a pseudocyst on MRI represents an underrecognized diagnostic pitfall. Rare entities have distinct , though sometimes overlapping, imaging appearances, and awareness of the full diagnostic spectrum is important for clinical management in this age group.

Keywords: Solid pseudopapillary neoplasm, pediatric pancreatic mass, pancreatoblastoma, diffuse large B-cell lymphoma, neuroendocrine tumor, MRI

ÖZ

Sonuç: SPN, pediyatrik ve genç erişkin hastalardaki pankreas kitlelerinin yaklaşık üçte ikisini oluşturmaktadır ve güvenilir ameliyat öncesi tanıyı destekleyen karakteristik görüntüleme özellikleri sergiler. MRG'de psödokisti taklit eden atipik kistik SPN paterni, yeterince tanınmayan bir tanısal tuzaktır. Nadir görülen antiteler belirgin ancak zaman zaman birbiriyle örtüşen görüntüleme bulguları taşır ve bu yaş grubundaki klinik yönetim için tüm tanısal yelpazenin farkında olunması önemlidir.

Anahtar Sözcükler: Solid psödopapiller neoplazm, pediyatrik pankreas kitlesi, pankreatoblastom, diffüz büyük B hücreli lenfoma, nöroendokrin tümör, MRG

INTRODUCTION

Pancreatic masses in children and young adults constitute a diagnostically distinct clinical entity compared with those encountered in older adults. The differential diagnosis is dominated by solid pseudopapillary neoplasm (SPN), which accounts for approximately 61% of primary pediatric pancreatic tumors and shows a striking predilection for female patients in the second and third decades of life (1-4).

Pancreatoblastoma is the second most common primary pancreatic tumor in this age group, comprising approximately 17% of cases and representing the most frequent pancreatic malignancy in children below 10 years of age (3). Other exocrine tumors, endocrine tumors, and sarcomas are rare and more commonly encountered in children aged 10 years or older (3). Lymphoma can involve the pancreas primarily or secondarily and represents the most common nonepithelial pancreatic tumor in this age group (5). Although infrequent, pancreatic lymphoma requires a fundamentally different management approach from epithelial tumors and should be recognized as a distinct diagnostic entity (6). At the other end of the spectrum, functional lesions such as focal form of congenital nesidioblastosis may present with no identifiable mass on conventional cross-sectional imaging, rendering the diagnosis dependent on clinical, biochemical, and subtle morphologic correlation (7).

Accurate preoperative characterization of pediatric pancreatic masses directly influences surgical planning, operative approach, and patient counseling. Multimodality imaging integrating ultrasonography (USG), computed tomography (CT), and magnetic resonance imaging (MRI), including diffusion-weighted imaging (DWI) and dynamic contrast enhancement, plays a central role in this process (5). However, imaging features may overlap between entities, and atypical presentations of otherwise characteristic tumors remain an important source of misdiagnosis. Pediatric case series describing the full diagnostic spectrum with detailed imaging-pathology correlation are scarce in the literature, particularly from institutions serving both pediatric and young adult populations (7).

The aim of this study was to describe the imaging characteristics and clinicopathologic features of pancreatic masses in pediatric and young adult patients managed at a single tertiary center, with particular emphasis on the dominant entity, SPN, including its atypical imaging manifestations, and on the salient imaging features of rare diagnoses.

MATERIALS AND METHODS

Study Design and Patients

This was a single-center retrospective study. This study was conducted in accordance with the Declaration of Helsinki. Ethical approval was obtained from the Gazi University Clinical Research Ethics Committee (decision number: 10, date: 02.06.2026). The requirement for informed consent was waived by the ethics commission due to the retrospective design of the study. All patient images included in the manuscript were fully anonymized, and no identifying information is present in the figures. Patients aged 40 years or younger who presented with a pancreatic mass between 2012 and 2025 were eligible. Patients with insufficient imaging, without a confirmed diagnosis, or without active radiologic follow-up were excluded. A total of 19 patients met the inclusion criteria in the final analysis.

Imaging Protocols

Fifteen patients underwent abdominal USG as the primary initial investigation, with Doppler interrogation performed to assess vascularity and vascular contact. CT examinations (available in n = 12 patients) were performed using intravenous iodinated contrast material with a slice thickness of 0.625–1 mm. MRI examinations (available in n = 16 patients)included axial and coronal T2-weighted sequences with and without fat suppression, fat-suppressed T1-weighted sequences before and after intravenous gadolinium contrast administration and DWI with b-value ≥500 s/mm^2. Magnetic resonance cholangiopancreatography was obtained when clinically indicated. Two patients underwent CT only; 10 patients had both CT and MRI; the remainder had multimodality imaging.

Image Analysis

All imaging studies were retrospectively reviewed by a radiologist with 10 years of abdominal imaging experience. The following parameters were recorded: location (head, uncinate process, neck, body, tail, or junction zones), maximum diameter (mm), internal structure (solid, mixed solid-cystic, or predominantly cystic), presence of a capsule or pseudocapsule, internal hemorrhage [T1 hyperintensity on MRI or hyperattenuation on non-contrast CT], calcification, main pancreatic duct (MPD) dilatation, vascular contact or encasement, biliary involvement, enhancement pattern on CT and MRI, and DWI signal characteristics. Distal parenchymal atrophy, when present, was noted.

Statistical Analysis

Continuous variables are expressed as median and interquartile range (IQR); categorical variables are expressed as frequency and percentage (%). Given the descriptive nature and small sample size, no inferential statistical testing was applied. Analyses were performed using SPSS version 22.0 (IBM Corp., Armonk, NY, USA).

RESULTS

Patient Demographics and Clinical Presentation

Nineteen patients (15 females, 4 males; median age 15 years, range 4–24 years) were included. SPN was the most common diagnosis (n = 12, 63.2%), followed by the following rare entities: pancreatoblastoma, diffuse large B-cell lymphoma (DLBCL) with pancreatic involvement, undifferentiated/anaplastic carcinoma, NET G1, focal nesidioblastosis, serous cystadenoma, and von Hippel-Lindau (VHL)-associated pancreatic cysts (n = 1 each). Patient characteristics and imaging modalities are detailed in Table 1.

Among SPN patients, abdominal pain was the predominant complaint (10/12), and symptom duration ranged from acute onset to two years. Two patients were diagnosed incidentally: one following blunt abdominal trauma and one during an obesity workup. A minority of cases exhibited associated symptoms, including nausea, vomiting, and dyspepsia.

Pancreatoblastoma, a rare entity, presented in the patient as a one-year history of intermittent abdominal pain and chronic diarrhea. The DLBCL patient presented with abdominal pain, nausea, and progressive clinical deterioration. The NET G1 patient had nonspecific abdominal pain without biochemical evidence of hormonal excess. The patient with nesidioblastosis presented with recurrent hypoglycemic episodes; biochemical workup confirmed hyperinsulinemic hypoglycemia with inappropriately elevated fasting insulin. The patient with a serous cystadenoma reported subacute abdominal pain without jaundice, weight loss, or steatorrhea. The undifferentiated carcinoma (UC) patient presented with abdominal pain and nausea, without a prior history of pancreatic disease. The VHL patient was asymptomatic, with pancreatic lesions detected on structured surveillance imaging.

Imaging Characteristics

The pancreatic head and uncinate process were the most common sites of involvement, accounting for the largest proportion of SPN lesions (5/12, 41.7%), pancreatoblastoma, and UC of the pancreas. Additional SPN locations included the body-tail (4/12, 33.3%), the body-head junction (2/12, 16.7%), and the neck (1/12, 8.3%); the SPN located in the neck was associated with distal parenchymal atrophy without MPD dilatation. Rare entities were distributed across the pancreatic body (DLBCL), head-body junction (UC of pancreas, NET G1, VHL cysts), uncinate process (serous cystadenoma), and tail (focal nesidioblastosis). The full imaging dataset is provided in Table 2.

Table 1. Demographic and clinical characteristics of all patients (n = 19).

No	Age (y)	Sex	Diagnosis	Presenting symptom	Modality	Surgery
1	12	M	SPN	Abdominal pain (1 month)	USG + CT + MRI	Whipple
2	10	F	SPN†	Abdominal pain	USG + CT + MRI	Refused
3	14	F	SPN	Right upper quadrant pain	USG +CT + MRI	Enucleation
4	18	F	SPN	Incidental (obesity workup)	USG+ MRI	Whipple
5	17	F	SPN	Abdominal pain, vomiting	CT only	Whipple
6	23	F	SPN	Abdominal pain	USG + MRI	Whipple
7	24	F	SPN	Abdominal pain, dyspepsia	USG + MRI	Distal Px
8	16	F	SPN	Abdominal pain, nausea	USG + CT + MRI	Distal Px*
9	12	M	SPN	Abdominal pain (2 years)	USG + CT + MRI	Whipple
10	12	F	SPN	Incidental (post-trauma USG)	USG + CT + MRI	Distal Px
11	12	F	SPN†	Abdominal pain, vomiting	USG + MRI	Refused
12	14	F	SPN	Abdominal pain	CT + MRI	Distal Px
13	15	M	Pancreatoblastoma	Abdominal pain, diarrhea (1 year)	USG + MRI	Enucleation
14	4	F	DLBCL	Abdominal pain, nausea, deterioration	CT only	Core biopsy
15	17	F	UC of pancreas	Abdominal pain, nausea	USG + CT + MRI	Whipple + hepatectomy
16	14	F	NET G1	Abdominal pain	USG + CT + MRI	Whipple
17	15	M	Focal nesidioblastosis	Hyperinsulinemic hypoglycemia	USG + MRI	None
18	21	F	Serous cystadenoma	Abdominal pain, nausea	USG + MRI	Whipple
19	17	M	VHL-associated pancreatic cysts	Incidental (known VHL, surveillance USG)	USG + CT + MRI	None

†Radiologic diagnosis; surgery refused; under follow-up. *Intraoperative perforation; margins not evaluable.
CT: Computed tomography, DLBCL: Diffuse large B-cell lymphoma, MRI: Magnetic resonance imaging, NET: Neuroendocrine tumor, Px: Pancreatectomy, SPN: Solid pseudopapillary neoplasm, UC: Undifferentiated carcinoma, USG: Ultrasonography, VHL: von Hippel-Lindau.

Table 2. Imaging findings for all patients (n = 19).

No	Location	Size (mm)	Structure	Capsule	Hemorrhage	Calcif.	DWI restr.	Enhancement pattern	MPD dil.
1	Head	× 41 × 40	Solid	+	+	–	+	Venous dominant	–
2	Body-head	× 55 × 55	Mixed solid-cystic	+	–	–	+ (periph.)	Peripheral heterogeneous	–
3	Head-uncinate	× 48 × 53	Mixed solid-cystic	+	+	–	N/R	Progressive septal	–
4	Neck	35 × 45	Solid	+	–	–	–	Homogeneous	–
5	Head	60 × 55	Solid	+	+	–	N/A	Heterogeneous	–
6	Uncinate	65 × 60	Hemorrhagic-cystic	+	+	+	–	Peripheral, no solid comp.	–
7	Body-tail	60 × 40	Predominantly cystic	+	–	+	–	No uptake (atypical)	–
8	Head-body	55 × 48	Predominantly cystic	+	–	–	–	No uptake (atypical)	–
9	Head	30 × 27	Mixed solid-cystic	+	–	–	–	Early complete, then wall	–
10	Body-tail	125 × 117	Mixed solid-cystic	+	+	–	+	Peripheral heterogeneous	–
11	Body-tail	26 × 22	Mixed solid-cystic	+	–	–	–	Peripheral solid	–
12	Tail	64 × 63 × 54	Solid-necrotic	+	+	–	N/R	Peripheral heterogeneous	–
13	Head-uncinate	75 × 65	Solid-necrotic	+	+	–	+	Late heterogeneous	Push
14	Body	28 × 22	Solid	–	–	–	N/A	Hypoattenuating	–
15	Head-body	95 × 100 × 115	Solid-necrotic	–	–	–	–	Heterogeneous, necrotic	Biliary
16	Head	51 × 47 × 52	Mixed solid-cystic	+	–	–	–	Mild	–
17	Tail	Hypertrophy	Focal hypertrophy	–	–	–	–	Mildly increased arterial	–
18	Uncinate	27 × 26	Cystic	+	–	–	–	Peripheral only	–
19	Head-body junction	12 × 8 (largest)	Multiple simple cysts (5–6)	–	–	–	–	No internal enhancement	–

Biliary: Biliary dilatation, calcif.: Calcification, comp.: Component, dil.: Dilatation, DWI: Diffusion-weighted imaging, MPD: Main pancreatic duct, MRI: Magnetic resonance imaging, N/A: Not applicable (no MRI), N/R: Not reported, periph.: Peripheral, Push: Ductal displacement without dilatation, restr.: Restriction. Size is given as the maximum dimension on cross-sectional imaging.

Lesion sizes ranged from 12 mm (VHL cysts) to 125 mm (the largest SPN); the median SPN size was 55 mm (IQR 40–61 mm). The UC of the pancreas was the largest among the rare entities (95–115 mm), followed by pancreatoblastoma (75 mm) and NET G1 (51 mm).

In SPNs, a well-defined capsule or pseudocapsule was identified in all 12 cases (100%) and was the most consistent imaging feature. Internal hemorrhage was detected in 7 of 12 patients (58.3%), typically as T1 hyperintensity on MRI. Calcification was present in two cases (16.7%), both of which were peripherally distributed. Mixed solid-cystic morphology was most prevalent (5/12, 41.7%), followed by solid or solid-necrotic morphology (4/12, 33.3%) and predominantly cystic morphology (3/12, 25%). Two of the three predominantly cystic cases demonstrated an atypical pattern (absent T1 hyperintensity, absent diffusion restriction, and absent internal enhancement) and were preoperatively misdiagnosed as either a pseudocyst or a congenital cyst. FNA was attempted in one case but failed to penetrate the thick capsule. DWI restriction was present in 3 of 11 MRI-evaluated patients (27.3%); MPD dilatation was absent in all SPN cases. A representative case is illustrated in Figure 1.

Vascular and ductal involvement was confined to malignant rare entities. The UC of the pancreas encased the portal vein and superior mesenteric vein, produced biliary dilatation by encircling the proximal common bile duct, and extended to fill the portal hilum. Doppler USG showed that the pancreatoblastoma caused ductal displacement without significant dilatation or inferior vena cava (IVC) compression. All SPN cases showed preservation of peripancreatic vascular planes and absence of ductal dilatation, regardless of size and location. Peripancreatic fat planes were preserved in the DLBCL case despite the extent of systemic disease. The NET G1 case demonstrated imaging-pathology size discordance, with a 51 mm mass apparent on imaging harboring a 0.9 cm tumor attributable to desmoplastic stroma.

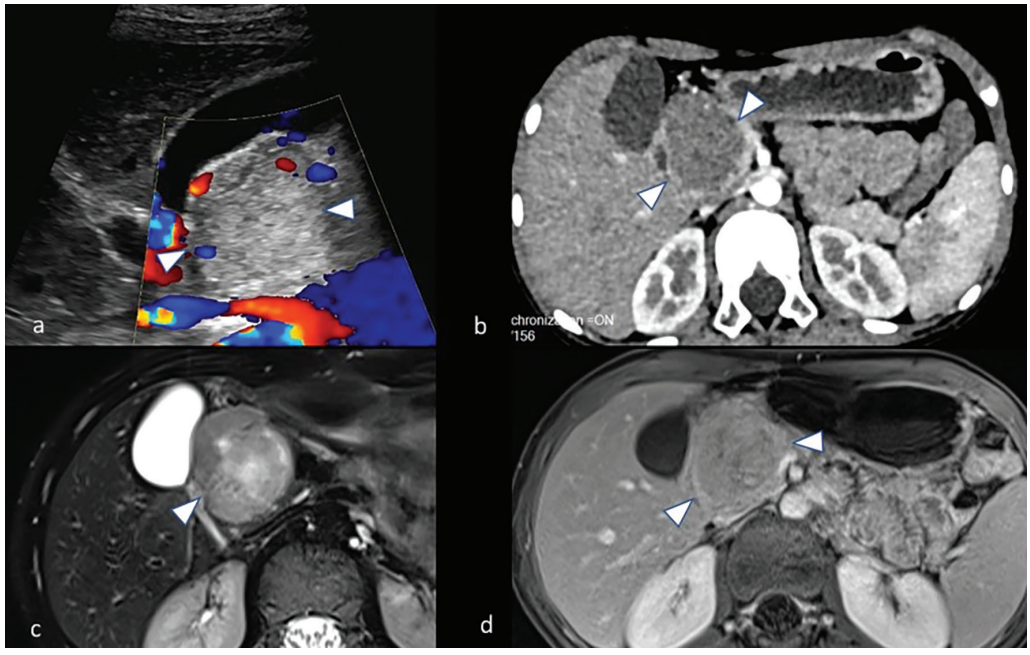

Figure 1. Solid pseudopapillary neoplasm of the pancreatic head in a 12-year-old male. (a) USG demonstrates a 42 × 37 mm well-defined mass with fine internal vascularity on Doppler interrogation. (b) Contrast-enhanced CT shows a heterogeneous solid mass with portal venous phase-dominant enhancement and less than 180° contact with the portal vein confluence and superior mesenteric vein. (c) T2-WI-MRI reveals heterogeneous signal intensity with central cystic foci. (d) Venous-phase contrast-enhanced MRI demonstrates heterogeneous enhancement. Posterior displacement of the inferior vena cava is noted; no peripancreatic lymphadenopathy was identified. Preoperative diagnosis was solid pseudopapillary neoplasm, confirmed on surgical pathology.

Surgical and Pathological Outcomes

Fourteen patients underwent surgical intervention. Pancreaticoduodenectomy was the most frequent operation (n = 8), followed by distal pancreatectomy (n = 4) and enucleation (n = 2). One pancreaticoduodenectomy was combined with hepatectomy in the patient with UC. Four patients were managed non-operatively: two SPN patients refused surgery and remain under imaging surveillance, the nesidioblastosis patient who is under endocrinologic follow-up, and the VHL patient who is on structured surveillance imaging.

Among surgically treated SPN patients (n = 10), histopathology confirmed SPN in all cases; four (40%) were staged as pT3. Surgical margins were negative in 7 of 9 evaluable cases (77.8%); one case could not be assessed due to intraoperative perforation. Two patients had positive anterior margins with uninvolved posterior margins. Perineural invasion (PNI) was identified in three patients (30%); lymphovascular invasion was absent in all ten patients. All dissected lymph nodes were reactive (8–12 nodes per case). Immunohistochemistry demonstrated nuclear and cytoplasmic beta-catenin positivity and chromogranin absence in all confirmed cases (10/10); Ki-67 was 1% in two patients and 5–10% in one patient.

Among rare entities, the pancreatoblastoma was staged as pT3 with negative margins and no perineural or lymphovascular invasion; immunohistochemistry showed nuclear beta-catenin, CK19, pankeratin, synaptophysin, chromogranin, trypsin, and focal AFP positivity. The UC was the only case with lymph node metastasis (pT3pN1, two metastatic nodes); margins were negative, and PNI was present. Immunohistochemistry revealed positivity for vimentin, pankeratin, CK7, and CK20 with negative staining for CD45, chromogranin, AFP, and glypican-3; intracytoplasmic mucin was confirmed by histochemistry. NET G1 pathology confirmed a 0.9-cm grade 1 tumor (Ki-67 1%) that was positive for synaptophysin and chromogranin. Serous cystadenoma was confirmed as a macrocystic/oligocystic type (CK7+, GLUT1+, CAIX+, inhibin+). DLBCL was confirmed on core needle biopsy (CD20+, BCL-2+, Ki-67 90–95%). No resection was performed.

Solid Pseudopapillary Neoplasm

SPN was identified in 12 patients (10 females, 2 males; median age 14 years, IQR 12–17, range 10–24). Ten of 12 patients (83.3%) were symptomatic; abdominal pain was the predominant complaint (10/12, 83.3%). Two patients were diagnosed incidentally: one on post-trauma USG and one on obesity workup USG. Ten patients (83.3%) underwent surgical resection; two refused surgery and remain under radiologic follow-up.

On cross-sectional imaging, SPN most commonly involves the pancreatic head or uncinate process (5/12, 41.7%), followed by body-tail (4/12, 33.3%), body-head junction (2/12, 16.7%), and neck (1/12, 8.3%). The neck lesion was associated with distal parenchymal atrophy without MPD dilatation. The median lesion size was 57 mm (IQR, 40–63; range, 26–125 mm). A well-defined capsule or pseudocapsule was identified in all 12 patients (100%). Internal hemorrhage was detected in 8 of 12 patients (66.7%) across all modalities. Calcification was present in two cases (16.7%), both peripherally distributed. MPD dilatation was absent in all 12 cases.

Internal structure varied across the cohort. Solid morphology was observed in three cases (25%), mixed solid-cystic morphology in 41.7% of cases, and predominantly cystic morphology in three cases (25%).

Two of the three predominantly cystic cases demonstrated an atypical imaging pattern on MRI: no T1 hyperintensity, no diffusion restriction, and no internal enhancement. Both were preoperatively interpreted as pseudocyst or congenital cyst, but surgical pathology confirmed SPN. In one of these cases, FNA was attempted, but it could not penetrate the thick capsule. Central necrosis was identified in two cases (16.7%), both on pathologic examination.

Of 11 patients evaluated with MRI, DWI restriction was present in three (27.3%). Enhancement was predominantly peripheral and heterogeneous in solid and mixed lesions, with venous-phase dominance; the two atypical cases that were predominantly cystic showed no meaningful contrast uptake. On USG, Doppler interrogation demonstrated an absence of significant internal vascularity in most cases.

Among the 10 operated patients, histopathology confirmed SPN in all cases. Surgical procedures included pancreaticoduodenectomy (Whipple; n = 5), distal pancreatectomy (n = 4), and enucleation (n = 1). Intraoperative perforation occurred in one case, precluding margin assessment. Surgical margins were negative in 7 of the remaining 9 cases (77.8%); two patients had positive anterior margins but uninvolved posterior margins. PNI was identified in three of the ten confirmed cases (30%) and lymphovascular invasion was absent in all ten confirmed cases. Four operated cases (40%) were staged as pT3. All dissected lymph nodes were reactive (range: 8–12 nodes per case). Immunohistochemistry revealed nuclear and cytoplasmic beta-catenin positivity and absence of chromogranin in all confirmed cases. Ki-67 was 1% in two patients and 5–10% in one. Imaging findings and pathologic data are summarized in Tables 2 and 3.

Table 3. Imaging and pathologic features of the SPN subgroup (n = 12).

Feature	Value	Notes
Sex (female)	10/12 (83.3%)	males: patients 1, 9
Median age, years (IQR)	(12–17)	Range 10–24
Pathologic confirmation	10/12 (83.3%)	refused surgery (pts 2, 11)
Symptomatic presentation	10/12 (83.3%)	2 incidentals: post-trauma USG, obesity workup
Location: head/uncinate	5/12 (41.7%)	Pts 1, 3, 5, 6, 9
Location: body-head junction	2/12 (16.7%)	Pts 2, 8
Location: neck	1/12 (8.3%)	Pt 4; with distal parenchymal atrophy
Location: body-tail	4/12 (33.3%)	Pts 7, 10, 11, 12
Median size, mm (IQR)	57 (41–64)	Range 26–125
Structure: solid/solid-necrotic	4/12 (33.3%)	Pts 1, 4, 5, 12
Structure: mixed solid-cystic	5/12 (41.7%)	Pts 2, 3, 9, 10, 11
Structure: predominantly cystic	3/12 (25%)	Pts 6, 7, 8 — 2 misdiagnosed as pseudocyst
Capsule present	12/12 (100%)	Present in all cases
Hemorrhage (imaging/pathology)	7/12 (58.3%)	Pts 1, 3, 5, 6, 10, 12; incl. pathologic hemorrhagic spaces
Calcification	2/12 (16.7%)	Pts 6, 7; peripherally distributed
MPD dilatation	0/12 (0%)	Absent in all
DWI restriction (MRI cases)	3/11 (27.3%)	11 SPN patients had MRI; pt 5 CT only
Atypical MRI (pseudocyst pattern)	2/11 (18.2%)	Pts 7, 8: no T1 signal, no DWI, no uptake
Central necrosis on pathology	2/10 (20%)	Pts 10, 12
Surgical resection	10/12 (83.3%)	2 refused surgery (pts 2, 11)
Whipple (pancreaticoduodenectomy)	5/10 (50%)	Head/uncinate lesions (pts 1, 4, 5, 6, 9)
Distal pancreatectomy	4/10 (40%)	Body-tail lesions (pts 7, 8, 10, 12)
Enucleation	1/10 (10%)	Pt 3
Negative surgical margins	7/9 (77.8%)	1 not evaluable (perforation, pt 8)
Positive anterior margin	2/9 (22.2%)	Pts 1, 9; posterior margins uninvolved
PNI	3/10 (30%)	Pts 1, 4, 9
LVI	0/10 (0%)	Absent in all operated cases
Lymph node metastasis	0/10 (0%)	All reactive
pT3 staging	4/10 (40%)	Peripancreatic fat or adjacent organ invasion
Beta-catenin nuclear + (IHC)	10/10 (100%)	All confirmed cases
Chromogranin – (IHC)	10/10 (100%)	Negative in all

*Intraoperative perforation; margins not evaluable. Atypical pseudocyst pattern: Two cases with no T1 hyperintensity, no DWI restriction, and no internal enhancement.

CT: Computed tomography, DWI: Diffusion-weighted imaging, IHC: Immunohistochemistry, IQR: Interquartile range, LVI: Lymphovascular invasion, MPD: Main pancreatic duct, MRI: Magnetic resonance imaging, PNI: Perineural invasion, pt/pts: Patient/patients, Px: Pancreatectomy, SPN: Solid pseudopapillary neoplasm, T1: T1-weighted imaging, USG: Ultrasonography.

Rare Entities: Case Descriptions

Pancreatoblastoma was confirmed in a 15-year-old male presenting with a one-year history of abdominal pain and diarrhea. USG demonstrated a 61 × 51 mm solid, lobulated pancreatic head mass with internal vascularity and IVC compression on Doppler. MRI confirmed a 65 × 75 mm mass involving the head and uncinate process, exhibiting internal microcystic foci, focal necrosis, and late-phase heterogeneous enhancement with associated ductal displacement. Total excision was performed; pathology revealed pancreatoblastoma (pT3, 8 cm) with squamoid nests, negative margins, and absent PNI and LVI. Imaging findings are illustrated in Figure 2.

DLBCL with pancreatic involvement was identified in a 4-year-old female who presented with abdominal pain, nausea, and clinical deterioration. CT demonstrated a 28 × 22 mm hypoattenuating mass in the pancreatic body, with multisegmental colonic wall thickening and diffuse ascites. Core needle biopsy confirmed high-grade B-cell lymphoma (Ki-67 90–95%); chemotherapy was initiated without surgical resection. Undifferentiated (anaplastic) carcinoma was identified in a 17-year-old female patient presenting with abdominal pain and nausea. CT and MRI revealed a 95–115 mm mass encasing the portal vein and the superior mesenteric vein, with biliary dilatation and cystic-necrotic areas. A Whipple procedure with hepatectomy yielded a 7-cm undifferentiated carcinoma (pT3pN1) with positive PNI and two metastatic peripancreatic lymph nodes (the only nodal metastases in the cohort). A diagnosis of NET G1 was confirmed in a 14-year-old female patient presenting with nonspecific abdominal pain. All three modalities demonstrated a 47–51 mm encapsulated mixed solid-cystic head mass; Whipple pathology confirmed a 0.9 cm grade 1 tumor surrounded by desmoplastic stroma, which accounted for the mass size apparent on imaging. Focal nesidioblastosis was suspected in a 15-year-old male with recurrent hyperinsulinemic hypoglycemia. MRI demonstrated focal tail hypertrophy with a lobulated contour, mildly elevated T1 signal, and slightly increased arterial enhancement without DWI restriction. No surgery was performed.

Serous cystadenoma was confirmed histologically in a 21-year-old woman with subacute abdominal pain. MRI demonstrated a 27 × 26 mm unilocular cystic uncinate lesion with peripheral enhancement and an absent solid component; pathology confirmed a macrocystic/oligocystic serous cystadenoma (CK7, GLUT1, CAIX, inhibin+). VHL-associated pancreatic cysts were identified in a 17-year-old male during structured surveillance. USG, CT, and MRI demonstrated 5–6 simple cysts, the largest measuring 12 × 8 mm, without solid components or MPD communication; no intervention was performed.

DISCUSSION

This single-center retrospective series of 19 pediatric and young adult patients demonstrates that SPN is the dominant entity, accounting for approximately two-thirds of cases, consistent with data from large multicenter registries (3,8). The remaining patients harbored a spectrum of diagnostically challenging lesions, including malignant tumors, functional disorders, syndromic cysts, and benign neoplasms, each with distinct but at times overlapping imaging features that directly influenced clinical management (8).

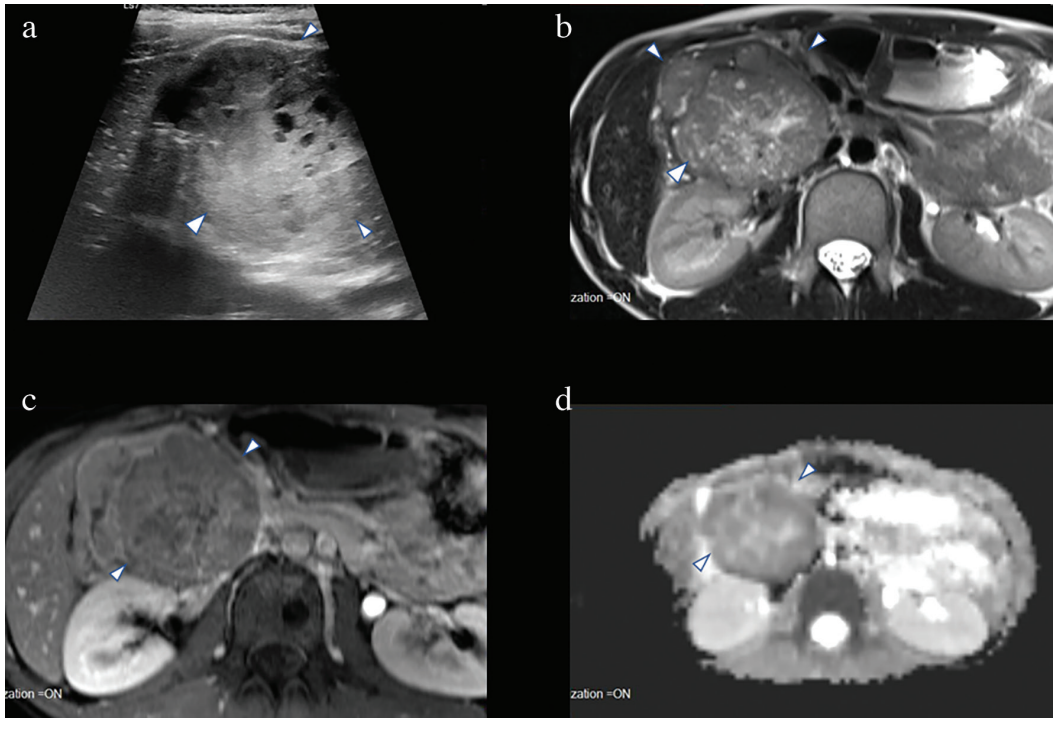

Figure 2. Pancreatoblastoma of the pancreatic head-uncinate process in a 15-year-old male. (a) USG demonstrates a 61 × 51 mm well-defined solid mass with lobulated superior-lateral contour, millimetric internal cysts, and inferior vena cava compression. (b) T2-WI-MRI reveals a large head-uncinate mass with internal microcystic foci and focal necrosis. (c) Late-phase contrast-enhanced MRI demonstrates heterogeneous enhancement. (d) DWI shows diffusion restriction within the lesion.

SPN represents approximately 1–3% of all exocrine pancreatic tumors and nearly 9% of cystic pancreatic neoplasms, with a marked predilection for young females; pooled analyses report female proportions of 84–88% and a mean age at diagnosis of 28–29 years (1,9). In the present cohort, 83.3% of patients were female, with a median age of 14 years; this is consistent with previously reported pediatric and young-adult series and likely reflects both earlier disease manifestation and referral patterns to tertiary pediatric centers. Abdominal pain was the predominant presenting symptom (83.3%), consistent with prior reports in which abdominal pain or discomfort was identified in 63.6% of patients as the most frequent complaint, though 38.1% were asymptomatic at diagnosis, while less frequent presentations included palpable mass, nausea, vomiting, and weight loss, with pancreatitis and jaundice occurring rarely (9). In our series, two cases were identified incidentally, supporting the well-recognized tendency of SPN to remain clinically silent until it reaches a considerable size or is detected on imaging performed for unrelated indications.

The fibrous capsule, present in 100% of our cases, is the most diagnostically reliable imaging feature of SPN. It has been identified as an independent predictor for differentiating SPN from pancreatic neuroendocrine neoplasms on both CT and MRI (10,11), typically appearing hypointense on T1- and T2-weighted sequences with moderate post-contrast enhancement, and is almost invariably present in tumors larger than 3 cm (12). The capsule arises from compressed peritumoral parenchyma and stroma, reflecting the expansile, non-infiltrative growth pattern that underlies SPN's low metastatic potential (13). Internal hemorrhage, detected in 58.3% of our cases, results from outgrowth of the central blood vessels and generates the characteristic T1-hyperintense foci on MRI. Reported rates in the literature range from 29% to 88.9%, and fluid-fluid levels may occasionally be observed (12,14,15).

The most common imaging appearance of SPN is a well-defined, encapsulated, heterogeneous mass with mixed solid-cystic morphology, reflecting variable degrees of intralesional hemorrhage and necrosis (16). This pattern was the most prevalent in our cohort (50%), consistent with published series. The solid component is typically peripheral while the cystic or necrotic component predominates centrally, although smaller lesions may present as predominantly solid masses (11,17). Two cases in our cohort demonstrated an atypical, predominantly cystic pattern with absent T1 hyperintensity, no diffusion restriction, and no internal enhancement; they were preoperatively interpreted as pseudocysts despite the absence of a history of pancreatitis or a known congenital cyst. This appearance arises when the solid component undergoes near-complete cystic degeneration and hemorrhagic products are reabsorbed (18). Atypical SPN may present across a wide imaging spectrum, ranging from purely cystic to predominantly solid lesions, and can mimic mucinous cystic neoplasms, pancreatic neuroendocrine tumors, or pseudocysts (18). Calcification, present in 18.2% of our cases and peripherally distributed in all, may provide an additional diagnostic clue (19). The presence of a preserved capsule and the clinical context of a young female patient with an encapsulated pancreatic lesion should prompt inclusion of SPN in the differential diagnosis, even in the absence of hemorrhagic signal. In equivocal cases, endoscopic ultrasound-guided fine needle aspiration may increase preoperative diagnostic yield without increasing the risk of metastasis or recurrence (20).

The reported incidence of MPD dilatation in SPN is approximately 10%, reflecting the typically soft and expansile growth pattern that displaces rather than obstructs the ductal system (21,22). In our cohort, MPD dilatation was absent in all 19 patients, irrespective of lesion size, location, or diagnosis; this included a pancreatoblastoma, which produced ductal displacement without dilatation, and an undifferentiated carcinoma, which caused biliary dilatation through common bile duct encasement without involvement of the MPD. Significant MPD dilatation should therefore prompt reconsideration of the diagnosis and raise suspicion for ductal adenocarcinoma or intraductal papillary mucinous neoplasm, both exceedingly rare in this age group (22).

Recent studies have identified several imaging features potentially associated with malignant behavior of SPN, including hepatic or peritoneal metastases, MPD obstruction, parenchymal infiltration, vascular encasement, capsular discontinuity, and tumor size exceeding 6 cm. In our series, three SPN cases exceeded 6 cm; the largest lesion measured 125 mm. None demonstrated vascular encasement, parenchymal infiltration, or nodal metastasis at surgery, underscoring the frequently indolent behavior of SPN even when size-based risk criteria are met. DWI restriction was present in 27.3% of MRI-evaluated SPN cases, likely reflecting high cellularity in solid components rather than overt malignant transformation, consistent with prior reports (23). ADC values in SPN are further influenced by cystic or hemorrhagic content, which may elevate measurements in mixed-morphology lesions and complicate threshold-based malignancy prediction (24). Detailed normative ADC data differentiating benign from malignant SPN behavior remain limited in the literature and represent an area that warrants prospective investigation.

Surgical resection is the standard of care for SPN regardless of size, given the risk of rupture and the excellent postoperative prognosis (25,26). Lymphovascular invasion was absent in all ten operated cases, and all dissected lymph nodes were reactive, consistent with the literature demonstrating that lymph node metastasis and lymphovascular spread are uncommon in SPN (27,28). PNI was identified in three of 10 patients (30%); however, its independent prognostic significance remains uncertain, as overall survival remains favorable even in the presence of adverse histopathologic features (28,29). Positive surgical margins were observed in two Whipple cases involving head-dominant lesions, reflecting the technical challenge of achieving clear margins at the superior mesenteric vein interface. Irtan et al. (30) identified positive surgical margins and age below 13.5 years as independent risk factors for recurrence, and several series have confirmed that R1 resection confers a higher recurrence risk than R0. Both margin-positive patients in our series have uninvolved posterior and lateral margins and remain under active follow-up, without evidence of recurrence.

Pancreatoblastoma is the most common malignant primary pancreatic tumor in children below 10 years, but may occur in older children and adolescents, as illustrated by our 15-year-old patient (31). Palpable abdominal mass, abdominal pain, and elevated AFP are the most frequent clinical presentations; however, AFP was

not measured preoperatively in our case, representing a limitation (31). On imaging, pancreatoblastoma typically presents as a large, well-circumscribed heterogeneous mass with solid and cystic components, internal septations, and variable calcifications; biliary duct dilatation is uncommon despite tumor size (31). In our case, IVC compression detected on USG highlights the importance of vascular interrogation in large head-uncinate lesions, as vascular encasement has direct implications for surgical planning. Nuclear beta-catenin positivity reflects shared Wnt-APC pathway activation with SPN; however, co-expression of trypsin, synaptophysin, lipase, BCL10, chromogranin, and AFP, alongside the defining squamoid nests on histology, reliably distinguishes pancreatoblastoma from SPN (32).

Among the rare entities in this series, several imaging-based diagnostic considerations merit emphasis. In the DLBCL case, the most discriminative feature was multisegmental extrapancreatic involvement, including colonic wall thickening and diffuse ascites accompanying a relatively small pancreatic body lesion. Vascular displacement without invasion and absent MPD dilatation favor lymphoma over ductal adenocarcinoma and should prompt image-guided biopsy rather than surgical exploration (33). The undifferentiated carcinoma case demonstrated vascular encasement and biliary obstruction, reflecting advanced locoregional disease. UC is an extremely rare and aggressive subtype, typically presenting as a large mass with variable imaging appearance; both biliary and pancreatic duct dilatation may occur due to the intraductal growth pattern (33). Large encasing pancreatic masses in young patients should not be reflexively attributed to lymphoma without a tissue diagnosis. In the NET G1 case, a disproportionately large imaging appearance relative to actual tumor size reflected prominent desmoplastic fibro-inflammatory stroma, a recognized pitfall that may lead to overestimation of tumor extent (34). VHL-associated pancreatic cysts develop in 60–72% of affected individuals and carry no malignant potential as isolated lesions (35). In our 17-year-old male patient, USG and MRI revealed multiple simple cysts without solid components or internal enhancement, consistent with VHL cysts without neoplastic transformation. The presence of multiple small pancreatic cysts in a young patient raises the possibility of underlying VHL disease. Surgical resection remains an option in symptomatic cases, though this is infrequent (35).

Study Limitations

This study has several limitations inherent to its retrospective single-center design. Different imaging modalities were used across patients according to clinical urgency and institutional availability, precluding a systematic cross-modality comparison. Two SPN patients refused surgery; their inclusion was based on concordant multiparametric imaging findings meeting established radiologic diagnostic criteria. Follow-up data were not uniformly available for survival analysis. Prospective multicenter studies with standardized imaging protocols and long-term follow-up are needed to validate imaging-prognostic correlations in this population.

CONCLUSION

SPN is the predominant pancreatic mass among pediatric and young adult patients and displays characteristic imaging features, including a well-defined capsule, internal hemorrhage, mixed solid-cystic morphology and absence of MPD dilatation that support a confident preoperative diagnosis in the majority of cases. An atypical, predominantly cystic SPN pattern that mimics a pseudocyst on MRI represents an underrecognized pitfall and should be considered in young female patients with an encapsulated pancreatic lesion lacking T1 hyperintensity. Each rare entity, including pancreatoblastoma, lymphoma, undifferentiated carcinoma, NET, nesidioblastosis, serous cystadenoma, and VHL-associated cysts, carries distinct imaging signatures that reflect its underlying biology and guide management; familiarity with this full diagnostic spectrum is required for appropriate clinical decision-making in this age group.

Ethics

Ethics Committee Approval: This study was conducted in accordance with the Declaration of Helsinki. Ethical approval was obtained from the Gazi University Clinical Research Ethics Committee (decision number: 10, date: 02.06.2026). The requirement for informed consent was waived by the ethics commission due to the retrospective design of the study.

Informed Consent: All patient images included in the manuscript were fully anonymized, and no identifying information is present in the figures. Patients aged 40 years or younger who presented with a pancreatic mass between 2012 and 2025 were eligible.

Footnotes

Authorship Contributions

Concept: M.Y., Design: M.Y., İ.A., Data Collection or Processing: M.Y., İ.A., Analysis or Interpretation: M.Y., İ.A., Literature Search: M.Y., Writing: M.Y.

Conflict of Interest: No conflict of interest was declared by the authors.

Financial Disclosure: The authors declared that this study received no financial support.

REFERENCES

1. Papavramidis T, Papavramidis S. Solid pseudopapillary tumors of the pancreas: review of 718 patients reported in English literature. J Am Coll Surg. 2005; 200: 965-72.
2. Yu P, Cheng X, Du Y, Yang L, Xu Z, Yin W, et al. Solid pseudopapillary neoplasms of the pancreas: a 19-year multicenter experience in China. J Gastrointest Surg. 2015; 19: 1433-40.
3. Eklund MJ, States LJ, Acord MR, Alazraki AL, Behr GG, El-Ali AM, et al. Imaging of pediatric pancreas tumors: a COG Diagnostic Imaging Committee/SPR Oncology Committee White Paper. Pediatr Blood Cancer. 2023; 70: e29975.
4. Fu C, Li X, Wang Y, Wang C, Jin H, Liu K, et al. Solid pseudopapillary neoplasm of the pancreas: a retrospective study of 195 cases. Front Oncol. 2024; 14: 1349282.
5. Shet NS, Cole BL, Iyer RS. Imaging of pediatric pancreatic neoplasms with radiologic-histopathologic correlation. AJR Am J Roentgenol. 2014; 202: 1337-48.
6. Ozcan HN, Oguz B, Sen HS, Akyuz C, Haliloglu M. Imaging features of primary malignant pancreatic tumors in children. AJR Am J Roentgenol. 2014; 203: 662-7.
7. Doi S, Yamada T, Kito Y, Obara S, Fujii Y, Nishimura T, et al. Adult-onset focal nesidioblastosis with nodular formation mimicking insulinoma. J Endocr Soc. 2022; 6: bvab185.

8. Patterson KN, Trout AT, Shenoy A, Abu-El-Haija M, Nathan JD. Solid pancreatic masses in children: a review of current evidence and clinical challenges. Front Pediatr. 2022; 10: 966943.
9. Law JK, Ahmed A, Singh VK, Akshintala VS, Olson MT, Raman SP, et al. A systematic review of solid-pseudopapillary neoplasms: are these rare lesions? Pancreas. 2014; 43: 331-7.
10. Khristenko E, Gaida MM, Tjaden C, Steinle V, Loos M, Krieger K, et al. Imaging differentiation of solid pseudopapillary neoplasms and neuroendocrine neoplasms of the pancreas. Eur J Radiol Open. 2024; 12: 100576.
11. Sunkara S, Williams T, Myers D, Kryvenko O. Solid pseudopapillary tumours of the pancreas: spectrum of imaging findings with histopathological correlation. Br J Radiol. 2012; 85: e1140-4.
12. Chae SH, Lee JM, Baek JH, Shin CI, Yoo MH, Yoon JH, et al. Magnetic resonance imaging spectrum of solid pseudopapillary neoplasm of the pancreas. J Comput Assist Tomogr. 2014; 38: 249-57.
13. Lu X, Chen H, Zhang T. Solid pseudopapillary neoplasm of the pancreas: current understanding on its malignant potential and management. Discov Oncol. 2024; 15: 77.
14. Ventriglia A, Manfredi R, Mehrabi S, Boninsegna E, Negrelli R, Pedrinolla B, et al. MRI features of solid pseudopapillary neoplasm of the pancreas. Abdom Imaging. 2014; 39: 1213-20.
15. Guerrache Y, Soyer P, Dohan A, Faraoun SA, Laurent V, Tasu JP, et al. Solid-pseudopapillary tumor of the pancreas: MR imaging findings in 21 patients. Clin Imaging. 2014; 38: 475-82.
16. Anil G, Zhang J, Al-Hamar NE, Nga ME. Solid pseudopapillary neoplasm of the pancreas: CT imaging features and radiologic-pathologic correlation. Diagn Interv Radiol. 2017; 23: 94-9.
17. Rogowska J, Semeradt J, Durko Ł, Małecka-Wojciesko E. Diagnostics and management of pancreatic cystic lesions: new techniques and guidelines. J Clin Med. 2024; 13: 4644.
18. Gao Y, Guo F, Lu Z, Xi C, Wei J, Jiang K, et al. Perioperative safety and prognosis following parenchyma-preserving surgery for solid pseudopapillary neoplasm of the pancreas. World J Surg Oncol. 2023; 21: 119.
19. Yao J, Song H. A review of clinicopathological characteristics and treatment of solid pseudopapillary tumor of the pancreas with 2450 cases in Chinese population. Biomed Res Int. 2020; 2020: 2829647.
20. Karsenti D, Caillol F, Chaput U, Perrot B, Koch S, Vuitton L, et al. Safety of endoscopic ultrasound-guided fine-needle aspiration for pancreatic solid pseudopapillary neoplasm before surgical resection: a European multicenter registry-based study on 149 patients. Pancreas. 2020; 49: 34-8.
21. Choi JY, Kim MJ, Kim JH, Kim SH, Lim JS, Oh YT, et al. Solid pseudopapillary tumor of the pancreas: typical and atypical manifestations. AJR Am J Roentgenol. 2006; 187: W178-86.
22. Kovac JD, Djikic-Rom A, Bogdanovic A, Jankovic A, Grubor N, Djuricic G, et al. The role of MRI in the diagnosis of solid pseudopapillary neoplasm of the pancreas and its mimickers: a case-based review with emphasis on differential diagnosis. Diagnostics. 2023; 13: 1074.
23. Perez ES, Towbin AJ, Morgan D, Towbin RB. Solid pseudopapillary tumor of the pancreas. Pediatr Imaging Case Ser. 2024; 20.
24. Quencer K, Kambadakone A, Sahani D, Guimaraes AS. Imaging of the pancreas: part 1. Appl Radiol. 2013; 42: 14-20.
25. Cruz MAA, Moutinho-Ribeiro P, Costa-Moreira P, Macedo G. Solid pseudopapillary neoplasm of the pancreas: unfolding an intriguing condition. GE Port J Gastroenterol. 2022; 29: 151-62.
26. Chen CC, Feng TY, Jan HC, Chou SJ, Chen TH, Wang SC. Rare case of solid pseudopapillary neoplasm of the pancreas with liver and splenic metastasis in a 19-year-old girl. Int J Surg Case Rep. 2024; 120: 109867.
27. Solakoğlu Kahraman D, Diniz G, Özamrak BG, Değirmenci M, Çalık B. Solid pseudopapillary neoplasm of the pancreas: clinicopathologic features, review of the literature. Anatol J Gen Med Res. 2025.
28. Lin YJ, Burkhart R, Lu TP, Wolfgang C, Wright M, Zheng L, et al. Solid pseudopapillary neoplasms of the pancreas across races demonstrate disparities with comparably good prognosis. World J Surg. 2022; 46: 3072-80.
29. Lee G, Sung YN, Kim SJ, Lee JH, Song KB, Hwang DW, et al. Large tumor size, lymphovascular invasion, and synchronous metastasis are associated with the recurrence of solid pseudopapillary neoplasms of the pancreas. HPB. 2021; 23: 220-30.
30. Irtan S, Galmiche-Rolland L, Elie C, Orbach D, Sauvat F, Elias D, et al. Recurrence of solid pseudopapillary neoplasms of the pancreas: results of a nationwide study of risk factors and treatment modalities. Pediatr Blood Cancer. 2016; 63: 1515-21.
31. Qiu L, Trout AT, Ayyala RS, Szabo S, Nathan JD, Geller JI, et al. Pancreatic masses in children and young adults: multimodality review with pathologic correlation. Radiographics. 2021; 41: 1766-84.
32. Omiyale AO. Adult pancreatoblastoma: current concepts in pathology. World J Gastroenterol. 2021; 27: 4172-84.
33. Veron Sanchez A, Santamaria Guinea N, Cayon Somacarrera S, Bennouna I, Pezzullo M, Bali MA. Rare solid pancreatic lesions on cross-sectional imaging. Diagnostics. 2023; 13: 2719.
34. Khanna L, Prasad SR, Sunnapwar A, Kondapaneni S, Dasyam A, Tammisetti VS, et al. Pancreatic neuroendocrine neoplasms: 2020 update on pathologic and imaging findings and classification. Radiographics. 2020; 40: 1240-62.
35. Charlesworth M, Verbeke CS, Falk GA, Walsh M, Smith AM, Morris-Stiff G. Pancreatic lesions in von Hippel-Lindau disease? A systematic review and meta-synthesis of the literature. J Gastrointest Surg. 2012; 16: 1422-1428.

Gazi Med J 2026;37(3):446-449

DOI: http://dx.doi.org/10.12996/gmj.2026.4679

Marked Hypercalcitoninemia without Medullary Thyroid Carcinoma: A Case Report

Medüller Tiroid Karsinomu Olmaksızın Belirgin Hiperkalsitoninemi: Olgu Sunumu

Seyit Murat Bayram, Hüseyin Demirci, Şule Canlar, Murat Cinel, Ceren Karaçalık, Erman Çakal

Clinic of Endocrinology, University of Health Sciences Türkiye, Ankara Etlik City Hospital, Ankara, Türkiye

ABSTRACT

This case report investigates the diagnostic difficulties associated with persistently elevated calcitonin levels in a patient with nodular thyroid disease, where biochemical evidence strongly indicated medullary thyroid carcinoma (MTC), yet histopathological analysis ultimately identified benign nodular hyperplasia with C cell activation.

We describe a 35-year-old male with hypothyroidism who exhibited persistently elevated serum calcitonin levels (35–47 ng/L). The diagnostic assessment comprised thyroid autoantibody panels, high-resolution ultrasound, serial fine-needle aspiration cytology (FNAC) with calcitonin washout measurements, a calcium stimulation test, and genetic testing for RET proto-oncogene mutations. The patient then had a total thyroidectomy and removal of the central lymph nodes.

The preoperative workup showed that the levels of anti-thyroglobulin and anti-thyroid peroxidase antibodies were very high, and the TSH level was also high (8.1 mIU/L). An ultrasound revealed two iso- to hypoechoic nodules and several cervical lymph nodes that appeared suspicious. FNAC results differed among samples: some were Bethesda II–III, while others were non-diagnostic. One nodule had a calcitonin washout level of 92 ng/L. The calcium stimulation test yielded a robust positive response, with peak calcitonin levels surpassing 500 ng/L (579 ng/L at 2 minutes). The genetic test for RET mutations came back negative. Following total thyroidectomy, histopathology confirmed nodular hyperplasia without evidence of MTC and all resected lymph nodes showed only reactive changes. After surgery, serum calcitonin levels returned to normal.

This case demonstrates that a combination of moderately elevated basal calcitonin levels, a positive calcitonin washout from FNAC, and a strong response to calcium stimulation—exceeding recently

ÖZ

Bu olgu sunumu, nodüler tiroid hastalığı olan bir hastada biyokimyasal bulguların medüller tiroid karsinomunu (MTK) güçlü bir şekilde işaret etmesine karşın histopatolojik analizin sonuçta benign nodüler hiperplazi ve C hücre aktivasyonunu tanımladığı, persistan yüksek kalsitonin düzeyleriyle ilişkili tanısal zorlukları incelemektedir.

Persistan yüksek serum kalsitonin düzeyleri (35–47 ng/L) sergileyen hipotiroidili 35 yaşında bir erkek hastayı tanımlıyoruz. Tanısal değerlendirme, tiroid otoantikor panelleri, yüksek çözünürlüklü ultrasonografi, seri ince iğne aspirasyon sitolojisi (İİAS) ve yıkama sıvısında kalsitonin ölçümü, kalsiyum stimülasyon testi ve RET proto-onkogen mutasyonları için genetik testten oluşmaktaydı. Hastaya ardından total tiroidektomi ve santral lenf nodlarının çıkarılması uygulandı.

Preoperatif değerlendirme, anti-tiroglobulin ve anti-tiroid peroksidaz antikor düzeylerinin oldukça yüksek olduğunu ve TSH düzeyinin de yüksek (8,1 mIU/L) olduğunu gösterdi. Ultrasonografi, iki adet izo-hipoekoik nodül ve şüpheli görünen birkaç servikal lenf nodu ortaya koydu. İİAS sonuçları her örnekte farklılık gösterdi; bazıları Bethesda II ile III arasında değerlendirilirken bazıları tanısal olarak değerlendirilemedi. Bir nodülde yıkama kalsitonin düzeyi 92 ng/L idi. Kalsiyum stimülasyon testi güçlü bir pozitif yanıt verdi; pik kalsitonin düzeyleri 500 ng/L'yi aştı (2. dakikada 579 ng/L). RET mutasyonlarına yönelik genetik test negatif sonuçlandı. Total tiroidektomi sonrasında histopatoloji, MTK bulgusu olmaksızın nodüler hiperplaziyi doğruladı ve çıkarılan tüm lenf nodlarında yalnızca reaktif değişiklikler izlendi. Cerrahi sonrasında serum kalsitonin düzeyleri normale döndü.

Bu olgu, orta derecede yüksek bazal kalsitonin düzeyleri, İİAS elde edilen pozitif yıkama kalsitonin sonucu ve yakın tarihte önerilen cinsiyete özgü eşik değerlerini aşan güçlü bir kalsiyum stimülasyon yanıtının bir arada

Cite this article as: Bayram SM, Demirci H, Canlar Ş, Cinel M, Karaçalık C, Çakal E. Marked Hypercalcitoninemia without medullary thyroid carcinoma: a case report. Gazi Med J. 2026;37(3):446-449

Address for Correspondence/Yazışma Adresi: Seyit Murat Bayram, Clinic of Endocrinology, University of Health Sciences Türkiye, Ankara Etlik City Hospital, Ankara, Türkiye
E-mail / E-posta: drmurat.endokrin@yandex.com
ORCID ID: orcid.org/0000-0003-1459-5765

Received/Geliş Tarihi: 02.04.2026
Accepted/Kabul Tarihi: 22.06.2026
Publication Date/Yayınlanma Tarihi: 10.07.2026

ABSTRACT

suggested sex-specific thresholds—does not conclusively indicate MTC. Nodular hyperplasia with functional C cell activation can closely resemble the biochemical profile of medullary carcinoma. Our results demonstrate the importance of integrating biochemical, cytological, and histopathological data to avoid overly aggressive surgery. Reporting these cases helps to improve diagnostic thresholds and shows that a careful, step-by-step approach is needed to evaluate hypercalcitoninemia, particularly in distinguishing between nodular hyperplasia and medullary carcinoma.

Keywords: Thyroid neoplasms, calcitonin, C-cell hyperplasia, Hashimoto's disease

ÖZ

bulunmasının MTK kesin olarak göstermediğini ortaya koymaktadır. Fonksiyonel C hücre aktivasyonu ile birlikte görülen nodüler hiperplazi, medüller karsinomun biyokimyasal profilini yakından taklit edebilir. Bulgularımız, aşırı agresif cerrahiden kaçınmak için biyokimyasal, sitolojik ve histopatolojik verilerin bütünleştirilmesinin ne denli önemli olduğunu göstermektedir. Bu tür olguların raporlanması, tanısal eşik değerlerin iyileştirilmesine katkı sağlamakta ve özellikle nodüler hiperplazi ile medüller karsinom arasında ayrım yapılmasında hiperkalsitoninemiyi değerlendirmek için dikkatli, adım adım ilerleyen bir yaklaşımın gerekliliğini vurgulamaktadır.

Anahtar Sözcükler: Tiroid neoplazileri, kalsitonin, C-hücre hiperplazisi, Hashimoto hastalığı

INTRODUCTION

Calcitonin is a peptide hormone made up of 32 amino acids that is released by the parafollicular C-cells in the thyroid gland (1). Calcitonin is a sensitive and specific biomarker for medullary thyroid carcinoma (MTC), and the number of C-cells in the blood directly reflects their number in the body (2,3). Elevated calcitonin levels are typically associated with malignancy, but nonmalignant such as C-cell hyperplasia (CCH), chronic thyroiditis, renal insufficiency, neuroendocrine tumors, and certain medications can also cause hypercalcitoninemia (4-6).

MTC is uncommon, making up only 2–3% of thyroid cancers in women and 4–5% in men (7). Its prevalence among patients with nodular thyroid disease has been reported to range from 0.3% to 1.4% (8,9). Some people have suggested that patients with thyroid nodules should have their serum calcitonin levels monitored regularly, but the cost-effectiveness of this strategy remains uncertain because MTC is rare and false-positive results can occur (9-12). In Europe, guidelines generally recommend that calcitonin levels be measured in patients with nodular thyroid disease. The American Thyroid Association, on the other hand, does not take a position (2,13). Assay interference, heterophilic antibodies, or natural factors like sex, age, and smoking (6,14-18) can all cause calcitonin levels to be falsely high. Furthermore, only 10–40% of individuals with both high basal calcitonin levels and thyroid nodules are eventually diagnosed with MTC (6,9). This gray area between normal and abnormal values makes it difficult to establish clear cutoff points. Basal calcitonin levels over 100 pg/mL are generally considered indicative of the need for surgery (2). However, levels below this threshold often require additional testing, such as immunocytochemistry, measurement of calcitonin in fine-needle aspiration washout fluid, or stimulation tests with pentagastrin or calcium (11,19-21).

CCH has been documented in conjunction with Hashimoto thyroiditis and multinodular goiter. Histologically, CCH is characterized by an elevated C cell density (>40 cells/cm²) or by the presence of multiple microscopic foci, each exceeding 50 C-cell per field. Hereditary CCH is thought to represent a precancerous stage of MTC, but there have also been reports of sporadic cases that did not progress to cancer (22-24).

Beyond the classical MTC framework, high calcitonin levels in nodular thyroid disease may result from benign C-cell activity, assay interference, or systemic factors such as medications and other comorbid conditions. If calcitonin levels return to normal after surgery and there is no histopathological evidence of MTC, the hormone excess likely originated from nodular thyroid tissue containing hyperplastic or functionally active C-cells. Such cases underscore the importance of combining biochemical markers with histopathological findings to avoid misclassification and unnecessarily aggressive management (25).

This case provides an opportunity to examine the broader context of the differential diagnosis of hypercalcitoninemia. It emphasizes the need for careful interpretation of calcitonin dynamics, strict adherence to assay methods, and a step-by-step diagnostic algorithm to avoid overtreatment of patients with nodular thyroid disease.

CASE PRESENTATION

A 35-year-old male patient was referred for testing because his serum calcitonin levels were consistently elevated. His medical history was otherwise unremarkable, with no family history of thyroid malignancy, chronic comorbidities, or alcohol or tobacco use. He was taking 50 mcg/day of levothyroxine for hypothyroidism.

Laboratory tests performed before surgery showed serum calcitonin levels ranging from 35 to 47 ng/L (normal range for men is less than 10 ng/L). The thyroid autoantibodies were positive. The anti-thyroglobulin (anti-TG) antibody was 596 IU/mL (reference: <115 IU/mL), and the anti-thyroid peroxidase (anti-TPO) antibody was 286 IU/mL (reference: <35 IU/mL). The thyroid-stimulating hormone level was elevated at 8.1 mIU/L (normal range: 0.4–4.0 mIU/L). Prolactin was 10 ng/mL (normal range: 4–15 ng/mL), which is within the normal range. The reference range for serum calcium is 8.5–10.5 mg/dL, and for gastrin is 0–100 pg/mL. The levels of catecholamine metabolites in the plasma were normal.

Thyroid ultrasound showed two iso-hypoechoic nodules: one in the right upper lobe, measuring 7 × 7 × 9.5 mm, and the other in the left lower lobe, measuring 5 × 6 × 7 mm. Some cervical lymph nodes were found in the central and lateral compartments. They ranged in size from 4 to 13 mm; some had a poorly defined echogenic hilum, which made them suspicious but not diagnostic for cancer.

Fine needle aspiration cytology (FNAC) was conducted on several occasions. The right upper nodule contained inflammatory infiltrates composed predominantly of lymphocytes and lacked thyrocytes in July 2024. There was no calcitonin washout. In September 2024, the same nodule was classified as benign follicular nodular disease

(Bethesda II), again without calcitonin washout. In November 2024, FNAC from the right upper nodule was non-diagnostic, but calcitonin washout was high at 92 ng/L. A second aspiration of the right upper lateral nodule did not yield useful information, and the calcitonin washout was less than 0.5 ng/L. FNAC of the left lower nodule showed a follicular lesion of unknown significance (Bethesda III) and a calcitonin washout of less than 0.5 ng/L.

Subsequently, provocative testing was performed. The omeprazole stimulation test was negative (Table 1). A calcium stimulation test showed a marked increase in serum calcitonin to levels exceeding 500 ng/L (Table 1). No evidence of the RET proto-oncogene by the genetic test.

Based on these results, a multidisciplinary tumor board suggested surgery. In December 2024, the patient had a total thyroidectomy and dissection of both central lymph nodes.

Histopathological analysis indicated nodular hyperplasia of the thyroid gland, with no signs of MTC. All examined lymph nodes exhibited reactive alterations without evidence of metastatic infiltration. After surgery, serum calcitonin levels returned to normal. This supports the idea that the high levels of calcitonin before surgery came from nodular thyroid tissue with hyperplastic or functionally active C-cells instead of medullary carcinoma.

DISCUSSION

In this case, a 35-year-old man had basal serum calcitonin levels that ranged from 35 to 50 ng/L, a fine-needle aspiration washout calcitonin level of 92 ng/L, and a calcium stimulation test that was markedly positive, with values of 579 ng/L at 2 minutes, 534 ng/L at 5 minutes, 524 ng/L at 7 minutes, and 468 ng/L at 10 minutes. Even though these biochemical results were present, histopathology after a total thyroidectomy showed only nodular hyperplasia and no MTC. After the surgery, calcitonin levels returned to normal. This result shows that nodular hyperplasia with C cell activation can mimic the biochemical profile of MTC without becoming malignant.

Calcitonin is a well-known biomarker for MTC, but it is not highly specific, especially when levels are only slightly to moderately elevated. False-positive results have been linked to autoimmune thyroiditis, multinodular goiter, differentiated thyroid carcinoma, renal insufficiency, and drugs like proton pump inhibitors. Both anti-TG and anti-TPO antibodies were markedly elevated in our patient, indicating autoimmune thyroiditis. This condition has also been linked to changes in calcitonin secretion. The 92 ng/L FNA washout calcitonin result supports the presence of active C-cells in the nodular tissue.

Table 1. Comparative table of stimulation tests applied to our patient.

Test type	Time point	Calcitonin (ng/L)	Gastrin (pg/mL)	Reference range (gastrin)
Omeprazole	Day 1	43.6	19.3	0–100 pg/mL
Omeprazole	Day 2	45.0	–	0–100 pg/mL
Omeprazole	Day 3	38.4	96.0	0–100 pg/mL
Omeprazole	Day 4	36.6	177.0	0–100 pg/mL
Calcium	Baseline	~45.0	–	N/A
Calcium	2 min	579.0	–	N/A
Calcium	5 min	534.0	–	N/A
Calcium	7 min	524.0	–	N/A
Calcium	10 min	468.0	–	N/A

The calcium stimulation test for this patient showed levels above 500 ng/L, which recent research suggests are highly suspicious for MTC. Sesti et al. (26) conducted a meta-analysis of individual-patient data and found different thresholds for calcium stimulation testing in men and women. They suggested that the cutoff values should be 562 pg/mL for men and 162 pg/mL for women. The pooled sensitivity for men was 0.79, specificity 0.89, and area under the curve 0.94, indicating that the test was highly accurate. The patient's peak value of 579 ng/L exceeded the male cutoff; however, histology showed no evidence of cancer. This shows that false positives can occur even when stimulated values exceed suggested thresholds. This difference highlights the importance of combining stimulation-test results with cytology, FNA-washout calcitonin, autoantibody status, and histopathology before deciding on aggressive surgery. Our case adds to this evidence by showing that nodular hyperplasia with C cell activation can cause values higher than the new male cutoff.

This case demonstrates several important points. Thresholds are not always accurate, and even sex-specific cutoffs from a meta-analysis may yield false positives. High levels of autoantibodies may indicate autoimmune thyroiditis, which is linked to C cell hyperplasia and a possible rise in calcitonin levels. If there are moderate basal elevations, you should obtain additional measurements, perform an FNA washout for calcitonin, and carefully consider the stimulation test results before surgery. Recording cases of non-MTC hypercalcitoninemia that normalize after surgery is useful for refining cutoff values and improving the specificity of clinical practice. Future studies examining procalcitonin, calcitonin, FNA washout calcitonin, and stimulation tests may help determine which hormone elevations are attributable to cancer and which are not.

This case demonstrates that a basal calcitonin level in the range of 45–50 ng/L, a positive fine-needle aspiration washout calcitonin level of 92 ng/L, and a calcium stimulation peak exceeding the recommended male cutoff of 562 pg/mL do not, in isolation, confirm the presence of MTC. Even though it was higher than what a recent meta-analysis suggested (26), histology showed nodular hyperplasia, and calcitonin levels returned to normal after surgery. To avoid unnecessarily aggressive treatments, doctors should interpret the results of stimulation tests in the broader clinical and pathological context. Reporting these cases contributes to refining diagnostic algorithms and underscores the need for prospective studies to validate sex-specific thresholds and to integrate additional markers in the evaluation of thyroid nodules.

Ethics

Informed Consent: Informed consent was obtained.

Footnotes

Authorship Contributions

Surgical and Medical Practices: S.M.B., H.D., Ş.C., M.C., C.K., E.Ç., Concept: S.M.B., E.Ç., Design: S.M.B., H.D., Data Collection or Processing: S.M.B., Ş.C., M.C., C.K., Analysis or Interpretation: S.M.B., H.D., E.Ç., Literature Search: S.M.B., C.K., Writing: S.M.B.

Conflict of Interest: No conflict of interest was declared by the authors.

Financial Disclosure: The authors declared that this study received no financial support.

REFERENCES

1. Felsenfeld AJ, Levine BS. Calcitonin, the forgotten hormone: does it deserve to be forgotten? Clin Kidney J. 2015; 8: 180-7.
2. Ringel MD, Sosa JA, Baloch Z, Bernet V, Brito JP, Cohen M, et al. 2025 American Thyroid Association management guidelines for adult patients with differentiated thyroid cancer. Thyroid. 2025; 35: 841-985.
3. Ozgen AG, Hamulu F, Bayraktar F, Yilmaz C, Tüzün M, Yetkin E, et al. Evaluation of routine basal serum calcitonin measurement for early diagnosis of medullary thyroid carcinoma in seven hundred seventy-three patients with nodular goiter. Thyroid. 1999; 9: 579-82.
4. Elisei R. Routine serum calcitonin measurement in the evaluation of thyroid nodules. Best Pract Res Clin Endocrinol Metab. 2008; 22: 941-53.
5. Turk Y, Makay O, Ozdemir M, Ertunc G, Demir B, Icoz G, et al. Routine calcitonin measurement in nodular thyroid disease management: is it worthwhile? Ann Surg Treat Res. 2017; 92: 173-8.
6. Toledo SP, Lourenço DM Jr, Santos MA, Tavares MR, Toledo RA, Correia-Deur JE. Hypercalcitoninemia is not pathognomonic of medullary thyroid carcinoma. Clinics. 2009; 64: 699-706.
7. Wells SA Jr, Asa SL, Dralle H, Elisei R, Evans DB, Gagel RF, et al. Revised American Thyroid Association guidelines for the management of medullary thyroid carcinoma: the American Thyroid Association Guidelines Task Force on Medullary Thyroid Carcinoma. Thyroid. 2015; 25: 567-610.
8. Cheung K, Roman SA, Wang TS, Walker HD, Sosa JA. Calcitonin measurement in the evaluation of thyroid nodules in the United States: a cost-effectiveness and decision analysis. J Clin Endocrinol Metab. 2008; 93: 2173-80.
9. Borget I, de Pouvourville G, Schlumberger M. Calcitonin determination in patients with nodular thyroid disease. J Clin Endocrinol Metab. 2007; 92: 425-7.
10. Cooper DS, Doherty GM, Haugen BR, Kloos RT, Lee SL, Mandel SJ, et al. Management guidelines for patients with thyroid nodules and differentiated thyroid cancer: the American Thyroid Association Guidelines Taskforce. Thyroid. 2006; 16: 109-42.
11. Costante G, Meringolo D, Durante C, Bianchi D, Nocera M, Tumino S, et al. Predictive value of serum calcitonin levels for preoperative diagnosis of medullary thyroid carcinoma in a cohort of 5817 consecutive patients with thyroid nodules. J Clin Endocrinol Metab. 2007; 92: 450-5.
12. LiVolsi VA. C cell hyperplasia/neoplasia. J Clin Endocrinol Metab. 1997; 82: 39-41.
13. Durante C, Hegedüs L, Czarniecka A, Paschke R, Russ G, Schmitt F, et al. 2023 European Thyroid Association clinical practice guidelines for thyroid nodule management. Eur Thyroid J. 2023; 12: e230067.
14. Aloia JF, Rasulo P, Deftos LJ, Vaswani A, Yeh JK. Exercise-induced hypercalcemia and the calciotropic hormones. J Lab Clin Med. 1985; 106: 229-32.
15. Karanikas G, Moameni A, Poetzi C, Kaserer K, Zettinig G, Dudczak R, et al. Frequency and relevance of elevated calcitonin levels in patients with neoplastic and nonneoplastic thyroid disease and in healthy subjects. J Clin Endocrinol Metab. 2004; 89: 515-9.
16. Kapoor D, Jones TH. Smoking and hormones in health and endocrine disorders. Eur J Endocrinol. 2005; 152: 491-9.
17. d'Herbomez M, Caron P, Bauters C, Cao CD, Schlienger JL, Sapin R, et al. Reference range of serum calcitonin levels in humans: influence of calcitonin assays, sex, age, and cigarette smoking. Eur J Endocrinol. 2007; 157: 749-55.
18. Papapetrou PD, Polymeris A, Karga H, Vaiopoulos G. Heterophilic antibodies causing falsely high serum calcitonin values. J Endocrinol Invest. 2006; 29: 919-23.
19. Rosário PW, Penna GC, Brandão K, Souza BÉ. Usefulness of preoperative serum calcitonin in patients with nodular thyroid disease without suspicious history or cytology for medullary thyroid carcinoma. Arq Bras Endocrinol Metabol. 2013; 57: 312-6.
20. Boi F, Maurelli I, Pinna G, Atzeni F, Piga M, Lai ML, et al. Calcitonin measurement in wash-out fluid from fine needle aspiration of neck masses in patients with primary and metastatic medullary thyroid carcinoma. J Clin Endocrinol Metab. 2007; 92: 2115-8.
21. Kudo T, Miyauchi A, Ito Y, Takamura Y, Amino N, Hirokawa M. Diagnosis of medullary thyroid carcinoma by calcitonin measurement in fine-needle aspiration biopsy specimens. Thyroid. 2007; 17: 635-8.
22. Guyetant S, Wion-Barbot N, Rousselet MC, Franc B, Bigorgne JC, Saint-Andre JP. C-cell hyperplasia associated with chronic lymphocytic thyroiditis: a retrospective quantitative study of 112 cases. Hum Pathol. 1994; 25: 514-21.
23. Verga U, Ferrero S, Vicentini L, Brambilla T, Cirello V, Muzza M, et al. Histopathological and molecular studies in patients with goiter and hypercalcitoninemia: reactive or neoplastic C-cell hyperplasia? Endocr Relat Cancer. 2007; 14: 393-403.
24. Barbot N, Guyetant S, Beldent V, Akrass M, Jeandrot A, Bigorgne JC, et al. Chronic autoimmune thyroiditis and C-cell hyperplasia: study of calcitonin secretion in 24 patients. Ann Endocrinol. 1991; 52: 109-12.
25. Fanget F, Demarchi MS, Maillard L, Lintis A, Decaussin M, Lifante JC. Medullary thyroid cancer outcomes in patients with undetectable versus normalized postoperative calcitonin levels. Br J Surg. 2021; 108: 1064-71.
26. Sesti F, Feola T, Dolce P, Alfano A, De Napoli L, Massa M, et al. Role of the calcium stimulation test in diagnosing medullary thyroid cancer: is it adequate to achieve a diagnosis in both sexes? An individual patient data meta-analysis. Eur Thyroid J. 2025; 14: e240347.

Gazi Med J 2026;37(3):450-459

DOI: http://dx.doi.org/10.12996/gmj.2026.4662

Harnessing *Mycobacterium tuberculosis*–Expanded γδ T-Cells for Tuberculosis Immunotherapy: Emerging Immunological Perspectives

Tüberküloz İmmünoterapisi için *Mycobacterium tuberculosis* ile Genişletilmiş γδ T-Hücrelerinden Yararlanma: Yeni Ortaya Çıkan İmmünolojik Bakış Açıları

Santosh Ramesh Achwani[1], Natarajan Suresh[2], R. Gayathri[3], V. Jhansi Lakshmi[4], Rajkumar Krishnan Vasanthi[5], Abhijit Dutta[6]

[1]Clinic of Family Medicine, Al Bateen Health Care Center, Abu Dhabi Health Services Company (SEHA), Abu Dhabi, United Arab Emirates
[2]Clinic of Pathology, Sree Balaji Medical College and Hospital, Chennai, India
[3]Clinic of Physiology, Bhaarath Medical College and Hospital, BIHER, Chennai, India
[4]Department of Pharmacology, Vignan Institute of Pharmaceutical Technology, Visakhapatnam, India
[5]Faculty of Health and Life Sciences, INTI International University, Nilai, Malaysia
[6]Royal School of Medical and Allied Sciences, The Assam Royal Global University, Guwahati, India

ABSTRACT

The rising incidence of multidrug-resistant and extensively drug-resistant tuberculosis and the persistent syndemic interaction between *Mycobacterium tuberculosis* (Mtb) and human immunodeficiency virus have substantially intensified the global tuberculosis burden. These challenges have renewed scientific interest in understanding the immunological mechanisms that regulate host resistance, as well as the sophisticated virulence strategies employed by Mtb. Tuberculosis infection is typically initiated through inhalation of aerosolized bacilli, which are first encountered by alveolar macrophages within the pulmonary microenvironment. Acting as frontline immunological sentinels, these cells recognize conserved microbial patterns through diverse pattern-recognition receptors—including Toll-like receptors, C-type lectin receptors, dendritic cell-specific intercellular adhesion molecule-3-grabbing non-integrin, and nucleotide-binding oligomerization domain-like receptors—thereby activating intracellular antimicrobial and inflammatory signaling pathways. Although tuberculosis immunology has been extensively investigated, earlier reviews have largely focused on conventional immune pathways, providing comparatively limited attention to the immunotherapeutic potential of Mtb–expanded gamma delta (γδ) T-cells. A comprehensive synthesis addressing their expansion

ÖZ

Çoklu ilaca dirençli ve yaygın ilaca dirençli tüberküloz vakalarının artması ve *Mycobacterium tuberculosis* (Mtb) ile insan immün yetmezlik virüsü (HIV) arasındaki sürekli sendemik etkileşim, küresel tüberküloz yükünü önemli ölçüde artırmıştır. Bu zorluklar, konak direncini düzenleyen immünolojik mekanizmaları ve Mtb tarafından kullanılan karmaşık virülans stratejilerini anlamaya yönelik bilimsel ilgiyi yeniden canlandırmıştır. Tüberküloz enfeksiyonu tipik olarak, akciğer mikroortamındaki alveoler makrofajlar tarafından ilk kez karşılaşılan aerosol halindeki basillerin solunmasıyla başlar. Ön cephe immünolojik bekçileri olarak hareket eden bu hücreler, Toll benzeri reseptörler, C tipi lektin reseptörleri, dendritik hücreye özgü hücreler arası yapışma molekülü-3 yakalayan non-integrin ve nükleotid bağlayıcı oligomerizasyon alanı benzeri reseptörler de dahil olmak üzere çeşitli patern tanıma reseptörleri aracılığıyla korunmuş mikrobiyal paternleri tanır ve böylece hücre içi antimikrobiyal ve inflamatuar sinyal yollarını aktive eder. Tüberküloz immünolojisi kapsamlı bir şekilde araştırılmış olsa da, önceki incelemeler büyük ölçüde geleneksel immün yollara odaklanmış ve Mtb tarafından genişletilmiş gama delta (γδ) T hücrelerinin immünoterapötik potansiyeline nispeten sınırlı bir dikkat göstermiştir. Genişleme mekanizmalarını, immünomodülatör fonksiyonlarını ve tüberküloz immünoterapisindeki translasyonel

Cite this article as: Achwani SR, Suresh N, Gayathri R, Lakshmi VJ, Vasanthi RK, Dutta A. Harnessing *Mycobacterium tuberculosis*–expanded γδ T-cells for tuberculosis immunotherapy: emerging immunological perspectives. Gazi Med J. 2026;37(3):450-459

Address for Correspondence/Yazışma Adresi: Abhijit Dutta, Royal School of Medical and Allied Sciences, The Assam Royal Global University, Guwahati, India
E-mail / E-posta: dutta.abhi2024@gmail.com
ORCID ID: orcid.org/0000-0002-0055-6696

Received/Geliş Tarihi: 16.03.2026
Accepted/Kabul Tarihi: 15.05.2026
Publication Date/Yayınlanma Tarihi: 10.07.2026

ABSTRACT

mechanisms, immunomodulatory functions, and translational significance in tuberculosis immunotherapy remains insufficiently explored. Consequently, a focused evaluation of the emerging role of γδ T-cells in host defense against tuberculosis is warranted. This review provides an integrated overview of the immunological functions and therapeutic relevance of γδ T-cells in tuberculosis. It discusses the role of γδ T-cells during Mtb infection, emphasizing their early antimicrobial responses and their contribution to innate-like immunity. The review further examines the interactions between γδ T-cells and dendritiC-cells, highlighting their cooperative role in antigen presentation and immune modulation. The mechanisms underlying γδ T-cell activation, interactions, and maturation during Mtb infection are addressed. Finally, emerging γδ T-cell–based immunotherapeutic strategies are being explored as potential host-directed approaches to complement conventional tuberculosis treatment. By consolidating recent advances in γδ T-cell biology and in understanding their role in tuberculosis immunity, this review addresses existing gaps in the literature and underscores their potential as targets for innovative therapeutic interventions against increasingly drug-resistant tuberculosis.

Keywords: *Mycobacterium tuberculosis*, γδ T-cells, tuberculosis immunology, host-directed therapy, dendritic cell interaction, drug-resistant tuberculosis

ÖZ

önemini ele alan kapsamlı bir sentez yeterince araştırılmamıştır. Sonuç olarak, tüberküloza karşı konak savunmasında γδ T hücrelerinin ortaya çıkan rolünün odaklanmış bir değerlendirmesi gereklidir. Bu inceleme, tüberkülozda γδ T hücrelerinin immünolojik fonksiyonları ve terapötik önemine ilişkin bütünleşik bir genel bakış sunmaktadır. Mtb enfeksiyonu sırasında γδ T hücrelerinin rolünü tartışarak, erken antimikrobiyal yanıtlarını ve doğuştan gelen bağışıklığa katkılarını vurgulamaktadır. İnceleme ayrıca, γδ T hücreleri ile dendritik hücreler arasındaki etkileşimleri inceleyerek, antijen sunumu ve immün modülasyondaki işbirlikçi rollerini vurgulamaktadır. Bu derlemede, Mtb enfeksiyonu sırasında γδ T hücre aktivasyonu, etkileşimleri ve olgunlaşmasının altında yatan mekanizmalar ele alınmaktadır. Son olarak, geleneksel tüberküloz tedavisini tamamlayıcı potansiyel konakçı odaklı yaklaşımlar olarak ortaya çıkan γδ T hücre tabanlı immünoterapötik stratejiler araştırılmaktadır. γδ T hücre biyolojisindeki ve tüberküloz bağışıklığındaki rollerinin anlaşılmasındaki son gelişmelerin bir araya getirilmesiyle, bu derleme literatürdeki mevcut boşlukları ele almakta ve giderek artan ilaç dirençli tüberküloza karşı yenilikçi terapötik müdahaleler için potansiyel hedefleri vurgulamaktadır.

Anahtar Sözcükler: *Mycobacterium tuberculosis*, γδ T-hücreleri, tüberküloz immunolojisi, konağa yönelik tedavi, dendritik hücre etkileşimi, ilaca dirençli tüberküloz

INTRODUCTION

The emergence of multidrug-resistant and extensively drug-resistant tuberculosis, compounded by the persistent syndemic interplay between *Mycobacterium tuberculosis* (Mtb) and human immunodeficiency virus (HIV), has profoundly aggravated the global tuberculosis burden. These converging pressures have renewed attention to the immunological architecture governing host resistance and to the sophisticated virulence mechanisms employed by the pathogen. Infection is initiated predominantly through inhalation of aerosolized bacilli, after which alveolar macrophages act as the primary immunological sentinels within the pulmonary milieu. Through diverse pattern-recognition receptors—including Toll-like receptors, C-type lectin receptors, dendritic cell (DC)-specific intercellular adhesion molecule-3-grabbing non-integrin, and nucleotide-binding oligomerization domain-like receptors—these cells identify conserved microbial signatures and activate intracellular antimicrobial cascades. In immunocompetent hosts, containment is typically achieved through the coordinated engagement of adaptive immunity, frequently evidenced by tuberculin skin test reactivity, which reflects immunologic sensitization rather than overt disease. Central to this containment is the granuloma, an organized cellular structure composed of activated macrophages, multinucleated giant cells, surrounded by T-lymphocytes, representing the histopathological hallmark of protective immunity. Its formation and maintenance depend largely upon T-cell–mediated processes. The variable efficacy of Bacillus Calmette–Guérin (BCG) vaccination and the limitations of existing chemotherapeutic regimens highlight the urgent need for innovative vaccine strategies and host-directed immunomodulatory approaches. Advancements in tuberculosis control require a more refined elucidation of immunopathogenic networks to identify dependable correlates of protection and inform the rational design of next-generation vaccines and adjunctive therapeutics.

Deterioration of host immune competence substantially compromises the ability to restrict Mtb replication. The bacillus subverts intracellular killing by interfering with phagolysosomal maturation, inhibiting vesicular acidification, and preventing phagosome–lysosome fusion (1), thereby establishing a permissive intracellular niche. Continued replication may ultimately induce host-cell necrosis, facilitating local tissue destruction and hematogenous dissemination. Protective immunity is orchestrated primarily by $CD4^+$ and $CD8^+$ T-lymphocytes, whose cytokine secretion profiles are indispensable for antimycobacterial defense (2). However, antigen-specific adaptive responses evolve slowly; several weeks are required for effective T-cell priming and accumulation at infection sites. This temporal delay enables substantial early bacillary expansion and constitutes a critical barrier to sterilizing immunity. Effective control depends on the differentiation of $CD4^+$ T-cells into functionally specialized subsets tailored to intracellular pathogens, particularly interferon-γ (IFN-γ)–producing T helper 1 (Th1) cells and, to a lesser extent, interleukin (IL)-4–secreting Th2 cells. While robust cell-mediated immunity is fundamental, additional immune components contribute to disease containment. Mtb produces structural and secreted virulence factors that modulate innate signaling pathways, and intrinsic host regulatory mechanisms often temper inflammatory responses, promoting equilibrium rather than complete eradication. Among the earliest lymphocyte populations mobilized during infection are gamma delta (γδ) T-cells, a highly responsive and functionally versatile subset that demonstrates distinct activation kinetics in both acute and chronic stages of mycobacterial disease in humans and experimental models.

A diverse array of T-cell lineages participates in immune responses to mycobacterial antigens, including $CD4^+$ and $CD8^+$ αβ T-cell receptor (TCR)–expressing lymphocytes, γδ TCR^+ cells, and CD1-restricted αβ T-cell subsets (3). Although the indispensable role of $CD4^+$ T-cells in human antimycobacterial immunity is well established, the precise

contributions and cooperative dynamics of other T-cell populations remain incompletely defined. Since the recognition of γδ TCR–bearing lymphocytes as a distinct lineage, studies in murine systems and human cohorts have substantiated their active engagement in host defense against Mtb (4). Conventionally, adaptive immunity is distinguished by antigen specificity and durable memory, whereas innate immunity relies on conserved recognition strategies and has historically been regarded as lacking memory capacity. γδ T-cells occupy an intermediate conceptual and functional position between these paradigms. Predominantly localized to peripheral tissues, the primary interfaces of microbial invasion act in concert with natural killer (NK) cells and interact closely with DCs, the principal antigen-presenting cells (APCs) responsible for translating localized inflammatory cues into systemic adaptive responses. Despite their relatively limited representation in peripheral blood, γδ T-cells exhibit distinctive migratory behavior and effector functions that differentiate them from conventional αβ T-lymphocytes. Emerging evidence, including observations from non-human primate studies, indicates that γδ T-cells may acquire adaptive-like attributes, notably memory-associated expansion. These cells recognize phosphoantigens generated during mycobacterial isoprenoid biosynthesis, in particular isopentenyl pyrophosphate (IPP) and (E)-1-hydroxy-2-methyl-but-2-enyl-4-diphosphate (HMBPP) (5). Experimental depletion of pulmonary γδ T-cells in macaque models has been associated with elevated bacterial burdens following Mtb challenge, stressing their crucial role in early containment. Collectively, these findings position γδ T-lymphocytes as pivotal immunological intermediaries that operate at the nexus of innate and adaptive immune defenses in tuberculosis.

γδ T-lymphocytes, long recognized for their participation in antimicrobial defense, also play a pivotal role in tumor immunosurveillance. Their antineoplastic capacity derives from an inherent ability to detect metabolic perturbations accompanying malignant transformation. Rapidly proliferating tumor cells exhibit increased flux through the mevalonate pathway, culminating in intracellular accumulation of IPP and related prenyl intermediates (6). These phosphoantigenic metabolites serve as potent stimuli for γδ T-cell activation, initiating cytotoxic effector responses. Beyond direct lysis of transformed cells, γδ T-lymphocytes augment antitumor immunity through dynamic interactions with other immune populations (7). Upon activation, they may acquire features of professional APCs, including expression of HLA-DR and delivery of costimulatory signals that promote αβ T-cell priming and differentiation into cytotoxic effectors. Modulation of receptors such as CD36 further facilitates clearance of tumor-derived debris and amplifies inflammatory signaling within the tumor microenvironment (8). Despite a comparatively restricted TCR repertoire, γδ T-cells recognize a broad array of phosphoantigenic structures, encompassing pyrophosphate-containing intermediates and prenyl metabolites generated by Mtb. In humans, the circulating Vγ9Vδ2 subset predominates in adulthood and constitutes the principal population responsive to mycobacterial phosphoantigens (9). These cells mediate antimycobacterial activity by granule-dependent cytotoxicity and by constraining bacillary replication within infected macrophages. γδ T-lymphocytes may function as unconventional APCs, promoting αβ T-cell expansion through CD40-mediated costimulation and reinforcing adaptive immune containment. Their capacity to enhance DC maturation and to engage in bidirectional TCR-dependent crosstalk further intensifies immune activation and contributes to the control of persistent intracellular infection.

During chronic Mtb infection, selective clonal expansion of discrete γδ T-cell subsets occurs, accompanied by acquisition of effector memory phenotypes characterized by increased cytokine secretion and augmented cytolytic potential (10). These expanded populations respond robustly to complex mycobacterial antigens, including whole-cell lysates, indicating participation in long-term immunological surveillance. γδ T-cells derived from tuberculosis-naïve infants exhibit measurable reactivity to mycobacterial lysates but display limited responsiveness to defined phosphoantigens such as HMBPP, suggesting that full functional maturation of this lineage depends on developmental progression and cumulative antigenic exposure. Although $CD4^+$ T-lymphocytes remain central to protective immunity against Mtb, their effectiveness may be diminished in states of immunodeficiency, particularly during HIV coinfection, wherein immune exhaustion attenuates antigen-specific responses. Under such circumstances, γδ T-cells may provide complementary or compensatory immune functions. Experimental murine models further delineate the context-dependent nature of γδ T-cell activation. Administration of complete Freund's adjuvant (CFA) induces marked expansion of γδ T-cells within draining lymph nodes (11). At the same time, repeated pulmonary exposure to purified protein derivative (PPD) increases the proportion of $CD3^+$ T-cells in lung tissue that CD4 and CD8 expression. Although CFA promotes in vivo proliferation of γδ T-lymphocytes within lymphoid organs, subsequent antigenic challenge does not elicit classical recall responses, implying that activation in this setting is driven primarily by inflammatory cues rather than by strict antigen specificity.

Functional studies provide additional insight into their role in host defense. Depletion of γδ T-cells exerts minimal impact on early bacterial loads following low-dose Mtb infection, indicating that they are not the principal mediators of initial microbial clearance (12). However, γδ TCR-deficient mice subjected to high-dose challenge exhibit disorganized granulomatous structures, characterized by enlarged lesions and excessive neutrophilic infiltration. These observations suggest that γδ T-lymphocytes contribute predominantly to immunoregulatory mechanisms that shape granuloma architecture (13), a structural determinant critical for containment of mycobacterial dissemination during advanced disease. Parallel findings in Listeria monocytogenes infection models, wherein γδ TCR-deficient animals display aberrant neutrophil recruitment and hepatic abscess formation, further stresses their role in orchestrating inflammatory patterning rather than serving as dominant antimicrobial effectors (14). Effective resistance to microbial invasion reflects the coordinated integration of innate and adaptive immunity. Because pathogens typically invade peripheral tissues while naïve αβ T-cells reside within secondary lymphoid compartments, early containment relies upon tissue-resident and rapidly mobilized immune populations. Within this interface, γδ T-lymphocytes occupy a distinctive intermediary position. Their antigen receptors exhibit structural diversity within complementarity-determining regions, enabling recognition of conserved molecular motifs independently of classical MHC restriction. This functional adaptability supports their characterization as rapid-response sentinels capable of exerting

both local and systemic immunomodulatory effects in accordance with the inflammatory context. Although numerically limited within the circulating lymphocyte pool, γδ T-cells constitute a phenotypically distinct $CD3^+$ subset with established contributions to both antimicrobial defense and tumor immunity.

Within the paradigm of tumor immunosurveillance, γδ T-lymphocytes are distinguished by their prompt secretion of IFN-γ and potent cytolytic capacity. They detect cellular distress through activating receptors most prominently NKG2D which engage stress-induced ligands such as MICA, MICB, and retinoic acid inducible molecules expressed on transformed or damaged cells (15). Upregulation of these ligands in malignant tissues, including melanoma, renders tumor cells more susceptible to γδ T-cell–mediated destruction. The interaction between activating receptors and their ligands provides critical costimulatory signals that facilitate targeted elimination of neoplastic cells. Unlike conventional αβ T-lymphocytes that recognize antigen in a major histocompatibility complex (MHC)-restricted manner and display extensive TCR variability, γδ T-cells exhibit comparatively constrained V-region diversity. In humans, the predominant Vγ9Vδ2 subset responds to low-molecular-weight, non-peptidic phosphorylated metabolites known as phosphoantigens (16), which arise from microbial biosynthetic routes or endogenous metabolic pathways. Among these, HMBPP, generated via the non-mevalonate pathway in numerous microbes and plants, represents one of the most potent activators (17). Endogenous IPP can stimulate these cells, generally at higher concentrations, while alkylamines enhance responsiveness by promoting intracellular accumulation of mevalonate pathway intermediates. Although TCR expression is unequivocally necessary for phosphoantigen recognition, an observation substantiated by gene-transfer studies, the precise molecular mechanisms underlying antigen sensing by γδ T-cells remain to be fully elucidated.

Accumulating data further indicate that Vγ9Vδ2 T-cells can acquire adaptive-like characteristics analogous to immunological memory (18). Investigations in nonhuman primate models of tuberculosis have demonstrated marked clonal expansion following primary immunization, accompanied by a more rapid and robust response upon re-exposure to antigen (19). In addition to these memory-like properties, γδ T-cells, alongside NK cells, serve as an early source of IFN-γ during the initial stages of immune activation, preceding the full participation of conventional αβ T-cells. This early cytokine output is principally driven by IL-12 and IL-18 produced by APCs, reflecting the intermediary role of γδ T-cells at the interface of innate and adaptive immunity (20). Their translational significance is underscored by ongoing early-phase oncologic studies assessing nonpeptidic pharmacological agents designed to selectively stimulate γδ T-cells, thereby highlighting their promise in vaccine development and cancer immunotherapy.

From a developmental standpoint, γδ T-cells constitute the earliest T-cell lineage to emerge in the murine thymus and subsequently colonize peripheral epithelial tissues. In the human fetal thymus, the dominant population typically expresses the Vδ1 chain paired with diverse Vγ chains and preferentially homes to epithelial compartments, particularly the intestinal mucosa (21). Although Vδ1 cells represent a minor fraction of circulating peripheral blood lymphocytes, they form a substantial component of intraepithelial lymphocytes and are often expanded in epithelial malignancies and certain lymphoproliferative conditions. Experimental depletion of pulmonary γδ T-cells has been associated with enhanced microbial clearance, suggesting a regulatory role in limiting excessive Th1-driven inflammatory responses. Moreover, both Vδ1 and Vδ2 subsets demonstrate cytotoxic activity *in vitro* against cells infected by viruses, parasites, or bacteria, as well as against transformed targets. Preferential expansion of Vδ1 T-cells has also been observed in individuals with HIV infection and in immunocompromised patients experiencing cytomegalovirus reactivation, stressing their integral role in host defense and immune homeostasis under conditions of immune perturbation.

γδ T in MTb Infection

γδ T-lymphocytes have been documented within granulomatous cutaneous lesions in patients with leprosy, and γδ T-cell lines established from these individuals demonstrate robust proliferative responses upon exposure to mycobacterial extracts (22). Accumulating experimental data further substantiate the capacity of MTb to directly stimulate γδ T-cells. Limiting dilution studies conducted by Kabelitz and co-investigators revealed that a substantial proportion of circulating γδ T-cells proliferate following stimulation with inactivated MTb, predominantly within the Vγ9/Vδ2 subset—the major γδ T-cell population in the peripheral blood of healthy adults (23). Parallel investigations by Havlir et al. (24) showed that monocytes harboring viable MTb possess a markedly enhanced ability to drive Vγ9/Vδ2 T-cell expansion compared with monocytes treated with heat-killed organisms or soluble mycobacterial derivatives such as PPD. These studies further clarified that heat shock protein 65 is not a strong mitogenic trigger for γδ T-cells.

Despite these observations, the precise antigenic determinants engaged by the Vγ9/Vδ2 TCR during MTb infection remain incompletely characterized. Although the Vγ and Vδ gene repertoires exhibit more restricted variability than the Vα and Vβ chains of conventional αβ T-lymphocytes, recombination events involving diversity (D) and joining (J) gene segments generate considerable junctional diversity, thereby enabling broad antigenic recognition (25). The definitive role of γδ T-cells in protective immunity against tuberculosis remains unresolved. Barnes and associates reported diminished *in vitro* expansion of γδ T-cells from individuals with pulmonary or disseminated tuberculosis following stimulation with heat-inactivated MTb and IL-2, although marked interindividual heterogeneity was observed (26). While certain studies have described elevated frequencies of circulating γδ T-cells in active tuberculosis and among healthcare workers with occupational exposure, these findings have not been uniformly replicated. Moreover, although γδ T-cells are present within pulmonary granulomas, their abundance does not surpass that of αβ TCR-expressing T-cells and generally mirrors the frequencies detected in peripheral blood or in unaffected lung parenchyma. Their localization within granulomatous tissue aligns with the role of alveolar macrophages as APCs capable of facilitating γδ T-cell activation.

Substantial evidence indicates a prominent expansion of Vγ9Vδ2 T-cells in the peripheral blood of patients with tuberculosis, as well as in diverse infectious conditions, including leprosy, malaria, Salmonella infection, and *Streptococcus pneumoniae* infection.

Furthermore, γδ T-cell clones isolated from the synovial fluid of individuals with rheumatoid arthritis recover proliferative capacity upon re-exposure to mycobacterial antigens after prior sensitization (27). Limiting dilution analyses provide compelling support for MTb-driven γδ T-cell activation, demonstrating significant expansion of peripheral γδ T-cells following interaction with killed bacilli. Within the pulmonary microenvironment, alveolar macrophages, the principal cellular targets of inhaled mycobacteria, function as non-MHC-restricted accessory cells that promote γδ T-cell activation. Significant functional distinctions exist between alveolar macrophages and circulating monocytes. Under steady-state conditions, where macrophages outnumber T-cells in the alveolar compartment, baseline γδ T-cell proliferation may be restrained through contact- and dose-dependent regulatory mechanisms. However, upon MTb infection, alveolar macrophages acquire enhanced immunostimulatory properties, thereby fostering localized γδ T-cell responses. Optimal γδ T-cell proliferation, cytokine secretion, and cytolytic activity require appropriate costimulatory signaling. Comparative analyses of MTb-stimulated $CD4^+$ and γδ T-cells from tuberculin-positive healthy donors have demonstrated comparable intracellular IFN-γ production, confirming the capacity of γδ T-cells to generate this critical effector cytokine (28). In contrast, $CD4^+$ T-cells produce greater amounts of IL-2, a difference that may partially account for the relatively limited proliferative expansion typically observed within γδ T-cell populations.

Administration of BCG has consistently been associated with preferential amplification of circulating Vγ9Vδ2 T-lymphocytes. At the same time, other γδ T-cell subsets exhibit comparatively limited fluctuations, underscoring the antigen-selective nature of this response during mycobacterial exposure. Beyond the peripheral blood, elevated frequencies of Vγ9Vδ2 cells have been observed in the pulmonary and intestinal compartments following systemic BCG immunization. In contrast, secondary lymphoid organs, including draining lymph nodes, demonstrate only modest changes. This spatial distribution implies that mucosal and barrier tissues constitute primary sites for γδ T-cell expansion and effector activity in the context of mycobacterial challenge. Both antigen dose and route of administration critically shape γδ T-cell dynamics; systemic delivery of BCG promotes dose-dependent increases in γδ, $CD4^+$, and $CD8^+$ T-cell populations, with particularly pronounced enrichment of γδ T-cells within the lung microenvironment (29). The dominant Vγ9Vδ2 subset detects non-peptidic phosphorylated intermediates via TCR–dependent recognition. These phosphoantigens originate predominantly from the mevalonate pathway, a fundamental metabolic cascade essential for sterol biosynthesis and cellular equilibrium. In parallel with TCR-mediated signaling, human γδ T-cells express diverse NK receptors that fine-tune activation thresholds. Stimulatory engagement of NKG2D by stress-inducible ligands such as MICA and MICB delivers crucial costimulatory signals, whereas inhibitory complexes, including CD94/NKG2A, restrain cytotoxic activity against targets bearing MHC class I molecules (30). Additional receptor pairings, notably CD94/NKG2C and various killer immunoglobulin-like receptors, further calibrate functional responsiveness.

The potential of Vγ9Vδ2 T-lymphocytes to establish long-lived immunological memory remains an area of active inquiry. Evidence from nonhuman primate tuberculosis models reveals clonal expansion of phosphoantigen-reactive Vγ9Vδ2 populations after primary immunization, followed by accelerated and augmented secondary responses upon re-exposure, consistent with memory-like attributes (31). The mechanism of γδ T-lymphocyte activation and immune response is illustrated in Figure 1. Phenotypic heterogeneity within this subset parallels the differentiation continuum characteristic of conventional αβ T-cells. It may be stratified by CD45RA and CD27 expression into naïve, central memory, effector memory, and terminal effector states. Early upregulation of CD45RO signifies commitment toward a memory phenotype analogous to developmental pathways described for $CD8^+$ T-cells. Effector memory cells display enhanced trafficking to peripheral tissues and may subsequently transition into $CD45RA^+CD27^-$ terminal effectors, distinguished by potent cytokine production and cytolytic capacity (32). Upon encountering infected or metabolically perturbed cells, Vγ9Vδ2 T-lymphocytes promptly secrete chemokines and Th1-polarized cytokines, mostly IFN-γ, thereby playing a pivotal role in the initiation and amplification of early antimicrobial defense mechanisms.

Extensive evidence obtained from histopathological analyses, rigorously controlled *in vitro* systems, and diverse animal models confirms the presence of persistent bidirectional crosstalk between γδ T-lymphocytes and myeloid-lineage cells. Such reciprocal communication highlights the distinctive placement of γδ T-cells at the interface of innate and adaptive immune responses. Experimental observations, including those reported by Ismaili and collaborators, have demonstrated that phosphoantigen-stimulated human γδ T-cells facilitate the differentiation and maturation of monocyte-derived DCs *in vitro* (33). This maturation is accompanied by a marked increase in the expression of antigen-presenting and co-stimulatory molecules, notably HLA-DR, CD86, and CD83. Mechanistically, these effects are largely mediated by cytokines, as activated γδ T-cells release substantial amounts of tumor necrosis factor-α and IFN-γ upon phosphoantigen exposure. The regulatory influence of γδ T-cells extends beyond soluble mediators; direct cell–cell interactions also play a pivotal role, forming an integrated and multifaceted network of immune modulation.

Within the peripheral circulation, the Vγ9Vδ2 subset constitutes the dominant γδ T-cell population and undergoes significant clonal

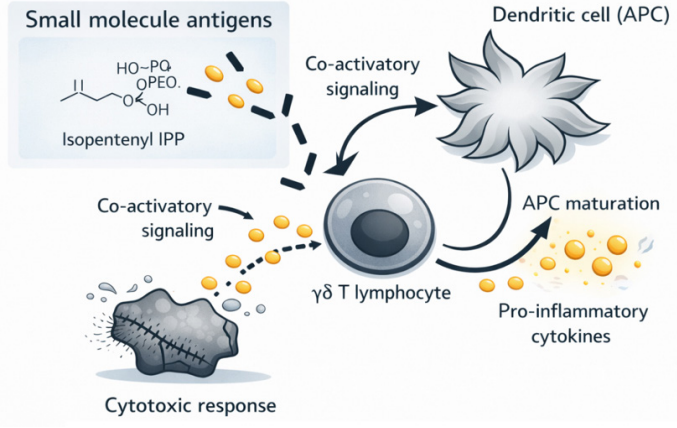

Figure 1. Mechanism of γδ T-lymphocyte activation and immune response. γδ T and dendritic cells.

γδ: Gamma delta.

expansion during infectious processes, occasionally comprising a considerable fraction of circulating T-lymphocytes. In contrast to conventional αβ T-cells, these cells exhibit a relatively restricted TCR repertoire, reflecting their evolutionarily conserved and specialized immunological functions. Their activation profile is contingent upon the nature of the stimulating signal. Pamidronate-induced activation requires close interaction with immature DCs to achieve full functional competence, whereas stimulation with IPP can occur independently of obligatory cellular contact (34). In both scenarios, cytokines within the microenvironment, particularly tumor necrosis factor-α and IFN-γ, serve as critical determinants of subsequent immune outcomes. Pamidronate, an aminobisphosphonate widely prescribed for osteoporosis and malignancy-associated bone disease, elicits robust γδ T-cell activation only in the presence of DCs, as reflected by upregulated expression of activation markers such as CD25 and CD69 and increased cytokine secretion; exposure in isolation produces comparatively modest effects (35). Moreover, γδ T-cells stimulated by IPP act synergistically with DCs undergoing lipopolysaccharide-driven maturation, leading to mutual amplification of activation signals and cytokine production. Collectively, these observations stress that microbial and pharmacologic stimuli enhance immune responsiveness through coordinated intercellular cooperation rather than isolated signaling events.

IL-15 further potentiates IFN-γ production by $CD4^+$ and $CD8^+$ T-lymphocytes, thereby reinforcing host defenses against mycobacterial pathogens. DCs infected and subsequently cultured with activated γδ T-cells display an increased capacity to direct naïve $CD4^+$ T-cells toward IFN-γ–producing phenotypes, compared with infected DCs maintained alone. This finding substantiates the concept that γδ T-cell engagement augments DC–mediated T-cell polarization and promotes pro-inflammatory cytokine responses. The pronounced expansion of γδ T-cells in response to BCG-infected DCs, even in the absence of supplemental cytokines, suggests the operation of self-sustaining reciprocal activation circuits that maintain localized inflammatory responses. Functional diversity emerges according to the mode of γδ T-cell expansion: Vγ9Vδ2 T cells expanded with IPP demonstrate limited capacity to restrict intracellular mycobacterial proliferation, whereas those expanded in response to BCG exhibit substantial antimycobacterial activity. These findings indicate that Vγ9Vδ2 T-cells play a critical role in preserving immunological homeostasis during bacterial infection by constraining pathogen dissemination, eliminating infected monocytes, and maintaining the antigen-presenting integrity of DCs. The interaction and activation pathways between DCs and Vγ9Vδ2 T-cells are illustrated in Figure 2.

Comprehensive transcriptomic profiling revealed that stimulation of peripheral blood mononuclear cells (PBMCs) with hemagglutinin antigen (HAg) induces a profound reorganization of global gene expression patterns. This remodeling was characterized by a significant enrichment of immunoregulatory signaling cascades, particularly those associated with tumour necrosis factor (TNF), IL-17, and JAK–STAT pathways. Quantitative real-time PCR validation corroborated these high-throughput findings, demonstrating robust upregulation of cytokine-encoding genes integral to antimycobacterial immunity following antigenic exposure. Functionally, γδ T-lymphocytes isolated from HAg-stimulated PBMCs of tuberculosis patients produced substantially higher levels of IFN-γ than those healthy individuals, indicating enhanced antigen sensitivity and effector competence. These HAg-primed γδ T-cells maintained IFN-γ secretion even under Th2-skewing conditions. This preserved functionality coincided with the expansion of Th1-like ($IFN\text{-}\gamma^+IL\text{-}4^-$) and Th0-like ($IFN\text{-}\gamma^+IL\text{-}4^+$) γδ T-cell subsets, alongside upregulation of the master transcription factors T-bet and GATA-3. Contrary to the classical model, which proposes mutual antagonism between these lineage regulators, the evidence does not support a definitive reciprocal inhibitory interaction. Experimental observations in murine systems further suggested that T-bet predominantly augments IFN-γ production while constraining IL-4 synthesis, whereas GATA-3 exerts limited suppressive influence on T-bet–mediated IFN-γ expression (36).

In addition to Th1-associated cytokines, HAg stimulation amplified γδ T-cell production of IL-17 and IL-22, with $Vδ2^+$ subsets exhibiting particularly pronounced responses following supplementation with exogenous IL-1β and IL-23 (37). Beyond γδ T-cells, NK cells demonstrated the capacity to develop durable, antigen-specific adaptive-like responses independent of classical B-cell and αβ T-cell pathways. $CD45RO^+$ NK cells isolated from pleural effusions of individuals with tuberculous pleuritis responded to HAg exposure by producing IL-22 and mounting recall responses against MTb, in contrast to NK cells from healthy PBMCs. Combined stimulation with IL-12, IL-15, and BCG further potentiated NK-cell activation, as reflected by increased expression of NKG2D, CD25, CD69, and granzyme B (38). These activated NK-cell populations were associated with the mitigation of inflammatory tissue injury and the preservation of pulmonary mucosal integrity. Collectively, these findings implicate HAg as a promising immunological adjuvant capable of strengthening BCG-induced protective immunity. Moreover, HAg-expanded γδ T-cells exhibited cytotoxic activity against hepatocellular carcinoma cells through mechanisms involving NKG2D engagement and ERK1/2 signaling (39). The role of Vγ9Vδ2 T-cells in tuberculosis-associated immune responses is summarized in Figure 3.

Contemporary models of host defense stress the importance of coordinated interactions among diverse immune cell subsets. Even numerically limited populations within infected tissues may exert substantial immunomodulatory effects through sustained communication with innate effector cells and APCs. During MTb infection, γδ-T-lymphocytes and DCs serve pivotal roles in

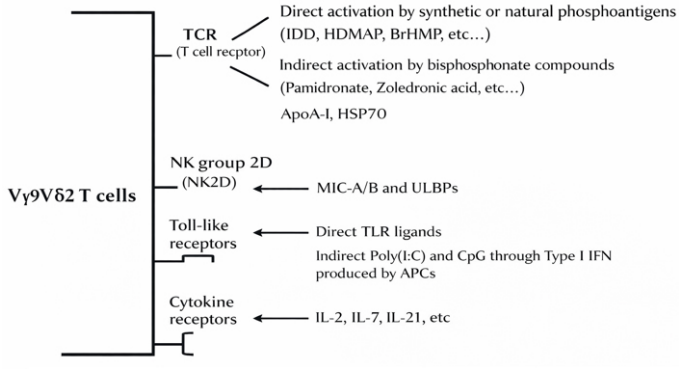

Figure 2. Activation pathways of Vγ9Vδ2 T-cells. γδ T interactions to MTb.
γδ: Gamma delta, MTb: Mycobacterium tuberculosis.

shaping early immune responses. Convergent evidence from histopathological studies, *in vitro* analyses, and *in vivo* models supports continuous, bidirectional crosstalk between γδ T-cells and myeloid compartments. Through secretion of pro-inflammatory mediators such as IFN-γ and TNF-α, as well as chemokines that enhance cytotoxic potential and modulate the local immune milieu, γδ T-cells contribute substantially to frontline antimycobacterial defense (40). Previous investigations have demonstrated that phosphoantigen-activated human γδ T-cells facilitate the maturation of monocyte-derived DCs. Although DCs are recognized as essential orchestrators of cellular immunity in tuberculosis, their functional behavior within infected tissues remains incompletely defined (41). In early disease stages, DCs accumulate at sites of inflammation, undergo pathogen-induced maturation, and subsequently migrate to secondary lymphoid organs, where they prime naïve T-cells by upregulating MHC molecules and co-stimulatory receptors and secreting cytokines such as IL-12.

In vivo studies further indicate that MTb can compromise DC migratory capacity and antigen-presenting function, thereby promoting bacterial persistence. Disruption of myeloid DC trafficking and competency appears to represent a strategic mechanism facilitating chronic infection. Under physiologically relevant conditions, particularly when Vγ9Vδ2 T-cells are activated in the context of incomplete DC maturation additional environmental cues likely influence the activation states of both cellular populations (42). Evidence suggests that Vγ9Vδ2 T-cells can drive the full maturation of MTb-infected immature DCs that would otherwise remain partially differentiated. Whereas infection alone elevates CD86 and HLA-DR expression without significantly increasing CD80 or CD40 expression, co-culture with Vγ9Vδ2 T-cells enhances CD80 and CD40 expression, sustains HLA-DR and CD86 expression, and markedly augments IL-12p70 secretion. Conversely, inadequate differentiation of Vγ9Vδ2 T-cells has been associated with insufficient IL-15 production by infected DCs. Given the critical role of IL-15 in promoting γδ T-cell differentiation toward an effector-memory phenotype—mediated through induction of Bcl-2 and enhanced resistance to apoptosis—deficiency of this cytokine may compromise the establishment of fully effective γδ T-cell–dependent protective immunity.

γδ T Maturation to MTb

Barnes and colleagues reported that patients with pulmonary or disseminated (miliary) tuberculosis exhibited a diminished *in vitro* proliferative response of γδ T-lymphocytes when these cells were stimulated with heat-inactivated Mtb in the presence of IL-2. However, the degree of impairment differed substantially among individuals. Data concerning the circulating proportions of γδ T-cells in individuals with tuberculosis and in healthcare workers exposed to the organism remain inconsistent; studies have reported divergent findings. Histological analyses have confirmed the presence of γδ T-cells within tuberculous pulmonary lesions; however, their abundance does not surpass levels detected in peripheral blood or uninvolved lung parenchyma. Their recruitment to infected tissue is consistent with the established role of alveolar macrophages as competent APCs capable of initiating γδ T-cell activation. Schwander et al. (43) further documented pronounced monocyte infiltration within the alveolar spaces of tuberculous lungs. Given that monocytes likewise possess antigen-presenting capacity, the inflammatory milieu within diseased lung tissue appears conducive to localized activation of γδ T-lymphocytes.

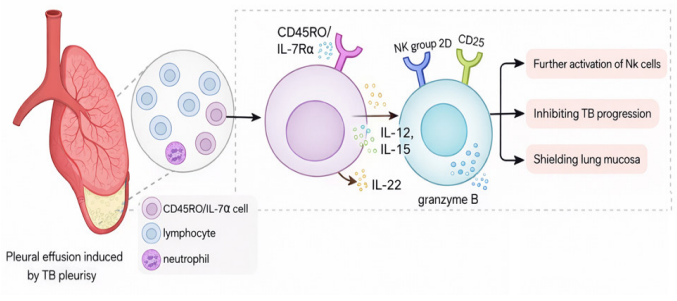

Figure 3. Role of Vγ9Vδ2 T-cells in tuberculosis-associated immune responses.

Robust expansion of Vγ9Vδ2 T-cells has been observed in neonates following BCG vaccination; this response is attributed to specific mycobacterial phosphoantigens. In the setting of active tuberculosis, circulating Vγ9Vδ2 T-cells exhibit transient phenotypic modulation that typically normalizes after successful antimicrobial therapy. Despite maintaining, or in some cases demonstrating, enhanced proliferative responsiveness, these cells produce lower quantities of IFN-γ than cells derived from healthy, tuberculin-reactive individuals. Dieli et al. (44) further demonstrated that this functional compromise extends beyond cytokine production to include reduced granulysin expression, thereby potentially attenuating antimycobacterial cytotoxic activity .

The mechanisms underlying this functional impairment remain incompletely defined. One proposed explanation implicates chronic antigenic stimulation *in vivo* as a driver of activation-induced cell death within the Vγ9Vδ2 subset. Alternatively, defective differentiation of central memory Vγ9Vδ2 cells into effector populations may result from suboptimal cytokine signals provided by Mtb-infected DCs. Experimental findings indicate that progression toward effector memory and terminally differentiated phenotypes depends critically on IL-15, whereas IL-7 is insufficient to substitute for this signal (45). IL-15 facilitates survival during this maturation process through induction of anti-apoptotic mechanisms, including upregulation of Bcl-2. Meraviglia et al. (46) have suggested that DCs harboring Mtb exhibit reduced IL-15 production, not because of an inherent defect in its induction, but as a consequence of pathogen-mediated suppression, thereby limiting effective Vγ9Vδ2 T-cell effector differentiation.

γδ T-based Immunotherapy

γδ T-lymphocytes possess potent antimicrobial and antineoplastic capabilities, attributable to their capacity to release proinflammatory cytokines, chemokines, and cytotoxic effector molecules, including perforin and granzymes (47). Through these mechanisms, they play a central role in immune surveillance and are increasingly regarded as valuable candidates in the development of next-generation immunotherapeutic strategies. In addition to their inherent cytolytic activity, γδ T-cells exert important immunomodulatory effects on DCs, promoting their maturation and enhancing antigen-presenting competence (48). This bidirectional interaction between innate-like and adaptive immune compartments is particularly relevant

for individualized immunotherapy, which requires coordinated immune activation. Although other unconventional lymphocyte subsets can stimulate DC function, circulating human γδ T-cells are distinguished by their relative abundance and their efficiency in amplifying DC-mediated immune responses. Their activation can be triggered by a wide array of endogenous and synthetic non-peptidic phosphoantigens, such as IPP, dimethylallyl diphosphate, geranylgeranyl pyrophosphate, and nitrogen-containing bisphosphonates, underscoring the diversity of metabolic and pharmacological signals capable of engaging this population.

Within the tumor microenvironment, malignant cells frequently circumvent immune detection by reducing the expression of tumor-associated antigens, downregulating MHC molecules, and impairing signaling pathways. Unlike conventional αβ T-lymphocytes, γδ T-cells recognize transformed targets in a largely MHC-independent fashion and exhibit diminished dependence on classical costimulatory signals, including CD28-mediated pathways (49). These properties provide a significant advantage in antitumor immunity. Experimental studies have demonstrated their protective function in murine models of chemically induced carcinogenesis and have shown robust cytotoxicity against diverse human tumor cell lines *in vitro* (50). Furthermore, adoptive transfer of *ex vivo* expanded human Vγ9Vδ2 T-cells into immunodeficient mice bearing xenografted malignancies has yielded therapeutic benefit in models of B-cell lymphoma, melanoma, and renal cell carcinoma (51). Pharmacological agents such as zoledronate have been reported to promote *in vivo* expansion of circulating γδ T-cells, thereby augmenting IFN-γ secretion and cytolytic potential (52). Early-phase clinical investigations in metastatic castration-resistant prostate cancer have established the feasibility and tolerability of Vγ9Vδ2 T-cell activation using zoledronate, either as monotherapy or in conjunction with low-dose IL-2, with preliminary signals of antitumor activity. The therapeutic impact observed in solid tumors likely reflects the dual functionality of γδ T-cells, encompassing direct tumor cell destruction following tissue infiltration and indirect enhancement of $CD8^+$ T-cell responses via DC modulation.

Studies in nonhuman primate models have provided additional insight into the adaptive-like attributes of γδ T-cells. Distinct peripheral γδ T-cell subsets —namely naïve, central memory ($CD27^+$), and effector memory ($CD27^-$) populations— have been phenotypically delineated across multiple primate species using monoclonal antibodies targeting human T-cell markers. Their *in vivo* proliferation following phosphoantigen stimulation has been shown to require IL-2. Enhanced immunogenicity to mycobacterial antigens has likewise been observed in cynomolgus macaques subjected to prime–boost vaccination with the H-1 fusion antigen formulated in Lipovac adjuvant, administered alone or together with the synthetic phosphoantigen Picostim (53). Although IC31 advanced to clinical evaluation in combination with the H-1 subunit vaccine, Lipovac was preferentially employed in experimental contexts due to its comparatively limited intrinsic immunostimulatory activity, thereby enabling clearer assessment of phosphoantigen-specific effects (54). Immunization strategies combining phosphoantigens and antituberculous subunit vaccines produced distinct T-cell kinetic patterns, in which booster administration attenuated γδ T-cell effector functions while simultaneously amplifying recall responses in αβ T-lymphocytes.

CONCLUSION

An expanding corpus of scientific literature has delineated the proliferative behavior, intracellular signaling networks, and functional effector properties of γδ T-lymphocytes within the intricate immunopathological landscape of tuberculosis. Findings from animal-based *in vivo* models, complemented by *in vitro* studies using human cellular systems, have progressively elucidated the contribution of γδ T-cells to orchestrating protective immune responses against Mtb. Their translation into clinical practice remains relatively limited. Only a modest number of clinical investigations have examined the therapeutic potential of γδ T-cells—particularly the Vγ9Vδ2 subset—within contemporary tuberculosis treatment frameworks. Unlike conventional αβ T-lymphocyte populations, γδ T-cells circulate at comparatively low frequencies under physiological conditions. Furthermore, the absence of well-established and phenotypically stable *in vitro* cell lines restricts comprehensive mechanistic exploration and translational advancement. Consequently, most experimental methodologies rely heavily on freshly isolated peripheral blood samples, which pose technical challenges associated with efficient cell purification, large-scale *ex vivo* expansion, and preservation of functional integrity and phenotypic stability, thereby imposing substantial practical limitations. Taken together, the unique capacity of γδ T-lymphocytes to function at the interface of innate and adaptive immunity, enabling rapid recognition of phosphoantigen-producing mycobacteria and other intracellular pathogens highlights their considerable promise as strategic candidates for the development of next-generation immunotherapeutic approaches in the management of tuberculosis.

Footnotes

Authorship Contributions

Surgical and Medical Practices: A.D., Concept: S.R.A., N.S., Design: S.R.A., N.S., Data Collection or Processing: A.D., Analysis or Interpretation: R.G., V.J.L., R.K.V., Literature Search: A.D., Writing: A.D.

Conflict of Interest: No conflict of interest was declared by the authors.

Financial Disclosure: The authors declared that this study received no financial support.

REFERENCES

1. Liu D, Wang J, Xu Z, Chen X, Jiao XA. Phagocytosis: strategies for macrophages to hunt *Mycobacterium tuberculosis*. One Health Adv. 2024; 2: 32.
2. Khanna H, Gupta S, Sheikh Y. Cell-mediated immune response against *Mycobacterium tuberculosis* and its potential therapeutic impact. J Interferon Cytokine Res. 2024; 44: 244-59.
3. Milton M, Mansour S. CD1-restricted T cells: are unconventional allies the key to future TB vaccines? Front Immunol. 2025; 16: 1629466.
4. Guo F, Song Y, Dong S, Wei J, Li B, Xu T, et al. Characterization and anti-tuberculosis effects of γδ T cells expanded and activated by *Mycobacterium tuberculosis* heat-resistant antigen. Virulence. 2025; 16: 2462092.
5. Comeau K, Paradis P, Schiffrin EL. Human and murine memory γδ T cells: evidence for acquired immune memory in bacterial and viral infections and autoimmunity. Cell Immunol. 2020; 357: 104217.

6. Yao Y, Zong Z, Zhang L. Unlocking γδ T cell power: pathways that boost cancer defense. Mol Biomed. 2024; 5: 5.
7. Park WH, Lee HK. Human γδ T cells in the tumor microenvironment: key insights for advancing cancer immunotherapy. Mol Cells. 2025; 48: 100177.
8. Xu Z, Kuhlmann-Hogan A, Xu S, Tseng H, Chen D, Tan S, et al. Scavenger receptor CD36 in tumor-associated macrophages promotes cancer progression by dampening type-I IFN signaling. Cancer Res. 2025; 85: 462-76.
9. Herrmann T, Karunakaran MM. Phosphoantigen recognition by Vγ9Vδ2 T cells. Eur J Immunol. 2024; 54: 2451068.
10. Huang Y, Jiang C, Zhu J, Lin L, Mao M, Yin T, et al. Expansion of effector memory Vδ2neg γδ T cells associates with cytomegalovirus reactivation in allogeneic stem cell transplant recipients. Front Immunol. 2024; 15: 1397483.
11. O'Brien RL, Born WK. Two functionally distinct subsets of IL-17 producing γδ T cells. Immunol Rev. 2020; 298: 10-24.
12. Vats D, Rani G, Arora A, Sharma V, Rathore I, Mubeen SA, Singh A. Tuberculosis and T cells: impact of T cell diversity in tuberculosis infection. Tuberculosis (Edinb). 2024; 149: 102567.
13. Bernal-Alferes B, Gómez-Mosqueira R, Ortega-Tapia GT, Burgos-Vargas R, García-Latorre E, Domínguez-López ML, et al. The role of γδ T cells in the immunopathogenesis of inflammatory diseases: from basic biology to therapeutic targeting. J Leukoc Biol. 2023; 114: 557-70.
14. Wang Y, Hu Y, Liu Y, Shi C, Yu L, Lu N, et al. Liver-resident CD44hiCD27– γδ T cells help to protect against *Listeria monocytogenes* infection. Cell Mol Gastroenterol Hepatol. 2023; 16: 923-41.
15. Arias-Badia M, Chang R, Fong L. γδ T cells as critical anti-tumor immune effectors. Nat Cancer. 2024; 5: 1145-57.
16. Herrmann T, Fichtner AS, Karunakaran MM. An update on the molecular basis of phosphoantigen recognition by Vγ9Vδ2 T cells. Cells. 2020; 9: 1433.
17. Xu Q, Sharif M, James E, Dismorr JO, Tucker JH, Willcox BE, et al. Phosphonodiamidate prodrugs of phosphoantigens (ProPAgens) exhibit potent Vγ9/Vδ2 T cell activation and eradication of cancer cells. RSC Med Chem. 2024; 15: 2462-73.
18. Gay L, Mezouar S, Cano C, Frohna P, Madakamutil L, Mège JL, et al. Role of Vγ9Vδ2 T-lymphocytes in infectious diseases. Front Immunol. 2022; 13: 928441.
19. Li F, Dang W, Du Y, Xu X, He P, Zhou Y, et al. Tuberculosis vaccines and T cell immune memory. Vaccines (Basel). 2024; 12: 483.
20. Linti AE, Göbel TW, Früh SP. Chicken γδ T cells proliferate upon IL-2 and IL-12 treatment and show a restricted receptor repertoire in cell culture. Front Immunol. 2024; 15: 1325024.
21. Hu Y, Hu Q, Li Y, Lu L, Xiang Z, Yin Z, et al. γδ T cells: origin and fate, subsets, diseases and immunotherapy. Signal Transduct Target Ther. 2023; 8: 434.
22. Pathak VK, Singh I, Sharma B, Turankar RP, Arora M, Singh SV, et al. Unveiling the role of NK cells, NKT-like cells, and γδ cells in pathogenesis of type 1 reactions in leprosy. Heliyon. 2024; 10: e25254.
23. Wei J, Guo F, Song Y, Feng T, Wang Y, Xu K, et al. Analysis of the components of *Mycobacterium tuberculosis* heat-resistant antigen (Mtb-HAg) and its regulation of γδ T-cell function. Cell Mol Biol Lett. 2024; 29: 70.
24. Havlir D.V., Ellner J.J., Chervenak K.A., Boom W.H., Selective expansion of human gamma delta T cells by monocytes infected with live *Mycobacterium tuberculosis*, J. Clin. Invest. 1991;87(2):729-33.
25. Sagar. Unraveling the secrets of γδ T cells with single-cell biology. J Leukoc Biol. 2024; 115: 47-56.
26. Kathamuthu GR, Kumar NP, Moideen K, Menon PA, Babu S. Decreased frequencies of gamma/delta T cells expressing Th1/Th17 cytokine, cytotoxic, and immune markers in latent tuberculosis-diabetes/pre-diabetes comorbidity. Front Cell Infect Microbiol. 2021; 11: 756854.
27. Feng X, Xu Y. The recent progress of γδ T cells and its targeted therapies in rheumatoid arthritis. Int J Rheum Dis. 2024; 27: e15381.
28. Nanda N, Alphonse MP. From host defense to metabolic signatures: unveiling the role of γδ T cells in bacterial infections. Biomolecules. 2024; 14: 225.
29. Moreo E, Jarit-Cabanillas A, Robles-Vera I, Uranga S, Guerrero C, Gómez AB, et al. Intravenous administration of BCG in mice promotes natural killer and T cell-mediated antitumor immunity in the lung. Nat Commun. 2023; 14: 6090.
30. Sánchez-Cerrillo I, Calzada-Fraile D, Triguero-Martínez A, Calvet-Mirabent M, Popova O, Delgado-Arévalo C, et al. MICa/b-dependent activation of natural killer cells by CD64+ inflammatory type 2 dendritic cells contributes to autoimmunity. EMBO J. 2023; 42: e113714.
31. Shen L, Huang D, Qaqish A, Frencher J, Yang R, Shen H, et al. Fast-acting γδ T-cell subpopulation and protective immunity against infections. Immunol Rev. 2020; 298: 254-63.
32. Yu XT, Cui J, Yang XG, Gao X, Yu L. Novel modulation of T effector memory cells-expressing CD45RA by prednisone in inoperable advanced type B thymoma patients. Genes Immun. 2025; 26: 222-8.
33. Wang B, Tian Q, Guo D, Lin W, Xie X, Bi H. Activated γδ T cells promote dendritic cell maturation and exacerbate the development of experimental autoimmune uveitis in mice. Immunol Invest. 2021; 50: 164-83.
34. Yazdanifar M, Barbarito G, Bertaina A, Airoldi I. γδ T cells: the ideal tool for cancer immunotherapy. Cells. 2020; 9: 1305.
35. Cieslak SG, Shahbazi R. Gamma delta T cells and their immunotherapeutic potential in cancer. Biomark Res. 2025; 13: 51.
36. Yang X, Sun M, Tang X, Zhang X, Shen W. T-bet: biological functions, molecular mechanisms, and therapeutic applications: a systematic review. Front Immunol. 2026; 17: 1671806.
37. Chojnacka-Purpurowicz J, Owczarczyk-Saczonek A, Nedoszytko B. The role of gamma delta T-lymphocytes in physiological and pathological conditions-focus on psoriasis, atopic dermatitis, autoimmune disorders, cancer and lymphomas. Int J Mol Sci. 2024; 25: 7960.
38. Tarannum M, Romee R. Cytokine-induced memory-like natural killer cells for cancer immunotherapy. Stem Cell Res. Ther. 2021; 12: 592.
39. Yang T, Zhang L, He S, Fan H, Li B, Li Z. Study on the effect of γδ T cells expanded *in vitro* to kill hepatocellular carcinoma cells. J Cancer Res Ther. 2023; 19: 45-56.
40. Qin Y, Xu J, Wang Q, Shi J. Cytotoxic granules and effector molecules from immune cells in tuberculosis: mechanisms of host defense and therapeutic potential. Virulence. 2025; 16: 2542466.
41. Larson EC, Ellis AL, Rodgers MA, Gubernat AK, Gleim JL, Moriarty RV, et al. Transiently boosting Vγ9+Vδ2+ γδ T cells early in Mtb coinfection of SIV-infected juvenile macaques does not improve Mtb host resistance. Infect Immun. 2024; 92: e00313-24.
42. Yuan M, Wang W, Hawes I, Han J, Yao Z, Bertaina A. Advancements in γδ T-cell engineering: paving the way for enhanced cancer immunotherapy. Front Immunol. 2024; 15: 1360237.
43. Schwander SK, Sada E, Torres M, Escobedo D, Sierra JG, Alt S, et al. T lymphocytic and immature macrophage alveolitis in active pulmonary tuberculosis. J. Infect. Dis. 1996;173(5):1267-72.

44. Dieli F, Sireci G, Caccamo N, Di Sano C, Titone L, Romano A, et al. Selective depression of interferon-γ and granulysin production with increase of proliferative response by Vγ9/Vδ2 T cells in children with tuberculosis. J. Infect. Dis. 2002;186:1835-9.
45. Lee H, Park SH, Shin EC. IL-15 in T-cell responses and immunopathogenesis. Immune Netw. 2024; 24: e11.
46. Meraviglia S, Caccamo N, Salerno A, Sireci G, Dieli F. Partial and ineffective activation of Vγ9Vδ2 T cells by *Mycobacterium tuberculosis*-infected dendritic cells. J. Immunol. 2010;185:1770- 6.
47. Subhi-Issa N, Tovar Manzano D, Pereiro Rodriguez A, Sanchez Ramon S, Perez Segura P, Ocaña A. γδ T cells: game changers in immune cell therapy for cancer. Cancers (Basel). 2025; 17: 1063.
48. Tyler CJ, Hoti I, Griffiths DD, Cuff SM, Andrews R, Keisker M, et al. IL-21 conditions antigen-presenting human γδ T-cells to promote IL-10 expression in naïve and memory $CD4^+$ T-cells. Discov Immunol. 2024; 3: kyae008.
49. Chen X, Sun G, Zhu X. γδ T cells in hematological malignancies: mechanisms and therapeutic strategies. Blood Sci. 2025; 7: 9-16.
50. Zheng HC, Xue H, Yun WJ. An overview of mouse models of hepatocellular carcinoma. Infect Agent Cancer. 2023; 18: 49.
51. Joalland N, Scotet E. Emerging challenges of preclinical models of anti-tumor immunotherapeutic strategies utilizing Vγ9Vδ2 T cells. Front Immunol. 2020; 11: 992.
52. Burnham RE, Zoine JT, Story JY, Garimalla SN, Gibson G, Rae A, et al. Characterization of donor variability for γδ T cell ex vivo expansion and development of an allogeneic γδ T cell immunotherapy. Front Med. 2020; 7: 588453.
53. Sefat KS, Kumar M, Kehl S, Kulkarni R, Leekha A, Paniagua MM, et al. An intranasal nanoparticle vaccine elicits protective immunity against *Mycobacterium tuberculosis*. Vaccine. 2024; 42: 125909.
54. Tait D, Diacon A, Borges ÁH, van Brakel E, Hokey D, Rutkowski KT, et al. Safety and immunogenicity of the H56:IC31 tuberculosis vaccine candidate in adults successfully treated for drug-susceptible pulmonary tuberculosis: a phase 1 randomized trial. J Infect Dis. 2024; 230: 1262-70.

Gazi Med J 2026;37(3):460

DOI: http://dx.doi.org/10.12996/gmj.2026.e001

Article corrected: Çelik E, Kanbur E, Bayram C, Aydoğan Ç, Köksal MB, Aydın SA, et al. *Polyethylenimine-Mediated Delivery of miR-379-5p Suppresses MTDH and FOXP2 in Colorectal Cancer Cells*. Gazi Med J. 2026;37(2):157-165. doi: 10.12996/gmj.2025.4598.

In the article titled "Polyethylenimine-Mediated Delivery of miR-379-5p Suppresses MTDH and FOXP2 in Colorectal Cancer Cells," published in Gazi Medical Journal, two references cited in the article were identified during post-publication review as retracted publications.

These retracted references were cited as supporting literature for the target-gene rationale and do not affect the experimental design, methodology, data analysis, results, interpretation, or conclusions of the article. Therefore, these retracted references should be replaced with appropriate non-retracted references at the same reference numbers.

The removed references are as follows:

"27. Hu W, Cao W, Liu J. RETRACTED: LncRNA-NEAT1 facilitates autophagy to boost pemetrexed resistance in lung adenocarcinoma via the miR-379-3p/HIF1A pathway. Human & Experimental Toxicology. 2025; 43.

35. He Q, Zhao L, Liu Y, Liu X, Zheng J, Yu H, et al. circ-SHKBP1 regulates the angiogenesis of U87 glioma-exposed endothelial cells through miR-544a/FOXP1 and miR-379/FOXP2 pathways. Mol Ther Nucleic Acids. 2018; 10: 331-48."

The corrected references should read as follows:

"27. Chen JS, Li HS, Huang JQ, Dong SH, Huang ZJ, Yi W, et al. MicroRNA-379-5p inhibits tumor invasion and metastasis by targeting FAK/AKT signaling in hepatocellular carcinoma. Cancer Lett. 2016; 375: 73-83.

35. Dhiman G, Srivastava N, Goyal M, Rakha E, Lothion-Roy J, Mongan NP, et al. Metadherin: a therapeutic target in multiple cancers. Front Oncol. 2019; 9: 349."

Accordingly, references 27 and 35 have been replaced in the reference list with the corrected references listed above. The relevant in-text citation "(27,35)" refers to the corrected references. No renumbering of the remaining references was required. These changes are technical in nature and do not alter the scientific content or conclusions of the article.